Université de Montréal

DÉCOUVERTE ET APPLICATION DE NOUVEAUX MOTIFS D'ASSOCIATION PROPRES À L'HEXAPHÉNYLBENZÈNE ET À SES DÉRIVÉS

par
Eric Gagnon

Département de Chimie
Faculté des Arts et des Sciences

Thèse présentée à la Faculté des Arts et des Sciences
en vue de l'obtention du grade de
Philosophiae Doctor (Ph.D.)
en chimie

novembre 2009

© Eric Gagnon, 2009

Université de Montréal
Faculté des Arts et des Sciences

Cette thèse intitulée :

DÉCOUVERTE ET APPLICATION DE NOUVEAUX MOTIFS D'ASSOCIATION PROPRES À L'HEXAPHÉNYLBENZÈNE ET À SES DÉRIVÉS

Présentée par :

Eric Gagnon

a été évaluée par un jury composé des personnes suivantes

Professeur Jeffrey W. Keillor	président-rapporteur
Professeur James D. Wuest	directeur de recherche
Professeur Gary S. Hanan	membre du jury
Professeur Eli Zysman-Colman	examinateur externe
Professeur Robert W. Cochrane	représentant du doyen de la FES

Sommaire

Les propriétés des matériaux moléculaires proviennent à la fois de la structure des composantes individuelles et de la façon dont elles s'associent. Ce dernier aspect reste difficile à contrôler, malgré de grandes avancées en science des matériaux. Pour mieux comprendre la relation structure-propriétés, nous avons entrepris une étude systématique de l'hexaphénylbenzène et de ses dérivés, qui offrent une charpente symétrique et rigide.

En premier lieu, nous avons attaché six groupements diaminotriazinyles sur l'hexaphénylbenzène afin de produire des réseaux tridimensionnels hautement poreux maintenus par des ponts hydrogène. En modifiant systématiquement le cœur moléculaire, nous avons excisé près du tiers de la molécule-mère, générant des réseaux supramoléculaires dont la porosité s'est élevée graduellement jusqu'à 75%, équivalant ainsi le record pour ce type de matériaux.

Ensuite, nous avons étudié le comportement de l'hexakis(4-nitrophényl)benzène. Dans les structures cristallines obtenues, des interactions non-covalentes entre groupements nitro démontrent leur potentiel en chimie supramoléculaire. Le cœur moléculaire ne joue qu'un rôle secondaire dans l'empilement des molécules : seules quelques interactions C-H···π impliquant le cycle aromatique central de l'hexaphénylbenzène sont évidentes.

Cette dernière observation nous a poussés à étudier le comportement à l'état cristallin de l'hexaphénylbenzène et ses dérivés. En scrutant attentivement neuf structures cristallines de ces composés, nous avons décerné la présence récurrente d'interactions C-H···π impliquant le cycle aromatique central. Cette association caractéristique a été exploitée pour créer des réseaux supramoléculaires maintenus par des interactions C-H···π sélectives entre un groupement éthynyle et le cycle aromatique central de l'hexaphénylbenzène.

Finalement, nous avons joint le côté sombre de l'ingénierie cristalline en utilisant nos connaissances dans le but d'empêcher la formation d'interactions directionnelles. En protégeant le cycle aromatique central de l'hexaphénylbenzène à l'aide de groupements alkyles, les interactions C-H···π ont été pratiquement éliminées. Ces résultats offrent la possibilité de créer de nouveaux matériaux amorphes.

Dans ces études, focalisées sur le système hexaphénylbenzène, nous avons mis en relief des phénomènes qui sont obscurcis dans d'autres familles de molécules. De plus, ce système a grandement facilité l'utilisation d'une approche méthodique pour explorer la relation structure-propriétés. Nos travaux nous ont amenés à des conclusions de valeur universelle en science des matériaux moléculaires.

Mots clés : Chimie supramoléculaire, ingénierie cristalline, cristallographie, pont hydrogène, interactions faibles, liens C–H···π, hexaphénylbenzène, (polyphényl)benzène, tectonique moléculaire, verres moléculaires.

Summary

The properties of molecular materials depend on the identity of individual components and on their organization. Unfortunately, it remains difficult to control molecular organization, despite advances in materials science. To better understand the relationship between molecular structure and collective properties, we undertook a systematic study of hexaphenylbenzene and its derivatives, which possess a rigid symmetric framework.

Our first study focused on using hydrogen bonds to control self-assembly in the solid state. By installing six diaminotriazinyl groups on a hexaphenylbenzene core, we predictably obtained highly porous three-dimensional hydrogen-bonded networks. Through systematic structural modifications of the molecular core, we excised nearly a third of the parent molecule, and the porosity of the networks gradually increased, matching the record of 75% previously obtained for this type of material.

We then turned to weaker interactions to control organization, as revealed by the packing of hexakis(4-nitrophenyl)benzene. In the crystal structures analyzed, non-covalent interactions between nitro groups were observed, demonstrating their potential in supramolecular chemistry. Careful examination of the structures showed that the hexaphenylbenzene moieties play only a secondary role in determining the overall packing; however, C-H···π interactions involving the central aromatic ring of hexaphenylbenzene were also observed.

To further document this unexpected behavior, we analyzed nine crystal structures of hexaphenylbenzene and derivatives, which showed that a C-H···π recognition pattern involving the central aromatic ring occurs consistently throughout the series. This motif was used to prepare supramolecular networks based exclusively on selective and directional C-H···π interactions involving ethynyl groups and the central aromatic ring of hexaphenylbenzene.

Finally, we joined the dark side of crystal engineering by using our knowledge of supramolecular chemistry to prevent the formation of directional interactions. By installing alkyl groups near the central aromatic ring of hexaphenylbenzene, C-H···π interactions were practically eliminated. These results were then used to devise new amorphous materials.

The hexaphenylbenzene system permitted a methodical analysis of structure-property relationships in molecular materials. This particular system exposed phenomena normally obscured in other families of molecules, and our analysis of its behavior has yielded conclusions of universal value in materials science.

Keywords : Supramolecular chemistry, crystal engineering, crystallography, hydrogen bond, weak interaction, C–H···π interaction, hexaphenylbenzene, (polyphenyl)benzene, molecular tectonics, molecular glasses.

Table des matières

Chapitre 1 : Introduction

Chapitre 2 : Historique et synthèse de l'hexaphénylbenzène et de ses dérivés

Chapitre 3 : Utilisation de l'hexaphénylbenzène dans la formation de réseaux poreux

Chapitre 4 : Étude des interactions intermoléculaires faibles dans les dérivés d'hexaphénylbenzène

Chapitre 5 : Utilisation des interactions C–H···π intermoléculaires pour contrôler l'organisation des dérivés d'hexaphénylbenzène

Liste des Tableaux

Liste des Schémas

Fin de l'article 1

Fin de l'article 4

Fin de l'article 5

Liste des Figures

Fin de l'article 2

Fin de l'article 4

Fin de l'article 5

Liste des abréviations

A	: accepteur (de pont hydrogène)
Å	: Ångström
Ac	: acétyle
ADN	: acide désoxyribonucléique
Anal.	: analyse
aq	: aqueux
Ar	: aryle
Bn	: benzyle
br	: *broad* (signal large, en RMN)
Bu	: butyle
°C	: degré Celsius
cm	: centimètre
calcd	: *calculated*
CPK	: Corey, Pauling et Koltun
δ	: déplacement chimique (en RMN)
°	: degré
Δ	: chaleur ou variation
D	: donneur (de pont hydrogène)
d	: doublet (en RMN)
D	: densité
d	: deutéré (solvant)
DAT	: 2,4-diamino-1,3,5-triazine
dba	: *dibenzylidene acetone*
dec.	: décomposition
DFT	: *density functional theory*
DMF	: *N,N*-diméthylformamide
DMSO	: diméthyl sulfoxyde
eq	: équivalent
ESI	: *electro-spray ionisation*
Et	: éthyle
Fig.	: figure
Fw	: *formula weight*
g	: gramme
GoF	: *goodness-of-fit*
h	: heure
hν	: sous irradiation
HOMO	: *highest occupied molecular orbital*
HPA	: hydrocarbure polyaromatique
HRMS	: *high-resolution mass spectrometry*
Hz	: hertz
I	: intensité (rayons-X)
*i*Pr	: isopropyle
IR	: infrarouge

J	: constante de couplage
K	: kelvin
kcal	: kilocalorie
kJ	: kilojoule
lit.	: littérature
LUMO	: *lowest unoccupied molecular orbital*
M	: molaire
μ	: coefficient d'absorption
m	: méta
m	: multiplet (en RMN)
m/e	: rapport masse/charge
Me	: méthyle
mg	: milligramme
MHz	: mégahertz
mL	: millilitre
mm	: millimètre
mM	: millimolaire
mmol	: millimole
mol	: mole
mp	: *melting point*
MS	: *mass spectrometry*
NMR	: *nuclear magnetic resonance*
o	: ortho
ORTEP	: *Oak Ridge Thermal Ellipsoid Program*
p	: para
Ph	: phényle
Pr	: propyle
PTFE	: poly(tétrafluoroéthylène)
q	: quadruplet (en RMN)
R_1	: facteur d'accord sur les réflexions observées
RMN	: résonance magnétique nucléaire
σ	: écart-type
s	: singulet (en RMN)
t	: triplet (en RMN)
T	: température
t-Bu	: *tert*-butyl
T_g	: température de transition vitreuse
TGA	: *thermogravimetric analysis*
THF	: tétrahydrofurane
TMS	: triméthylsilyl
μ	: coefficient d'absorption
μm	: micromètre
ωR_2	: facteur d'accord pondéré
w/v	: *weight per volume*
RMN	: résonance magnétique nucléaire
RT	: *room temperature*

ν	: fréquence (de vibration en infrarouge)
Z	: nombre d'unités formulaires par maille

Remerciements

Dans un premier temps, j'aimerais remercier le professeur James D. Wuest pour m'avoir accepté dans son groupe de recherche. Il m'a laissé une grande liberté dans le choix de mes projets de recherche et m'a soutenu tout au long de mes études graduées, ce dont je lui suis très reconnaissant. Je souhaite ardemment qu'il continu à transmettre son professionnalisme, son soucis du détail et sa patience aux étudiants qui joignent son groupe.

Je tiens aussi à remercier le professeur Kenneth E. Maly, mon second mentor. C'est grâce à lui que j'ai pu apprécier pleinement le travail de chimiste. Son éthique de travail exemplaire, sa bonne humeur contagieuse et son support scientifique et moral ont été des facteurs déterminants au travers de mes études graduées. J'espère que nous allons continuer à collaborer encore longtemps.

Ensuite, on ne peut passer sous silence la contribution majeure de Thierry Maris. Son expertise en cristallographie est tout simplement phénoménale et je suis toujours à la recherche de la question à laquelle il ne pourra répondre. Sa patience et son professionnalisme font de lui un modèle pour n'importe quel scientifique.

J'aimerais aussi remercier tous les membres du groupe Wuest, passés et présents, pour avoir contribué à l'ambiance au laboratoire. Plus particulièrement je remercie Pat, avec qui je continue de rire de nos infortunes et qui reste à mes yeux un modèle de persévérance. Je ne dois pas oublier Émilie, Olivier, Greg, Daniel, Janie, Dom, Mike et Demers qui ont fait de mon passage dans le groupe un moment des plus agréables.

De plus, je voudrais souligner le rôle prépondérant qu'ont joué les gens du Département de chimie. Merci aux professeurs, aux employés des laboratoires de résonance magnétique nucléaire, de cristallographie et de spectrométrie de masse, aux gens de l'atelier mécanique ainsi qu'aux employés du secrétariat.

Finalement, j'aimerais remercier ma famille et plus particulièrement Caroline et notre petite Rachel pour m'avoir fait découvrir tout un monde au-delà de la chimie.

Merci à tous.

Notes et contributions personnelles

Voici quelques notes concernant le format de cette thèse ainsi que les contributions personnelles d'Eric Gagnon aux travaux rapportés.

1. La numérotation des figures, schémas, tableaux, molécules et références de chaque article est indépendante de celle du reste de la thèse afin de rester consistant avec les documents publiés en ligne.
2. Les parties supplémentaires des articles 1 et 2, jugées non nécessaires à la compréhension immédiate du texte, sont disponibles sur internet sur les sites de l'*American Chemical Society* et de *Elsevier* respectivement.
3. Les travaux présentés dans cette thèse s'appuient fortement sur des résultats d'études cristallographiques. Afin de confirmer qu'une structure cristalline représente bien la totalité de l'échantillon, des diagrammes de diffraction de poudres ont été mesurés. Ces analyses, effectuées dans le cadre des articles 3, 4 et 5, sont disponibles dans leurs annexes respectives.
4. Tous les articles, à l'exception de l'article 1, ont été écrits par Eric Gagnon et corrigés par le professeur James D. Wuest. Le professeur Kenneth E. Maly a écrit l'article 1 et a aussi participé à la correction des articles 2, 3 et 5.

Contributions détaillées d'Eric Gagnon aux articles

Premier article

- Le travail expérimental a été effectué à parts égales par Eric Gagnon et Kenneth E. Maly.
- Les études cristallographiques ont été menées par Thierry Maris et ont été analysées par Eric Gagnon, Kenneth E. Maly et Thierry Maris.

Deuxième article

- Le travail expérimental a été fait par Eric Gagnon.
- Les études cristallographiques ont été effectuées par Eric Gagnon et Thierry Maris.

Troisième article

- Tous les composés ont été préparés et cristallisés par Eric Gagnon, à l'exception de deux composés préparés et cristallisés par Pierre-Marc Arseneault et Kenneth E. Maly.
- Les études cristallographiques ont été faites par Eric Gagnon, aidé par Thierry Maris.
- Thierry Maris a mesuré les diagrammes de poudre cristalline.

Quatrième article

- La synthèse et les analyses cristallographiques de tous les composés ont été faites par Eric Gagnon.
- Les mesures de diffraction de poudre ont été effectuées par Valérie Métivaud.
- Les calculs théoriques ont été effectués par le professeur Alain Rochefort de l'École polytechnique.

Cinquième article

- La synthèse et la caractérisation de tous les composés ont été effectuées par Eric Gagnon à l'exception d'un composé, préparé par Shira Halperin sous la direction du professeur Kenneth E. Maly (Université Wilfrid-Laurier).
- Les études cristallographiques ont été faites par Eric Gagnon, à l'exception des diagrammes de diffraction de poudre qui ont été mesurés par Valérie Métivaud.

Chapitre 1

Introduction

1.1 De la Nature à la chimie supramoléculaire

La Nature fait bien les choses. Ces quelques mots résument l'essence même de ce que beaucoup de scientifiques s'efforcent de faire : comprendre le fonctionnement des systèmes les plus perfectionnés qui soient. Les systèmes de la Nature, si bien rodés dans toutes leurs facettes, sont une source d'inspiration inépuisable. Les capacités de la science moderne, malgré un torrent de percées, demeurent encore limitées par rapport à ce qu'elles peuvent devenir. Une citation souvent répétée, provenant d'un discours des plus visionnaires donné par Richard P. Feynman près de 50 ans auparavant, résume ce que l'Homme tente de faire :

> *What would the properties of materials be if we could really arrange the atoms the way we want them? They would be very interesting to investigate theoretically. I can't see exactly what would happen, but I can hardly doubt that when we have some control of the arrangement of things on a small scale we will get an enormously greater range of possible properties that substances can have, and of different things that we can do.*
>
> Richard P. Feynman,
> Tiré de: There's plenty of room at the bottom, 29 décembre 1959

Si le discours de Feynman avait été donné au début de la création de l'Univers, nous aurions pu postuler que la Nature elle-même était dans l'audience. En effet, ses prouesses dans l'utilisation de structures précises afin d'obtenir des propriétés voulues sont époustouflantes.

Par exemple, les protéines sont construites majoritairement à base d'acides α-aminés reliés les uns aux autres par des liens peptidiques. Seulement une vingtaine d'acides α-aminés sont utilisés pour construire les chaînes peptidiques, c'est-à-dire la structure primaire. Par la suite, l'élaboration d'un réseau de ponts hydrogène entre différentes sections de la chaîne d'acides α-aminés mène à la formation de structures

secondaires telles que les hélices-α et les feuillets-β. La structure tertiaire décrit la conformation finale de la protéine dans l'espace, encore une fois due à des interactions non-covalentes entre différentes sections de la protéine. La liste des interactions impliquées dans le repliement des protéines s'allongent de plus en plus : on parle entre autre de ponts hydrogène, d'interactions hydrophobiques, d'interactions dipôle-dipôle, d'empilement-π et de liens C-H···π. Finalement, on retrouve aussi des protéines formant des structures quaternaires, c'est-à-dire qui assemblent plus d'une chaîne peptidique par des interactions intermoléculaires. Un exemple bien connu est l'hémoglobine, qui combine quatre chaînes peptidiques (Figure 1.1).

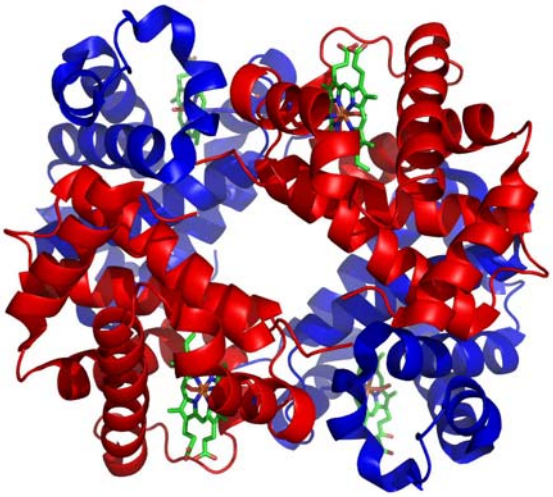

Figure 1.1. Structure quaternaire d'une molécule d'hémoglobine liée à 4 molécules d'oxygène. On observe quatre sous-unités protéiques, deux représentées en bleu et deux en rouge.[1]

Ainsi, à partir d'une banque limitée d'acides α-aminés, la Nature arrive à générer une structure tridimensionnelle élaborée avec une fonction précise (transporter des molécules d'oxygène dans le cas d'hémoglobine). Avec les mêmes acides aminés naturels, la Nature peut créer une multitude de protéines avec une vaste gamme de fonctions différentes, telles que la catalyse (anhydrase carbonique) ou le stockage (ferritine).

[1] Paoli, M.; Liddington, R.; Tame, J.; Wilkinson, A.; Dodson, G. *J. Mol. Biol.* **1996**, *256*, 775-792.

L'étude des protéines et des autres systèmes du vivant suggère fortement que la structure tridimensionnelle a une importance capitale quant à la fonction. Ainsi, la première étape pour arriver à répliquer et éventuellement améliorer la fonction réside dans le contrôle de la structure. Pour y arriver, les chimistes ont développé une discipline nommée chimie supramoléculaire, qui s'intéresse particulièrement aux interactions non-covalentes qui sont à l'origine des structures complexes observées jusqu'à maintenant.

1.2 De la chimie à la chimie supramoléculaire

La Nature a toujours été une source inépuisable d'inspiration pour le chimiste. On n'a qu'à penser à toutes les réactions mises au point dans l'objectif de reproduire la structure de produits naturels. Par ailleurs, les approches synthétiques elles-mêmes sont quelques fois calquées sur la biosynthèse des produits naturels.[2] La chimie de synthèse procède donc à des séries de réactions dont le but ultime est de créer la connectivité atomique désirée. Le réseau de liens covalents obtenu, le produit, est donc une molécule.

Par opposition, la chimie supramoléculaire, qualifiée de « chimie par-delà la molécule »,[3] couvre le domaine des interactions non-covalentes. Ses unités constitutionnelles sont des molécules et ses produits sont des assemblages supramoléculaires. Il s'ensuit que, pour contrôler l'assemblage d'une molécule à l'état cristalline, on doit connaître et exploiter les interactions intermoléculaires de la même façon qu'un chimiste de synthèse doit contrôler la formation de liens covalents afin d'obtenir le produit désiré. Les liens utilisés en chimie supramoléculaire ont toutefois des propriétés très différentes de celles de la chimie moléculaire, comme on peut le constater au Tableau 1.1.

---

2 (a) Nicolaou, K. C.; Sorensen, E. J. *Classics in Total Synthesis: Targets, Strategies, Methods*, Wiley-VCH, Weinheim, 1996. (b) Nicolaou, K. C.; Snyder, S. A. *Classics in Total Synthesis: More Targets, Strategies, Methods*, Wiley-VCH, Weinheim, 2003.

3 Lehn, J.-M. *Angew. Chem. Int. Ed. Engl.* **1988**, *27*, 89-112.

Tableau 1.1. Analogie entre la chimie moléculaire traditionnelle et la chimie supramoléculaire.

	Chimie moléculaire	Chimie supramoléculaire
Unités	Atomes	Molécules
Interactions	Liens (simples) covalents [~ 200 - 400 kJ mol^{-1}]	Interactions intermoléculaires [~ 1 - 150 kJ mol^{-1}]
Produits	Molécules	Assemblages supramoléculaires

La chimie supramoléculaire tient ses origines des travaux de Charles J. Pedersen. Son impressionnant article rapportant la découverte des éthers-couronnes (**1.1**, Figure 1.2)[4] a attiré rapidement l'attention de Pr. Jean-Marie Lehn et de Pr. Donald J. Cram; ceux-ci ont entrepris respectivement des travaux qui ont mené à la découverte des cryptands[5] et des sphérands[6] (**1.2** et **1.3**, Figure 1.2). Ces trois molécules forment des complexes avec des cations métalliques qui sont maintenus par des interactions de type cation-dipôle. Les travaux menés par Pedersen, Cram et Lehn n'ont pas passé inaperçus, leurs carrières atteignant un point culminant en 1987 lorsqu'ils ont reçu le prix Nobel de chimie.

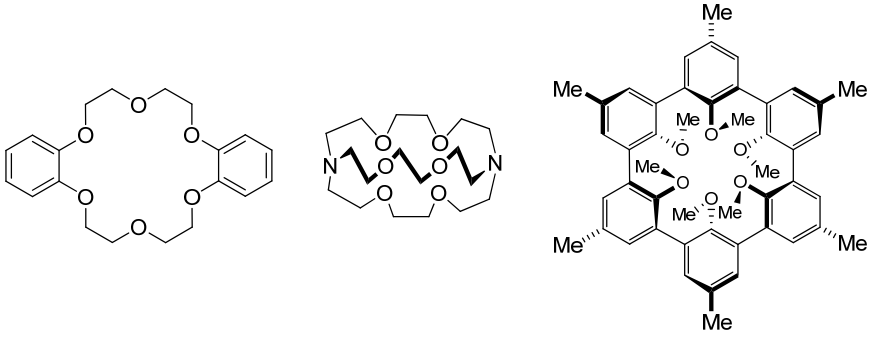

Figure 1.2. Structures représentatives des trois classes de molécules créées par Pedersen, Cram et Lehn.

[4] Pedersen, C. J. *J. Am. Chem. Soc.* **1967**, *89*, 7017-7036.
[5] Lehn, J.-M. *Angew. Chem. Int. Ed. Engl.* **1988**, *27*, 89-112.
[6] Cram, D. J. *Angew. Chem. Int. Ed. Engl.* **1988**, *27*, 1009-1020.

La puissance de cette chimie vient en partie du délicat équilibre des forces en jeu. Les interactions non-covalentes, telles que les ponts hydrogène, l'empilement-π, les interactions dipôle-dipôle ou encore certains liens de coordination ont toutes la possibilité d'être réversibles, contrairement à la majorité des liens covalents. Le pont hydrogène, par exemple, est sensible à la température, au médium dans lequel il a lieu et à la concentration des espèces interagissant ensemble.[7] En modifiant ces variables, il est alors possible de contrôler le degré d'association de deux molécules liées par des ponts hydrogène.

De plus, les interactions non-covalentes bénéficient de l'effet du nombre. Ainsi, les liaisons par ponts hydrogène peuvent être cumulées afin d'obtenir un système supramoléculaire stable. Cette coopérativité permet à l'ADN de conserver sa structure à double brins dans les conditions ambiantes ou encore aux fibres de Kevlar de posséder d'excellentes propriétés mécaniques dues aux interactions entre les chaînes polymériques (Figure 1.3).[8,9]

En ayant comme thème commun ces interactions non-covalentes, plusieurs sous-disciplines de la chimie supramoléculaire ont vu le jour.[10] On retrouve maintenant des récepteurs pour des cations, des anions et des molécules neutres, des polymères supramoléculaires maintenus par des ponts hydrogène ou des liens de coordinations, des cages moléculaires, des rotaxanes et des nœuds moléculaires. Cette liste non-exhaustive souligne l'étendue des systèmes supramoléculaires qu'il est possible de créer en utilisant les interactions non-covalentes.

---

7 Jeffrey, G.A. *An Introduction to Hydrogen Bonding*, Oxford University Press, New York, 1997.
8 Northolt, M. G. *Eur. Polym. J.* **1974**, *10*, 799-804.
9 Tashiro, K.; Kobayashi, M.; Tadokoro, H. *Macromolecules* **1977**, *10*, 413-420.
10 Steed, J. W.; Atwood, J. L. *Supramolecular Chemistry*, John Wiley & Sons, Ltd, Chichester, 2000.

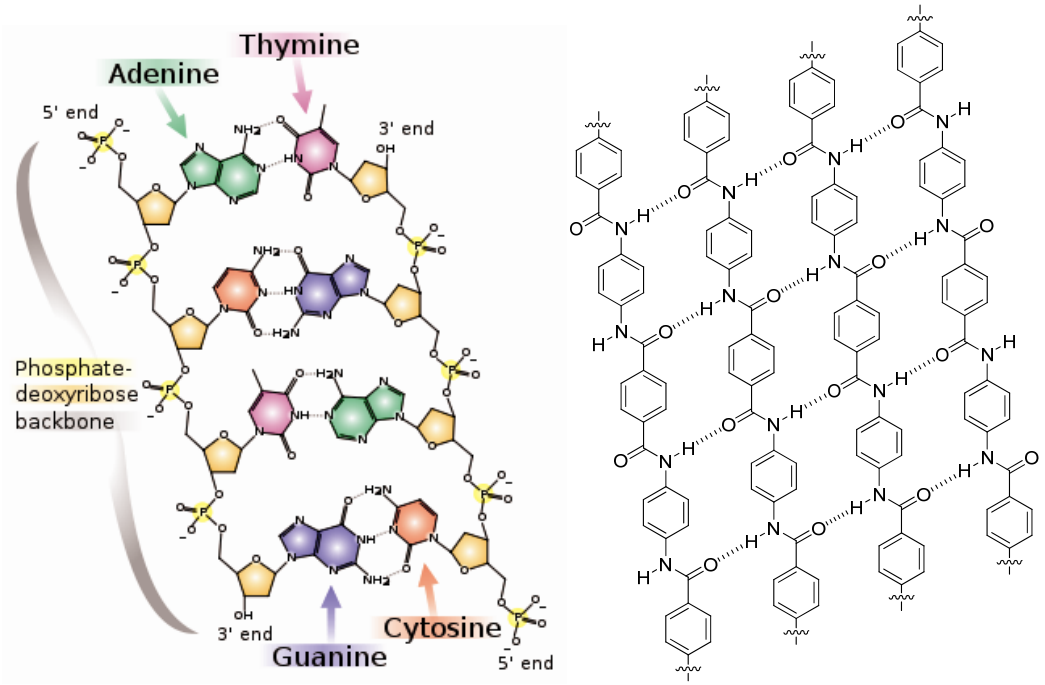

Figure 1.3. Additivité des ponts hydrogène dans l'ADN (gauche)[11] et le Kevlar (droite). Les ponts hydrogène sont indiqués par des lignes pointillées.

Par contre, le titre de « supermolécule par excellence » revient aux cristaux.[12] Le phénomène d'agrégation qu'est la cristallisation implique l'assemblage autonome et spontané de millions de molécules via la formation d'interactions non-covalentes. L'étude de ces structures périodiques a défini une autre sous-discipline de la chimie supramoléculaire : l'ingénierie cristalline.

1.3 L'ingénierie cristalline

L'origine de cette discipline remonte aux travaux de Schmidt sur la photodimérisation de dérivés de l'acide cinnamique à l'état solide.[13] En fonction de la substitution de l'acide cinnamique (**1.4**), deux classes de structures photoréactives peuvent être obtenues. Dans les polymorphes α (**1.5**) et β (**1.7**), les liaisons doubles sont suffisamment près l'une de l'autre pour qu'une photodimérisation [2+2] ait lieu.

[11] http://en.wikipedia.org/wiki/File:DNA_chemical_structure.svg
[12] Dunitz, J. D. *Pure Appl. Chem.* **1991**, *63*, 177-185.
[13] (a) Cohen, M. D.; Schmidt, G. M. J.; Sonntag, F. I. *J. Chem. Soc.* **1964**, 2000-2013. (b) Schmidt, G. M. J. *Pure Appl. Chem.* **1971**, *27*, 647-678.

Toutefois, la différence se situe au niveau de la symétrie au niveau cristallin : dans la structure de type α, les liaisons doubles réactives sont reliées par un centre d'inversion, tandis que dans la structure de type β, elles sont reliées par un plan miroir. Cette symétrie à l'échelle cristalline se répercute en symétrie moléculaire une fois la réaction de photodimérisation effectuée (Schéma 1.1). Toutefois, il existe aussi des dérivés d'acide cinnamique qui cristallisent dans des structures de type γ.[14] Celles-ci sont caractérisées par une distance trop élevée entre les alcènes, ce qui confère une photostabilité à ces composés. Ce premier exemple montre bien l'impact que l'empilement tridimensionnel des molécules peut avoir sur les propriétés du solide. Il s'avère toutefois très difficile de contrôler le positionnement même approximatif des molécules l'une par rapport à l'autre et un mélange de persévérance et de chance est souvent nécessaire pour y arriver.

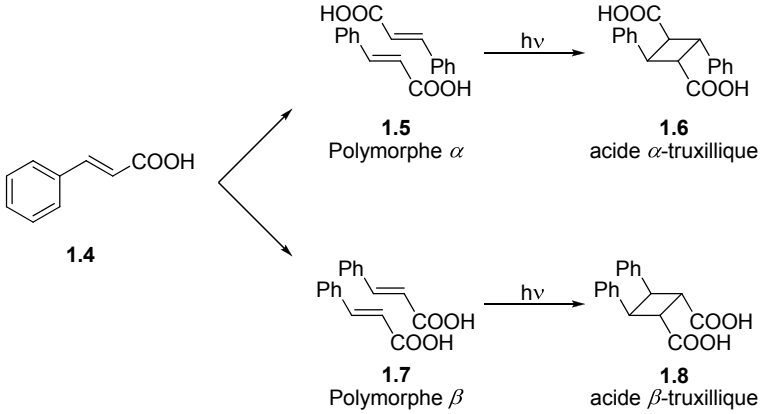

Schéma 1.1. Premier exemple d'ingénierie cristalline. L'acide *trans*-cinnamique cristallise en deux formes polymorphiques qui génèrent les isomères α et β de l'acide truxillique une fois les cristaux irradiés.

Prévoir la façon dont les molécules s'associent à l'état cristallin constitue donc un des plus grands défis contemporains. Il est encore triste de constater qu'il est impossible de déduire la structure tridimensionnelle d'un tel assemblage à partir de la structure de la molécule étudiée, aussi simple soit-elle. Ce constat a été fait en 1988 par John Maddox dans la revue *Nature*[15] et malheureusement, il a été réitéré à quelques

[14] Cohen, M. D.; Schmidt, G. M. J.; Sonntag, F. I. *J. Chem. Soc.* **1964**, 2000-2013.
[15] Maddox, J. *Nature* **1988**, *335*, 201.

reprises depuis.[16] L'origine de l'incapacité d'effectuer ce genre de prédiction a été résumé par Hosseini :

> *It is worth noting that because of our limited knowledge of all intermolecular interactions governing the formation of the crystalline phases, the complete understanding of the packing of molecular entities is currently impossible.*[17]

L'ingénierie cristalline est une discipline totalement dédiée à l'étude du phénomène de la cristallisation et de ses impacts. Elle a été définie comme étant « la compréhension des interactions intermoléculaires dans les cristaux et l'utilisation de ces connaissances pour créer de nouveaux solides avec des propriétés physiques et chimiques souhaitées. »[18] On reconnait alors que le but ultime est d'obtenir des propriétés en contrôlant l'assemblage de molécules afin d'obtenir des structures cristallines précises et de façon prévisible.[19]

Au fil du temps, plusieurs outils ont été développés pour rationnaliser la structure tridimensionnelle des cristaux moléculaires. La formation des solides cristallins a d'abord été décrite grossièrement comme étant l'emboîtement optimal des surfaces convexes et concaves de molécules adjacentes. Kitaigorodskii a remarqué que les molécules sont positionnées de cette façon afin d'éliminer les espaces vacants, c'est-à-dire que l'empilement compact (*close packing*) est favorisé.[20] Ces espaces vacants ne peuvent être totalement comblés à cause de la forme irrégulière des molécules; on observe typiquement environ 30% de vide interstitiel dans les cristaux moléculaires tel qu'évalué par le *Kitaigorodskii packing index*.[20,21]

---

16 (a) Gavezzotti, A. *Acc. Chem. Res.* **1994**, *27*, 309-314. (b) Dunitz, J. D. *Chem. Commun.* **2003**, 545-548.
17 Hosseini, M. W. *CrystEngComm* **2004**, *6*, 318-322.
18 Desiraju, G. R. *Crystal Engineering : The Design of Organic Solids*, Elsevier, Amsterdam, 1989.
19 Braga, D.; Brammer, L.; Champness, N. R. *CrystEngComm* **2005**, *7*, 1-19.
20 Kitaigorodskii, A. I. *Organic Chemical Crystallography*,Consultants Bureau, New York, 1961.
21 (a) Spek, A. L. *PLATON, A Multipurpose Crystallographic Tool,* Utrecht University, Utrecht, 2001. (b) van der Sluis, P.; Spek, A. L. *Acta Crystallogr.* **1990**, *A46*, 194-201.

On retrouve aussi les règles d'Etter,[22] s'appliquant aux interactions par ponts hydrogène. Ces règles proposent une hiérarchie quant à la formation de ces liens non-covalents, la plus importante étant que le meilleur donneur s'associe préférablement avec le meilleur accepteur. Plus récemment, Desiraju a proposé l'utilisation des synthons supramoléculaires,[23] qui se veulent être un recueil d'interactions intermoléculaires favorisées, tel qu'observé statistiquement.[24] En effet, la *Cambridge Structural Database* regroupe plus de 469 000 structures cristallographiques de composés organiques et organo-métalliques,[25] permettant de déterminer la fréquence et la géométrie de contacts intermoléculaires. Ce condensé d'informations structurelles permet de savoir si deux groupements fonctionnels ont une tendance ou non à s'associer à l'état solide.

Tous ces outils font en sorte que l'ingénierie cristalline poursuit son essor de façon inlassable, tout en créant de nouveaux concepts. Éventuellement, il a été reconnu qu'un choix judicieux de groupes fonctionnels permet d'obtenir avec une bonne sélectivité l'empilement désiré : c'est le concept de la tectonique moléculaire.

1.4 La tectonique moléculaire

Initialement introduite par Wuest en 1991,[26] la tectonique moléculaire est une discipline liée à l'ingénierie cristalline qui vise à exploiter les interactions intermoléculaires fortes pour diriger l'assemblage de molécules de façon périodique. Cette stratégie se fonde sur le concept du *tecton*, une molécule capable d'orienter dans l'espace des groupements fonctionnels pouvant participer dans des interactions intermoléculaires qui sont suffisamment fortes et directionnelles pour guider la topologie du cristal résultant. Un tecton est donc une combinaison judicieuse de

---

22 *Etter, M. C. Acc. Chem. Res.* **1990**, *23*, 120-126.
23 Desiraju, G. R. *Angew. Chem. Int. Ed. Engl.* **1995**, *34*, 2311-2327.
24 Allen, F. H.; Motherwell, W. D. S.; Raithby, P. R.; Shields, G. P.; Taylor, R. *New J. Chem.* **1999**, *23*, 25-34.
25 En date du 1er janvier 2009, tiré du site de Cambridge Crystallographic Data Centre, http://www.ccdc.cam.ac.uk/
26 Simard, M.; Su, D.; Wuest, J. D. *J. Am. Chem. Soc.* **1991**, *113*, 3696-3698.

groupements de reconnaissance fiables et de cœurs moléculaires qui orientent les sites de reconnaissance de manière prévisible. Un exemple devenu classique qui illustre bien le concept du tecton est celui de l'acide adamantane-1,3,5,7-tétracarboxylique rapporté par Ermer (**1.9**, Schéma 1.2).[27] Dans ce composé, le squelette rigide tricyclique ordonne le positionnement des groupements carboxyles, qui interagissent par la formation de ponts hydrogène caractéristiques pour générer une structure tridimensionnelle ayant une architecture prédéterminée.

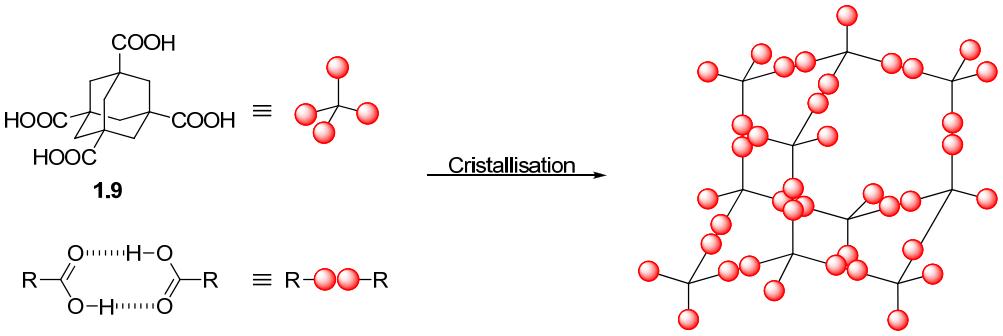

Schéma 1.2. Formation de réseaux tridimensionnels par l'acide adamantane-1,3,5,7-tétracarboxylique. Les sphères rouges représentent les acides carboxyliques qui agissent comme groupements de reconnaissance. Leur association en dimères, conjugué à la géométrie tétragonale de l'adamantane, force le réseau supramoléculaire à définir une structure diamantoïde.

Un cristal est un arrangement périodique tridimensionnel obtenu par la translation d'une maille cristalline. Il s'ensuit qu'en gouvernant l'assemblage d'une molécule avec ses voisins immédiats, on contrôle aussi l'assemblage de molécules à l'échelle macroscopique. De cette façon, il est possible de contrôler la topologie d'un cristal à partir de la structure d'une molécule. Dans le cas de l'acide adamantane-1,3,5,7-tétracarboxylique, on observe alors la formation de réseau diamantoïde, soit une réplique à plus grande échelle de la structure de l'adamantane (Schéma 1.2).

Toutefois, la tectonique moléculaire n'est pas limitée à l'utilisation de ponts hydrogène. Pour diriger l'assemblage supramoléculaire, il suffit d'utiliser des interactions qui sont suffisamment fortes pour dominer celles de l'ensemble de la structure. Il est donc nécessaire de déterminer quelles interactions remplissent ce critère.

---

[27] Ermer, O. *J. Am. Chem. Soc.* **1988**, *110*, 3747-3754.

Un coup d'œil à la Figure 1.4 nous permet de constater qu'il existe une multitude d'interactions pouvant remplir ce critère.

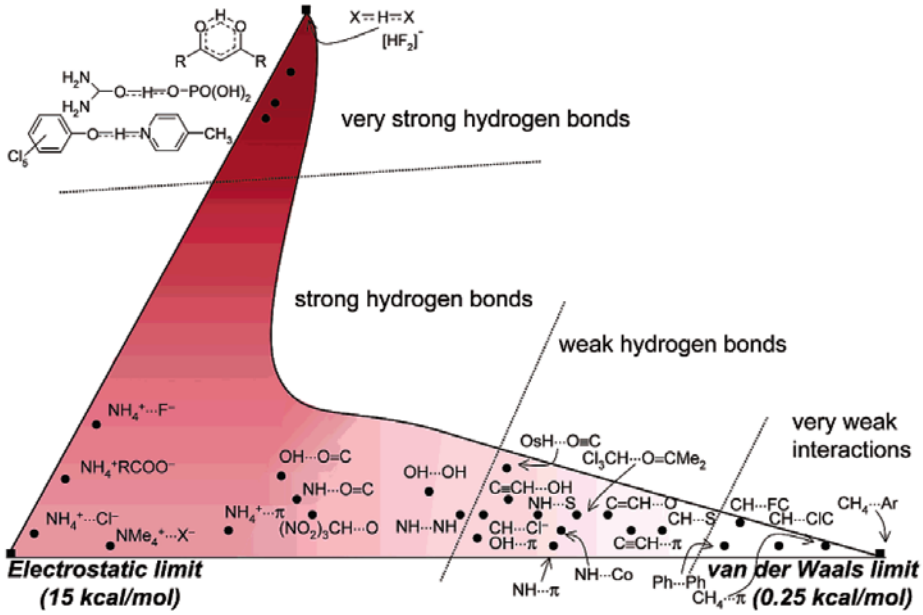

Figure 1.4. Comparaison des forces de liaisons différentes générées par des interactions non-covalentes. Tiré de la référence 28.

La clé réside dans l'introduction d'une interaction dominante par rapport aux autres. Ceci est accompli facilement dans le cas de cages moléculaires métalliques ou des réseaux de coordination qui exploitent la force des liens métal-ligand, ou encore dans les réseaux maintenus par des ponts hydrogène. Toutefois, la tâche devient plus délicate si on désire diriger un assemblage à l'état cristallin avec des interactions plus faibles.

1.5 Objectif de la thèse

Tel que nous l'avons établi, les propriétés des matériaux moléculaires proviennent de l'identité des composantes et de la nature de leurs assemblages. Toutefois, le contrôle des interactions non-covalentes reste ardu et les assemblages obtenus reflètent trop souvent une inaptitude à prévoir et exploiter les phénomènes de reconnaissance moléculaire. Notre contribution au domaine de la chimie

[28] Desiraju, G. R. *Acc. Chem. Res.* **2002**, *35*, 565-573.

supramoléculaire se retrouve à ce niveau : documenter, analyser, développer et possiblement maîtriser ne serait-ce qu'une partie du phénomène de l'assemblage à l'état cristallin.

Pour y arriver, nous avons choisi d'utiliser la molécule d'hexaphénylbenzène comme unité centrale. Puisque cette molécule est le point focal de cette thèse, sa chimie est présentée selon un aspect historique. Le chapitre 2 couvre ses principales voies de synthèse et de substitution qui seront utilisées lors des chapitres subséquents. Par la suite, nous présentons nos résultats en tectonique moléculaire basée sur l'utilisation de ponts hydrogène. La symétrie élevée et la rigidité de l'hexaphénylbenzène nous ont permis d'obtenir des réseaux poreux, analogues aux zéolites. Le chapitre 3 rapporte nos efforts vers la formation de réseaux supramoléculaires perméables aux molécules invitées et possédant une solidité accrue comparativement aux systèmes étudiés précédemment. Le chapitre suivant tient compte de la faible tendance de l'hexaphénylbenzène à participer dans des interactions impliquant la surface π de ses groupements aromatiques, contrairement aux unités centrales telles que le tétraphénylméthane, le spirobifluorène, le tétraphényl éther du pentaerythritol ou la triarylamine. La conformation particulière de l'hexaphénylbenzène diminue de beaucoup les risques que ces interactions entrent en compétition avec celles issues de ses substituants. Nous avons donc étudié l'assemblage par interactions faibles des hexaphénylbenzènes substitués par des groupements nitro. Tel qu'escompté, l'élimination de la contribution importante du squelette hydrocarboné nous a permis de mettre à jour la reconnaissance particulière de ce groupement fonctionnel. Le chapitre 5 explore l'empilement à l'état solide de l'hexaphénylbenzène et de ses dérivés. Bien que nous ayons assumé une reconnaissance amoindrie de ce squelette hydrocarboné, une étude minutieuse de la structure déjà connue de l'hexaphénylbenzène a mis à jour certains détails structurels mettant en jeu les interactions de type C–H···π. Dans un premier temps, nous avons documenté ce comportement en cristallisant une série de benzènes substitués par plusieurs groupements phényles, puis nous avons tenté d'exploiter ce comportement afin de former de nouveaux assemblages supramoléculaires. Le chapitre 6 exploite les connaissances acquises au fil des chapitres

précédents. À l'opposé du chapitre 5, nous avons tenté d'empêcher l'hexaphénylbenzène d'établir des interactions non-covalentes directionnelles. Ces travaux s'inscrivent dans l'optique de mieux comprendre la formation de matériaux amorphes, totalement désordonnés.

Finalement, nous présentons un retour sur les multiples propriétés attribuées à l'hexaphénylbenzène et ses dérivés. Grâce à leurs structures bien définies ainsi que leurs caractéristiques citées ci-haut, ces molécules nous ont permis d'étudier une série de phénomènes d'association exploitant les interactions non-covalentes. Toutefois, la portée des conclusions tirées de l'ensemble de nos travaux est loin d'être limitée à l'utilisation de l'hexaphénylbenzène et ses dérivés; nous terminerons donc sur la démonstration de l'applicabilité générale de nos résultats, concluant ainsi cette thèse.

Chapitre 2

Historique et synthèse de l'hexaphénylbenzène et de ses dérivés

2.1 Introduction

Notre quête des matériaux moléculaires ordonnés nous a dirigés vers l'utilisation de la molécule d'hexaphénylbenzène (**2.3**) comme unité centrale. Puisqu'il s'agit d'un thème commun à l'ensemble de cette thèse, il est important de décrire les voies de synthèse principales de l'hexaphénylbenzène. D'abord, la section 2.2 place le développement de ces approches dans un contexte historique. Par la suite, la section 2.3 couvre brièvement les façons de substituer ou de modifier cette molécule. Finalement, la section 2.4 détaille nos choix d'approches synthétiques lors de nos travaux.

2.2.1 Synthèse par les réactions de Hart et de Suzuki

En 1930, Durand a rapporté la première synthèse de l'hexaphénylbenzène (**2.3)**.[1] Celle-ci consiste en le traitement de l'hexabromobenzène (**2.1**) ou de l'hexaiodobenzène (**2.2**) par le bromure de phénylmagnésium (Schéma 2.1). Quatre ans plus tard, Dilthey a démontré, par comparaison avec un échantillon pur obtenu par une voie synthétique indépendante, que le produit de la réaction de Durand était plutôt le 1,2,4,5-tétraphénylbenzène (**2.5**).[2] Il a été postulé que la réaction procède par l'intermédiaire di-magnésien **2.4** qui, une fois hydrolysé, donne le 1,2,4,5-tétraphénylbenzène (**2.5**). En effet, lorsque traité avec du dioxyde de carbone, le réactif de Grignard **2.4** réagit pour générer le diacide carboxylique **2.6** correspondant (Schéma 2.1).[3]

1 Durand, J. F.; Hsun, L.-W. *Compt. Rend.* **1930**, *191*, 1460-1463.
2 Dilthey, W.; Hurtig, G. *Chem. Ber.* **1934**, *67B*, 2004-2007.
3 Geissman, T. A.; Mallatt, R. C. *J. Am. Chem. Soc.* **1939**, *61*, 1788-1790.

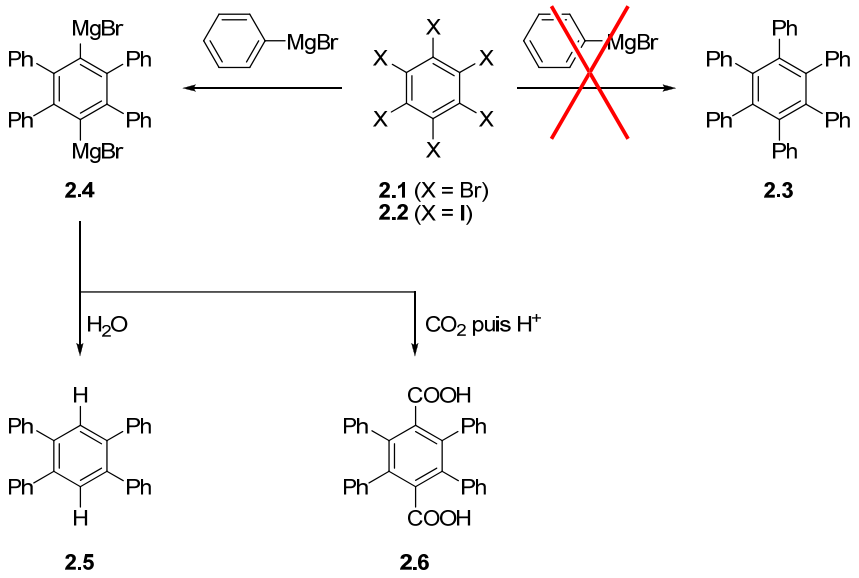

Schéma 2.1. Première tentative de synthèse de l'hexaphénylbenzène par la réaction entre des benzènes hexahalogénés et un réactif de Grignard.

En 1969, une étude a démontré que le traitement de l'hexabromobenzène par du bromure de phénylmagnésium forme du tétrabromobenzyne (**2.8**). Celui-ci a pu être piégé *in situ* par des diènes tels que le benzène ou encore le furane pour donner les adduits correspondants **2.9** et **2.10** (Schéma 2.2).[4]

En traitant le 1,2,4,5-tétrabromo-3,6-dichlorobenzène (**2.11**) avec un large excès de réactif de Grignard, Hart a préparé plus d'une dizaine de benzènes substitués par des groupements aryles aux positions 1,2,4,5 dans des rendements allant de 50 à 73%.[5] De plus, en s'appuyant sur les travaux de Berry et Wakefield,[4] il a proposé un mécanisme expliquant la formation sélective des benzènes substitués aux positions 1,2,4,5. Sa contribution la plus importante en vue de la synthèse de l'hexaphénylbenzène a cependant été l'halogénation des réactifs de Grignard intermédiaires. En effet, le traitement d'intermédiaires magnésiens (**2.12** ou **2.14**) avec du brome[5] ou de l'iode[6] lui a permis d'isoler les composés halogénés correspondants (**2.13** et **2.15**, Schéma 2.3).

4 Berry, D. J.; Wakefield, B. J. *J. Chem. Soc. (C)* **1969**, 2342-2346.
5 Harada, K.; Hart, H.; Du, C.-J. F. *J. Org. Chem.* **1985**, *50*, 5524-5528.
6 Du, C.-J. F.; Hart, H.; Ng, K.-K. D. *J. Org. Chem.* **1986**, *51*, 3162-3165.

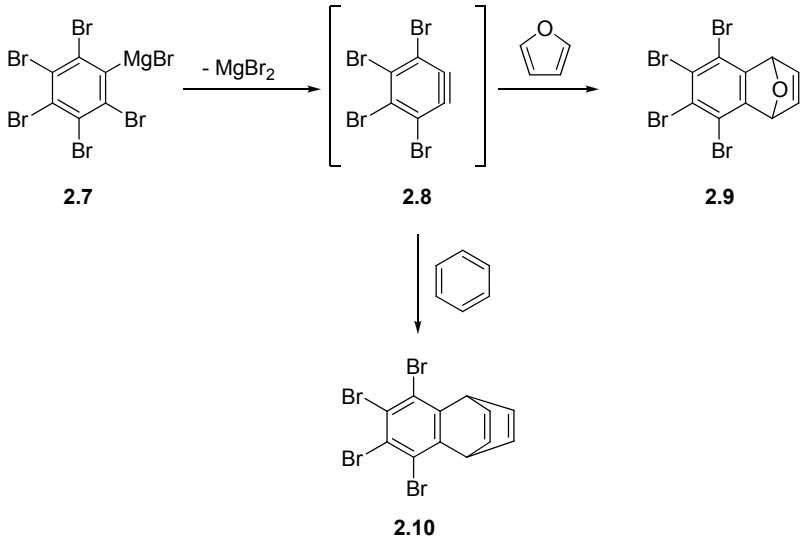

Schéma 2.2. Formation du tétrabromobenzyne à partir du bromure de pentabromophénylmagnésium. L'intermédiaire réactif est piégé par une réaction de Diels-Alder avec le furane ou le benzène.

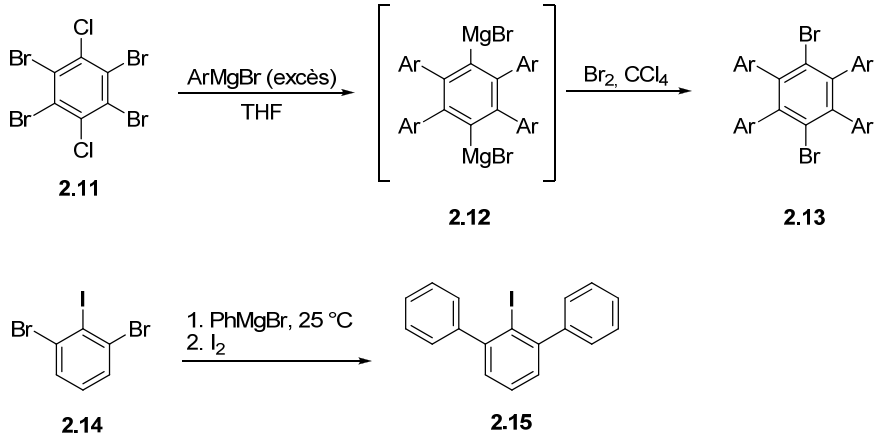

Schéma 2.3. Réactions de Hart et parachèvement avec du brome ou de l'iode.

Récemment, le groupe de Müllen a rapporté une synthèse de l'hexaphénylbenzène par un couplage catalysé au palladium.[7] En parachevant l'intermédiaire di-magnésien avec de l'iode, ils ont réussi à obtenir en une étape le 1,4-diiodo-2,3,5,6-tétraphénylbenzène (**2.16**) dans 40% de rendement (Schéma 2.4). Ce composé a pu être réagi avec l'acide phénylboronique en présence d'un catalyseur de palladium pour générer l'hexaphénylbenzène (**2.17**, Ar^1 = Ph).

[7] Yang, X.; Dou, X.; Müllen, K. *Chem. Asian. J.* **2008**, *3*, 759-766.

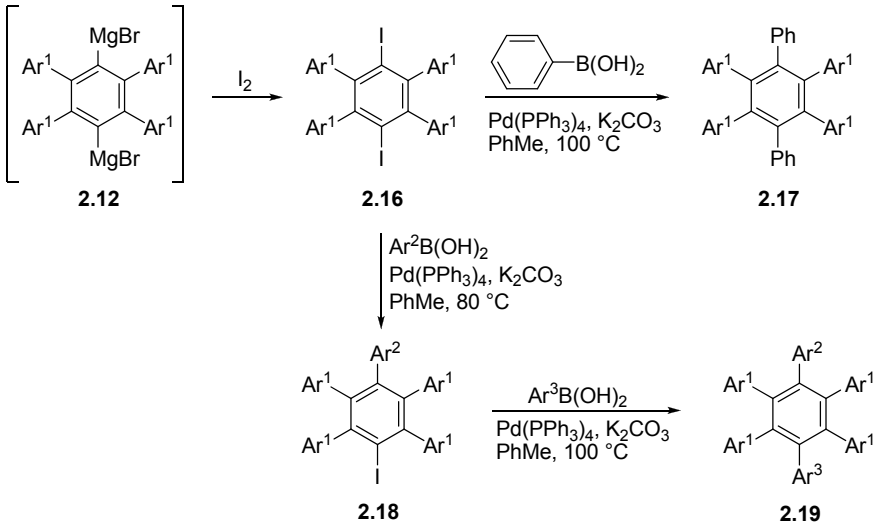

Schéma 2.4. Réaction de Hart appliquée à la synthèse de l'hexaphénylbenzène. Le patron de substitution peut être modifié par l'utilisation d'une ou de deux réactions de Suzuki séquentielles.

Cette approche comporte toutefois une sérieuse limitation : l'intermédiaire iodé **2.16** possède nécessairement quatre groupements aryles identiques aux positions 1,2,4,5. Par contre, les deux dernières positions peuvent être substituées en même temps ou de façon séquentielle. Cette possibilité amène donc un minimum de flexibilité quant à la répartition des substituants autour du benzène central (Schéma 2.4).

2.2.2 Synthèse par la cyclotrimérisation d'alcynes

En 1886, la synthèse du benzène par la cyclotrimérisation de l'acétylène a été rapportée.[8] Cette réaction très peu efficace doit être menée à des températures supérieures à 400 °C et produit une grande variété de sous-produits.[9] En 1948, la cyclotrimérisation de l'acétylène catalysée par un complexe de nickel a été rapportée.[10] Les conditions réactionnelles utilisées sont plus douces ($Ni(PPh_3)_2(CO)_2$, 60-80 °C, 15 atmosphères) et les rendements nettement supérieurs que ceux obtenus par cyclotrimérisation thermique. Onze ans plus tard, l'hexaphénylbenzène (**2.3**) a été

[8] Bertholet, M. C. R. *Held. Seances. Acad. Sci.* **1866**, 905.
[9] Badger, G. M.; Lewis, G. E.; Napier, I. M. *J. Chem. Soc.* **1960**, 2825-2827.
[10] Reppe, W.; Sweckendiek, W. J. *Liebigs Ann. Chem.* **1948**, *560*, 93-104.

obtenu en traitant le diphénylacétylène (**2.20**) avec un mélange de tris(isobutyl)aluminium et de tétrachlorure de titane (Schéma 2.5).[11]

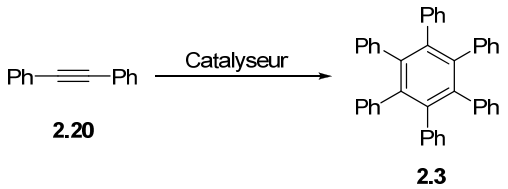

2.20 **2.3**

Schéma 2.5. Préparation de l'hexaphénylbenzène par cyclotrimérisation du diphénylacétylène.

Depuis, plusieurs autres systèmes catalytiques ont été développés pour effectuer la conversion du diphénylacétylène en hexaphénylbenzène. Dans les dix dernières années seulement, on retrouve dans la littérature des catalyseurs à base de titane,[12] de fer,[13] de cobalt,[14] de nickel,[15] de zirconium,[16] de molybdène,[17] de rhodium,[18] de palladium,[19] de platine[20] et d'osmium/antimoine[21] pouvant effectuer cette transformation. Toutefois, seuls les catalyseurs à base de cobalt sont employés couramment à cette fin.[22]

---

[11] Franzus, B.; Canterino, P. J.; Wickliffe, R. A. *J. Am. Chem. Soc.* **1959**, *81*, 1514.

[12] (a) Eisch, J. J.; Gitua, J. N.; Otieno, P. O.; Shi, X. *J. Organomet. Chem.* **2001**, *624*, 229-238. (b) Morohashi, N.; Yokomakura, K.; Hattori, T.; Miyano, S. *Tetrahedron Lett.* **2006**, *47*, 1157-1161. (c) Eisch, J. J.; Gitua, J. N.; Otieno, P. O.; Shi, X. *J. Organomet. Chem.* **2001**, *624*, 229-238.

[13] Breschi, C.; Piparo, L.; Pertici, P.; Caporusso, A. M.; Vitulli, G. *J. Organomet. Chem.* **2000**, *607*, 57-63.

[14] (a) Yong, L.; Butenschön, H. *Chem. Commun.* **2002**, 2852-2853. (b) Hilt, G.; Vogler, T.; Hess, W.; Galbiati, F. *Chem. Commun.* **2005**, 1474-1475. (c) Shukla, R.; Lindeman, S. V.; Rathore, R. *J. Am. Chem. Soc.* **2006**, *128*, 5328-5329. (d) Shukla, R.; Lindeman, S. V.; Rathore, R. *Chem. Commun.* **2007**, 3717-3719.

[15] (a) Eisch, J. J.; Ma, X.; Han, K. I.; Gitua, J. N.; Krüger, C. *Eur. J. Inorg. Chem.* **2001**, 77-88. (b) Müller, C.; Lachicotte, R. J.; Jones, W. D. *Organometallics* **2002**, *21*, 1975-1981.

[16] Calderazzo, F.; Pampaloni, G.; Pallavicini, P.; Straehle, J.; Wurst, K. *Organometallics* **1991**, *10*, 896-901.

[17] Goodyear, J. W.; Hemingway, C. W.; Harrington, R. W.; Wiseman, M. R.; Brisdon, B. J. *J. Organomet. Chem.* **2002**, *664*, 176-181.

[18] (a) Yoshida, K.; Morimoto, I.; Mitsudo, K.; Tanaka, H. *Chem. Lett.* **2007**, *36*, 998-999. (b) Yoshida, K.; Morimoto, I.; Mitsudo, K.; Tanaka, H. *Tetrahedron* **2008**, *64*, 5800-5807. (c) Uozumi, Y.; Nakazono, M. *Adv. Synth. Catal.* **2002**, *344*, 274-277. (d) Toganoh, M.; Matsuo, Y.; Nakamura, E. *J. Organomet. Chem.* **2003**, *683*, 295-300.

[19] (a) Fu, Y.-S.; Yu, S., J. *Angew. Chem. Int. Ed.* **2001**, *40*, 437-440. (b) Lin, Y.-Y.; Tsai, S.-C.; Yu, S., J. *J. Org. Chem.* **2008**, *73*, 4920-4928. (c) Carvalho, M. F. N. N.; Almeida, F. M. T.; Galvão, A. M.; Pombeiro, A. J. L. *J. Organomet. Chem.* **2003**, *679*, 143-147.

[20] Müller, C.; Lachicotte, R. J.; Jones, W. D. *Organometallics* **2002**, *21*, 1118-1123.

[21] Deng, M.; Leong, W. K. *Organometallics* **2002**, *21*, 1221-1226.

[22] Saito, S.; Yamamoto, Y. *Chem. Rev.* **2000**, *100*, 2901-2915.

Malgré la grande diversité de catalyseurs pouvant effectuer la réaction de cyclotrimérisation d'alcynes, il existe un mécanisme général illustré conceptuellement au Schéma 2.6.[23] Certains des intermédiaires proposés dans ce mécanisme ont pu être isolés et caractérisés. Par exemple, la réaction entre un composé de zirconium, Zr(η^6-benzène)($AlCl_4$)$_2$, et trois équivalents de diphénylacétylène (**2.20**) mène à la formation du métallocycle **2.22** (Schéma 2.7). Tel qu'escompté, un traitement thermique de cet intermédiaire a libéré l'hexaphénylbenzène (**2.3**) dans un rendement de 60%, supportant ainsi le mécanisme proposé. La structure de l'intermédiaire-clé **2.22** a été résolue par la diffraction des rayons-X et est représentée à la Figure 2.1.

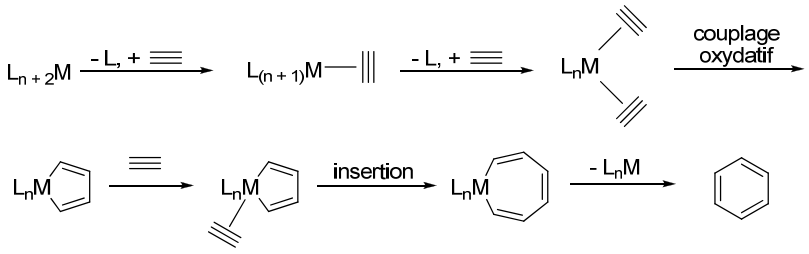

Schéma 2.6. Mécanisme général de la cyclotrimérisation d'acétylène catalysée par des métaux, adapté de la référence 23c.

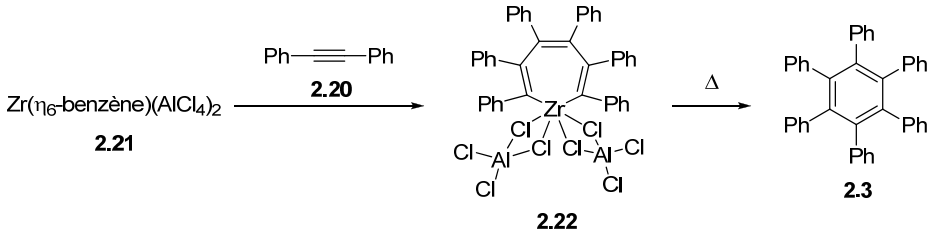

Schéma 2.7. Formation et décomposition thermique du métallocycle **2.22**.

[23] (a) Vollhardt, K. P. C. *Acc. Chem. Res.* **1977**, *10*, 1-8. (b) Collman, J. P.; Hegedus, L. S.; Norton, J. R.; Finke, R. G. *Principles and Applications of Organotransition Metal Chemistry*; University Science Books : Sausalito, 1987, pp 509–511. (c) Schore, N. E. *Chem. Rev.* **1988**, *88*, 1081-1119.

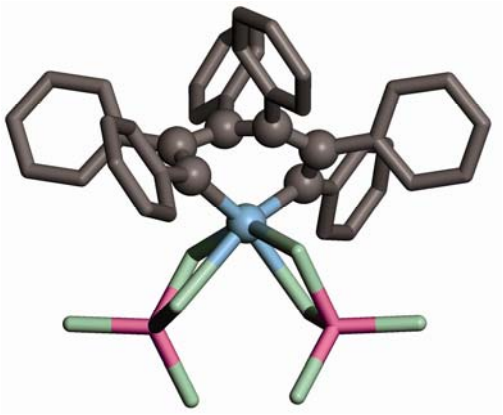

Figure 2.1. Structure à l'état cristallin du composé **2.22** obtenue par diffraction des rayons-X. Les atomes faisant partie du métallocycle sont représentés par de petites sphères. Les atomes sont identifiés par la couleur comme suit : aluminium, rose; carbone, gris; chlore, vert; zirconium, bleu.

Plus récemment, le groupe de Vollhardt a réussi à isoler une série de composés du type métallocyclopentadiène coordonné à un alcyne (**2.23**, Schéma 2.8).[24] Lorsque chauffé en présence de monoxyde de carbone, le produit se décompose pour former le cycle benzénique issu de la cyclotrimérisation (**2.24**, Schéma 2.8). Cette transformation comporte toutefois deux limitations majeures. D'abord, l'utilisation de plus d'un type d'alcyne mène à des mélanges de produits, sauf dans des cas bien particuliers.[23a] On est donc restreint à n'utiliser qu'un type d'alcyne, ce qui limite les motifs de substitution possibles. Ensuite, lorsque des acétylènes substitués par deux groupements différents sont utilisés, on obtient un mélange d'isomères. Par exemple, la cyclotrimérisation du phénylacétylène (**2.24**) mène à deux triphénylbenzènes isomériques **2.25** et **2.26** tel qu'illustré au Schéma 2.9.[25]

[24] Diercks, R.; Eaton, B. E.; Gürtzgen, S.; Jalisatgi, S.; Matzger, A. J.; Radde, R. H.; Vollhardt, K. P. C. *J. Am. Chem. Soc.* **1998**, *120*, 8247-8248.

[25] Hilt, G.; Hengst, C.; Hess, W. *Eur. J. Org. Chem.* **2008**, 2293-2297.

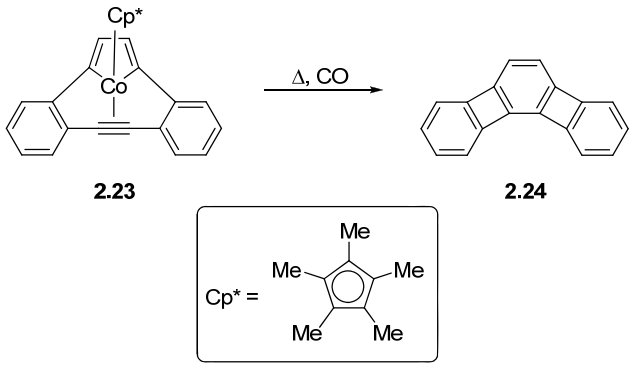

Schéma 2.8. Intermédiaire du type métallocyclopentadiène isolé par le groupe de Vollhardt.

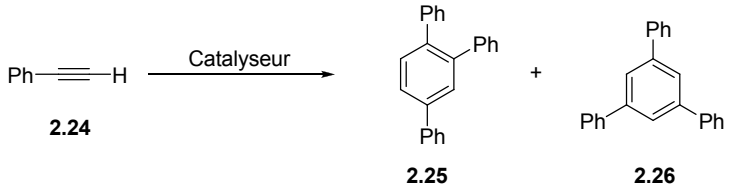

Schéma 2.9. Formation des isomères 1,2,4- et 1,3,5-triphénylbenzène lors de la cyclotrimérisation du phénylacétylène.

La cyclotrimérisation d'acétylènes est une méthode à privilégier lors de la préparation des benzènes substitués par six groupements identiques. Plusieurs groupes fonctionnels sont tolérés, ce qui a permis de préparer des hexaphénylbenzènes substitués par des groupements acétyles,[26] alkoxy,[27] alkyles saturés[28] ou partiellement fluorés,[29] amide,[30] amines tertiaires,[31] aryle,[32] benzoyle,[33] cyano,[34] esters,[35] ainsi que des

---

[26] Chebny, V. J.; Gwengo, C.; Gardinier, J. R.; Rathore, R. *Tetrahedron Lett.* **2008**, *49*, 4869-4872.

[27] (a) Wang, Z.; Dötz, F.; Enkelmann, V.; Müllen, K. *Angew. Chem. Int. Ed.* **2005**, *44*, 1247-1250. (b) Weiss, K.; Beernink, G.; Dötz, F.; Birkner, A.; Müllen, K.; Wöll, C. H. *Angew. Chem. Int. Ed.* **1999**, *38*, 3748-3752.

[28] (a) Kastler, M.; Pisula, W.; Wasserfallen, D.; Pakula, T.; Müllen, K. *J. Am. Chem. Soc.* **2005**, *127*, 4286-4296. (b) Herwig, P. T.; Enkelmann, V.; Schmelz, O.; Müllen, K. *Chem. Eur. J.* **2000**, *6*, 1834-1839. (c) Ito, S.; Wehmeier, M.; Brand, J. D.; Kübel, C.; Epsch, R.; Rabe, J. P.; Müllen, K. *Chem. Eur. J.* **2000**, *6*, 4327-4342. (d) Stabel, A.; Herwig, P.; Müllen, K.; Rabe, J. P. *Angew. Chem. Int. Ed. Engl.* **1995**, *34*, 1609-1611.

[29] (a) Aebischer, O. F.; Tondo, P.; Alameddine, B.; Jenny, T. A. *Synthesis* **2006**, 2891-2896. (b) Alameddine, B.; Aebischer, O. F.; Amrein, W.; Donnio, B.; Deschenaux, R.; Guillon, D.; Savary, C.; Scanu, D.; Scheidegger, O.; Jenny, T. A. *Chem. Mater.* **2005**, *17*, 4798-4807.

[30] Kobayashi, K.; Kobayashi, N.; Ikuta, M.; Therrien, B.; Sakamoto, S.; Yamaguchi, K. *J. Org. Chem.* **2005**, *70*, 749-752.

[31] (a) Rosokha, S. V.; Neretin, I. S.; Sun, D.; Kochi, J. K. *J. Am. Chem. Soc.* **2006**, *128*, 9394-9407. (b) Lambert, C.; Nöll, G. *Angew. Chem. Int. Ed.* **1998**, *37*, 2107-2110. (c) Lambert, C.; Nöll, G. *Chem. Eur. J.* **2002**, *8*, 3467-3477.

groupements plus élaborés tels que des dendrons,[36] des chaînes polyéthylène glycol[37] ou encore des sucres.[38]

2.2.3 Synthèse par la réaction de Diels-Alder

C'est en 1933 qu'a été rapportée la réaction à haute température entre la tétraphénylcyclopentadiènone (**2.27**) et le diphénylacétylène (**2.20**). Celle-ci permet d'isoler l'hexaphénylbenzène suite à une réaction de Diels-Alder suivie de l'expulsion d'une molécule de monoxyde de carbone (Schéma 2.10).[39]

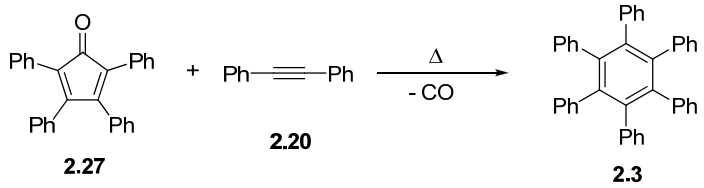

Schéma 2.10. Première synthèse de l'hexaphénylbenzène par une réaction de Diels-Alder suivie d'une élimination chélétropique de monoxyde de carbone.

La tétraphénylcyclopentadiènone et ses dérivés sont facilement préparés à partir d'un benzil (**2.28**) et d'une 1,3-diarylacétone (**2.29**). La double condensation d'aldol de ces réactifs génère les cyclopentadiènones (**2.30**) qui peuvent être réagi avec l'alcyne désiré (**2.31**, Schéma 2.11).[40] Alternativement, si une des trois composantes (**2.28**, **2.29** ou **2.31**) est non-symétrique, on peut préparer des composés avec une répartition différente des substituants (Schéma 2.12).

---

[32] (a) Iyer, V. S.; Wehmeier, M.; Brand, J. D.; Keegstra, M. A.; Müllen, K. *Angew. Chem. Int. Ed. Engl.* **1997**, *36*, 1603-1607. (b) Shen, X.; Ho, D. M.; Pascal, R. A., Jr *J. Am. Chem. Soc.* **2004**, *126*, 5798-5805.

[33] (a) Rathore, R.; Burns, C. L.; Abdelwahed, S. A. *Org. Lett.* **2004**, *6*, 1689-1692. (b) Rathore, R.; Burns, C. L.; Guzei, I. A. *J. Org. Chem.* **2004**, *69*, 1524-1530.

[34] Kobayashi, K.; Kobayashi, N.; Ikuta, M.; Therrien, B.; Sakamoto, S.; Yamaguchi, K. *J. Org. Chem.* **2005**, *70*, 749-752.

[35] Kobayashi, K.; Shirasaka, T.; Horn, E.; Furukawa, N. *Tetrahedron Lett.* **2000**, *41*, 89-93.

[36] Hahn, U.; Maisonhaute, E.; Amatore, C.; Nierengarten, J.-F. *Angew. Chem. Int. Ed.* **2007**, *46*, 951-954.

[37] Lu, Y.; Suzuki, T.; Zhang, W.; Moore, J. S.; Mariñas, B. J. *Chem. Mater.* **2007**, *19*, 3194-3204.

[38] Das, S. K.; Trono, M. C.; Roy, R. *Methods Enzymol.* **2003**, *362*, 3-17.

[39] Dilthey, I. W.; Schommer, W.; Trosken, O. *Chem. Ber.* **1933**, *B66*, 1627-1628.

[40] Ogliaruso, M. A.; Romanelli, M. G.; Becker, E. I. *Chem. Rev.* **1965**, *65*, 261-367.

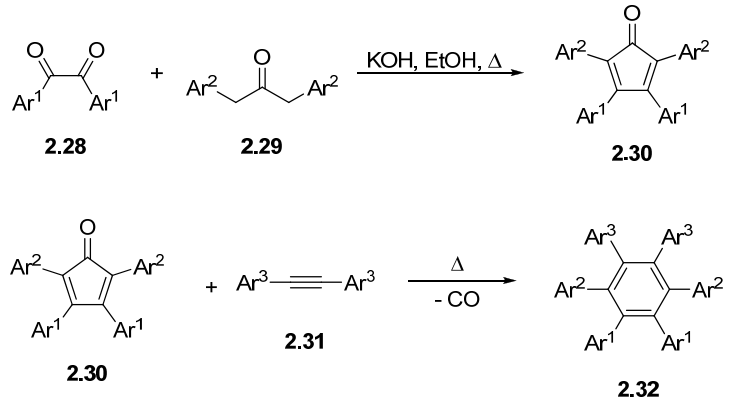

2.28 **2.29** **2.30** **2.31** **2.32**

Schéma 2.11. Synthèse de benzènes polysubstitués par la combinaison de trois fragments substitués adéquatement.

Cette approche nécessite beaucoup plus de travail synthétique que la synthèse par les réactions de Hart/Suzuki ou la cyclotrimérisation d'alcynes. Toutefois, la flexibilité synthétique permet d'adapter facilement la synthèse pour obtenir une variété de composés similaires à partir des mêmes produits de départ. De plus, les synthèses typiques de la tétraphénylcyclopentadiénone (**2.27**)[41] et de l'hexaphénylbenzène (**2.3**)[42] par cette voie sont très efficaces à grande échelle.

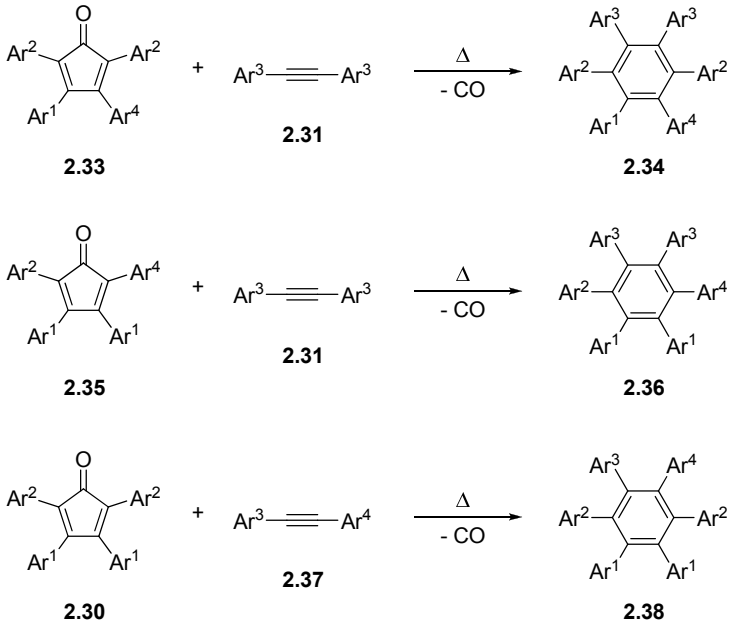

2.33 **2.31** **2.34**

2.35 **2.31** **2.36**

2.30 **2.37** **2.38**

Schéma 2.12. Préparation de benzènes polysubstitués non-symétriques.

[41] Johnson, J. R.; Grummitt, O. *Org. Synth.* **1943**, *23*, 92-93.
[42] Fieser, L. F. *Org. Synth.* **1966**, *46*, 44-48.

Section 2.3.1 Préparation d'hexaphénylbenzènes substitués

Bien qu'on puisse utiliser des intermédiaires préalablement substitués lors de la synthèse de l'hexaphénylbenzène, il est aussi possible de le substituer en une étape par des réactions aromatiques électrophiles. De cette façon, on accède rapidement, et avec d'excellents rendements, aux dérivés bromé (**2.39**),[43] iodé (**2.40**),[44] nitré (**2.41**)[45] ou chlorosulfonylé (**2.42**).[46] La sélectivité de la réaction est excellente pour la position *para* sur les six cycles aromatiques pour des raisons stériques et électroniques. L'introduction de groupements *tert*-butyles à cette position a aussi été tentée avec un succès limité.[47] Les conditions utilisées sont aussi connues pour induire une réaction de Scholl intramoléculaire (Schéma 2.14).

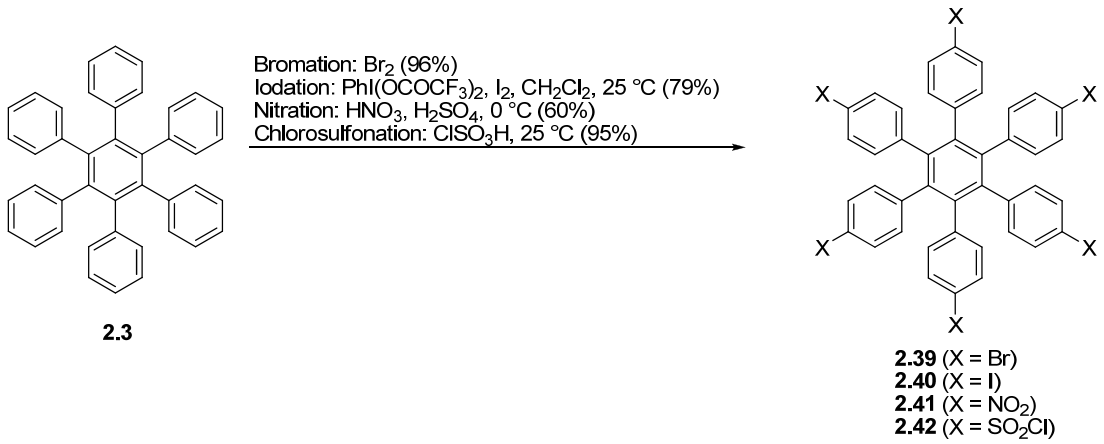

Schéma 2.13. Réactions de substitution électrophile aromatique connues de l'hexaphénylbenzène.

[43] Rathore, R.; Burns, C. L. *Org. Synth.* **2005**, *82*, 30-32.
[44] Kobayashi, K.; Kobayashi, N.; Ikuta, M.; Therrien, B.; Sakamoto, S.; Yamaguchi, K. *J. Org. Chem.* **2005**, *70*, 749-752.
[45] (a) Bergmann, P. *Z. Chem.* **1971**, *11*, 341-342. (b) Gagnon, E.; Maris, T.; Maly, K. E.; Wuest, J. D. *Tetrahedron* **2007**, *63*, 6603-6613.
[46] Tugsu, N.; Park, S. K.; Moore, J. A.; Cramer, S. M. *Ind. Eng. Chem. Res.* **2002**, *41*, 6482-6492.
[47] Rathore, R.; Burns, C. L. *J. Org. Chem.* **2003**, *68*, 4071-4074.

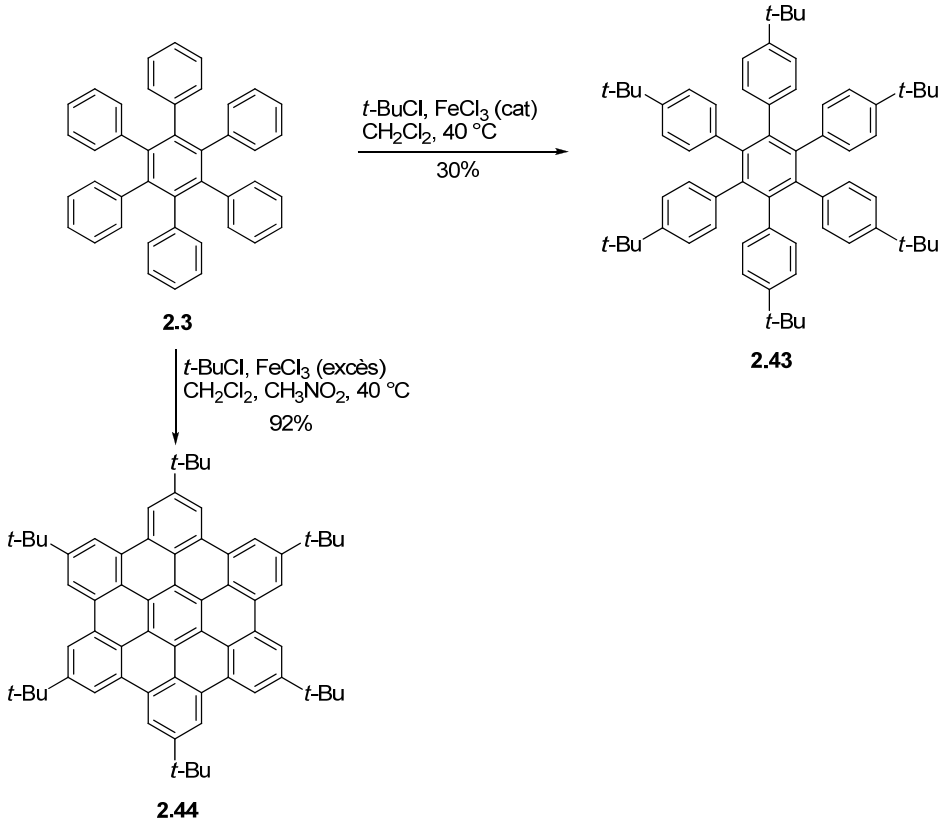

Schéma 2.14. Formation du hexakis(4-*tert*-butylphenyl)benzène catalysée par $FeCl_3$ et réaction de Scholl concomitante lorsqu'en présence d'une quantité élevée de $FeCl_3$.

2.3.2 Réaction de Scholl des hexaphénylbenzènes

Tel que vu dans la section précédente, le traitement de l'hexaphénylbenzène par du chlorure de fer (III), qui agit à la fois comme acide de Lewis et oxydant, permet de former six nouveaux liens carbone-carbone en une étape. Cette réaction est applicable à des systèmes beaucoup plus grands : un article rapporte la formation de 126 liens carbone-carbone en une étape.[48] Deux mécanismes sont postulés, impliquant soit des intermédiaires de type cation arénium ou radical-cation. Une étude théorique approfondie du sujet supporte davantage le mécanisme par cation arénium, surtout dans

[48] Simpson, C. D.; Mattersteig, G.; Martin, K.; Gherghel, L.; Bauer, R. E.; Räder, H. J.; Müllen, K. *J. Am. Chem. Soc.* **2004**, *126*, 3139-3147.

le cas de systèmes très grands comme l'hexaphénylbenzène.[49] Cette transformation s'accompagne de la planarisation du squelette hydrocarboné.

Cette réaction a ravivé l'intérêt de la communauté scientifique pour les dérivés de l'hexaphénylbenzène puisqu'ils sont des précurseurs immédiats pour toute une série d'hydrocarbones polyaromatiques (HPA) utiles en chimie des matériaux. On retrouve par exemple des HPAs considérés comme des fragments de graphène[50,51] (**2.46**, Schéma 2.15) ou encore des composés positionnant plusieurs de ces HPAs en hélice[52] (**2.49**, Schéma 2.16). Par contre, ils ont surtout été utilisés pour élaborer des cristaux liquides discotiques interagissant par empilement-π (**2.50** et **2.52**, Schéma 2.17).[53]

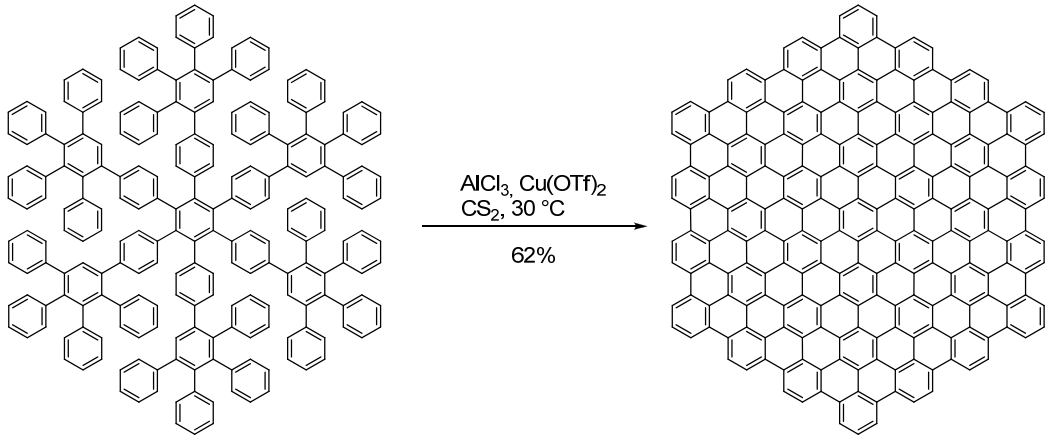

2.45 **2.46**

Schéma 2.15. Fragment de graphène par cyclodéshydrogénation éliminant 108 atomes d'hydrogène et formant 54 nouveaux liens carbone-carbone.

[49] Rempala, P.; Kroulík, J.; King, B. T. *J. Org. Chem.* **2006**, *71*, 5067-5081.
[50] Iyer, V. S.; Wehmeier, M.; Brand, J. D.; Keegstra, M. A.; Müllen, K. *Angew. Chem. Int. Ed. Engl.* **1997**, *36*, 1603-1607.
[51] Simpson, C. D.; Brand, J. D.; Berresheim, A. J.; Przybilla, L.; Räder, H. J.; Müllen, K. *Chem. Eur. J.* **2002**, *8*, 1424-1429.
[52] Simpson, C. D.; Mattersteig, G.; Martin, K.; Gherghel, L.; Bauer, R. E.; Räder, H. J.; Müllen, K. *J. Am. Chem. Soc.* **2004**, *126*, 3139-3147.
[53] (a) Ito, S.; Wehmeier, M.; Brand, J. D.; Kübel, C.; Epsch, R.; Rabe, J. P.; Müllen, K. *Chem. Eur. J.* **2000**, *6*, 4327-4342. (b) Aebischer, O. F.; Alameddine, B.; Jenny, T. A. *Chimia* **2008**, *62*, 967-973.

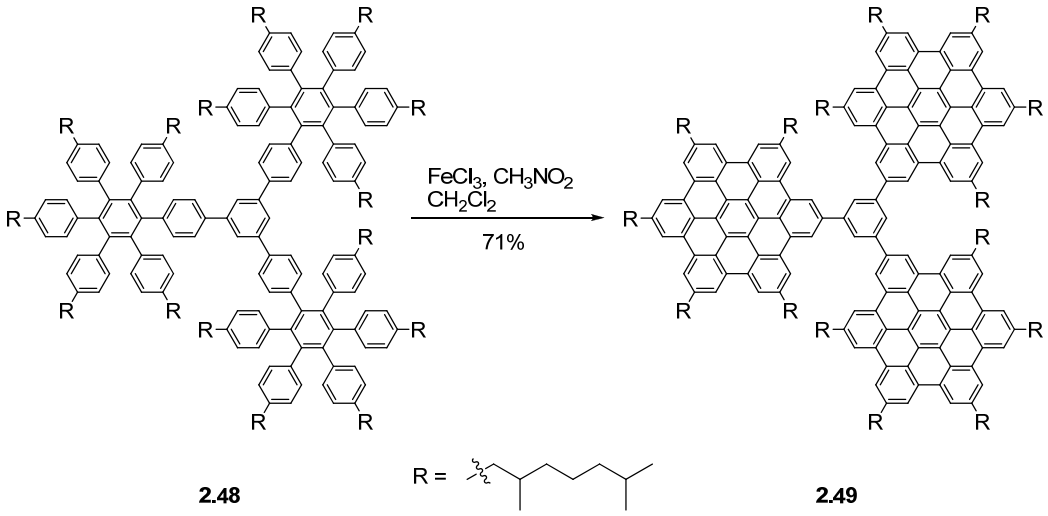

Schéma 2.16. Fragments de graphène positionnés en hélices, obtenus par cyclodéshydrogénation, élimination de 36 atomes d'hydrogène et formation conséquente de 18 nouveaux liens carbone-carbone.

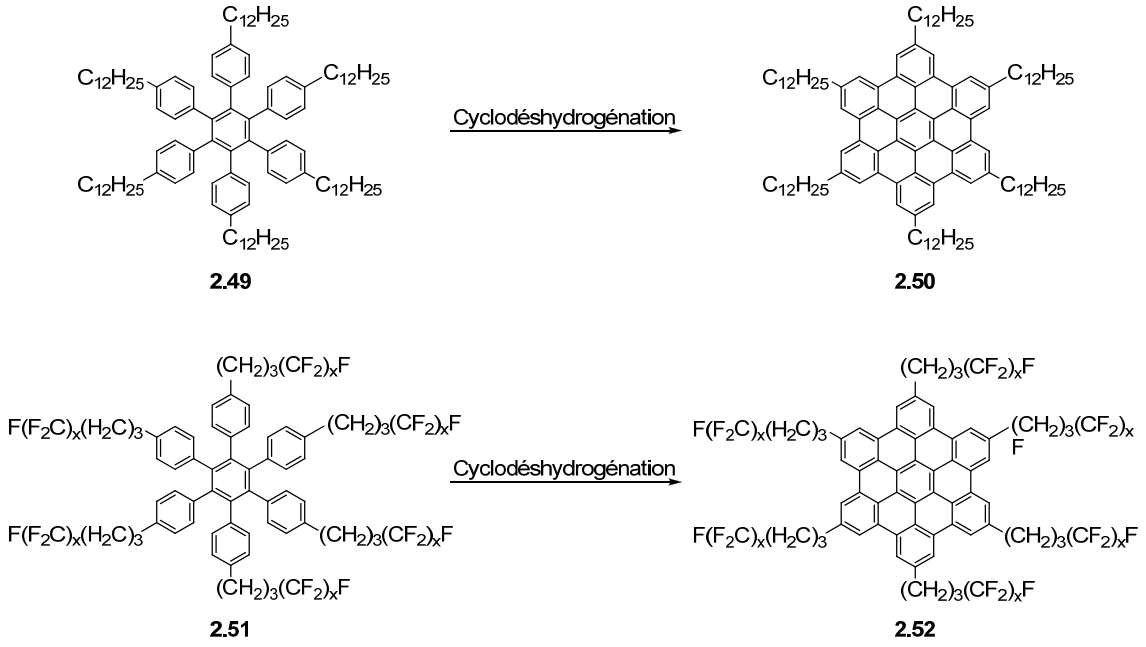

Schéma 2.17. Synthèse de HPA possédant des chaînes alkyles ou alkyles partiellement fluorées. Ces composés forment des phases liquides cristallines.

2.4 Conclusion

Ce chapitre couvre l'historique des premières synthèses de l'hexaphénylbenzène. Les trois méthodes de synthèse présentent chacune plusieurs avantages et inconvénients. Dans l'intérêt de nos études, nous avons eu besoin d'accéder facilement à des produits substitués souvent de façon non-symétrique. L'approche par la réaction de Diels-Alder permet d'obtenir des benzènes substitués par des groupements aromatiques, mais aussi des groupements alkyles ou encore des atomes d'hydrogène. Cette flexibilité quant au choix de la structure des réactifs est l'élément-clé qui justifie notre décision d'utiliser l'approche par la réaction de Diels-Alder dans les chapitres subséquents.

De plus, les benzènes substitués obtenus de cette façon offrent la possibilité d'être substitués rapidement et efficacement par des réactions de substitution électrophile aromatique. Nous avons donc pu préparer plusieurs composés avec des structures reliées, qui ont fait l'objet d'études cristallographiques approfondies. Ces résultats sont présentés dans les chapitres suivants.

Chapitre 3

Utilisation de l'hexaphénylbenzène dans la formation de réseaux poreux

3.1 Introduction

Les zéolites, du grec « pierre qui bout », sont des aluminosilicates qui possèdent une charpente anionique poreuse dans laquelle se situent des cations qui contrebalancent les charges.[1] Ces derniers ne remplissent pas totalement les cavités; on y retrouve d'autres molécules telles que de l'eau ou divers gaz pour les combler. La structure d'une zéolite représentative est illustrée à la Figure 3.1.

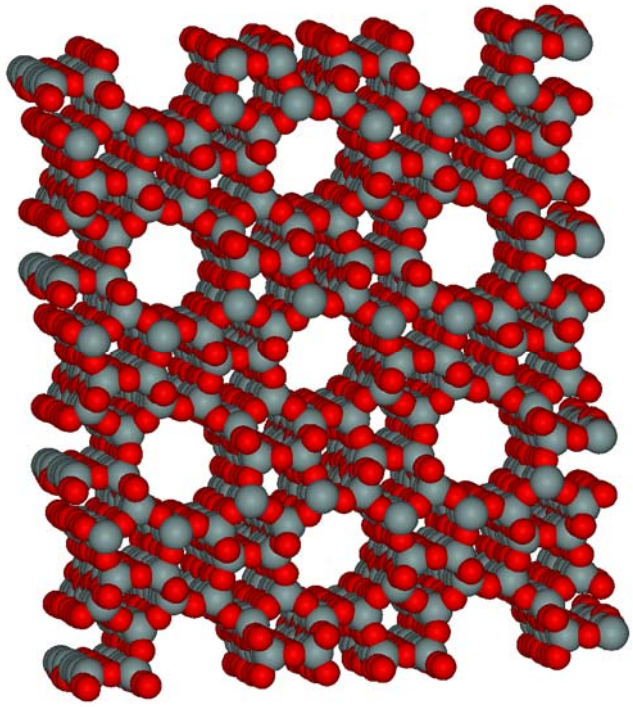

Figure 3.1. Structure de la zéolite ZSM-5.[2] Les atomes d'oxygène (O^{2-}) sont représentés en rouge et les atomes de silicium (Si^{4+}) ou d'aluminium (Al^{3+}) sont représentés en gris. Lorsqu'un atome d'aluminium est présent, un cation supplémentaire (tel que, mais non limité à, H^{+} ou Na^{+}) doit être inclus dans les cavités pour balancer la charge du réseau.

Une des applications les plus connues des zéolites en chimie organique est, sans contredit, le tamis moléculaire. La grosseur des pores de ces zéolites est idéale pour que de petites molécules telles que l'eau puissent y pénétrer et être piégées, tout en

1 Steed, J. W.; Atwood, J. L. *Supramolecular Chemistry*; John Wiley & Sons: Chichester. 2000.
2 http://en.wikipedia.org/wiki/File:Zeolite-ZSM-5-3D-vdW.png

empêchant des molécules plus volumineuses d'y entrer. Cette sélectivité permet d'utiliser des zéolites pour sécher très efficacement des solvants organiques.[3] Les zéolites sont également très utilisées en catalyse sélective. Par exemple, la zéolite ZSM-5 possède une application intéressante en pétrochimie. Ses pores sont suffisamment larges pour que le *p*-xylène y diffuse, mais ils empêchent le *o*-xylène et le *m*-xylène d'y arriver efficacement.[1] De plus, l'intérieur de ses cavités (Figure 3.1) contient des sites réactifs acides, capables de catalyser l'isomérisation des *o*- et *m*-xylènes en *p*-xylène, qui peut ensuite sortir de la zéolite. Ces processus impliquent des phénomènes de séparation, de séquestration, de catalyse et de sélectivité. Ces applications ne seraient pas possibles si cette zéolite n'avait pas la topologie requise, des grosseurs de pores idéales et des sites réactifs efficaces.

Un but important en sciences des matériaux est de développer de nouveaux aluminosilicates ainsi que d'autres matériaux inorganiques possédant des propriétés analogues à celles des zéolites. Un objectif additionnel consiste à élaborer des matériaux moléculaires possédant des caractéristiques similaires.[4] Bien que les zéolites possèdent une certaine flexibilité quant à leur contenu, et qu'il existe quelques centaines de zéolites différentes, la chimie organique offre une flexibilité structurale inégalée. La possibilité de créer pratiquement atome par atome des structures moléculaires est un avantage important lorsque l'on veut obtenir des matériaux moléculaires avec des propriétés précises.

Ainsi, il est possible de générer des molécules avec une précision chirurgicale. Par contre, leurs auto-assemblages relèvent en partie de la chance. Pour augmenter la probabilité que les composantes moléculaires s'associent de façon prévisible, nous pouvons exploiter la stratégie de la tectonique moléculaire, dans laquelle l'organisation supramoléculaire est contrôlée par des interactions spécifiques, fortes et directionnelles qui orientent chaque molécule de manière prévisible par rapport à ses voisines. Les ponts hydrogène se sont avérés particulièrement efficaces pour diriger la formation de

---

[3] Armarego, W. L. F.; Chai, C. L. L. *Purification of Laboratory Chemicals, fifth edition*; Elsevier, 2003.
[4] Wuest, J. D. *Chem. Commun.* **2005**, 5830-5837.

réseaux moléculaires. La prochaine section (3.2) discute des caractéristiques des ponts hydrogène. La section suivante (3.3) présente quelques précédents en tectonique moléculaire qui sont dignes de mention. On expliquera ensuite les motivations derrière l'utilisation de l'hexaphénylbenzène (section 3.4) en tectonique moléculaire, puis un premier article sera présenté (section 3.5). Le chapitre sera clos par une courte récapitulation de nos résultats ainsi qu'une série d'idées dérivées de ceux-ci.

3.2 Les ponts hydrogène

Les assemblages supramoléculaires présentés dans ce chapitre exploitent tous les propriétés exceptionnelles des ponts hydrogène. Ces assemblages sont caractérisés généralement par des études de diffraction des rayons-X. Ces études révèlent sans-équivoque la structure des assemblages mais ne montrent pas directement la force motrice favorisant l'assemblage et les contributions individuelles des interactions non-covalentes en jeu. Toutefois, il existe des caractéristiques structurelles très fiables qui relient la position des atomes participants dans des interactions à la force de celles-ci. Afin de mettre en contexte nos données structurelles, il est nécessaire de décrire brièvement le pont hydrogène lui-même, une interaction dominante dans les structures présentées dans ce chapitre.

Les ponts hydrogène tirent avantage de l'électronégativité de l'atome donneur pour diminuer la densité électronique au terminus du lien D–H (Figure 3.2). Ce dipôle peut alors interagir avec une autre source de densité électronique, l'accepteur A, qui peut être un atome possédant un doublet d'électrons ou encore un système conjugué possédant des électrons π, tel que le benzène.

Figure 3.2. Pont hydrogène. D est le donneur du pont hydrogène, H est l'hydrogène partagé et A est l'accepteur du pont hydrogène.

À l'origine, seuls les atomes d'azote, d'oxygène et de fluor étaient considérés comme assez électronégatifs pour participer dans un pont hydrogène.[5] Bien entendu, ces éléments sont parmi les plus électronégatifs du tableau périodique et ils établissent les ponts hydrogène les plus forts. Toutefois, la définition des ponts hydrogène s'est grandement élargie avec le temps. Maintenant, des donneurs aussi faibles que les liens C-H du méthane sont considérés, ce qui soulève des débats quant à la frontière séparant les ponts hydrogène des interactions de van der Waals.[6] On peut par contre classifier les ponts hydrogène qualitativement en fonction de plusieurs de leurs propriétés, tel qu'indiqué au Tableau 3.1.

Tableau 3.1. Reproduction partielle des propriétés des ponts hydrogène forts, modérés et faibles, tiré du livre de Jeffrey.[7]

	Fort	Modéré	Faible
Interaction D-H···A	Majoritairement covalente	Majoritairement électrostatique	Électrostatique
Longueur de liens			
H···A (Å)	~1,2-1,5	~1,5-2,2	~2,2-3,2
D···A (Å)	2,2-2,5	2,5-3,2	3,2-4,0
Angles des liens (°)	175-180	130-180	90-150
Énergie des liens (kcal mol^{-1})	14-40	4-15	< 4
Variation relative des vibrations v_s (cm^{-1})	25%	10-25%	< 10%
Exemples	· Complexes de HF · Éponges à proton · Dimères d'acides forts en phase gazeuse	· Molécules biologiques · Phénols · Alcools · Acides carboxyliques	Ponts hydrogène faibles tels que : · C–H···O/N · O/N–H···π

On remarque premièrement que les ponts hydrogène forts forment des liens dont l'énergie approche celle des interactions covalentes les plus faibles (voir Tableau 1.1). Ceux-ci sont toutefois formés plus souvent qu'autrement par des composantes ioniques

[5] Pauling, L. *The Nature of the Chemical Bond and the Structure of Molecules and Crystals - An Introduction to Modern Structural Chemistry, 2nd Edition*, Oxford University Press, London, 1940.
[6] Une discussion des interactions impliquant des liens C-H est disponible au chapitre 5.
[7] Jeffrey, G. A. *An Introduction to Hydrogen Bonding*, Oxford University Press, Oxford, 1997.

impliquant des groupements tels que des sels d'ammonium (agissant comme donneur) ou un alcoolate (en tant qu'accepteur). Les ponts hydrogène les plus communs, tels que ceux dirigeant la structure des protéines, font partie de la catégorie « modéré ». Ils sont aussi qualifiés de ponts hydrogène « normaux ». Finalement, on retrouve les ponts hydrogène faibles, dont les donneurs et/ou les accepteurs sont faiblement polarisés. On remarque aussi au Tableau 3.1 que l'énergie du pont hydrogène est directement reliée aux partenaires impliqués dans l'interaction. Les données structurelles obtenues par la diffraction des rayons-X (composition de la molécule, distance entre les atomes et géométrie de l'interaction) nous permettent donc de classer un pont hydrogène dans l'une des trois catégories.

La tectonique moléculaire exploite typiquement les forces des ponts hydrogène modérés. Plusieurs de leurs propriétés utiles peuvent être extrapolées en étudiant plus attentivement le Tableau 3.1. Dans un premier temps, on note que l'énergie de ces ponts hydrogène est relativement faible. Toutefois, la sommation de l'énergie de plusieurs de ces interactions peut rapidement atteindre plusieurs dizaines, voire centaines de kJ mol^{-1}. Ainsi, les assemblages supramoléculaires créés peuvent posséder une stabilité très élevée. À l'opposée, ces interactions sont encore suffisamment faibles pour être réversibles dans certaines conditions. Ceci permet aux molécules de se dissocier si la reconnaissance intermoléculaire ne s'est pas faite de façon optimale. On évite alors d'obtenir des agrégats non-cristallins. Finalement, la géométrie des ponts hydrogène couvre une large gamme de distances et d'angles entre les atomes impliqués et leurs énergies peuvent rester pratiquement constantes malgré une déformation sensible de leurs géométries.[7] Ces dernières propriétés se révèlent très utiles puisque la charpente cristalline peut s'adapter aux variations de grosseurs et de formes des molécules invitées. Ainsi, c'est en tenant compte des forces et des faiblesses des ponts hydrogène que des assemblages supramoléculaires fonctionnels ont été obtenus par l'approche de la tectonique moléculaire.

3.3 Des tectons aux propriétés intéressantes

La tectonique moléculaire a pris son envol en 1991 lorsque la tétrapyridone **3.1** (Figure 3.3) a été cristallisée dans un mélange d'acide butyrique, de méthanol et d'hexane.[8] L'étude des cristaux obtenus a démontré que l'association dimérique des 2-pyridones[9] peut être étendue en trois dimensions afin d'obtenir des réseaux diamantoïdes maintenus par des ponts hydrogène (Figure 3.4). Ces cristaux ont une porosité limitée de 28%,[10] à cause du phénomène d'interpénétration des réseaux diamantoïdes. Cette démonstration de concept a pavé la voie pour les études subséquentes.

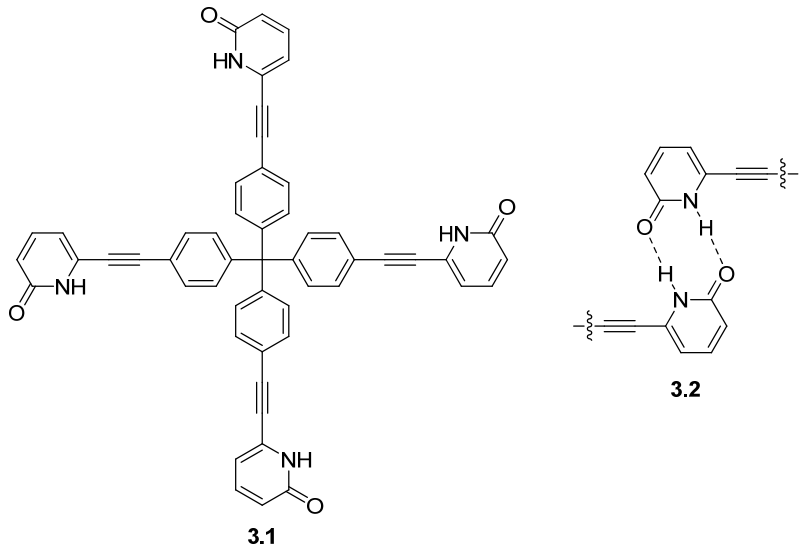

Figure 3.3. Structure de la tétrapyridone **3.1** et le motif d'association par ponts hydrogène typique des 2-pyridone (**3.2**).

Plus récemment, on retrouve une étude de Brunet *et al.* qui exploite également la géométrie particulière du tétraphénylméthane.[11] L'incorporation de groupements diaminotriazinyles (DAT) sur celui-ci a apporté une importante contribution à la tectonique moléculaire (**3.3**, Figure 3.5). La présence de multiples donneurs et accepteurs de ponts hydrogène sur les groupements DAT apporte un avantage non-négligeable : le nombre d'interactions intermoléculaires par molécule augmente afin de

[8] Simard, M.; Su, D.; Wuest, J. D. *J. Am. Chem. Soc.* **1991**, *113*, 4696-4698.
[9] Ducharme, Y.; Wuest, J. D. *J. Org. Chem.* **1988**, *53*, 5787-5789.
[10] La porosité est évaluée par le volume occupé par les molécules invitées.
[11] Brunet, P.; Simard, M.; Wuest, J. D. *J. Am. Chem. Soc.* **1997**, *119*, 2737-2738.

contribuer à la stabilité du réseau supramoléculaire. Par contre, la prédiction des motifs de reconnaissance des tectons devient plus ardue : trois modes d'association sont fréquemment observés (Figure 3.5).

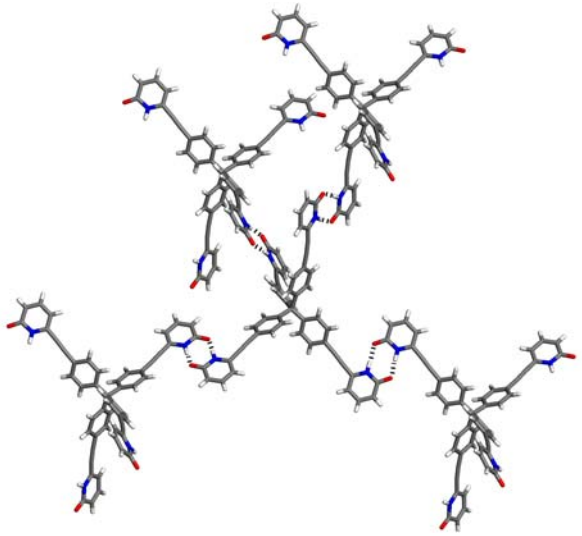

Figure 3.4. Voisins immédiats d'une molécule de tétrapyridone **3.2**. Tel qu'escompté, l'association en dimère des 2-pyridones dirige l'assemblage supramoléculaire. Les ponts hydrogène sont représentés par des traits hachurés.

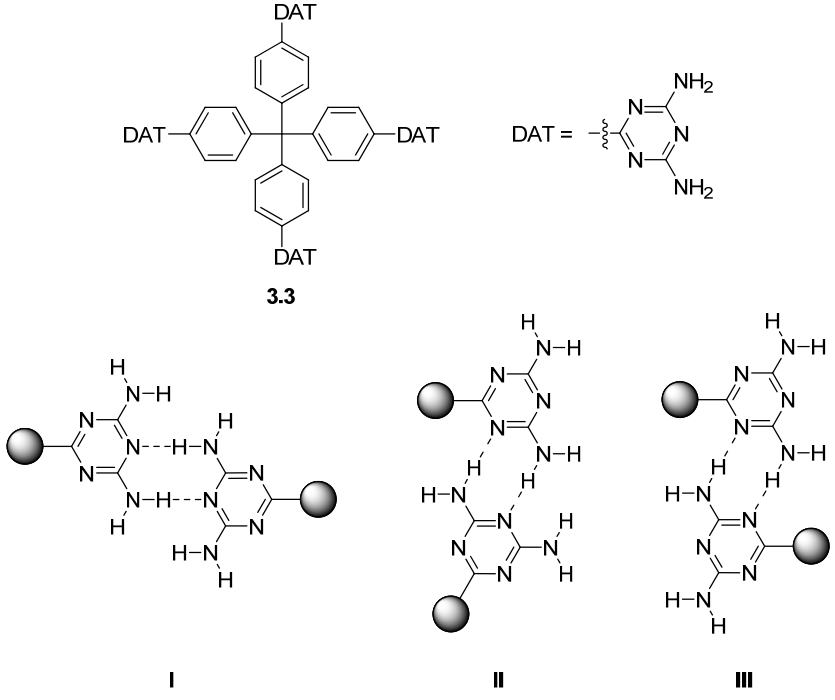

Figure 3.5. Structure du tecton **3.3** et modes normaux de reconnaissance des groupements diaminotriazinyles (DAT) : **I** (face-à-face); **II** (face-à-côté); et **III** (côté-à-côté).

Le réseau supramoléculaire obtenu par la cristallisation du tecton **3.3** dans un mélange d'acide formique et de dioxane possède une porosité évaluée à 42 %. Tel qu'observé à la Figure 3.6, l'association des molécules selon les motifs de reconnaissance favorisés des groupements DAT définit des canaux relativement larges. Selon les conditions exactes de cristallisation, ces pores sont occupés par une proportion variable de dioxane et d'acide formique. Le réseau est donc isostructural peu importe l'identité des molécules invitées. De plus, en suspendant des cristaux du tecton **3.3** dans le dioxane, l'acétonitrile ou l'eau, un échange complet du contenu des pores peut être effectué. Finalement, il a été démontré que les canaux peuvent être vidés de jusqu'à 63 % de leurs contenus, sans détérioration majeure de l'assemblage supramoléculaire.

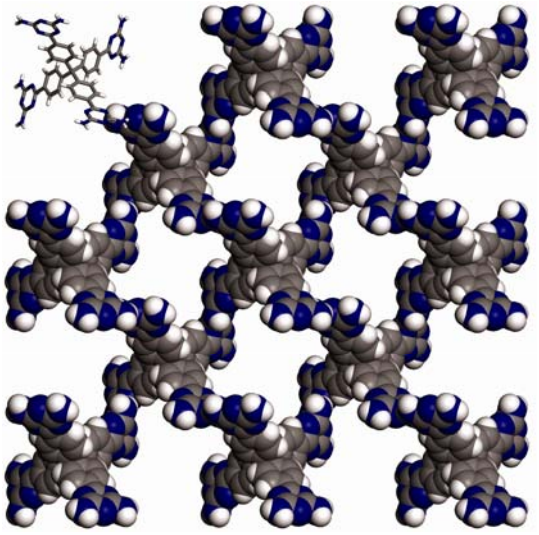

Figure 3.6. Représentation de l'assemblage supramoléculaire formé par 2 × 2 × 1 mailles élémentaires du tecton **3.3**. On remarque en haut à gauche la structure d'une seule molécule.

Le tétraphénylméthane a ensuite été modifié par des groupements de reconnaissance dérivés des DAT. Ces nouveaux groupements de reconnaissance permettent à la fois de former un réseau supramoléculaire selon les motifs d'assemblage typiques des DAT, tout en introduisant des sites réactifs allyliques (**3.4**, Schéma 3.1).[12] Le résultat est un édifice supramoléculaire maintenu par des ponts hydrogène et comportant de larges cavités (11,4 Å × 7,8 Å) dans lesquelles on retrouve du dioxane

[12] Brunet, P.; Demers, E.; Maris, T.; Enright, G. D.; Wuest, J. D. *Angew. Chem. Int. Ed.* **2003**, *42*, 5303-5306.

ainsi que les groupements allyles. Ces cristaux sont perméables et lorsque le dioxane est échangé pour du méthanethiol et que les cristaux sont irradiés avec une lampe au mercure, les groupements thiométhyles s'additionnent sur les groupements allyles (Schéma 3.1). Similairement, si on diffuse de l'éthane-1,2-dithiol dans les canaux puis qu'on irradie les cristaux, une réticulation du réseau a lieu suite à l'addition du dithiol sur les groupements allyles de deux molécules distinctes. Le produit obtenu est une macromolécule insoluble et cristalline, qui fige par des liens covalents le réseau supramoléculaire initial.

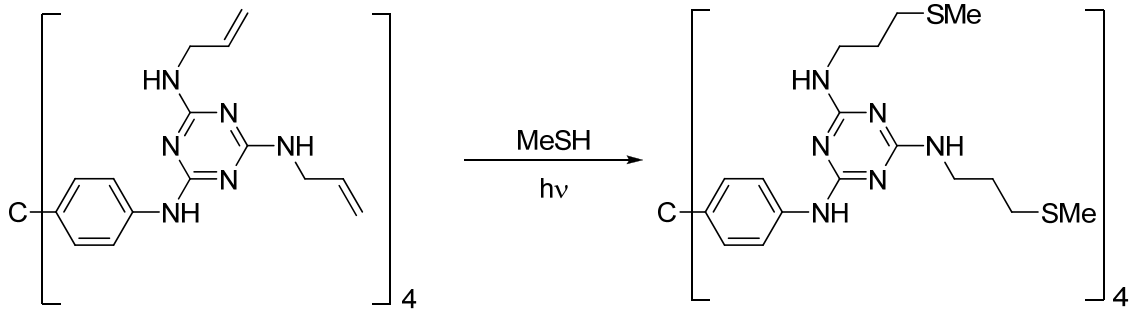

3.4 **3.5**

Schéma 3.1. Réaction d'addition photochimique des groupements allyles du tectons **3.4** avec du méthanethiol.

Finalement, le tecton **3.6** a été rapporté par Fournier *et al*.[13] L'unité centrale utilisée dans ce cas est le 9,9'-spirobifluorène. Lorsque substitué par des groupements de reconnaissance dérivés de la diaminotriazine, le tecton **3.6** cristallise en formant des réseaux hautement poreux. La particularité de ces cristaux consiste surtout en la quantité de solvant incluse : les molécules de dioxane, de DMSO et d'eau occupent 75% du volume du cristal, ce qui en fait un des réseaux supramoléculaires maintenus par des ponts hydrogène parmi les plus poreux connus.

[13] Fournier, J.-H.; Maris, T.; Wuest, J. D. *J. Org. Chem.* **2004**, *69*, 1762-1775.

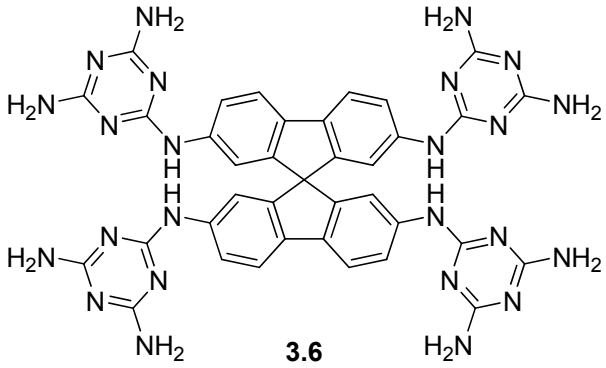

3.6

L'évolution graduelle de la tectonique moléculaire a permis de recréer plusieurs propriétés qui étaient propres à celles des zéolites, dont la conservation de la structure tridimensionnelle lors de l'échange ou le retrait de molécules invitées, la sélectivité lors de l'inclusion de molécules invitées, l'échange de molécules invitées, la réactivité à l'intérieur des cavités et une porosité très élevée. Afin de repousser davantage les limites de la tectonique moléculaire, nous avons utilisé de nouveaux cœurs moléculaires : l'hexaphénylbenzène et ses dérivés.

3.4 Nos objectifs

La principale raison d'introduire l'hexaphénylbenzène en tectonique moléculaire réside dans le nombre accru de groupements de reconnaissance (jusqu'à six) qu'on peut y installer, comparativement aux cœurs moléculaires plus fréquemment étudiés (seulement quatre dans les cas du tétraphénylméthane et du 9,9'-spirobifluorène). Le nombre de ponts hydrogène par molécule devrait donc augmenter, en ayant pour conséquence de solidifier davantage le réseau supramoléculaire. De plus, la structure rigide de l'hexaphénylbenzène permet de diriger précisément les groupements de reconnaissances dans l'espace, de façon à former des réseaux poreux avec une structure prédictible. Finalement, grâce à la flexibilité synthétique de l'approche par Diels-Alder présentée au Chapitre 2, les dérivés analogues de l'hexaphénylbenzène sont facilement accessibles.

3.5 Article 1

Engineering Hydrogen-Bonded Molecular Crystals Built from Derivatives of Hexaphenylbenzene and Related Compounds

Kenneth E. Maly,[1] Eric Gagnon,[2] Thierry Maris, and James D. Wuest

Journal of the American Chemical Society, **2007**, *129*, 4306-4322

Reproduced with permission from *Journal of the American Chemical Society*
Copyright 2007 American Chemical Society

Abstract

Hexakis[4-(2,4-diamino-1,3,5-triazin-6-yl)phenyl]benzene (**4**) incorporates a disc-shaped hexaphenylbenzene core and six peripheral diaminotriazine groups that can engage in hydrogen bonding according to established motifs. Under all conditions examined, compound **4** crystallizes as planned to give closely related noninterpenetrated three-dimensional networks built from sheets in which each molecule has six hydrogen-bonded neighbors. In the structure of compound **4**, the number of hydrogen bonds per molecule and the percentage of volume accessible to guests approach the highest values so far observed in molecular networks. Analogue **5** (which has the same hexaphenylbenzene core but only four diaminotriazine groups at the 1,2,4,5-positions) and analogue **7** (in which the two unsubstituted phenyl groups of compound **5** are replaced by methyl groups) crystallize according to a closely similar pattern. Analogues with flatter pentaphenylbenzene or tetraphenylbenzene cores crystallize differently, underscoring the importance of maintaining a consistent molecular shape in attempts to engineer crystals with predetermined properties.

Introduction

Designing molecules to form crystals with particular structures and properties has become a very active area of research.[3] An especially productive strategy in crystal engineering builds structures from molecules that engage in multiple specific interactions with neighbors.[4-7] Such molecules, which have been called tectons,[8] are well suited for the purposeful construction of new materials. Hydrogen bonds have been widely exploited in this strategy because their strength and directionality tend to favor the formation of crystals in which neighboring molecules are positioned predictably.[9] The resulting structures can be described as networks of molecules connected by hydrogen bonds.

These networks often have a significant degree of openness because efficient packing cannot normally be achieved at the same time that hydrogen bonding is

optimized. In such cases, an important percentage of the volume of the resulting crystals can be occupied by included guests. Systematic efforts to increase the openness of the resulting networks have yielded molecular crystals in which as much as 75% of the volume is accessible to guests.[5,6,10,11] Initially, these permeable molecular crystals were exotic curiosities; increasingly, however, they are serving as inspiration for scientists studying subjects of immediate practical importance, such as ways to make new porous materials for selectively storing guests,[12] to make solids react without using solvents to dissolve them,[13] and to create new types of gels, liquid crystals, films, glasses, and other materials in which particular degrees of order, porosity, and molecular diffusion must be maintained.[14]

Diverse tectons can be made conveniently by attaching appropriate hydrogen-bonding groups or other sticky sites to the periphery of cores with well-defined geometries. Many previously studied networks have been built from tectons with nominally tetrahedral cores, which tend to favor diamondoid architectures. In such structures, the volume available for including guests is often diminished or even eliminated by the interpenetration of independent networks.[15] Increasing the permeability of molecular crystals requires new types of tectons that yield networks in which interpenetration is disfavored or impossible. In addition, to ensure that the resulting networks are highly robust, each tecton must form many hydrogen bonds with its neighbors.

As part of a systematic effort to construct highly open and robust hydrogen-bonded networks, we turned our attention to tectons with complex aromatic cores related to hexaphenylbenzene. In noteworthy earlier work in crystal engineering, Kobayashi and co-workers showed that compounds **1**-**3**, which have simple hydrogen-bonding groups attached to each of the six radiating phenyl arms of hexaphenylbenzene, form open networks without interpenetration.[16-18] A summary of key features of these structures appears in Table 1. Hexakis(4-hydroxyphenyl) benzene (**1**) was shown to crystallize from two different solvent systems as inclusion compounds that both consist of hydrogen-bonded sheets.[16] In each of these two structures, the percentage of volume

accessible to guests is relatively modest (42% and 48%), as is the number of hydrogen bonds in which each tecton participates (four and eight). Hexakis(4-carboxyphenyl) benzene (**2**) also crystallizes as sheets, which are held together by self-association of the carboxyl groups as cyclic hydrogen-bonded pairs.[17] This leads to a structure in which the number of hydrogen bonds per tecton increases to 12 but the percentage of accessible volume is still modest (46%). Hexakis-(4-carbamoylphenyl)benzene (**3**) was found by Kobayashi and co-workers to crystallize from three solvent systems as different three-dimensional hydrogen-bonded networks.[18] Again, the percentages of volume accessible to included guests (59%, 48%, and 7%) are significantly lower than those of the most permeable molecular crystals currently known,[5,6] and the cohesive forces are modest, as measured by the number of hydrogen bonds per tecton.

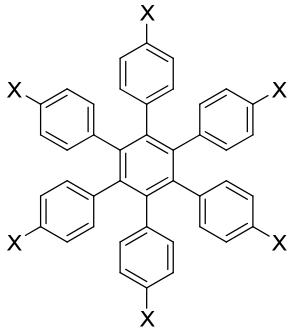

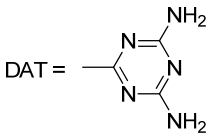

1 (X = OH)
2 (X = COOH)
3 (X = $CONH_2$)
4 (X = DAT)

Table 1. Summary of Key Structural Features of the Hydrogen-Bonded Networks in Crystals of Hexaphenylbenzenes **1**-**5** and Related Compounds **6**-**8.**

Compound (conditions of crystallization in parentheses)	% volume accessible to guests[10,11]	Number of hydrogen-bonded Neighbors per tecton[a]	Number of hydrogen bonds per tecton[a]	Dimensionality of hydrogen-bonded network
1 (Et_2O)[16]	48	6	8	2D
1 (DMF)[16]	42	4	4	2D
2 (MeOH)[17]	46	6	12	2D
3 (DMSO)[18]	59	8	12	3D
3 (*n*-PrOH/H_2O)[18]	48	6	12	3D
3 (H_2O)[18]	7	10 10[c]	12 20[c]	3D
4 (DMSO/THF)	70	8	16	3D
4 (DMSO/toluene)	56	8	16	3D
4 (DMSO/benzene)	72	6	12	3D
4 (HCOOH/EtOH)	56	12	36	3D
5 (DMSO/MeCN)	60	6	12	3D
6 (DMSO/acetone)	55	4	8	3D
7 (DMSO/dioxane)	75	6	16	3D
7 (DMSO/MeOH)	39[b]	4	14	2D
8 (DMSO/acetone)	64	2	4	1D

[a] Hydrogen bonds involving guests are excluded. [b] This value is abnormally low in the series of compounds **4**-**8** because the network is 2-fold interpenetrated. [c] The unit cell contains two independent molecules.

Tectons **1-3** are structurally similar, but the resulting networks display widely different architectures for reasons that have not been delineated. Moreover, the percentages of volume accessible to guests are all less than 60%, in some cases by a large margin, and the number of hydrogen bonds per tecton does not normally exceed 12 (Table 1). Taken together, these properties do not point to tectons derived from hexaphenylbenzene as especially promising precursors for engineering highly permeable molecular crystals. However, we were encouraged to note that none of the networks formed by compounds **1-3** exhibits interpenetration, possibly because of the geometry of the hexaphenylbenzene core. These observations encouraged us to undertake a systematic study of derivatives of hexaphenylbenzene as sources of highly porous hydrogen-bonded networks not compromised by interpenetration.

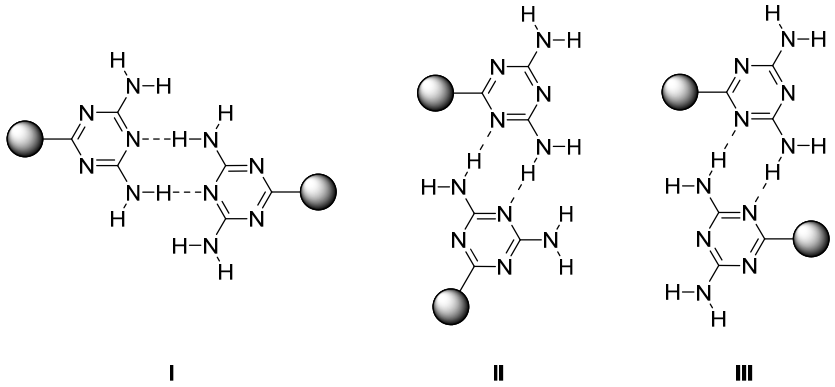

I **II** **III**

Our initial target was tecton **4**, which incorporates six diaminotriazine groups on the periphery of the hexaphenylbenzene core. Diaminotriazines are known to self-associate reliably in the solid state by forming hydrogen-bonded motifs **I-III**.[5,6,19] Motif **I** is particularly favorable because it involves hydrogen bonding remote from sterically congested sites where the diaminotriazine groups are attached to the molecular core. For this reason, we expected tecton **4** to crystallize by associating according to motif **I**. This would lead to the formation of sheets represented by Figure 1a, in which each tecton has six hydrogen-bonded neighbors and takes part in a total of 12 hydrogen bonds. In addition, the sheets shown in Figure 1a could potentially be further connected by secondary hydrogen-bonding interactions according to motif **II** or **III**, giving a three-dimensional network and increasing the number of hydrogen bonds per tecton. In the resulting network, the sheets would be held apart and spaced by hydrogen bonding. For

these reasons, we expected compound **4** to generate structures with higher percentages of volume accessible to guests, larger numbers of hydrogen bonds per tecton, and more consistent three-dimensional architectures than those produced by the simpler hexaphenylbenzenes studied by Kobayashi et al.[16-18]

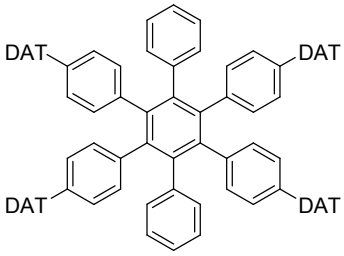

5

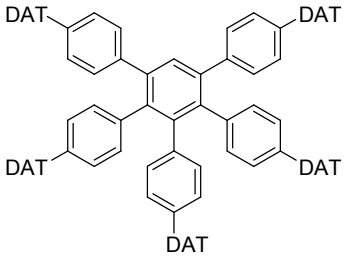

6

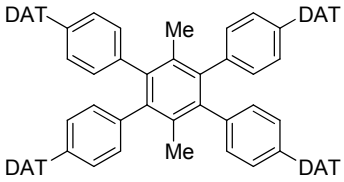

7

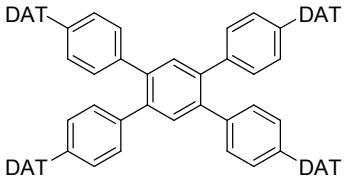

8

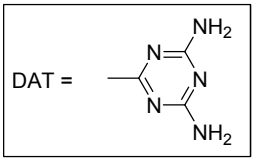

In addition, we recognized that the hexaphenylbenzene core offers an attractive opportunity to modify networks rationally by changing the number and position of the hydrogen-bonding substituents. For example, removing selected hydrogen-bonding groups from the core can produce hexaphenylbenzenes such as compound **5**, and more dramatic mutations of the core itself can yield derivatives such as pentaphenylbenzene **6** and tetraphenylbenzenes **7** and **8**. We undertook these systematic alterations with the expectation that analysis of the resulting structures would deepen our understanding of how molecular crystals can be engineered.

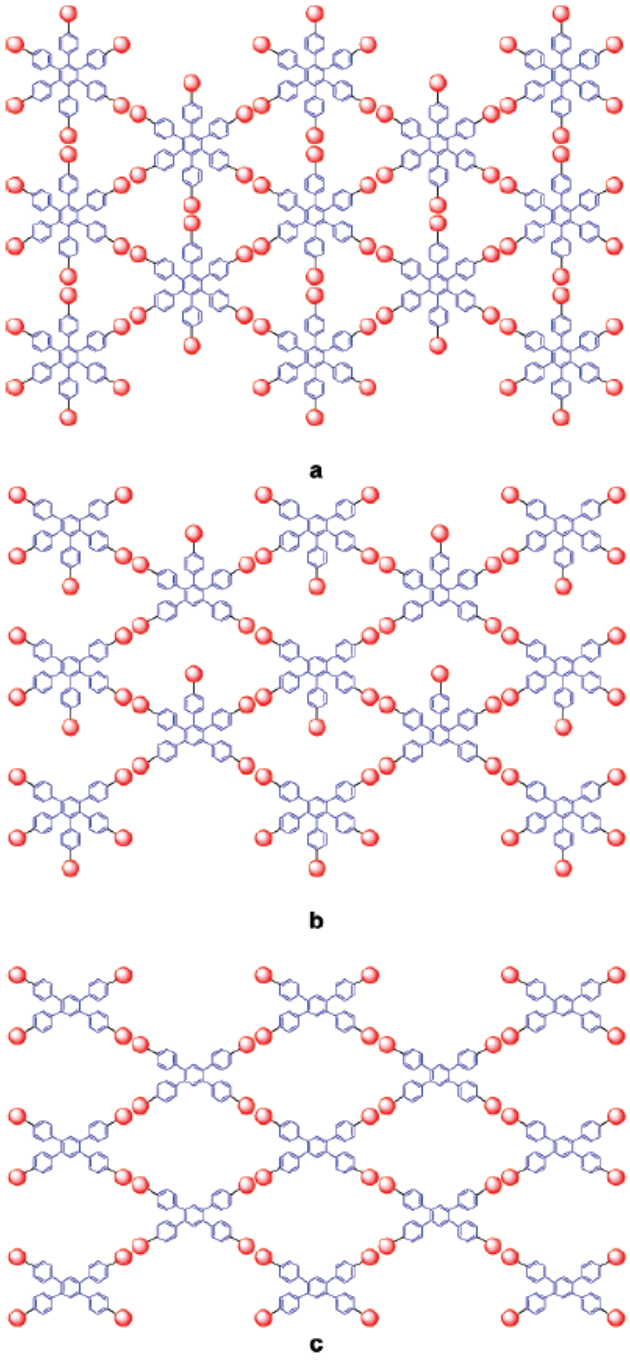

Figure 1. Schematic representations of possible networks derived from (a) a hexaphenylbenzene with six hydrogen-bonding substituents at the para position of each phenyl group (such as tecton **4**); (b) a pentaphenylbenzene with five hydrogen-bonding substituents (such as tecton **6**); and (c) a 1,2,4,5-tetraphenylbenzene with four hydrogen-bonding substituents (such as tecton **7**). In all images, red circles represent hydrogen-bonding substituents.

Scheme 1.

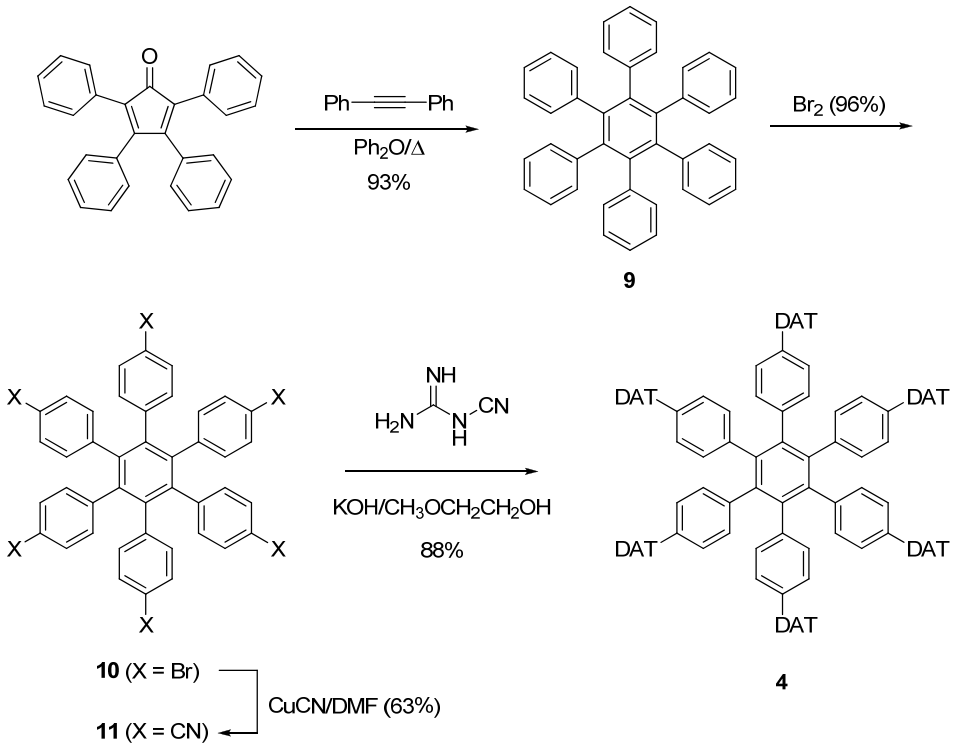

Results and Discussion

Synthesis of Tecton 4. Target **4** was prepared in four steps in an overall yield of 47% by the route outlined in Scheme 1. Hexaphenylbenzene (**9**) was synthesized in 93% yield via the Diels-Alder reaction of tetraphenylcyclopentadienone with diphenylacetylene.[20] Treatment with neat bromine then produced hexakis(4-bromophenyl)benzene (**10**) in 96% yield.[21,22] Reaction of hexabromide **10** with CuCN gave hexakis(4-cyanophenyl)benzene (**11**) in 63% yield,[23,24] and treatment of the product with dicyandiamide under basic conditions provided target **4** in 88% yield.[25]

Synthesis of Tecton 5. To synthesize derivative **5**, in which two diaminotriazine groups have been removed from opposing positions on the hexaphenylbenzene core, we took advantage of the flexibility inherent in the Diels-Alder strategy employed in Scheme 1. The reaction of 4,4'-dibromobenzil with 1,3-diphenylacetone gave dibrominated tetraphenylcyclopentadienone **12** in 85% yield (Scheme 2).[26] The Diels-Alder reaction of compound **12** with bis(4-bromophenyl)acetylene,[27] followed by loss of

CO, produced tetrabrominated hexaphenylbenzene **13** in 84% yield. Treatment of compound **13** with CuCN gave the corresponding tetranitrile **14** in 60% yield, and further reaction with dicyandiamide under standard conditions provided target **5** in 83% yield.

Scheme 2.

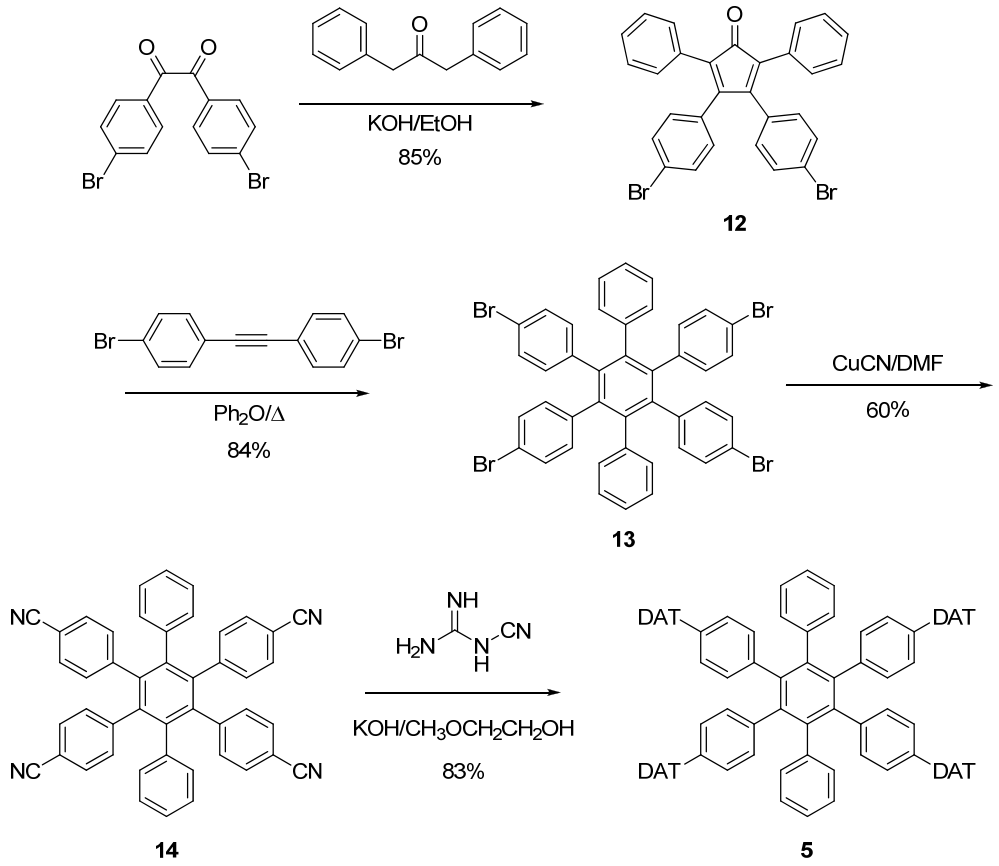

Synthesis of Tecton 6. Pentaphenylbenzene **6** was prepared by an analogous route (Scheme 3). The reaction of tetraphenylcyclopentadienone with phenylacetylene in refluxing diphenyl ether gave pentaphenylbenzene (**15**) in 91% yield.[28] Subsequent bromination in neat bromine produced pentakis(4-bromophenyl)benzene (**16**) in 58% yield. Treatment of compound **16** with CuCN in DMF provided pentakis(4-cyanophenyl)benzene (**17**) in 31% yield. Finally, the reaction of pentanitrile **17** with dicyandiamide under standard conditions gave compound **6** in 76% yield.

Scheme 3.

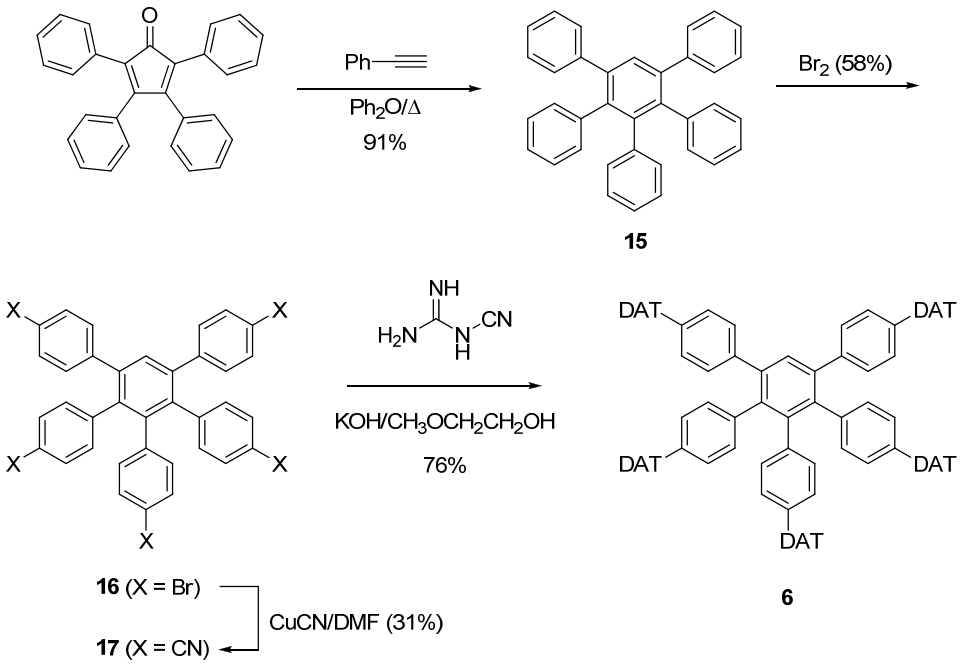

Synthesis of Tecton 7. Tetraphenylbenzene **7** was prepared from the commercially available dimer of 2,5-dimethyl-3,4-diphenylcyclopentadienone, which reacted with diphenylacetylene in hot diphenyl ether to give 1,4-dimethyl-2,3,5,6-tetraphenylbenzene (**18**) in 81% yield (Scheme 4).[29] Bromination using neat bromine produced the desired tetrabromide **19** in 81% yield. This reaction was carried out in the dark to avoid benzylic bromination. The subsequent reaction of tetrabromide **19** with CuCN in DMF provided the corresponding tetranitrile **20** in 66% yield. Finally, treatment of compound **20** with dicyandiamide under standard conditions gave target **7** in 78% yield.

Scheme 4.

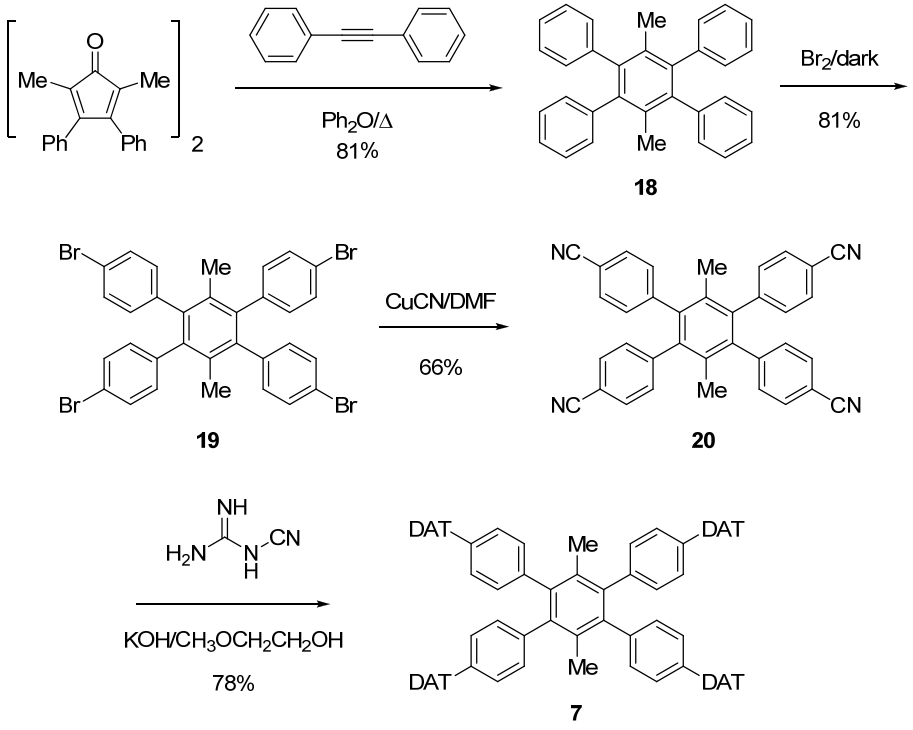

Scheme 5.

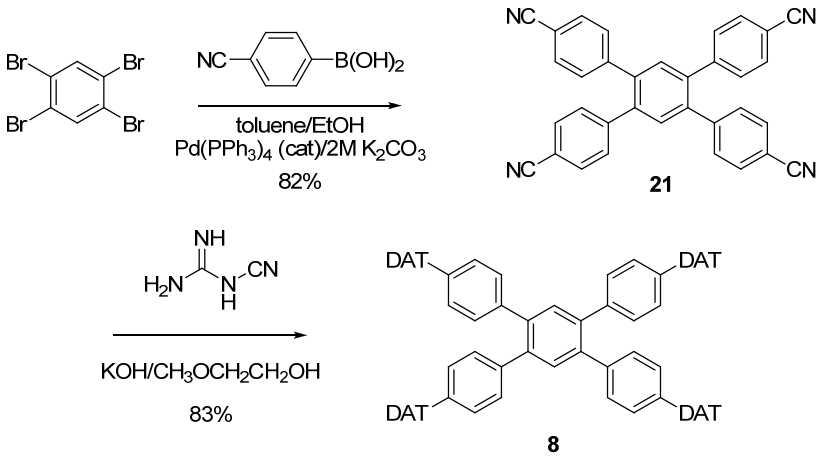

Synthesis of Tecton 8. Tetraphenylbenzene **8** was most conveniently prepared by an alternative approach involving a fourfold Suzuki-Miyaura coupling of commercially available 1,2,4,5-tetrabromobenzene with 4-cyanophenylboronic acid[30] to give 1,2,4,5-tetrakis(4-cyanophenyl)benzene (**21**) in 82% yield (Scheme 5). Subsequent treatment of tetranitrile **21** with dicyandiamide under standard conditions gave target **8** in 83% yield.

Structures of Crystals of Tecton 4. Hexaphenylbenzene **4** showed low solubility in most organic solvents but could be crystallized by allowing vapors of suitable cosolvents to diffuse into solutions in DMSO or formic acid. Crystals suitable for study by X-ray diffraction were obtained from DMSO/THF, DMSO/toluene, DMSO/benzene, and formic acid/methanol. Their structures were solved to allow comparison of the resulting hydrogen-bonded networks.

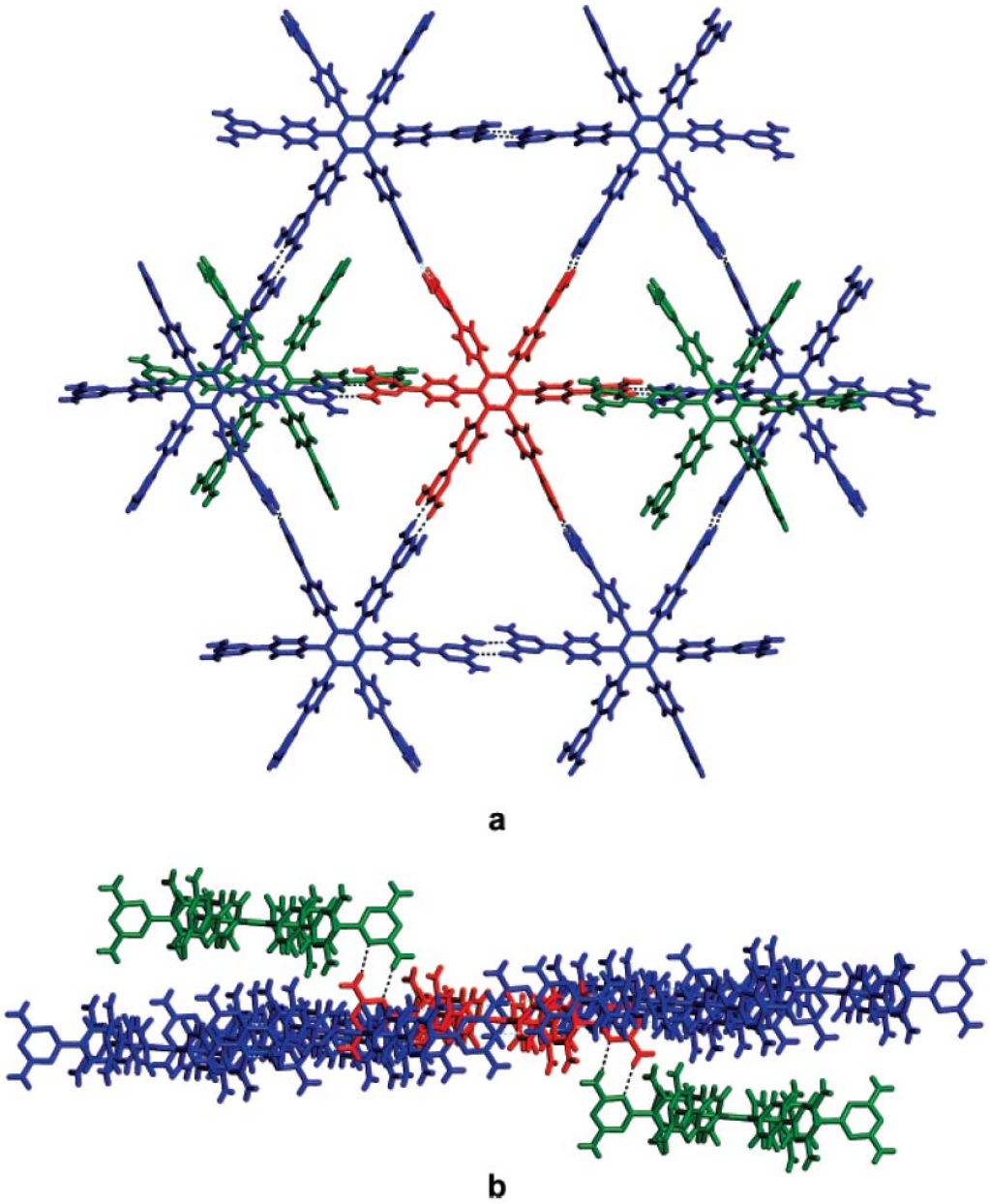

Figure 2. (a) View of the structure of crystals of tecton **4** grown from DMSO/THF, showing a central molecule (red) and its eight hydrogen-bonded neighbors (blue and green). Six of the neighbors (blue) lie approximately in the plane of the central molecule and interact according to motif **I**, and the other two (green) lie above and below the plane and form hydrogen bonds of type **III** with the central molecule (red). (b) Side view showing the two neighbors in green above and below the plane. In both views, guests are omitted for clarity, and hydrogen bonds are represented by broken lines.

Table 2. Conformations Adopted by the Arylbenzene Cores in Crystals of Hexaphenylbenzenes **4**-**5** and Related Compounds **6**-**8**.

compound (conditions of crystallization in parentheses)	angles (°) between the average planes of the aryl substituents and central ring of the arylbenzene core
4 (DMSO/THF)	67.0(2), 63.3(2), 68.4(2), 67.7(2), 62.3(2), 66.2(2)
4 (DMSO/toluene)	66.4(3), 74.1(2), 89.8(2)
4 (DMSO/benzene)	66.08(11)
4 (HCOOH/EtOH)	88.88(15)
5 (DMSO/MeCN)	59.88(9), 80.48(9), 85.63(9) (2x), 88.59(10) (2x)
6 (DMSO/acetone)	41.9(2) (2x), 56.09(19), 62.4(2) (2x)
7 (DMSO/dioxane)	84.50(12)
7 (DMSO/MeOH)	67(1), 72(1), 80(1), 81(1)
8 (DMSO/acetone)	40.06(16) (2x), 65.17(16) (2x)

Structure of Crystals of Tecton 4 Grown from DMSO/ THF. The crystals were found to belong to the triclinic space group *P*-1 and to have the approximate composition **4**•9DMSO•7THF•*x*H_2O.[31] As anticipated (Figure 1a), the six diaminotriazine groups of each tecton form hydrogen bonds according to motif **I** with six neighbors, thereby defining parallel sheets held together by 12 hydrogen bonds per tecton (Figure 2a). The hexaphenylbenzene core of compound **4** adopts a characteristic chiral propeller-shaped conformation with approximate 6-fold symmetry, as observed in many other derivatives of hexaphenylbenzene.[23,32] The angles between the average plane of the central aromatic ring and those of the six aryl substituents lie in the range 62.3(2)°-68.4(2)° (Table 2). The sheets consist of equal numbers of the two enantiomers.

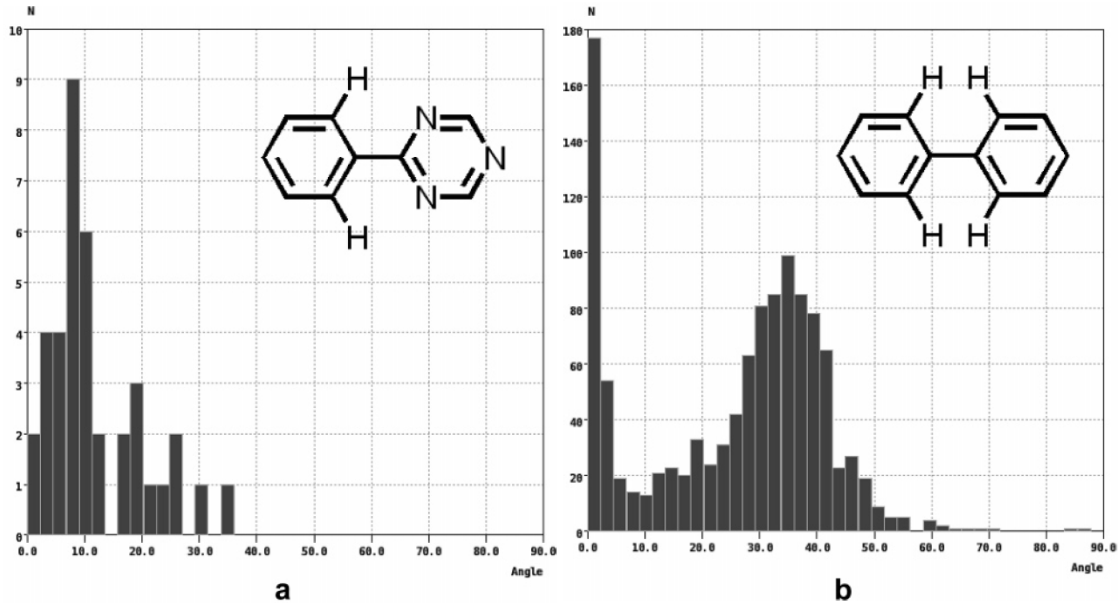

Figure 3. Histograms showing the frequency of torsional angles between the average planes of the aromatic rings in 2-phenyl-1,3,5-triazines and biphenyls, as observed in crystal structures compiled in the Cambridge Structural Database (Version 5.27). Structures containing metals or with atoms other than hydrogen at the indicated positions were not included in the analysis to avoid torsional effects arising from coordination or from ortho substitution. In addition, phenyltriazines in which the atoms of nitrogen were protonated or otherwise substituted were removed individually from the set of data.

A subtle but important element in the design of hexaphenylbenzene **4**, modified tectons **5**-**8**, and related compounds is the strong tendency of 2-phenyl-1,3,5-triazines to adopt conformations in which the phenyl and triazine rings are nearly coplanar. In 2,4,6-triphenyl-1,3,5-triazine, for example, the planes of the three phenyl substituents are tilted by an average of only 8.5° with respect to the plane of the triazine core.[33] Similar conformational preferences have been noted in many other simple phenyltriazines.[34] Data compiled in the Cambridge Structural Database (Version 5.27) demonstrate that torsional angles in 2-phenyl-1,3,5-triazines (Figure 3a) tend to be significantly smaller than those observed for biphenyls (Figure 3b), and those found in 2-phenylpyrimidines are similarly small.[35] In crystals of tecton **4** grown from DMSO/THF, the average deviation from coplanarity is 12.9(3)°. This ensures that the diaminotriazine groups are oriented in a way that extends the propeller shape of the hexaphenylbenzene core and

directs hydrogen-bonding sites out of the plane defined by each tecton and its six principal neighbors.

As a result, each tecton can form another four hydrogen bonds of type **III** to two additional neighbors in adjacent sheets (Figure 2b). This links the sheets into a three-dimensional network, and each tecton participates in a total of 16 intertectonic hydrogen bonds involving eight neighbors (Table 1). As expected, no interpenetration of independent networks is observed; instead, a single open network is favored, and 70% of the volume of the crystal is accessible to guests, which are partly disordered.[10,11] The guests occupy interconnected channels that in principle give new guests access to the interior of the crystal. The largest channels are triangular and aligned with the *b*-axis, and smaller channels run along the *a*-axis (Figure 4).

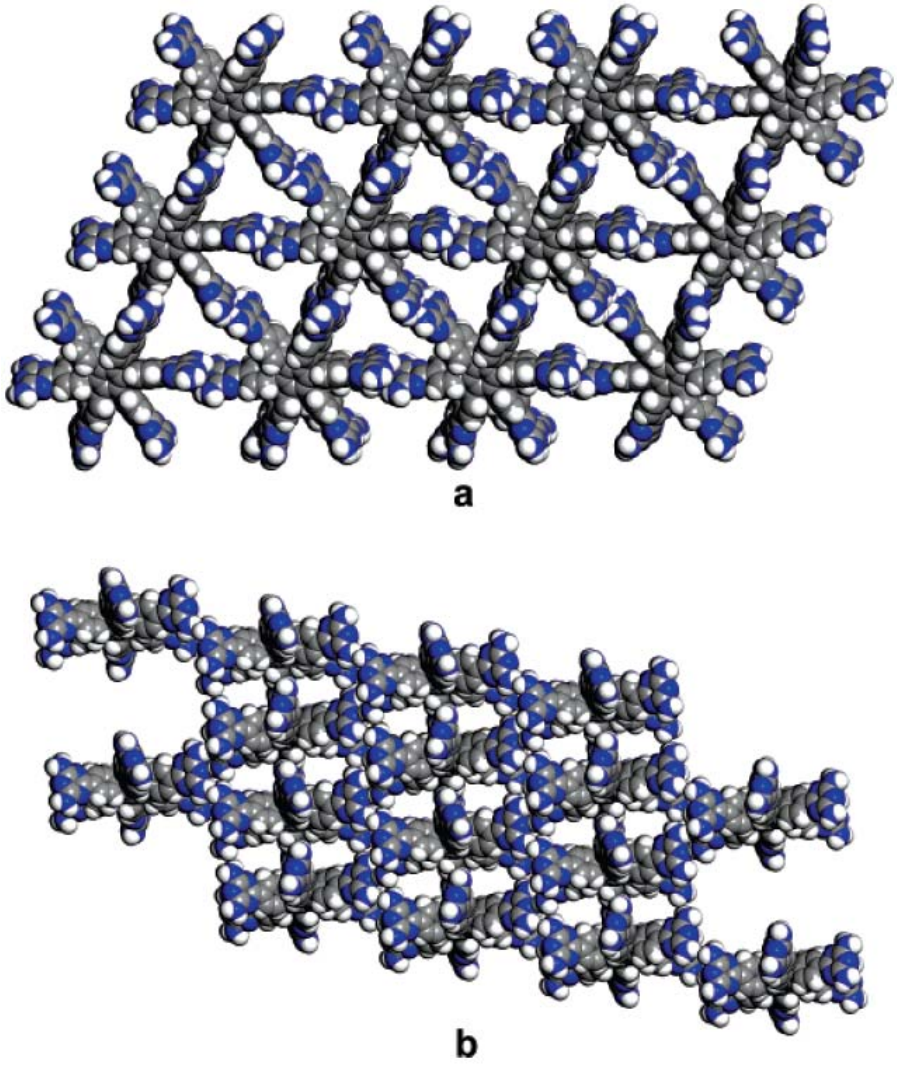

Figure 4. Views of the structure of crystals of tecton **4** grown from DMSO/THF, showing (a) large triangular channels along the *b*-axis and (b) smaller channels along the *a*-axis. Both views show a 3 × 2 × 3 array of unit cells. Guests are omitted for clarity, and atoms are represented by spheres of van der Waals radii to show the cross sections of the channels. Atoms of hydrogen appear in white; carbon in gray; and nitrogen in blue.

Examination of the overall structure confirms that multiple key features result predictably from design. In particular, compound **4** crystallizes as a non-interpenetrated three-dimensional hydrogen-bonded network built from sheets in which each tecton interacts as planned with six neighbors. In this design, the natural tendency of hexaphenylbenzenes and other disc-shaped molecules to form layered structures is strongly reinforced by intrasheet hydrogen bonding. As planned, the six diaminotriazine

groups of compound **4** are nearly coplanar with the phenyl arms of the hexaphenylbenzene core, thereby extending its propeller conformation predictably. This ensures the formation of additional intersheet hydrogen bonds, although we acknowledge that the precise mode of stacking of the sheets and the nature of the resulting channels could not have been foreseen with confidence. As measured by the volume accessible to guests and the number of hydrogen bonds per tecton, the network formed by compound **4** is significantly more open and robust than those built from simpler analogues **1**-**3**, placing it among the most impressive molecular networks observed so far.

Structure of Crystals of Tecton 4 Grown from DMSO/Toluene. Our assertion that key features of the structure resulted from rational design was tested rigorously by searching for pseudopolymorphs formed under other conditions. Crystals grown by allowing vapors of toluene to diffuse into a solution of tecton **4** in DMSO also proved to belong to the triclinic space group *P*-1. Their composition was determined by crystallography to be **4**•6DMSO•H_2O. Again, each tecton interacts with six neighbors according to hydrogen-bonding motif **I** to define sheets.[35] The hexaphenylbenzene core is characteristically nonplanar (Table 2), allowing four additional hydrogen bonds to link each tecton to two neighbors located in adjacent sheets.[35] The resulting network is three-dimensional and held together by a total of 16 hydrogen bonds per tecton (Table 1), like that found in crystals grown from DMSO/THF. The only significant architectural difference between the two networks is in the precise way the sheets are connected.[35] Packing of the sheets appears to be somewhat more efficient in crystals grown from DMSO/toluene, leading to a smaller percentage of volume accessible to guests (56%).[10,11] The guests occupy large parallel triangular channels that run along the a-axis and are similar to those observed in crystals grown from DMSO/THF (Figure 4a), but they are not interconnected by other significant channels. Despite these minor differences, the structures of crystals grown from DMSO/THF and DMSO/toluene show close overall similarity, supporting the conclusion that the observed networks are the result of logical design.

Structure of Crystals of Tecton 4 Grown from DMSO/Benzene. A further test of this conclusion was carried out by analyzing crystals grown by the diffusion of vapors of benzene into a solution of tecton **4** in DMSO. The resulting crystals were found to belong to the trigonal space group *R*-3 and to have the approximate composition **4**•12DMSO•12benzene•*x*H_2O.[31] The network formed is similar to the two already described, although some new features appear. Again, each tecton interacts directly with six neighbors by hydrogen bonding according to motif **I**. However, the neighbors lie alternately above and below the plane defined by the central tecton, giving rise to an irregular sheet in which the neighbors cannot interact directly but instead are bridged by hydrogen bonds to intervening molecules of DMSO (Figure 5). In this way, each molecule of hexaphenylbenzene **4** participates in 12 hydrogen bonds with neighboring tectons and 12 more with included molecules of DMSO (Table 1). The resulting network is highly open, and 72% of the volume is accessible to guests, which occupy interconnected channels.[10,11] The largest channels are triangular and aligned with the *c*-axis (Figure 6), and smaller channels lie in other directions. The included DMSO is hydrogen-bonded to tecton **4** and ordered, whereas included benzene and the phenyl arms of the hexaphenylbenzene core are statistically disordered (Table 2).

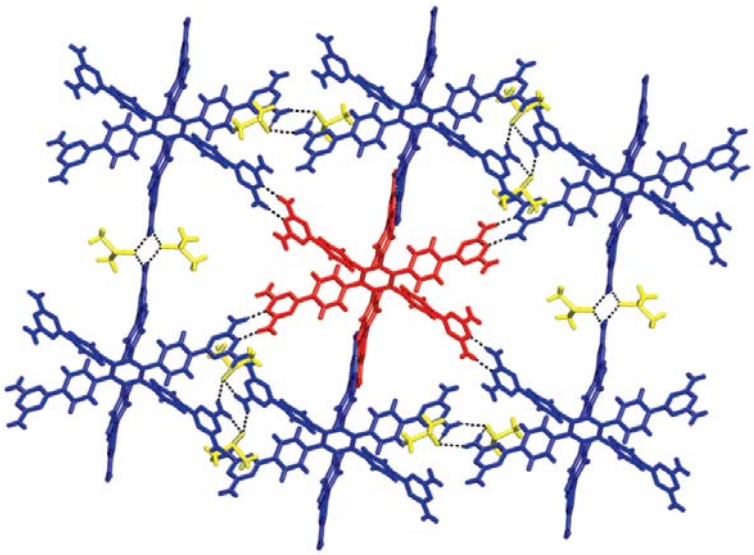

Figure 5. View of the structure of crystals of tecton **4** grown from DMSO/benzene, showing a central molecule (red) and its six hydrogen-bonded neighbors (blue). The six neighbors (blue) lie alternately above and below the plane of the central molecule (red), and they are bridged by hydrogen bonds to molecules of DMSO (yellow). Guests are omitted for clarity, and hydrogen bonds are represented by broken lines.

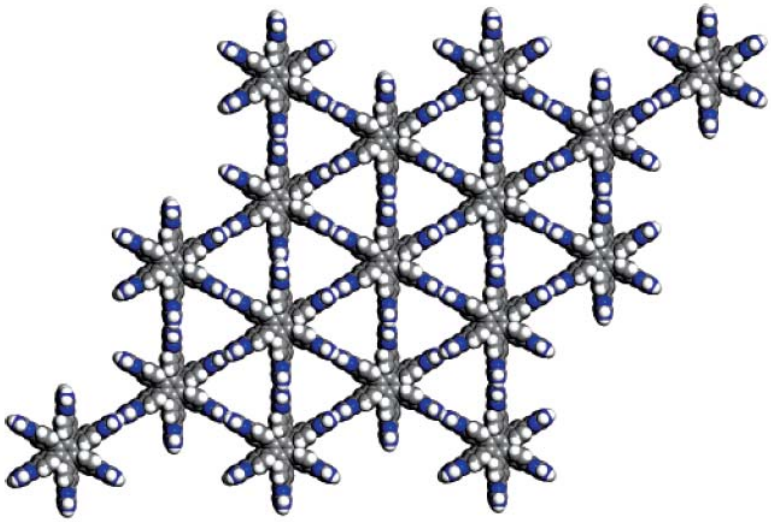

Figure 6. View of the structure of crystals of tecton **4** grown from DMSO/benzene, showing a 2 × 2 × 2 array of unit cells along the *c*-axis. Guests are omitted for clarity, and atoms are represented by spheres of van der Waals radii to show the cross sections of the channels. Atoms of hydrogen appear in white; carbon in gray; and nitrogen in blue.

Structure of Crystals of Tecton 4 Grown from Formic Acid/Methanol. The marked tendency of hexaphenylbenzene **4** to form three-dimensional networks built from sheets in which each tecton interacts with six neighbors by forming 12 hydrogen bonds according to motif **I** was further tested by growing crystals under distinctly different conditions. Vapors of methanol were allowed to diffuse into a solution of compound **4** in formic acid, and the resulting crystals were found to belong to the trigonal space group *R*-3. Included solvent proved to be disordered, and the composition could not be determined accurately by crystallography. Again, each tecton interacts with six neighbors in the expected way, leading to the formation of sheets closely similar to those observed in crystals grown from DMSO/THF and DMSO/toluene.[35] In each tecton, the six phenyl arms of the hexaphenylbenzene core are virtually perpendicular to the central benzene ring (Table 2). This conformation allows each tecton to engage in a total of 24 additional hydrogen bonds of type **III** with six other neighbors, of which three are in each of the two adjacent sheets.[35] The resulting network is three-dimensional, each tecton participates in a total of 36 hydrogen bonds, and 56% of the volume is accessible to guests (Table 1).[10,11] In this structure, adjacent sheets are offset in a way that prevents the formation of conspicuous channels perpendicular to the plane of the characteristic sheets (Figure 7).

Together, the structures of the four pseudopolymorphs described above provide strong evidence that tecton **4** has been successfully engineered to favor crystals with the following specific features: (1) Each structure is built from a heptameric unit in which a central tecton forms hydrogen bonds of type **I** with six neighbors; (2) further association of these heptameric units leads to the formation of sheets; (3) the characteristic nonplanar conformations adopted by the hexaphenylbenzene core, in conjunction with the tendency of the triazine rings to lie close to the planes of the phenyl arms to which they are grafted, promote hydrogen bonding between sheets, thereby leading to the formation of three-dimensional networks held together by up to 36 hydrogen bonds per tecton; (4) no interpenetration of independent networks is observed; and (5) spaces between and within the sheets allow the inclusion of guests, and the percentage of accessible volume (56%-72%) consistently approaches the highest values so far

observed in molecular networks. Although the networks produced by tecton **4** under different conditions of crystallization are not strictly identical, their close similarity supports a key principle of molecular tectonics: molecules with well-defined geometries and multiple sites of strong directional interactions do not tend to crystallize in widely divergent polymorphic forms.[7]

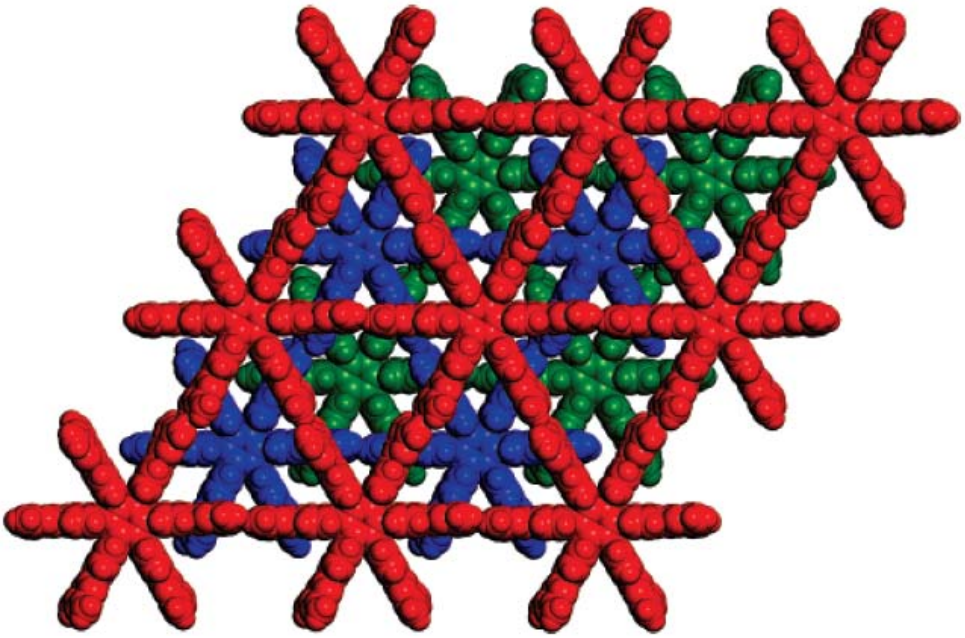

Figure 7. Representation of the structure of crystals of tecton **4** grown from formic acid/methanol, showing a 2 × 2 × 2 array of unit cells viewed along the *c*-axis. Three successive offset sheets are colored in red, blue, and green. Guests are omitted for clarity, and atoms are represented by spheres of van der Waals radii to confirm the absence of channels perpendicular to the sheets.

Hydrogen-Bonded Networks Formed by Mutated Tectons 5-8. Having demonstrated an important degree of control in constructing networks from hexaphenylbenzene **4**, we then put our understanding to a further test by probing the effect of selected structural modifications. Analogues **5-8** were synthesized and crystallized to reveal how removal of specific diaminotriazine groups or phenyl groups from the hexaphenylbenzene core would change how crystallization occurs.

Structure of Crystals of Tecton 6 Grown from DMSO/Acetone. In tecton **6**, one of the phenyl arms of the hexaphenylbenzene core has been excised, thereby

producing a pentaphenylbenzene with five attached diaminotriazine groups. Crystals grown by diffusion of vapors of acetone into a solution of tecton **6** in DMSO proved to belong to the monoclinic space group *C*2/*c* and to have the approximate composition **6**•8DMSO•*x*H2O.[31] In the resulting structure, each tecton uses four of its five diaminotriazine groups to form a total of eight hydrogen bonds of type **I** with four neighbors (Figure 8). The fifth group does not form hydrogen bonds with neighboring tectons and interacts instead with included molecules of DMSO. The resulting pentameric motif generates the hydrogen-bonded sheets represented by Figure 1b and shown from the side in Figure 9. Removal of one of the arms of the hexaphenylbenzene core allows the remaining phenyl spacers to adopt orientations closer to the plane of the central benzene ring (Table 2). This flattening of the molecular structure prevents tectons in one sheet from engaging in direct hydrogen bonding with tectons in adjacent sheets. Instead, the sheets are linked into an offset three dimensional network by hydrogen bonds involving bridging molecules of DMSO. No interpenetration is observed, and 55% of the volume of the crystal is accessible to guests (Table 1).[10,11] Guests occupy distinct channels that lie along the *c*-axis and incorporate the unpaired diaminotriazine groups. The accessible volume is slightly lower than that observed in structures of tecton **4**, even though removal of a significant part of the molecule might have been expected to increase porosity. This is presumably because the flattened pentaphenylbenzene core permits closer packing of the sheets. Despite this important change, however, mutated tecton **6** continues to resemble hexaphenylbenzene **4** in key ways. Specifically, a sheet structure maintained by multiple hydrogen bonds of type **I** is retained, and the resulting network is noninterpenetrated and highly porous.

Structure of Crystals of Tecton 5 Grown from DMSO/Acetonitrile. The behavior of pentaphenylbenzene **6** helped clarify the importance of the conformation of the core and suggested that analysis of derivatives of tecton **4** with an intact hexaphenylbenzene core but less than six diaminotriazine groups would be informative. Crystals of tetrasubstituted hexaphenylbenzene **5** were grown by allowing vapors of acetonitrile to diffuse into a solution in DMSO. The crystals were found to belong to the monoclinic space group *C*2/*c* and to have the composition **5**•8DMSO•6CH_3CN. The

observed structure is closely consistent with the pattern established by hexasubstituted analogue **4**. In particular, tecton **5** engages in a total of eight hydrogen bonds of type **I** with four neighbors, and the resulting pentameric unit defines a sheet (Figure 10a). The hexaphenylbenzene core of each tecton adopts a characteristic nonplanar conformation (Table 2), which permits the formation of four additional hydrogen bonds to two other tectons in adjacent sheets (Figure 10b). The resulting network is noninterpenetrated and highly open, with 60% of the volume of the crystal accessible to guests (Table 1).[10,11] Again, the guests occupy channels that run perpendicular to the plane of the sheets (Figure 11), and the unsubstituted phenyl groups face one another across the channels, as represented schematically by Figure 1c. The closely parallel behavior of hexaphenylbenzenes **4** and **5** provides a compelling example of successful crystal engineering and underscores the importance of maintaining a consistent molecular shape.

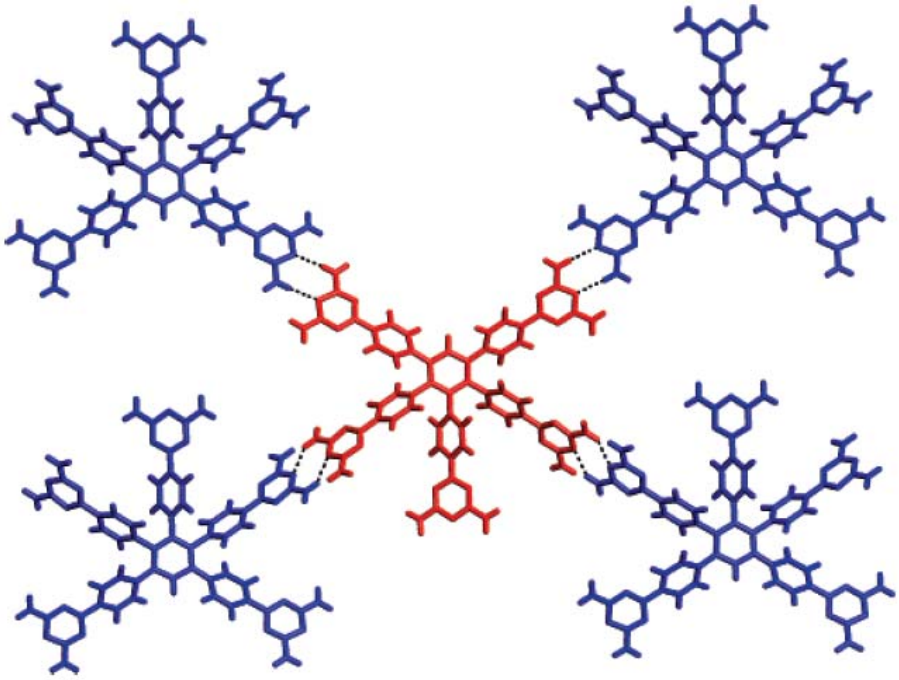

Figure 8. View of the structure of crystals of tecton **6** grown from DMSO/acetone, showing a central molecule (in red) and its four coplanar neighbors (blue), which are linked to the central molecule by hydrogen bonds of type **I**. Guests are omitted for clarity, and hydrogen bonds are represented by broken lines.

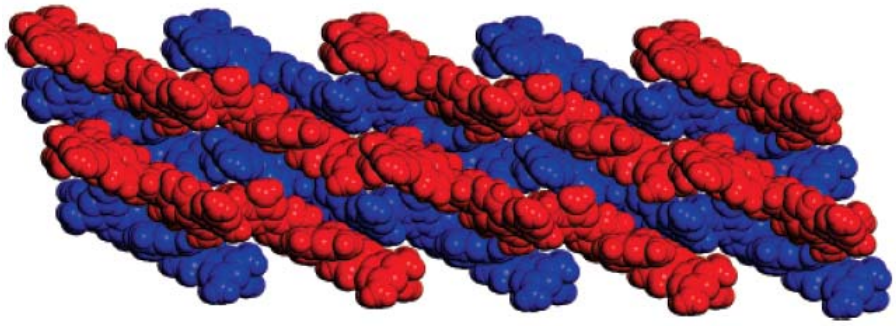

Figure 9. View of the structure of crystals of tecton **6** grown from DMSO/acetone, showing a 2 × 2 × 2 array of unit cells viewed along the *b*-axis with successive sheets colored in red and blue. Guests are omitted for clarity, and atoms are represented by spheres of van der Waals radii.

Structure of Crystals of Tecton 7 Grown from DMSO/Dioxane. In tetraphenylbenzene **7**, the two unsubstituted phenyl groups of hexaphenylbenzene **5** have been replaced by methyl groups. The new substituents were chosen to be (1) large enough to force tecton **7** to adopt a conformation similar to that of tecton **5**, with the remaining four phenyl groups held well out of the plane of the central aromatic ring, but (2) small enough to yield crystals in which the volume accessible to guests is increased significantly. Crystals were obtained by allowing dioxane to diffuse slowly into a solution of compound **7** in DMSO. The crystals proved to belong to the monoclinic space group *C*2/*m*, to have the approximate composition **7**•10DMSO•*x*H2O[31] and to adopt a structure in close agreement with expectations. In particular, tecton **7** forms eight hydrogen bonds of type **I** with four neighbors to define a sheet (Figure 12a). As planned, the methyl groups enforce a conformation in which the central aromatic ring forms large dihedral angles with the four remaining phenyl arms (Table 2). Moreover, the established preference for nearly coplanar alignment of the triazines then allows the formation of four additional hydrogen bonds of type **III** to two tectons in adjacent sheets (Figure 12b). The resulting network is noninterpenetrated and defines large channels (Figures 13- 15).[36] The most impressive are aligned with the *c*-axis and measure approximately 9.6 × 15 Å^2, and 75% of the volume of the crystals is accessible to guests (Table 1).[10,11] The porosity equals the current record for crystals built from small molecules.[5,6] By yielding a network with an architecture closely similar to that of model

5, and by increasing the volume accessible to guests from 60% to 75%, tecton **7** behaved according to plan, demonstrating how new structures with predictable features can be engineered by following the guidelines of molecular tectonics.

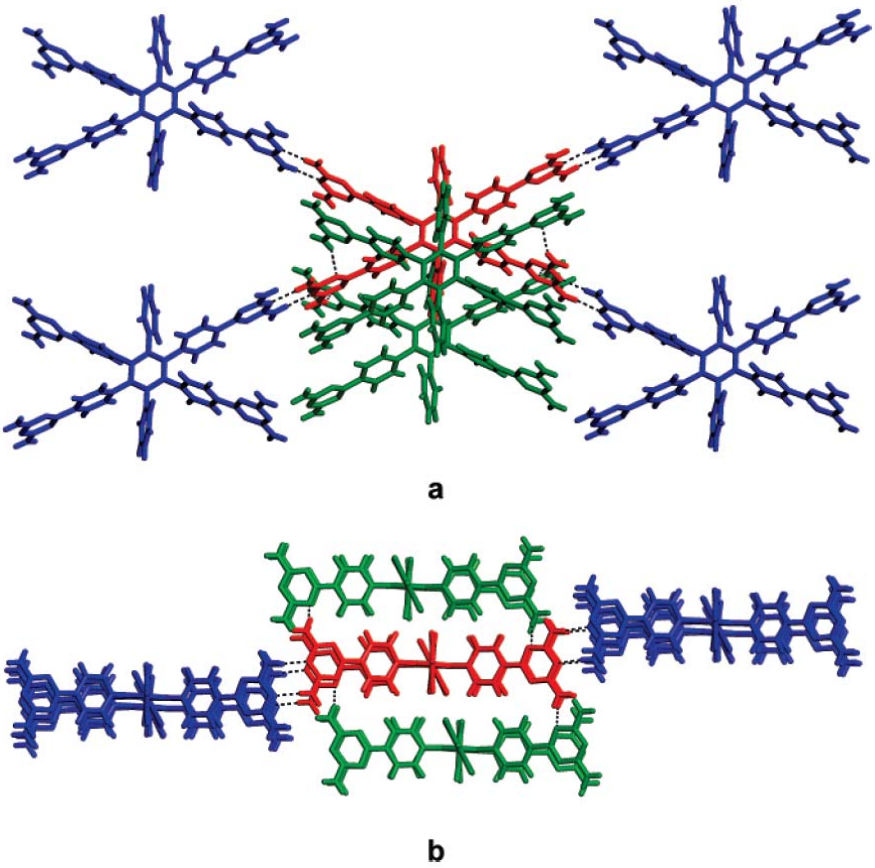

Figure 10. (a) View of the structure of crystals of tecton **5** grown from DMSO/acetonitrile, showing a central molecule (red) and its six hydrogen-bonded neighbors (blue and green). Four of the neighbors (blue) lie approximately in the plane of the central molecule and form hydrogen bonds to it via motif **I**. The remaining two neighbors (green) lie above and below the sheet. (b) Side view of the central molecule (red) and its six hydrogen-bonded neighbors (blue and green). In both views, guests are omitted for clarity, and hydrogen bonds are represented by broken lines.

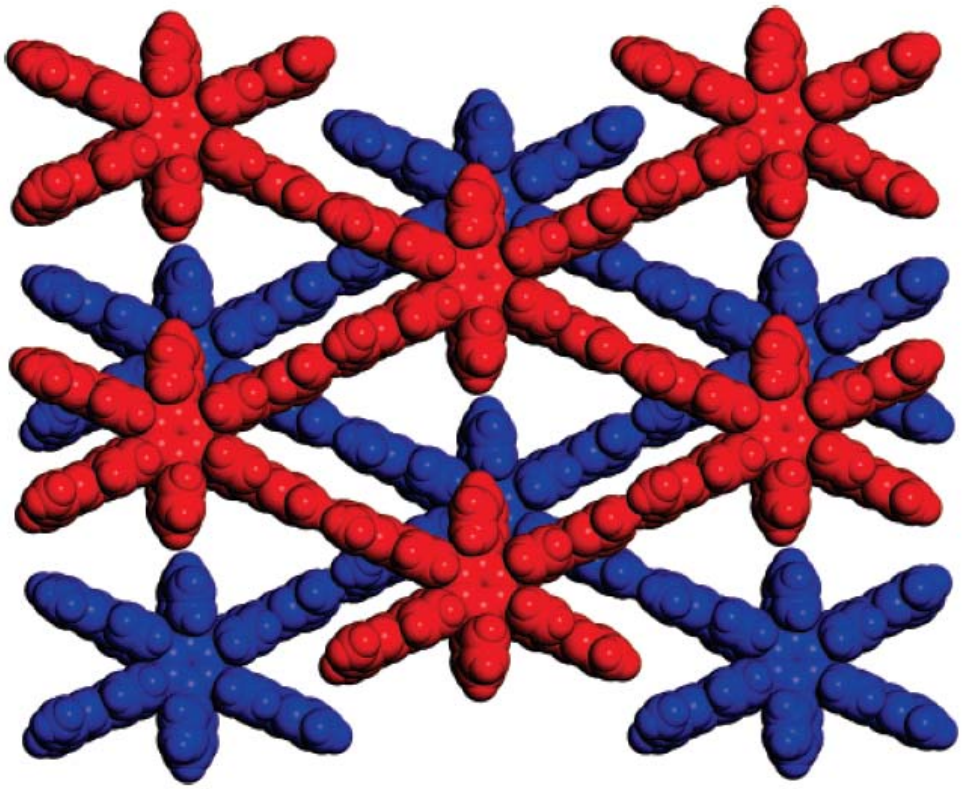

Figure 11. Representation of the structure of crystals of tecton **5** grown from DMSO/acetonitrile, showing two successive offset hydrogen-bonded sheets in red and blue. The image shows a 1 × 2 × 2 array of unit cells viewed along the *c*-axis, with guests omitted for clarity and atoms represented by spheres of van der Waals radii to reveal the cross sections of channels.

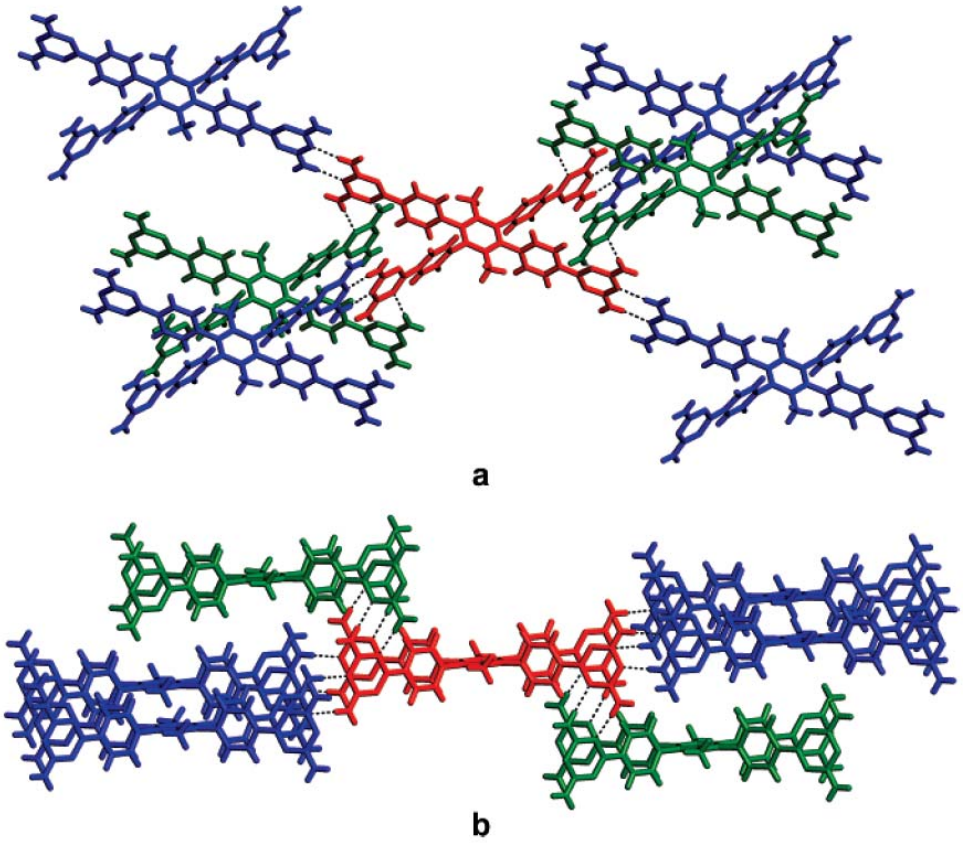

Figure 12. (a) View of the structure of crystals of tecton **7** grown from DMSO/dioxane, showing a central molecule (red) and its six hydrogen-bonded neighbors (blue and green). Four of the neighbors (blue) interact according to motif **I** and lie approximately in the plane of the central molecule, and the other two (green) form hydrogen bonds of type **III** and lie above and below the plane. (b) Side view showing the two neighbors in green above and below the plane. In both views, guests are omitted for clarity, and hydrogen bonds are represented by broken lines.

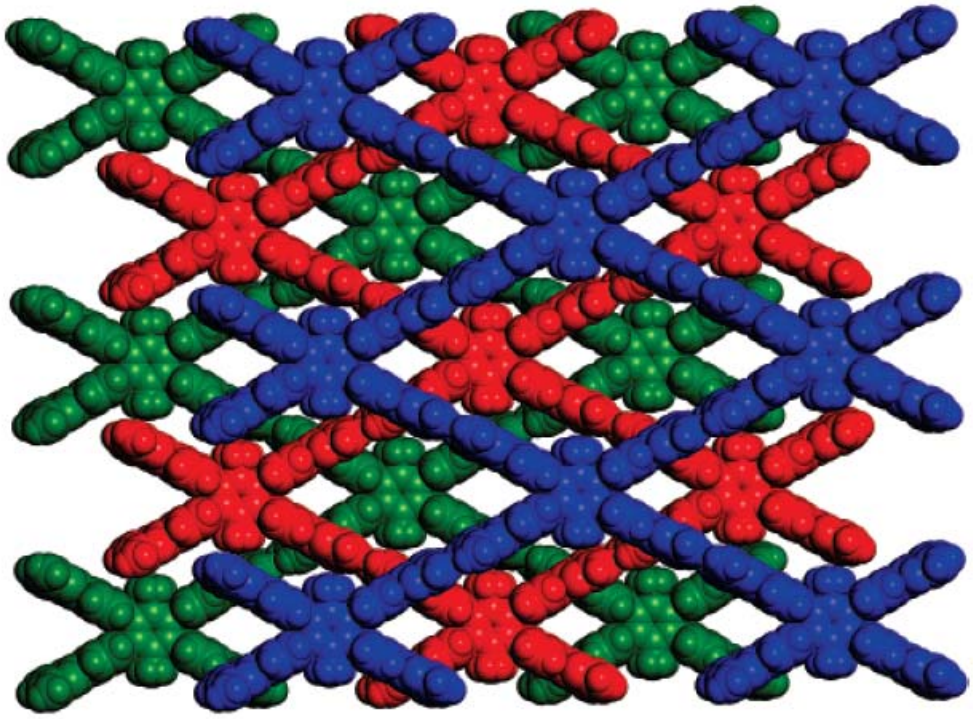

Figure 13. Representation of the structure of crystals of tecton **7** grown from DMSO/dioxane, showing three successive offset sheets colored in red, blue, and green. Guests are omitted for clarity, and atoms are represented by spheres of van der Waals radii.

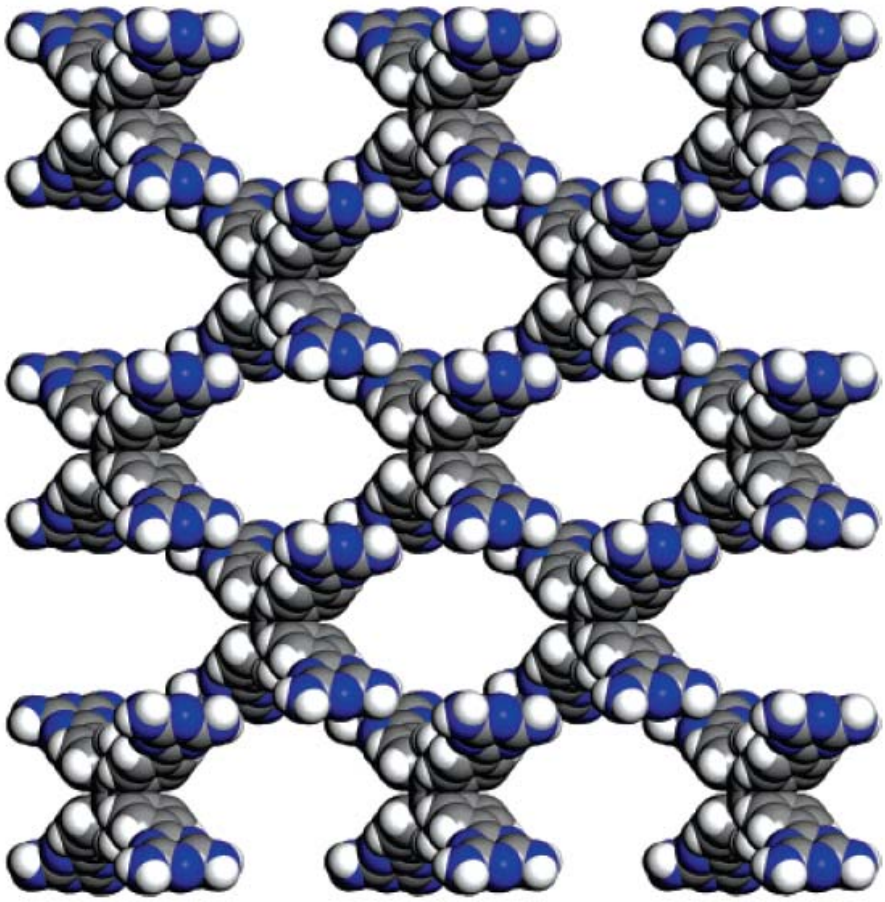

Figure 14. View of the structure of crystals of tecton **7** grown from DMSO/dioxane, showing a 2 × 2 × 2 array of unit cells along the *c*-axis. Guests are omitted for clarity, and atoms are represented by spheres of van der Waals radii to show the cross sections of the channels. Atoms of hydrogen appear in white; carbon in gray; and nitrogen in blue.

Figure 15. Representation of channels along the *c*-axis in the network resulting from crystallization of tecton **7** from DMSO/dioxane. The image shows a 2 × 2 × 2 array of unit cells. The outsides of the channels appear in dark gray, and light gray is used to show where the channels are cut by the boundaries of the array. The surface of the channels is defined by the possible loci of the center of a sphere of diameter 6 Å as it rolls over the surface of the ordered network.[36]

Structure of Crystals of Tecton 7 Grown from DMSO/Methanol. To test the reliability of these guidelines, we searched for pseudopolymorphs formed under other conditions. Crystals grown by slow diffusion of methanol into a solution of compound **7** in DMSO were found to belong to the monoclinic space group *P*21/*c* and to have the composition **7**•8DMSO•4H_2O. In the resulting structure, one of the diaminotriazine groups is disordered over two positions, which complicates analysis of the hydrogen bonding. Each tecton forms hydrogen bonds with four neighbors, thereby generating a sheet (Figure 16). Unlike all previously analyzed structures, in which the characteristic sheets are maintained by hydrogen bonds of type **I**, those generated when tecton **7** is crystallized from DMSO/methanol are held together by hydrogen bonds of types **II** and **III**. Moreover, adjacent sheets do not appear to form hydrogen bonds with each other, despite the nonplanar conformation of tecton **7** (Table 2). In addition, the network is 2-fold interpenetrated (Figure 17), and only 39% of the volume is accessible to guests

(Table 1). Together, the observations of significantly lower porosity, interpenetration, and deviations from established patterns of hydrogen bonding show that significant alterations of the hexaphenylbenzene core of tectons **4** and **5** can have subtle and unexpected effects. In the particular case of tecton **7**, key conformational features of the aromatic core are successfully maintained, but the smaller methyl groups appear to allow neighboring molecules to approach more closely.

Structure of Crystals of Tecton 8 Grown from DMSO/Acetone. Further confirmation of the importance of an intact hexaphenylbenzene core was obtained by studying the behavior of tecton **8**, which is derived from 1,2,4,5-tetraphenylbenzene. Crystals grown by diffusion of vapors of acetone into a solution of compound **8** in DMSO were found to belong to the monoclinic space group $P2_1/c$ and to have the composition **8**•12DMSO. As expected, tecton **8** adopts a flattened conformation (Table 2) and generates a hydrogen-bonded network that is very different from those derived from analogous hexaphenylbenzenes. Only two diaminotriazine groups in each tecton interact with those of neighbors, thereby producing chains that extend along the *b*-axis and are held together by hydrogen bonds of type **I** (Figure 18a). The remaining diaminotriazine groups engage in hydrogen bonding with included molecules of DMSO, which form bridges to neighboring tectons (Figure 18b). The resulting network is open, and 64% of the volume is accessible to guests (Table 1).

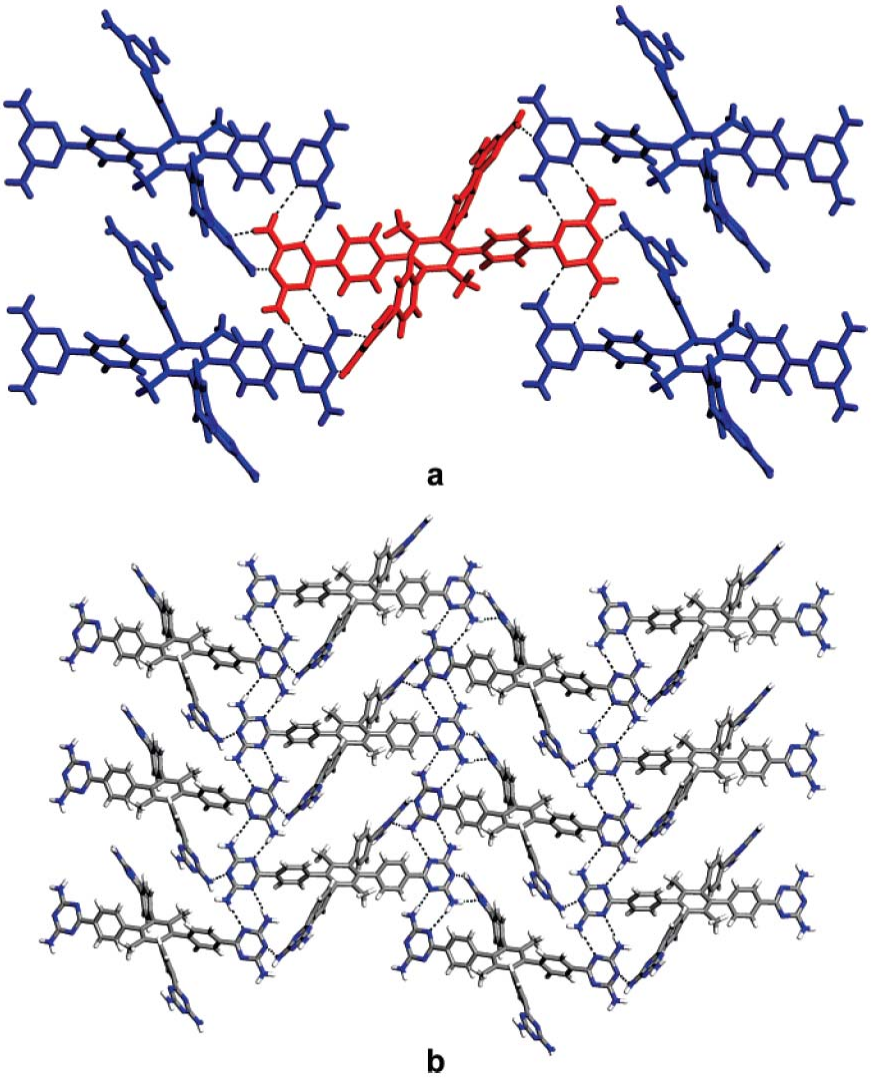

Figure 16. (a) View of the structure of crystals of tecton **7** grown from DMSO/methanol, showing a central molecule (red) and its four hydrogen-bonded neighbors (blue). (b) View of the resulting hydrogen-bonded sheet, with atoms of hydrogen appearing in white; carbon in gray; and nitrogen in blue. In both views, guests are omitted for clarity, and hydrogen bonds are represented by broken lines.

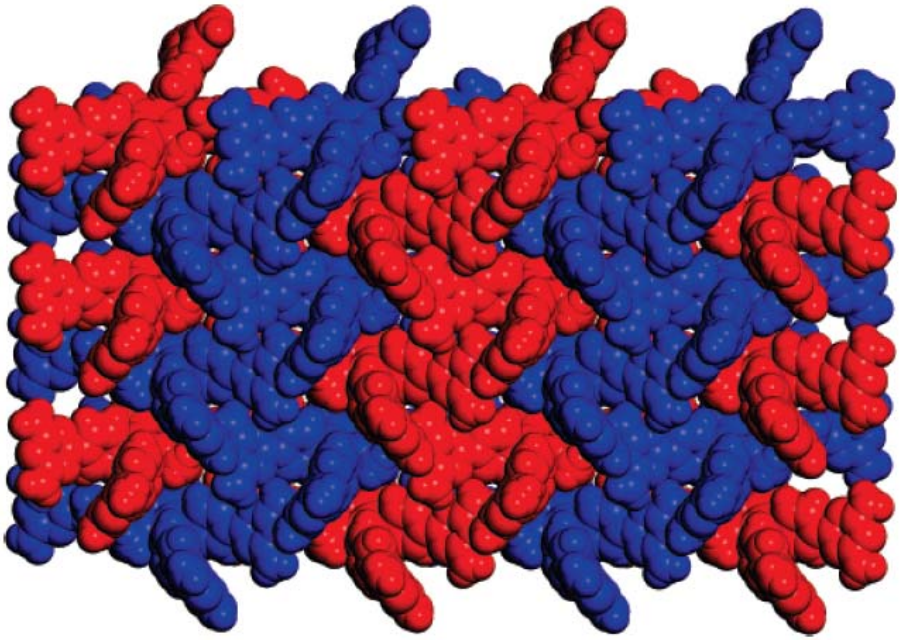

Figure 17. Representation of the structure of crystals of tecton **7** grown from DMSO/methanol, showing the 2-fold interpenetration of hydrogen-bonded sheets (red and blue). Guests are omitted for clarity, and atoms are represented by spheres of van der Waals radii.

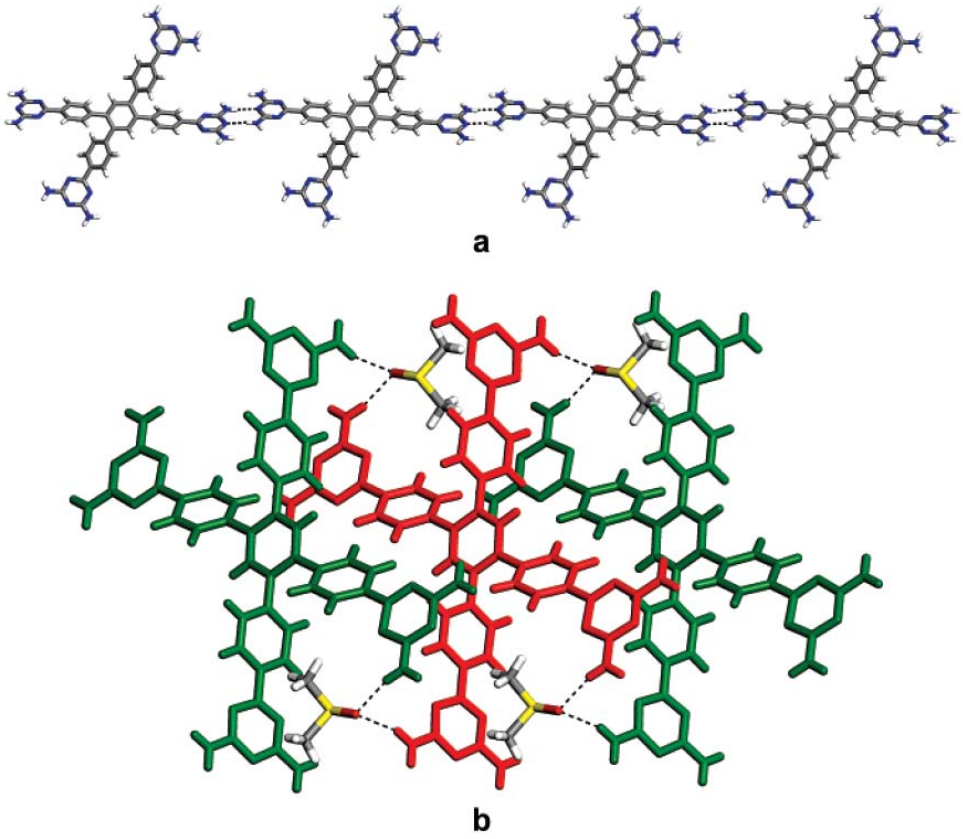

Figure 18. (a) View of the structure of crystals of tecton **8** grown from DMSO/acetone, showing how molecules are linked into chains by hydrogen bonds of motif **I**. Atoms of hydrogen appear in white; carbon in gray; and nitrogen in blue. (b) Additional view of the structure showing how hydrogen bonds involving bridging molecules of DMSO link each tecton (red) to two additional neighbors in adjacent chains (green).

Conclusions

Our study of hydrogen-bonded networks derived from hexaphenylbenzene and related compounds, together with earlier work reported by Kobayashi et al.,[16-18] has yielded a deeper understanding of how to create molecular crystals by design. By examining the behavior of a single compound under multiple conditions of crystallization, and by analyzing the effects of a series of systematic structural modifications, we have tested molecular tectonics as a strategy for engineering crystals with predetermined properties, and we have clearly delineated its current strengths and limitations.

Our results underscore the importance of the geometry of the hexaphenylbenzene core, which reliably adopts nonplanar conformations and has a disc-like shape that inherently favors parallel molecular packing and the formation of layered structures. In tectons **4** and **5**, this tendency has been powerfully reinforced by grafting diaminotriazine groups to the periphery of the hexaphenylbenzene core, thereby ensuring the formation of multiple hydrogen bonds in the molecular plane. Simultaneously, the characteristic nonplanar conformation of the core, along with the preference for nearly coplanar alignment of phenyl-substituted triazines, ensures that additional hydrogen bonds are formed between the sheets, creating three-dimensional networks. Our results show that when a consistent molecular shape is maintained, the results of crystallization have a high degree of predictability. Under all conditions examined, hexaphenylbenzene **4** crystallizes as planned to give noninterpenetrated three-dimensional networks built from sheets in which each tecton forms hydrogen bonds of type **I** with six neighbors. In addition, the behavior of analogues **5** and **7**, which have conformationally similar cores but only four diaminotriazine groups, is closely parallel. In these structures, the number of hydrogen bonds per tecton and the percentage of volume accessible to guests consistently exceed those reported for the simpler derivatives studied earlier by Kobayashi et al., and they reach the highest values so far observed in molecular networks. Together, these results provide an impressive demonstration of the ability of molecular tectonics to control crystallization, and they suggest that new tectons with more complex nonplanar aromatic cores and multiple sites of hydrogen bonding can be designed to produce networks with even higher degrees of porosity and robustness.

Our results also demonstrate that major structural alterations of the hexaphenylbenzene core can change the architecture of the resulting network significantly. In particular, analogues with flatter pentaphenylbenzene and tetraphenylbenzene cores yield crystals with different features. It is important to note that we have not been able to compare the structures of crystals of tectons **4**-**8** grown under identical conditions. However, our thorough investigation of the pseudopolymorphs of compound **4** has established that key structural features are

maintained in all crystals examined. Moreover, the networks generated by tectons **4**-**8** have many shared properties despite significant differences in the conditions of crystallization. For these reasons, we believe that our work defines the current state of the art in crystal engineering and illustrates primarily the systematic effect of modifying the molecular components of crystals, not the conditions of crystallization.

Experimental Section

All reagents and solvents were purchased from commercial sources and used without further purification unless otherwise indicated. Hexakis(4-cyanophenyl)benzene (**11**) was prepared from hexakis(4-bromophenyl)benzene (**10**)[21,22] as described previously.[23] Anhydrous and oxygen-free solvents (DMF and toluene) were obtained by passage through columns packed with activated alumina and supported copper catalyst (Glass Contour, Irvine, CA). NMR spectra were recorded using a Bruker AV400 spectrometer, and high-resolution mass spectra were obtained using an Agilent LC-MSD TOF spectrometer. Elemental analyses were performed at the Université de Montréal.

Hexakis[4-(2,4-diamino-1,3,5-triazin-6-yl)phenyl]benzene (4). Hexakis(4-cyanophenyl)benzene (**11**) (315 mg, 0.460 mmol)[23,24] was combined with dicyandiamide (474 mg, 5.64 mmol) and KOH (75 mg, 1.34 mmol) in 2-methoxyethanol (10 mL), and the mixture was heated at reflux for 15 h. The resulting mixture was then cooled to 25 °C, and volatiles were removed by evaporation in vacuo. The residue was suspended in water, and the solid fraction was separated by filtration and then washed with hot water, ethanol, and methanol. The product was dried to give hexakis[4-(2,4-diamino-1,3,5-triazin-6-yl)phenyl]benzene (**4**; 467 mg, 0.393 mmol, 85%) as a colorless solid. A sample was further purified for analysis by recrystallization from formic acid/ ethyl acetate: mp > 300 °C; ^{1}H NMR (400 MHz, DMSO-d_6) δ 6.62 (s, 24H), 6.96 (d, 12H, ^{3}J = 8 Hz), 7.67 (d, 12H, ^{3}J = 8 Hz); ^{13}C NMR (100 MHz, DCOOD) δ 127.3, 127.6, 132.4, 139.6, 146.0, 160.7, 163.4; HRMS (ESI) calcd for $C_{60}H_{48}N_{30}$ + H

m/e 1189.47510, found 1189.47404. Anal. Calcd for $C_{60}H_{48}N_{30}$ + HCOOH: C, 59.31; H, 4.08; N, 34.02. Found: C, 59.79; H, 4.11; N, 33.83.

3,4-Bis(4-bromophenyl)-2,5-diphenyl-2,4-cyclopentadien-1-one (12).[26] A solution of KOH (0.29 g, 5.2 mmol) in ethanol (5 mL) was added to a mixture of 4,4'-dibromobenzil (3.68 g, 10.0 mmol) and 1,3-diphenylacetone (2.10 g, 10.0 mmol) in ethanol (20 mL). The resulting mixture was heated at reflux for 1 h. The mixture was then cooled to 0 °C, and the resulting precipitate was collected by filtration and dried to give 3,4-bis(4-bromophenyl)-2,5-diphenyl-2,4-cyclopentadien-1-one (**12**; 4.61 g, 8.50 mmol, 85%) as a dark purple solid: ^{1}H NMR (400 MHz, $CDCl_3$) δ 6.80 (d, 4H, ^3J = 8.4 Hz), 7.1-7.3 (m, 10H), 7.35 (d, 4H, ^3J = 8.4 Hz); ^{13}C NMR (100 MHz, $CDCl_3$) δ 123.6, 126.3, 128.3, 128.7, 130.5, 130.6, 131.4, 131.9, 132.1, 153.0, 200.0.

1,2,4,5-Tetrakis(4-bromophenyl)-3,6-diphenylbenzene (13). A mixture of 3,4-bis(4-bromophenyl)-2,5-diphenyl-2,4-cyclopentadien-1-one (**12**; 2.16 g, 3.98 mmol) and bis(4-bromophenyl)acetylene (1.34 g, 3.99 mmol)[27] in diphenyl ether (5 mL) was heated at reflux under N_2 for 48 h. The resulting mixture was cooled to 25 °C and then diluted with ethanol. The precipitate was collected by filtration, washed with ethanol and hexane, and dried to give 1,2,4,5-tetrakis(4-bromophenyl)-3,6-diphenylbenzene (**13**; 2.83 g, 3.33 mmol, 84%) as a nearly colorless solid: ^{1}H NMR (400 MHz, $CDCl_3$) δ 6.67 (d, 8H, ^3J = 8.4 Hz), 6.78 (m, 4H), 6.94 (m, 6H), 7.04 (d, 8H, ^3J = 8.4 Hz). Anal. Calcd for $C_{42}H_{26}Br_4$: C, 59.33; H, 3.08. Found: C, 59.11; H, 2.75.

1,2,4,5-Tetrakis(4-cyanophenyl)-3,6-diphenylbenzene (14). 1,2,4,5-Tetrakis(4-bromophenyl)-3,6-diphenylbenzene (**13**; 1.70 g, 2.00 mmol) was combined with CuCN (1.08 g, 12.1 mmol) in dry DMF (10 mL). The mixture was heated at reflux under N_2 for 21 h. The resulting mixture was then cooled to 25 °C and diluted with water. The precipitate was collected by filtration, washed with a mixture of water and ethylenediamine, and extracted with CH_2Cl_2. The extracts were washed several times with a mixture of water and ethylenediamine, 1 M aqueous HCl, and brine. The organic phase was then dried ($MgSO_4$) and filtered, and volatiles were removed by evaporation

under reduced pressure. The crude residue was purified by passage through a short column of silica gel (100% CH_2Cl_2) to yield 1,2,4,5-tetrakis(4-cyanophenyl)-3,6-diphenylbenzene (**14**; 780 mg, 1.23 mmol, 61%) as a nearly colorless solid: mp > 300 °C; ^{1}H NMR (400 MHz, $CDCl_3$) δ 6.72 (m, 4H), 6.90 (d, 8H, ^3J = 8.2 Hz), 6.94 (m, 6H), 7.21 (d, 8H, ^3J = 8.2 Hz); ^{13}C NMR (100 MHz, $CDCl_3$) δ 110.7, 118.8, 127.3, 128.0, 131.1, 131.5, 132.0, 138.4, 139.8, 140.9, 144.6; HRMS (ESI) calcd for $C_{46}H_{26}N_4$ + H *m/e* 635.2230, found 635.2232. Anal. Calcd for $C_{46}H_{26}N_4$: C, 87.04; H, 4.13; N, 8.83. Found: C, 86.93; H, 3.77; N, 8.88.

1,2,4,5-Tetrakis[4-(2,4-diamino-1,3,5-triazin-6-yl)phenyl]-3,6-diphenylbenzene (5). 1,2,4,5-Tetrakis(4-cyanophenyl)-3,6-diphenylbenzene (**14**; 160 mg, 0.252 mmol) and dicyandiamide (106 mg, 1.26 mmol) were added to a solution of KOH (55 mg, 0.98 mmol) in 2-methoxyethanol (5 mL), and the mixture was heated at reflux for 12 h. The resulting mixture was cooled to 25 °C and diluted with water. The precipitate was collected by filtration, washed with hot water and ethanol, and dried to give 1,2,4,5-tetrakis[4-(2,4-diamino-1,3,5-triazin-6-yl)phenyl]-3,6-diphenylbenzene (**5**; 204 mg, 0.210 mmol, 83%) as a colorless solid: mp > 300 °C; ^{1}H NMR (400 MHz, DMSO-d_6) δ 6.61 (br s, 16H), 6.8-6.9 (m, 10H), 6.95 (d, 8H, ^3J = 8.4 Hz), 7.67 (d, 8H, ^3J = 8.4 Hz); ^{13}C NMR (100 MHz, DCOOD) δ 126.7, 126.7, 127.2, 127.5, 131.3, 132.5, 138.8, 139.6, 140.4, 147.1, 160.8, 163.4; HRMS (ESI) calcd for $C_{54}H_{42}N_{20}$ + H *m/e* 971.3974, found 971.4007.

Pentaphenylbenzene (15).[28] Tetraphenylcyclopentadienone (3.84 g, 9.99 mmol) and phenylacetylene (1.1 mL, 10 mmol) were combined in diphenyl ether (10 mL), and the mixture was heated at reflux under N_2 for 30 min. During this time, the mixture became light orange. The mixture was cooled to 25 °C and diluted with ethanol (150 mL). The resulting precipitate was collected by filtration, washed with ethanol and hexane, and dried to give pentaphenylbenzene (**15**; 4.16 g, 9.07 mmol, 91%) as a colorless solid: ^{1}H NMR (400 MHz, $CDCl_3$) δ 6.83 (m, 2H), 6.90 (m, 7H), 6.96 (m, 6H), 7.19 (m, 10 H), 7.63 (s, 1H); ^{13}C NMR (100 MHz, $CDCl_3$) δ 125.8, 126.0, 126.7, 127.1, 127.4, 128.0, 130.4, 131.8, 131.9, 132.0, 139.7, 140.4, 140.8, 141.2, 142.1, 142.2.

Pentakis(4-bromophenyl)benzene (16). Pentaphenylbenzene (**15**; 1.73 g, 3.77 mmol) was spread in a thin layer at the bottom of a beaker and covered with neat bromine (6.5 mL, 130 mmol). The mixture was allowed to stand overnight at 25 °C. The crude product was washed with ethanol and hexane, dried, recrystallized from xylenes, and dried again to give pure pentakis(4-bromophenyl)benzene (**16**; 1.88 g, 2.20 mmol, 58%) as a colorless solid: mp > 300 °C; ^{1}H NMR (400 MHz, $CDCl_3$) δ 6.59 (d, 2H, ^3J = 8.4 Hz), 6.65 (d, 4H, ^3J = 8.4 Hz), 6.95 (d, 4H, ^3J = 8.4 Hz), 7.07 (d, 2H, ^3J = 8.4 Hz), 7.13 (d, 4H, ^3J = 8.3 Hz), 7.32 (d, 4H, ^3J = 8.4 Hz), 7.45 (s, 1H); ^{13}C NMR (100 MHz, $CDCl_3$) δ 120.8, 121.0, 121.6, 129.3, 130.9, 131.1, 131.5, 131.7, 133.1, 133.2, 138.4, 138.7, 138.7, 140.1, 140.5, 141.0. Anal. Calcd for $C_{36}H_{21}Br_5$: C, 50.69; H, 2.48. Found: C, 51.29; H, 2.39.

Pentakis(4-cyanophenyl)benzene (17). Pentakis(4-bromophenyl)-benzene (**16**; 1.34 g, 1.57 mmol) and CuCN (1.05 g, 11.7 mmol) were combined in dry DMF (10 mL), and the mixture was heated at reflux under N_2 for 18 h. The resulting mixture was then cooled to 25 °C and poured into water. The precipitate was collected by filtration and washed with water and then with water/ethylenediamine (3:1 v/v). The solid residue was suspended in CH_2Cl_2 and washed repeatedly with water/ethylenediamine until the aqueous washings were colorless. The organic phase was then washed with 1 M aqueous HCl and brine, dried over $MgSO_4$, and filtered. Removal of volatiles by evaporation under reduced pressure left a residue that was purified by flash chromatography (100% CH_2Cl_2) to give pentakis(4-cyanophenyl)benzene (**17**; 0.280 g, 0.480 mmol, 31%) as a colorless solid: mp > 300 °C; ^{1}H NMR (400 MHz, $CDCl_3$) δ 6.85 (d, 2H, ^3J = 8.2 Hz), 6.91 (d, 4H, ^3J = 8.2 Hz), 7.20 (d, 4H, ^3J = 8.3 Hz), 7.27 (d, 2H, ^3J = 8.2 Hz), 7.32 (d, 4H, ^3J = 8.2 Hz), 7.52 (d, 4H, ^3J = 8.3 Hz), 7.56 (s, 1H); ^{13}C NMR (100 MHz, $CDCl_3$) δ 111.6, 111.8, 112.1, 118.3, 118.3, 118.6, 130.7, 131.8, 131.9, 132.0, 132.1, 132.2, 132.5, 138.7, 140.5, 140.8, 143.1, 143.4, 144.6; HRMS (ESI) calcd for $C_{41}H_{21}N_5$ + Na *m/e* 606.16892, found 606.16852. Anal. Calcd for $C_{41}H_{21}N_5$ + 0.25 CH_2Cl_2: C, 81.91; H, 3.58; N, 11.58. Found: C, 82.03; H, 3.59; N, 11.63.

Pentakis[4-(2,4-diamino-1,3,5-triazin-6-yl)phenyl]benzene (6). Pentakis(4-cyanophenyl)benzene (**17**; 255 mg, 0.437 mmol), dicyandiamide (370 mg, 4.40 mmol), and KOH (123 mg, 2.19 mmol) were combined in 2-methoxyethanol (5 mL), and the mixture was heated at reflux for 19 h. The resulting mixture was cooled to 25 °C and poured into water. The precipitate was collected by filtration, washed with hot water and methanol, and then dried to give pentakis[4-(2,4-diamino-1,3,5-triazin-6-yl)phenyl]benzene (**6**; 335 mg, 0.334 mmol, 76%) as a colorless solid: mp > 300 °C; ^{1}H NMR (400 MHz, DMSO-d_6) δ 6.6- 6.8 (br m, 20H), 6.93 (d, 2H, ^3J = 8.4 Hz), 6.97 (d, 4H, ^3J = 8.2 Hz), 7.27 (d, 4H, ^3J = 8.2 Hz), 7.69 (s, 1H), 7.70 (d, 2H, ^3J = 8.4 Hz), 7.75 (d, 4H, ^3J = 8.2 Hz), 8.02 (d, 4H, ^3J = 8.2 Hz); ^{13}C NMR (100 MHz, DMSO-d_6) δ 127.0, 127.3, 128.0, 130.4, 131.9, 132.0, 132.0, 135.4, 135.7, 136.2, 139.5, 141.0, 141.8, 142.8, 143.2, 144.2, 168.1, 168.2, 168.2, 170.7, 170.9, 170.9; HRMS (ESI) calcd for $C_{51}H_{41}N_{25}$ + H *m/e* 1004.40495, found 1004.40531.

1,4-Dimethyl-2,3,5,6-tetraphenylbenzene (18).[29] A stirred mixture of the dimer of 2,5-dimethyl-3,4-diphenylcyclopentadienone (2.00 g, 3.84 mmol) and diphenylacetylene (2.05 g, 11.5 mmol) in diphenyl ether (5 mL) was heated at reflux for 2 h. During this time, the mixture turned deep red and then faded to orange. Slow cooling yielded crystals after 24 h, which were collected by filtration and washed with hexane. The product was further purified by recrystallization from xylenes, giving 1,4-dimethyl-2,3,5,6-tetraphenylbenzene (**18**; 2.54 g, 6.19 mmol, 81%) as a colorless solid: mp > 300 °C (lit.[29] 363-365 °C); ^{1}H NMR (400 MHz, $CDCl_3$) δ 1.80 (s, 6H), 7.05 (m, 12H), 7.13 (m, 8H).

1,4-Dimethyl-2,3,5,6-tetrakis(4-bromophenyl)benzene (19). 1,4-Dimethyl-2,3,5,6-tetraphenylbenzene (**18**; 3.50 g, 8.52 mmol) was powdered and covered with neat bromine (35 mL). The mixture was kept at 25 °C in the dark for 24 h and was then added to stirred ethanol (125 mL) precooled to -78 °C. The resulting solid was separated by filtration and washed with cold ethanol (25 mL) and then with small portions of 5% (w/v) aqueous $Na_2S_2O_3$ (total of 75 mL). Recrystallization from xylenes afforded 1,4-dimethyl-2,3,5,6-tetrakis(4-bromophenyl)benzene (**19**; 5.00 g, 6.89 mmol, 81%) as a

colorless solid. An analytically pure sample was obtained by further recrystallization from toluene: mp > 300 °C; ^{1}H NMR (400 MHz, $CDCl_3$) δ 1.72 (s, 6H), 6.88 (d, 8H, ^3J = 8.2 Hz), 7.31 (d, 8H, ^3J = 8.2 Hz). Anal. Calcd for $C_{32}H_{22}Br_4$: C, 52.93; H, 3.05. Found: C, 52.57; H, 2.72.

1,4-Dimethyl-2,3,5,6-tetrakis(4-cyanophenyl)benzene (20). A mixture of 1,4-dimethyl-2,3,5,6-tetrakis(4-bromophenyl)benzene (**19**; 0.500 g, 0.689 mmol) and CuCN (0.617 g, 6.89 mmol) in dry DMF (40 mL) was heated at reflux under N_2 for 42 h. The mixture was cooled to 25 °C, water (80 mL) was added, and the resulting precipitate was collected by filtration. The solid was then washed with a 30% aqueous solution of ethylenediamine until the washings were colorless. The solid was treated with CH_2Cl_2, and the suspension was washed with 30% aqueous ethylenediamine, then with water, and finally with brine. The organic phase was dried over anhydrous $MgSO_4$ and filtered, and volatiles were then removed by evaporation under reduced pressure. Flash chromatography on silica gel (100% CH_2Cl_2) afforded 1,4-dimethyl-2,3,5,6-tetrakis(4-cyanophenyl)benzene (**20**; 0.231 g, 0.452 mmol, 66%) as a colorless solid: mp > 300 °C; ^{1}H NMR (400 MHz, CD_2Cl_2) δ 1.72 (s, 6H), 7.15 (d, 8H, ^3J = 8.4 Hz), 7.50 (d, 8H, ^3J = 8.4 Hz); ^{13}C NMR (100 MHz, CD_2Cl_2) δ 19.5, 111.3, 119.1, 131.3, 131.7, 132.4, 140.3, 145.7; HRMS (ESI) calcd for $C_{36}H_{22}N_4$ + H *m/e* 511.19172, found 511.19221.

1,2,4,5-Tetrakis[4-(2,4-diamino-1,3,5-triazin-6-yl)phenyl]-3,6-dimethyl-benzene (7). 1,4-Dimethyl-2,3,5,6-tetrakis(4-cyanophenyl)benzene (**20**; 0.200 g, 0.392 mmol), dicyandiamide (0.527 g, 6.27 mmol), and powdered KOH (0.056 g, 1.0 mmol) were suspended in 2-methoxyethanol (5 mL). The reaction mixture was heated at reflux for 24 h, cooled to 25 °C, and treated with water (5 mL). The resulting precipitate was separated by filtration and washed successively with boiling water, methanol, and dichloromethane to give 1,2,4,5-tetrakis[4-(2,4-diamino- 1,3,5-triazin-6-yl)phenyl]-3,6-dimethylbenzene (**7**; 0.260 g, 0.307 mmol, 78%) as a colorless solid. Further purification could be achieved by (1) dissolving the compound (40 mg) in DMSO (20 mL) with the assistance of slight heating and sonication, (2) filtering the resulting mixture through a 0.45 μm PTFE filter, (3) adding a supernatant layer of anhydrous

ethanol (120 mL) on top of the filtered solution, and (4) keeping the mixture undisturbed in a closed vessel overnight until small crystals appeared: mp > 300 °C; ^{1}H NMR (400 MHz, DMSO-d_6) δ 1.79 (s, 6H), 6.68 (br s, 16H), 7.17 (d, 8H, ^3J = 8.3 Hz), 8.00 (d, 8H, ^3J = 8.3 Hz); HRMS (ESI) calcd for $C_{44}H_{38}N_{20}$ + H *m/e* 847.3661, found 847.3663.

1,2,4,5-Tetrakis(4-cyanophenyl)benzene (21). A mixture of 1,2,4,5-tetrabromobenzene (0.394 g, 1.00 mmol) and 4-cyanophenylboronic acid (0.882 g, 6.00 mmol) in toluene (80 mL), ethanol (40 mL), and aqueous K_2CO_3 (40 mL, 2 M) was degassed by allowing N_2 to bubble through it. $Pd(PPh_3)_4$ (115 mg, 0.100 mmol) was then added, and the mixture was degassed again. The mixture was heated at 90 °C for 24 h under N_2 and was then exposed to air for 1 h to oxidize the catalyst. The resulting mixture was partitioned between toluene (100 mL) and aqueous NaOH (50 mL, 1 M). The organic phase was separated and treated with acetone cyanohydrin (3 mL) and triethylamine (3 mL). As the mixture was stirred for 1 h, it turned from black to yellow. The mixture was filtered through silica gel, using $CHCl_3$ to help elute the product. Volatiles were then removed from the filtrate by evaporation under reduced pressure. Recrystallization of the residue from dioxane, followed by repeated dissolution of the product in $CHCl_3$ and evaporation to eliminate dioxane, yielded 1,2,4,5-tetrakis(4-cyanophenyl)benzene (**21**; 0.396 g, 0.821 mmol, 82%) as a colorless solid: mp > 300 °C; ^{1}H NMR (400 MHz, DMSO-d_6) δ 7.44 (d, 8H, ^3J = 8.2 Hz), 7.63 (s, 2H), 7.80 (d, 8H, ^3J = 8.2 Hz); ^{13}C NMR (100 MHz, DMSO-d_6) 111.06, 119.49, 131.61, 133.13, 133.66, 139.52, 144.98; HRMS (ESI) calcd for $C_{34}H_{18}N_4$ + H *m/e* 483.16042, found 483.15952.

1,2,4,5-Tetrakis[4-(2,4-diamino-1,3,5-triazin-6-yl)phenyl]benzene (8). 1,2,4,5-Tetrakis(4-cyanophenyl)benzene (**21**; 0.340 g, 0.705 mmol), dicyandiamide (0.296 g, 3.52 mmol), and powdered KOH (0.198 g, 3.53 mmol) were suspended in 2-methoxyethanol (10 mL). The mixture was heated at reflux for 24 h, cooled to 25 °C, and treated with water (10 mL). The resulting suspension was filtered, and the solid was washed with boiling water and then with cold methanol. Drying in air yielded 1,2,4,5-tetrakis[4-(2,4-diamino-1,3,5-triazin-6-yl)phenyl]benzene (**8**; 0.479 g, 0.585 mmol,

83%) as a colorless solid. Further purification was achieved by dissolving the product in hot DMSO, filtering, and reprecipitating the solid by adding four volumes of ethyl acetate. The product was collected by filtration and freed of DMSO by trituration with ethyl acetate: mp > 300 °C; ^{1}H NMR (400 MHz, DMSO-d_6) δ 6.75 (br s, 16H), 7.32 (d, 8H, ^3J = 8.3 Hz), 7.65 (s, 2H), 8.10 (d, 8H, ^3J = 8.3 Hz); ^{13}C NMR (100 MHz, DMSO-d_6) δ 127.4, 129.4, 132.1, 135.6, 139.0, 142.6, 167.3, 169.8; HRMS (ESI) calcd for $C_{42}H_{34}N_{20}$ + H *m/e* 819.3348, found 819.3346.

X-ray Crystallographic Studies. Data were collected using (1) a Bruker AXS SMART 4K/Platform diffractometer or (2) a Bruker Microstar diffractometer with Cu Kα radiation at 100, 200, or 240 K. Structures were solved by direct methods using SHELXS-97 and refined using SHELXL-97.[37] All non-hydrogen atoms were refined anisotropically, whereas hydrogen atoms were placed in ideal positions and defined as riding atoms.

Structure of Crystals of Hexakis[4-(2,4-diamino-1,3,5-triazin-6-yl)phenyl]benzene (4) Grown from DMSO/THF. Crystals were found to belong to the triclinic space group *P*-1 with a = 17.770(2) Å, b = 21.235(3) Å, c = 21.691(2) Å, α = 98.400(6)°, β = 110.518(5)°, γ = 103.475(6)°, V = 7217.9(14) Å^3, D_{calcd} = 1.128 g/cm^3, and Z = 2. Full-matrix least-squares refinements on F^2 led to final residuals R_f = 0.1160, R_w = 0.2902, and GOF = 1.096 for 23 987 reflections with $I > 2\sigma(I)$.

Structure of Crystals of Hexakis[4-(2,4-diamino-1,3,5-triazin-6-yl)phenyl]benzene (4) Grown from DMSO/Toluene. Crystals were found to belong to the triclinic space group *P*-1 with a = 8.4178(11) Å, b = 16.424(2) Å, c = 20.251(3) Å, α = 105.291(5)°, β = 97.289 (6)°, γ = 93.544(6)°, V = 2665.7(6) Å^3, D_{calcd} = 1.347 g/cm^3, and Z = 2. Full-matrix least-squares refinements on F^2 led to final residuals R_f = 0.0792, R_w = 0.1865, and GOF = 1.045 for 5999 reflections with $I > 2\sigma(I)$.

Structure of Crystals of Hexakis[4-(2,4-diamino-1,3,5-triazin-6-yl)phenyl]benzene (4) Grown from DMSO/Benzene. Crystals were found to belong to

the trigonal space group *R*-3 with $a = b = 38.6740(9)$ Å, $c = 10.010(3)$ Å, $V = 12966(4)$ Å^3, $D_{calcd} = 1.177$ g/cm^3, and $Z = 3$. Full-matrix least-squares refinements on F^2 led to final residuals $R_f = 0.0587$, $R_w = 0.1369$, and GOF = 1.028 for 5226 reflections with $I > 2\sigma(I)$.

Structure of Crystals of Hexakis[4-(2,4-diamino-1,3,5-triazin-6-yl)phenyl]benzene (4) Grown from Formic Acid/Methanol. Crystals were found to belong to the trigonal space group *R*-3 with $a = b = 22.8070(9)$ Å, $c = 17.2915(16)$ Å, $V = 7789.3(8)$ Å^3, $D_{calcd} = 0.761$ g/cm^3, and $Z = 3$. Full-matrix least-squares refinements on F^2 led to final residuals $R_f = 0.0614$, $R_w = 0.1513$, and GOF = 1.048 for 1912 reflections with $I > 2\sigma(I)$.

Structure of Crystals of 1,2,4,5-Tetrakis[4-(2,4-diamino-1,3,5- triazin-6-yl)phenyl]-3,6-diphenylbenzene (5) Grown from DMSO/Acetonitrile. Crystals were found to belong to the monoclinic space group *C*2/*c* with $a = 40.3960(13)$ Å, $b = 20.6327(7)$ Å, $c = 12.0265(4)$ Å, $\beta = 99.926(2)°$, $V = 9873.8(6)$ Å^3, $D_{calcd} = 1.239$ g/cm^3, and $Z = 4$. Full-matrix least-squares refinements on F^2 led to final residuals $R_f = 0.0622$, $R_w = 0.1476$, and GOF = 1.003 for 6853 reflections with $I > 2\sigma(I)$.

Structure of Crystals of Pentakis[4-(2,4-diamino-1,3,5-triazin- 6-yl)phenyl]benzene (6) Grown from DMSO/Acetone. Crystals were found to belong to the monoclinic space group *C*2/*c* with $a = 31.282(15)$ Å, $b = 24.617(3)$ Å, $c = 11.704(9)$ Å, $\beta = 108.302(4)°$, $V = 8557(8)$ Å^3, $D_{calcd} = 1.265$ g/cm^3, and Z = 4. Full-matrix least-squares refinements on F^2 led to final residuals $R_f = 0.0890$, $R_w = 0.1426$, and GOF = 1.00 for 8129 reflections with $I > 2\sigma(I)$.

Structure of Crystals of 1,2,4,5-Tetrakis[4-(2,4-diamino-1,3,5-triazin-6-yl)phenyl]-3,6-dimethylbenzene (7) Grown from DMSO/ Dioxane. Crystals were found to belong to the monoclinic space group *C*2/*m* with $a = 20.4638(8)$ Å, $b = 21.4603(8)$ Å, $c = 15.8607(6)$ Å, $\beta = 104.885(2)°$, $V = 6307.2(4)$ Å^3, $D_{calcd} = 0.940$

g/cm^3, and Z = 2. Full-matrix least-squares refinements on F^2 led to final residuals R_f = 0.0730, R_w = 0.1611, and GOF = 1.181 for 1988 reflections with $I > 2\sigma(I)$.

Structure of Crystals of 1,2,4,5-Tetrakis[4-(2,4-diamino-1,3,5-triazin-6-yl)phenyl]-3,6-dimethylbenzene (7) Grown from DMSO/ Methanol. Crystals were found to belong to the monoclinic space group $P2_1/c$ with a = 34.706(2) Å, b = 14.9704(9) Å, c = 12.064(7) Å, β = 91.318(2)°, V = 6246.8(7) Å^3, D_{calcd} = 1.271 g/cm^3, and Z = 4. Full-matrix least-squares refinements on F^2 led to final residuals R_f = 0.0794, R_w = 0.1704, and GOF = 1.115 for 8635 reflections with $I > 2\sigma(I)$.

Structure of Crystals of 1,2,4,5-Tetrakis[4-(2,4-diamino-1,3,5-triazin-6-yl)phenyl]benzene (8) Grown from DMSO/Acetone. Crystals were found to belong to the monoclinic space group $P2_1/c$ with a = 8.9750(3) Å, b = 22.7525(6) Å, c = 21.9316(8) Å, β = 101.4980(10)°, V = 4388.6(2) Å^3, D_{calcd} = 1.329 g/cm^3, and Z = 2. Full-matrix least-squares refinements on F^2 led to final residuals R_f = 0.0651, R_w = 0.1491, and GOF = 1.085 for 7838 reflections with $I > 2\sigma(I)$.

Acknowledgment

We are grateful to the Natural Sciences and Engineering Research Council of Canada, the Ministère de l'Éducation du Québec, the Canada Foundation for Innovation, the Canada Research Chairs Program, and Université de Montréal for financial support. We thank Dr. Alexandra Furtos and Karine Venne for obtaining mass spectra. In addition, we are grateful to Prof. Jurgen Sygusch for providing access to a diffractometer equipped with a rotating anode.

Supporting Information Available. Additional crystallographic details, including ORTEP drawings and tables of structural data for compounds **4-8**. This material is available free of charge via the Internet at http://pubs.acs.org.

Notes and references

1. Fellow of the Natural Sciences and Engineering Research Council of Canada, 2003-2004.

2. Fellow of the Natural Sciences and Engineering Research Council of Canada, 2003-2007.

3. Braga, D. *Chem. Commun.* **2003**, 2751-2754. Biradha, K. *CrystEngComm* **2003**, *5*, 374-384. Hollingsworth, M. D. *Science* **2002**, *295*, 2410-2413. *Crystal Engineering: From Molecules and Crystals to Materials*; Braga, D., Grepioni, F., Orpen, A. G., Eds.; Kluwer: Dordrecht, Netherlands, 1999. Desiraju, G. R. *Crystal Engineering: The Design of Organic Solids*; Elsevier: Amsterdam, 1989.

4. For recent examples, see: Sokolov, A. N.; Friščić, T.; MacGillivray, L. R. *J. Am. Chem. Soc.* **2006**, *128*, 2806-2807. Roques, N.; Maspoch, D.; Wurst, K.; Ruiz-Molina, D.; Rovira, C.; Veciana, J. *Chem.-Eur. J.* **2006**, *12*, 9238-9253. Pigge, F. C.; Dighe, M. K.; Rath, N. P. *Cryst. Growth Des.* **2006**, *6*, 2732-2738. Saha, B. K.; Nangia, A.; Nicoud, J.-F. *Cryst. Growth Des.* **2006**, *6*, 1278-1281. Jayaraman, A.; Balasubramaniam, V.; Valiyaveettil, S. *Cryst. Growth Des.* **2006**, *6*, 636-642. Suslick, K. S.; Bhyrappa, P.; Chou, J.-H.; Kosal, M. E.; Nakagaki, S.; Smithenry, D. W.; Wilson, S. R. *Acc. Chem. Res.* **2005**, *38*, 283-291. Aakeröy, C. B.; Desper, J.; Urbina, J. F. *Chem. Commun.* **2005**, 2820-2822. Braga, D.; Brammer, L.; Champness, N. R. *CrystEngComm* **2005**, *7*, 1-19. Sisson, A. L.; del Amo Sanchez, V.; Magro, G.; Griffin, A. M. E.; Shah, S.; Charmant, J. P. H.; Davis, A. P. *Angew. Chem., Int. Ed.* **2005**, *44*, 6878-6881. Malek, N.; Maris, T.; Perron, M.-È.; Wuest, J. D. *Angew. Chem., Int. Ed.* **2005**, *44*, 4021-4025. Voogt, J. N.; Blanch, H. W. *Cryst. Growth Des.* **2005**, *5*, 1135-1144. Lee, S.-O.; Shacklady, D. M.; Horner, M. J.; Ferlay, S.; Hosseini, M. W.; Ward, M. D. *Cryst. Growth Des.* **2005**, *5*, 995-1003. Saied, O.; Maris, T.; Wang, X.; Simard, M.; Wuest, J. D. *J. Am. Chem. Soc.* **2005**, *127*, 10008-10009. Custelcean, R.; Gorbunova, M. G.; Bonnesen, P. V. *Chem.-Eur. J.* **2005**, *11*, 1459-1466. Moorthy, J. N.; Natarajan, R.; Venugopalan, P. *J. Org. Chem.* **2005**, *70*, 8568-8571. Soldatov, D. V.;

Moudrakovski, I. L.; Ripmeester, J. A. *Angew. Chem., Int. Ed.* **2004**, *43*, 6308-6311. Alshahateet, S. F.; Nakano, K.; Bishop, R.; Craig, D. C.; Harris, K. D. M.; Scudder, M. L. *CrystEngComm* **2004**, *6*, 5-10.

5. Malek, N.; Maris, T.; Simard, M.; Wuest, J. D. *J. Am. Chem. Soc.* **2005**, *127*, 5910-5916.

6. Fournier, J.-H.; Maris, T.; Wuest, J. D. *J. Org. Chem.* **2004**, *69*, 1762-1775.

7. For recent overviews of the strategy, see: Wuest, J. D. *Chem. Commun.* **2005**, 5830-5837. Hosseini, M. W. *Acc. Chem. Res.* **2005**, *38*, 313-323.

8. Simard, M.; Su, D.; Wuest, J. D. *J. Am. Chem. Soc.* **1991**, *113*, 4696-4697.

9. For reviews, see: Steiner, T. *Angew. Chem., Int. Ed.* **2002**, *41*, 48-76. Prins, L. J.; Reinhoudt, D. N.; Timmerman, P. *Angew. Chem., Int. Ed.* **2001**, *40*, 2382-2426.

10. We estimate the percentage of volume accessible to guests by using the PLATON program.[11] PLATON calculates the accessible volume by allowing a spherical probe of variable radius to roll over the van der Waals surface of the network. PLATON uses a default value of 1.20 Å for the radius of the probe, which is an appropriate model for small guests such as water.

11. Spek, A. L. *PLATON, A Multipurpose Crystallographic Tool*; Utrecht University: Utrecht, The Netherlands, 2001. van der Sluis, P.; Spek, A. L. *Acta Crystallogr.* **1990**, *A46*, 194-201.

12. Nangia, A. *Curr. Opin. Solid State Mater. Sci.* **2001**, *5*, 115-122. Langley, P. J.; Hulliger, J. *Chem. Soc. Re*V. **1999**, *28*, 279-291.

13. Brunet, P.; Demers, E.; Maris, T.; Enright, G. D.; Wuest, J. D. *Angew. Chem., Int. Ed.* **2003**, *42*, 5303-5306.

14. For recent references, see: Lebel, O.; Maris, T.; Perron, M.-È.; Demers, E.; Wuest, J. D. *J. Am. Chem. Soc.* **2006**, *128*, 10372-10373. Nath, K. G.; Ivasenko, O.; Miwa, J. A.; Dang, H.; Wuest, J. D.; Nanci, A.; Perepichka, D. F.; Rosei, F. *J. Am. Chem. Soc.* **2006**, *128*, 4212-4213. Lebel, O.; Perron, M.-È.; Maris, T.; Zalzal, S.

F.; Nanci, A.; Wuest, J. D. *Chem. Mater.* **2006**, *18*, 3616-3626. Maly, K. E.; Dauphin, C.; Wuest, J. D. *J. Mater. Chem.* **2006**, *16*, 4695-4700.

15. For discussions of interpenetration in networks, see: Batten, S. R. *CrystEngComm* **2001**, 76-82. Batten, S. R.; Robson, R. *Angew. Chem., Int. Ed.* **1998**, *37*, 1460-1494.

16. Kobayashi, K.; Shirasaka, T.; Sato, A.; Horn, E.; Furukawa, N. *Angew. Chem., Int. Ed*. **1999**, *38*, 3483-3486.

17. Kobayashi, K.; Shirasaka, T.; Horn, E.; Furukawa, N. *Tetrahedron Lett.* **2000**, *41*, 89-93.

18. Kobayashi, K.; Sato, A.; Sakamoto, S.; Yamaguchi, K. *J. Am. Chem. Soc.* **2003**, *125*, 3035-3045.

19. Demers, E.; Maris, T.; Wuest, J. D. *Cryst. Growth Des.* **2005**, *5*, 1227-1235.

20. Fieser, L. F. *Org. Synth.* **1966**, *46*, 44-48. Fieser, L. F. *Organic Syntheses*; Wiley: New York, 1973; Collect. Vol. V, pp 604-608.

21. Rathore, R.; Burns, C. L.; Guzei, I. A. *J. Org. Chem.* **2004**, *69*, 1524-1530. Rathore, R.; Burns, C. L. *Org. Synth.* **2004**, *82*, 30-33.

22. Wu, J.; Watson, M. D.; Zhang, L.; Wang, Z.; Müllen, K. *J. Am. Chem. Soc.* **2004**, *126*, 177-186.

23. Maly, K. E.; Maris, T.; Gagnon, E.; Wuest, J. D. *Cryst. Growth Des*. **2006**, *6*, 461-466.

24. Kobayashi, K.; Kobayashi, N.; Ikuta, M.; Therrien, B.; Sakamoto, S.; Yamaguchi, K. *J. Org. Chem.* **2005**, *70*, 749-752.

25. Simons, J. K.; Saxton, M. R. *Org. Synth.* **1953**, *33*, 13-15. Simons, J. K.; Saxton, M. R. *Organic Syntheses*; Wiley: New York, 1963; Collect. Vol. IV, pp 78-80.

26. Coan, S. B.; Trucker, D. E.; Becker, E. I. *J. Am. Chem. Soc.* **1955**, *77*, 60-66.

27. Misumi, S.; Kuwana, M.; Nakagawa, M. *Bull. Chem. Soc. Jpn.* **1962**, *35*, 135-142. Barber, H. J.; Slack, R. *J. Chem. Soc*. **1944**, 612-615.

28. Kübel, C.; Eckhardt, K.; Enkelmann, V.; Wegner, G.; Müllen, K. *J. Mater. Chem.* **2000**, *10*, 879-886.

29. Padwa, A.; Goldstein, S. I.; Rosenthal, R. J. *J. Org. Chem.* **1987**, *52*, 3278-3285. Regan, T. H.; Miller, J. B. *J. Org. Chem.* **1967**, *32*, 592-596.

30. Nishimura, M.; Ueda, M.; Miyaura, N. *Tetrahedron* **2002**, *58*, 5779-5787.

31. The composition was estimated by X-ray diffraction and by ^{1}H NMR spectroscopy of dissolved samples. The amount of any H_2O included could not be determined accurately.

32. Gagnon, E.; Maly, K. E.; Maris, T.; Wuest, J. D. *Acta Crystallogr.* **2007**, *C63*, o4-o6.

33. Damiani, A.; Giglio, E.; Ripamonti, A. *Acta Crystallogr.* **1965**, *19*, 161-168.

34. Ishi-i, T.; Kuwahara, R.; Takata, A.; Jeong, Y.; Sakurai, K.; Mataka, S. *Chem.-Eur. J.* **2006**, *12*, 763-776. Janczak, J.; Kubiak, R. *J. Mol. Struct.* **2005**, *751*, 74-84. Díaz-Ortiz, Á.; Elguero, J.; Foces-Foces, C.; de la Hoz, A.; Moreno, A.; Mateo, M. d. C.; Sánchez-Migallón, A.; Valiente, G. *New J. Chem.* **2004**, *28*, 952-958.

35. See the Supporting Information for details.

36. Representations of channels were generated by the Cavities option in the program ATOMS Version 5.1 (Shape Software, 521 Hidden Valley Road, Kingsport, Tennessee 37663 U.S.A.; www.shapesoftware.com).

37. Sheldrick, G. M. *SHELXS-97, Program for the Solution of Crystal Structures* and *SHELXL-97, Program for the Refinement of Crystal Structures*; Universität Göttingen: Germany, 1997.

3.6 Conclusions

Lors de cette étude, nous avons adopté une approche systématique pour modifier l'hexaphénylbenzène et obtenir des réseaux présentant une porosité de plus en plus élevée. Cette approche, typique de l'ingénierie cristalline, nous a permis de mettre à jour des facteurs conformationnels qui ont un impact sur l'architecture supramoléculaire obtenue. On retient en particulier l'importance des conformations que peuvent adopter les cœurs moléculaires. Celles-ci peuvent avoir des effets majeurs sur les assemblages supramoléculaires générés. La structure moléculaire de l'hexakis[4-(2,4-diamino-1,3,5-triazin-6-yl)phényl]benzène, représentée partiellement par le composé **3.7**, illustre bien ces effets : les facteurs stériques du cœur moléculaire, couplés à la tendance de l'unité phényle-diaminotriazine à être coplanaire favorisent la formation de motifs de reconnaissances de type **III** entre des couches de molécules adjacentes (voir Figure 3.5). Dans un composé plus flexible tel que le tecton **3.3**, la rotation autour du lien C(sp^3)-C(sp^2) élimine en partie l'intérêt portée à la coplanarité de l'unité phényle-diaminotriazine. Ainsi, en combinant intelligemment des cœurs moléculaires et des unités de reconnaissance, on peut amplifier le potentiel d'association des tectons obtenus.

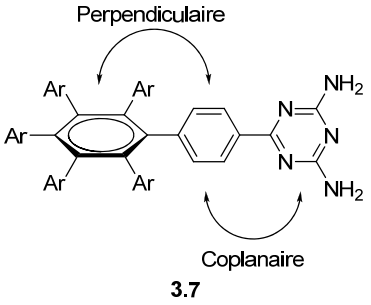

3.7

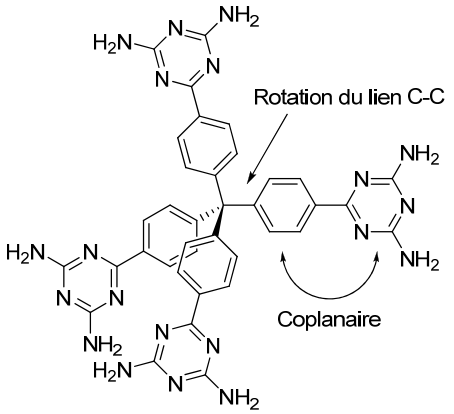

3.3

Finalement, on remarque dans la série de composés étudiés que les réseaux supramoléculaires sont structurellement très similaires, malgré la scission de près du tiers de la molécule initiale lorsqu'on passe du tecton **3.8** au tecton **3.9**. Cette

impressionnante tolérance aux modifications structurelles laisse envisager que d'autres fonctionnalités pourraient être introduites dans ce type de réseau supramoléculaire. On peut imaginer des composés tels que les tectons **3.10** et **3.11**, dans lesquels deux des six groupements diaminotriazinyles du tecton **3.8** ont été remplacés par des fonctions aldéhyde ou époxyde. La cristallisation des tectons **3.10** et **3.11** donnerait potentiellement des réseaux poreux analogues à ceux obtenus avec les tectons **3.8** et **3.9**. De plus, l'introduction de fonctions aldéhyde ou époxyde ajoute la possibilité de réticuler de façon covalente les réseaux obtenus, soit par la formation de liens imines à partir des groupements aldéhyde ou par des attaques nucléophiles sur les groupements époxydes. Ces deux composés offrent un point de départ intéressant pour la formation de réseaux covalents organiques stables, analogues aux zéolites.

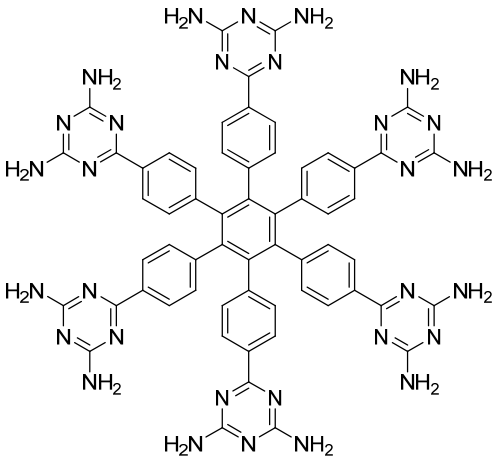

3.8

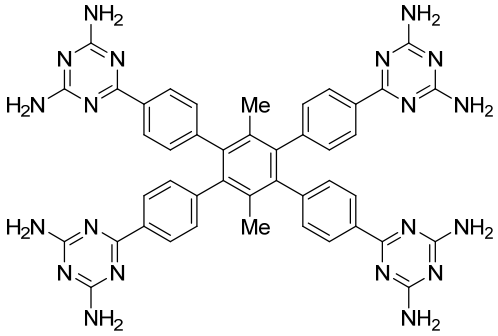

3.9

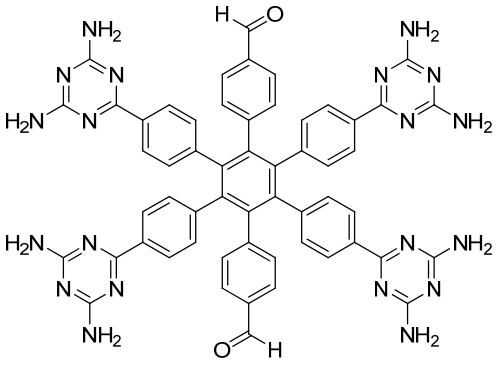

3.10

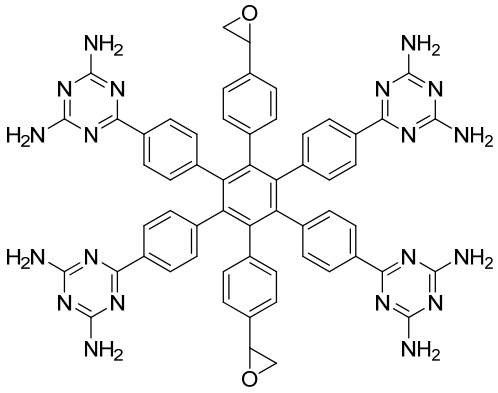

3.11

Chapitre 4

Études des interactions intermoléculaires faibles dans les dérivés d'hexaphénylbenzène

4.1 Introduction

L'ingénierie cristalline exploite la force et la directionnalité des interactions non-covalentes, telles que les ponts hydrogène, pour positionner des molécules de manière prévisible. Idéalement, ces interactions seraient suffisamment fortes pour diriger l'assemblage des molécules à l'état solide, mais les détails de la structure sont souvent régis par l'établissement d'une série d'interactions plus faibles, présentes en grande quantité. Celles-ci sont difficiles à prévoir, à classifier et à observer. Afin d'augmenter le contrôle que nous avons sur la formation d'assemblages supramoléculaires, il est essentiel de mieux comprendre ces interactions.

Certains problèmes peuvent survenir lorsque les interactions dites « faibles » sont à l'étude. Deux en particuliers ont été soulevés par Desiraju.[1] Premièrement, les cœurs moléculaires que nous utilisons pour maintenir les groupements fonctionnels en place peuvent être impliqués dans des interactions de type π···π ou C–H···π. Bien que l'énergie de ces dernières soit souvent de l'ordre de quelques kJ mol^{-1}, elles sont tout à fait capables de rivaliser avec les interactions dites « faibles ».[2] Deuxièmement, le nombre d'interactions non-covalentes possible augmente rapidement avec la dimension de la molécule et le nombre de groupements fonctionnels qu'elle contient. Il devient alors ardu d'étudier les interactions intermoléculaires émanant d'un groupe fonctionnel précis.

Le cœur moléculaire qu'est l'hexaphénylbenzène est idéal pour aborder le sujet des interactions faibles. Nous avons porté une attention toute particulière au groupement nitro, qui est connu pour participer dans des interactions faibles.[3] Nous avons donc préparé l'hexakis(4-nitrophényl)benzène (**4.1**). Dans la prochaine section (4.2), la

---

1 Desiraju, G. R. *Angew. Chem. Int. Ed.* **2007**, *46*, 8342-8356.

2 Le chapitre 5 est entièrement dédié à l'étude des interactions π–π et C–H···π. Une discussion plus approfondie y est présentée.

3 Afin que ce document conserve une longueur raisonnable, nous avons décidé de limiter notre discussion à l'étude des groupements nitro. Pour un aperçu de nos résultats relatifs aux interactions faibles impliquant des groupements cyano, le lecteur est invité à consulter les articles suivants : Maly, K. E.; Maris, T.; Gagnon, E.; Wuest, J. D. *Cryst. Growth Des.* **2006**, *6*, 461-466. Gagnon, E.; Maly, K. E.; Maris, T.; Wuest, J. D. *Acta Crystallogr.* **2007**, *C63*, o4-o6.

contribution essentielle du cœur moléculaire dans cette étude est discutée. Ensuite (Section 4.3), les interactions non-covalentes typiques des groupements nitro sont présentées. Finalement, l'article 2 (Section 4.4) qui décrit nos résultats est suivi d'une conclusion (Section 4.5) qui complète ce chapitre.

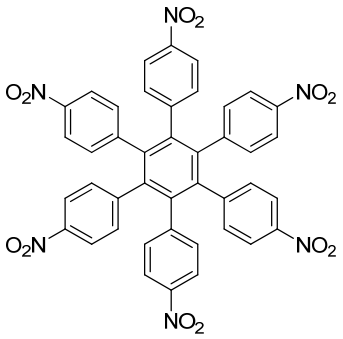

4.1

4.2 L'importance du cœur moléculaire

Les molécules utilisées en tectonique moléculaire sont toutes construites de la même façon : une charpente moléculaire oriente dans l'espace les groupements de reconnaissance. Les cœurs moléculaires utilisés dans notre groupe de recherche sont majoritairement aromatiques, rigides et hautement symétriques. Quelques exemples typiques sont illustrés à la Figure 4.1.

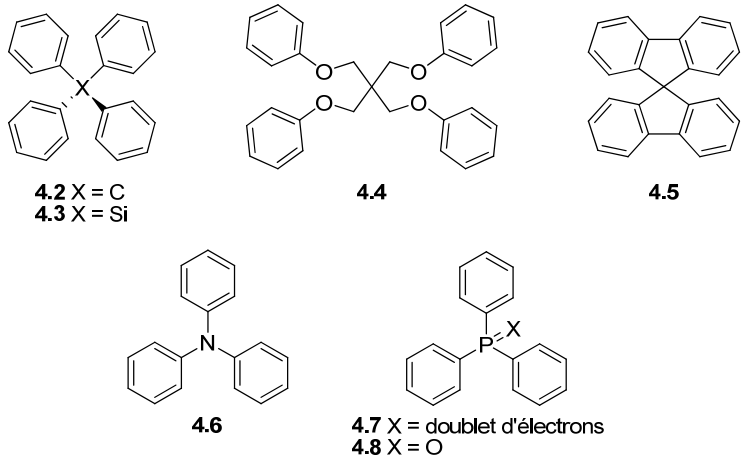

4.2 X = C
4.3 X = Si

4.4

4.5

4.6

4.7 X = doublet d'électrons
4.8 X = O

Figure 4.1. Cœurs moléculaires typiques déjà utilisés en tectonique moléculaire.

On remarque rapidement que tous ces cœurs moléculaires ont des cycles aromatiques peu encombrés. Si on étudie les structures cristallographiques du

tétraphénylméthane (**4.2**),[4] du tétraphénylsilane (**4.3**),[5] du tétraphényl éther du pentaerythritol (**4.4**),[6] du spirobifluorène (**4.5**),[7] de la triarylamine (**4.6**),[8] de la triphénylphosphine (**4.7**)[9] ou de son oxyde (**4.8**),[10] il apparait que ces cycles aromatiques établissent une grande quantité d'interactions C-H···π et/ou d'empilement-π à l'état solide. En particulier, les groupements trityles, triphénylsilyles, triphénylphosphines et le tétraphényl ether du pentaerythritol sont bien connus pour former des embrassements phényliques.[11]

La nitration du tétraphénylméthane permet d'obtenir aisément le tétrakis(4-nitrophényl)méthane (**4.9**). Ce composé a été l'objet d'une étude approfondie sur son comportement à l'état cristallin.[12] En effet, quatorze structures cristallines différentes ont été obtenues en variant le solvant de cristallisation utilisé. Les groupements nitro prennent part dans des interactions du type C–H···$O_{(nitro)}$ et la présence des cycles aromatiques ajoutent dans chaque cas une série d'interactions C–H···π et d'empilement-π. Ce composé illustre l'effet de la compétition entre les interactions faibles issus des groupements nitro et ceux venant du tétraphénylméthane.

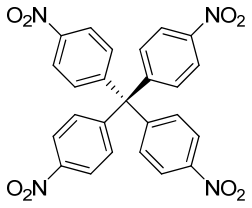

4.9

---

4 Robbins, A.; Jeffrey, G. A.; Chesick, J. P.; Donohue, J.; Cotton, F. A.; Frenz, B. A.; Murillo, C. A. *Acta Crystallogr.* **1975**, *B31*, 2395-2399.

5 Claborn, K.; Kahr, B.; Kaminsky, W. *CrystEngComm* **2002**, *4*, 252-256.

6 Laliberté, D.; Maris, T.; Wuest, J. D. *Acta Crystallogr.* **2003**, *E59*, o799-o901.

7 (a) Schenk, H. *Acta Crystallogr.* **1972**, *B28*, 625-628. (b) Douthwaite, R. E.; Taylor, A.; Whitwood, A. C. *Acta Crystallogr.* **2005**, *C61*, o328-301.

8 Sobolev, A. N.; Belsky, V. K.; Romm, I. P.; Chernikova, N. Y.; Guryanova, E. N. *Acta Crystallogr.* **1985**, *C41*, 967-971.

9 Dunne, B. J.; Orpen, A. G. *Acta Crystallogr.* **1991**, *C47*, 345-347.

10 Thomas, J. A.; Hamor, T. A. *Acta Crystallogr.* **1993**, *C49*, 355-357.

11 (a) Dance, I.; Scudder, M. *J. Chem. Soc., Chem. Commun.* **1995**, 1039-1040. (b) Steiner, T. *New J. Chem.* **2000**, *24*, 137-142. (c) Scudder, M.; Dance, I. *CrystEngComm* **2001**, *12*, 1-4. (d) Dance, I.; Scudder, M. *New J. Chem.* **2001**, *25*, 1510-1515. (e) Karlen, S. D.; Khan, S. I.; Garcia-Garibay, M. A. *Cryst. Growth Des.* **2005**, *5*, 53-55. (f) Dance, I.; Scudder, M. *CrystEngComm* **2009**, *11*, 2233-2247.

12 Thaimattam, R.; Xue, F.; Sarma, J. A. R. P.; Mak, T. C. W.; Desiraju, G. R. *J. Am. Chem. Soc.* **2001**, *123*, 4432-4445.

À l'opposé, la structure cristallographique de l'hexaphénylbenzène révèle que les cycles aromatiques sont beaucoup moins exposés aux molécules environnantes (Figure 4.2)[13] La formation d'interactions non-covalentes de type π-π ou C-H···π est donc très limitée pour des raisons stériques. Cet aspect de l'hexaphénylbenzène suggère qu'il peut remplir le rôle de cœur moléculaire efficacement, tout en interférant minimalement dans les phénomènes d'association intermoléculaire.

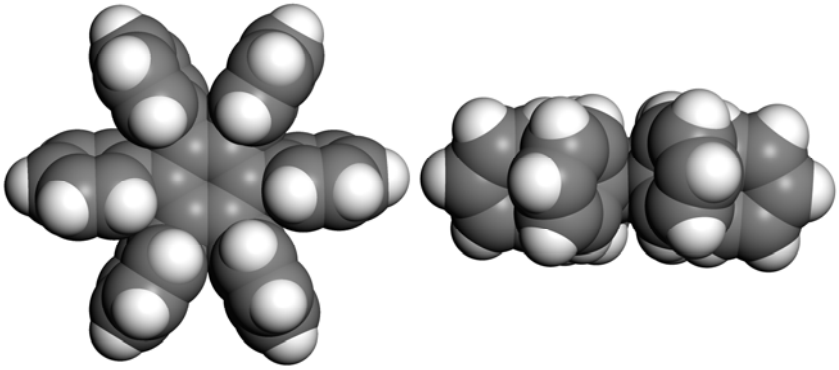

Figure 4.2. Structure par diffraction des rayons-X de l'hexaphénylbenzène, représenté par un modèle CPK. Gauche : vue du dessus, droite : vue de côté.

4.3.1 Interactions faibles des groupements nitro

Le groupement nitro comporte trois atomes électronégatifs maintenus par des liaisons σ et π. Cette combinaison particulière permet au groupement nitro d'interagir très fortement avec un cycle aromatique par effet inductif et par résonance (Figure 4.3). On note que l'on attribue toujours une charge positive à l'atome d'azote et que celui-ci est lié à deux atomes d'oxygène très électronégatifs. On peut donc supposer qu'un groupement nitro a le potentiel de former des interactions très similaires à celles des groupements carbonyles : c'est-à-dire, participer dans des interactions de type dipôle-dipôle[14] ou encore former des ponts hydrogène en agissant comme accepteur.[15] Par

[13] Bart, J. C. J. *Acta Crystallogr.* **1968**, *B24*, 1277-1287.

[14] (a) Gavezzotti, A. *J. Phys. Chem.* **1990**, *94*, 4319-4325. (b) Allen, F. H.; Baalham, C. A.; Lommerse, J. P. M.; Raithby, P. R. *Acta Crystallogr.* **1998**, *B54*, 320-329. (c) Lee, S.; Mallik, A. B.; Fredrickson, D. C. *Cryst. Growth Des.* **2004**, *4*, 279-290.

[15] (a) Wood, P. A.; Pidcock, E.; Allen, F. H. *Acta Crystallogr.* **2008**, *B64*, 491-496. (b) Lommerse, J. P. M.; Price, S. L.; Taylor, R. *J. Comput. Chem.* **1997**, *18*, 757-774.

contre, une recherche plus approfondie de la littérature révèle une plus grande diversité d'interactions non-covalentes.

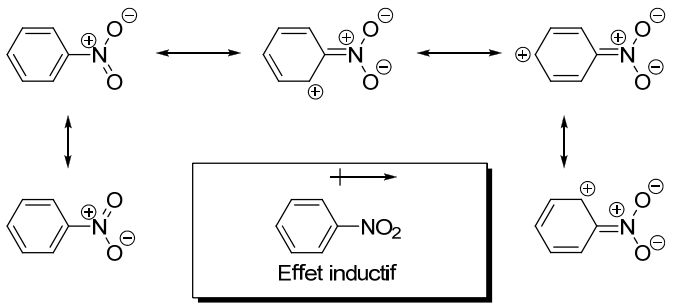

Figure 4.3. Effet inductif et effet de résonance dans le nitrobenzène.

4.3.2 Le groupement nitro, accepteur de ponts hydrogène

Le groupement nitro est un moins bon accepteur de ponts hydrogène que d'autres groupements fonctionnels oxydés, tels que les aldéhydes, les cétones et les esters. Cet effet est expliqué par la présence de l'atome d'azote, qui est plus électronégatif que le carbone, ainsi que par la résonance qui diminue la disponibilité des doublets d'électrons des atomes d'oxygène.[16] On retrouve par contre certains motifs plus fiables que d'autres. Par exemple, l'étude cristallographique d'une série de nitroanilines a permis d'observer deux types de ponts hydrogène, **4.10** et **4.11** (Figure 4.4).[17]

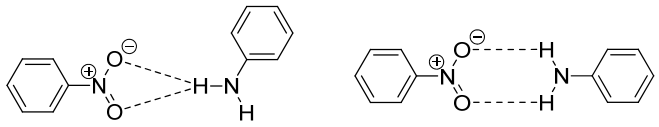

4.10 **4.11**

Figure 4.4. Ponts hydrogène chélatés (gauche) et cycliques (droite) entre un groupement nitro et le groupement amino d'une aniline.

Le groupement nitro forme aussi d'autres motifs de reconnaissance de façon récurrente. Par exemple, plusieurs structures cristallines contenant un groupement nitro

[16] Robinson, J. M. A.; Philp, D.; Harris, K. D. M.; Kariuki, B. M. *New J. Chem.* **2000**, *24*, 799-806.
[17] (a) Panunto, T. W.; Urbánczyk-Lipkowska, Z.; Johnson, R.; Etter, M. C. *J. Am. Chem. Soc.* **1987**, *109*, 7786-7797. (b) Etter, M. C. *Acc. Chem. Res.* **1990**, *23*, 120-126.

et un groupement diméthylamino forment des hétérodimères cycliques.[18] Ainsi, la co-cristallisation de l'acide 4-nitrobenzoïque et de l'acide 4-(*N*,*N*-diméthylamino)benzoïque[18a] permet d'obtenir une chaîne supramoléculaire (Figure 4.5). Les acides carboxyliques s'associent pour former des dimères (**A**) tandis que le groupement nitro s'associe au groupement diméthylamino par la formation de deux liens C-H···$O_{(nitro)}$ (**B**).

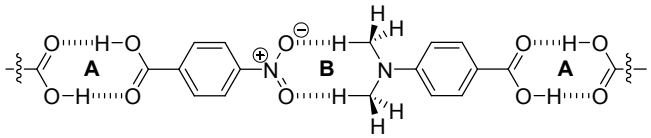

4.12

Figure 4.5. Formation de chaînes supramoléculaires dans le co-cristal de l'acide 4-nitrobenzoïque et de l'acide 4-(*N*,*N*-diméthylamino)benzoïque.

Étant donné la capacité des groupements nitro d'accepter des ponts hydrogène, certains auteurs se sont penchés sur la possibilité de former des associations sélectives avec des groupements éthynyles terminaux. Ceux-ci sont de meilleurs donneurs de ponts hydrogène que les liens C-H hybridés sp^2 et sp^3 et établissent facilement des ponts hydrogène chélatés avec les groupements nitro. La cristallisation du 1-éthynyl-4-nitrobenzène (**4.13**) génère comme attendu une chaîne supramoléculaire maintenue par des interactions C-H···$O_{(nitro)}$ (Figure 4.6).[19] De plus, cette interaction est suffisamment forte pour favoriser la co-cristallisation du 1,4-diéthynylbenzène et du 1,4-dinitrobenzène (**4.14**), illustrée dans la Figure 4.6.[20]

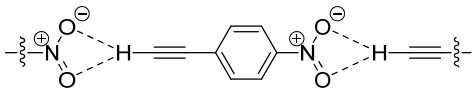

4.13

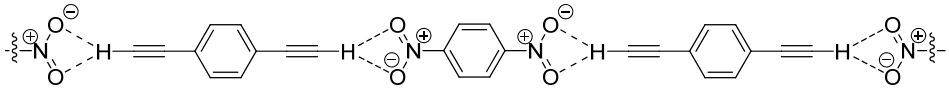

4.14

Figure 4.6. Exemples de groupements nitro impliqués dans des ponts hydrogène chélatés avec des groupements éthynyles.

---

[18] (a) Sharma, C. V. K.; Panneerselvam, K.; Pilati, T.; Desiraju, G. R. *J. Chem. Soc., Chem. Commun.* **1992**. (b) Sharma, C. V. K.; Desiraju, G. R. *J. Chem. Soc., Perkin Trans. 2* **1994**, 2345-2352.

[19] Langley, P. J.; Hulliger, J.; Thaimattam, R.; Desiraju, G. R. *New J. Chem.* **1998**, *22*, 1307-1309.

[20] Robinson, J. M. A.; Philp, D.; Kariuki, B. M.; Harris, K. D. M. *Chem. Commun.* **1999**, 329-330.

4.3.3 Interactions nitro-iodo

Les atomes d'oxygène du groupement nitro sont riches en électrons. Tel que présenté ci-haut, cet effet permet aux groupements nitro d'établir une série d'interactions non-covalentes avec des atomes d'hydrogène polarisés positivement. Les atomes d'halogènes liés à un atome de carbone ont aussi un grand potentiel en chimie supramoléculaire. Les liens C-X (X = Cl, Br, I) ont une distribution électronique anisotrope; l'extrémité du lien est polarisée positivement alors que la circonférence du lien C-X est polarisée négativement (Figure 4.7).[21]

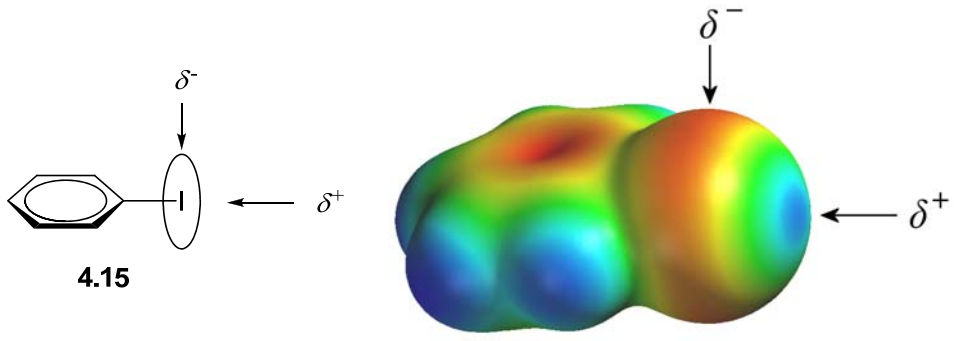

Figure 4.7. La distribution schématisée des électrons dans un lien C-I (à gauche) et le potentiel électrostatique de l'iodobenzène (à droite). La densité électronique augmente en allant du bleu au vert au rouge.

Il s'ensuit qu'une interaction non-covalente linéaire analogue au pont hydrogène peut être établie entre un lien C-X et un groupement nitro. Un autre facteur important est la polarisabilité de l'atome d'halogène; plus celui-ci est polarisable, plus l'interaction avec un groupement nitro est probable.[22] L'iode est alors tout indiqué pour établir ces interactions non-covalentes.

---

[21] (a) Bosch, E.; Barnes, C. L. *Cryst. Growth Des.* **2002**, *2*, 299-392. (b) Awwadi, F. F.; Willett, R. D.; Peterson, K. A.; Twamley, B. *Chem. Eur. J.* **2006**, *12*, 8952-8960. (c) Metrangolo, P.; Meyer, F.; Pilati, T.; Resnati, G.; Terraneo, G. *Angew. Chem. Int. Ed.* **2008**, *47*, 6114-6127.

[22] (a) Desiraju, G. R.; Harlow, R. L. *J. Am. Chem. Soc.* **1989**, *111*, 6757-6764. (b) Allen, F. H.; Lommerse, J. P. M.; Hoy, V. J.; Howard, J. A. K.; Desiraju, G. R. *Acta Crystallogr.* **1997**, *B53*, 1006-1016.

Cette possibilité a été démontrée dès 1994 par la co-cristallisation du 1,4-diiodobenzène et du 1,4-dinitrobenzène, qui génère le motif **4.16** (Figure 4.8).[23] Des interactions linéaires chélatées formées par le contact entre un atome d'iode et les deux atomes d'oxygène d'un groupement nitro sont observées. Ceci n'est pas sans rappeler le pont hydrogène nitro-éthynyle vu ci-haut (Figure 4.6). Similairement, la cristallisation du 4-iodonitrobenzène (**4.17**),[24] la cristallisation du 4-iodo-4'-nitrobiphényle (**4.18**)[25] ou encore la co-cristallisation du 1,4-dinitrobenzène et de l'acide 4-iodocinnamique (**4.19**)[26] mènent à la formation de chaînes linéaires formées par ces interactions relativement robustes (Figure 4.8).

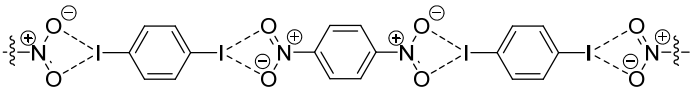

4.16

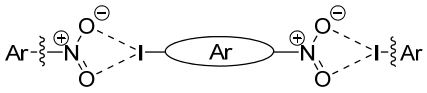

4.17 Ar = phényle
4.18 Ar = biphényle

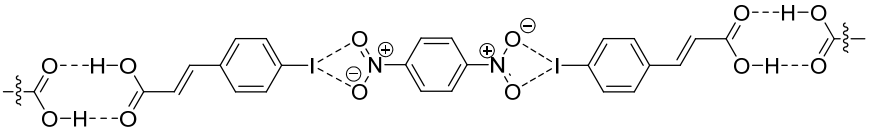

4.19

Figure 4.8. Interactions supramoléculaires entre un groupement nitro et un atome d'iode.

4.3.4 Interactions impliquant le dipôle du groupement nitro

Les interactions non-covalentes présentées jusqu'ici possèdent toutes une géométrie quasi-linéaire. Par contre, les groupements nitro peuvent aussi former des

---

[23] Allen, F. H.; Goud, B. S.; Hoy, V. J.; Howard, J. A. K.; Desiraju, G. R. *J. Chem. Soc., Chem. Commun.* **1994**, 2729-2730.

[24] Thalladi, V. R.; Goud, B. S.; Hoy, V. J.; Allen, F. H.; Howard, J. A. K.; Desiraju, G. R. *Chem. Commun.* **1996**, 401-402.

[25] (a) Sarma, J. A. R. P.; Allen, F. H.; Hoy, V. J.; Howard, J. A. K.; Thaimattam, R.; Biradha, K.; Desiraju, G. R. *Chem. Commun.* **1997**, 101-102. (b) Hulliger, J.; Langley, P. J. *Chem. Commun.* **1998**, 2557-2558. (c) Masciocchi, N.; Bergamo, M.; Sironi, A. *Chem. Commun.* **1998**, 1347-1348.

[26] Thalladi, V. R.; Goud, B. S.; Hoy, V. J.; Allen, F. H.; Howard, J. A. K.; Desiraju, G. R. *Chem. Commun.* **1996**, 401-402.

interactions orthogonales dans lesquelles les deux groupements interagissant ensemble sont disposés à 90° l'un de l'autre.[27] Ces interactions non-covalentes sont possibles grâce à la présence de dipôles à l'intérieur du groupement nitro : c'est-à-dire que l'atome d'azote est appauvri en électrons par les deux atomes d'oxygène. On peut alors espérer voir des interactions dipôle-dipôle comme celles observées avec les groupements carbonyles[28] ou cyano.[29] Par exemple, dans une série de structures reliées au picrate, on dénote ce type d'interaction dans laquelle un atome d'oxygène appartenant à un groupement nitro s'approche de l'atome d'azote d'un second groupement.[30] Les auteurs représentent ce contact par un tétraèdre formé par les atomes d'un groupement C-NO_2 et l'atome d'oxygène interagissant avec celui-ci (Figure 4.9).

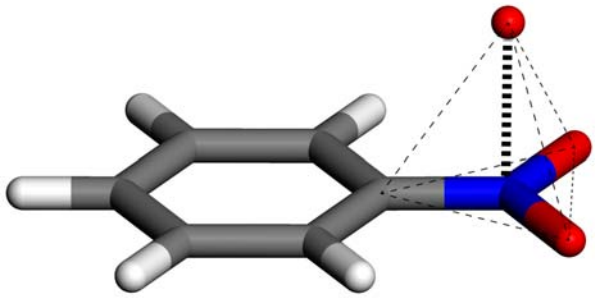

Figure 4.9. Interaction schématisée entre un atome d'oxygène et un groupement nitro, représentée par un trait large hachuré. On peut définir un tétraèdre en reliant ensemble les atomes liés à l'atome d'azote du groupement nitro.

Ce comportement a été observé à quelques reprises, comme dans les structures du 1,3,5-trinitrobenzène[31] et de la 2,4,6-tris(4-nitrophenoxy)-1,3,5-triazine.[32] Plus étonnamment, les structures de deux isomères d'acide nitro-α-résorcylique contiennent aussi ces motifs de reconnaissance, malgré la présence de groupements hydroxyles et

---

27 (a) Paulini, R.; Müller, K.; Diederich, F. *Angew. Chem. Int. Ed.* **2005**, *44*, 1788-1805. (b) Voth, A. R.; Khuu, P.; Oishi, K.; Ho, P. S. *Nature Chem.* **2009**, *1*, 74-79.

28 Allen, F. H.; Baalham, C. A.; Lommerse, J. P. M.; Raithby, P. R. *Acta Crystallogr.* **1998**, *B54*, 320-329.

29 Wood, P. A.; Borwick, S. J.; Watkin, D. J.; Motherwell, W. D. S.; Allen, F. H. *Acta Crystallogr.* **2008**, *B64*, 393-396.

30 Wozniak, K.; He, H.; Klinowski, J.; Jones, W.; Grech, E. *J. Phys. Chem.* **1994**, *98*, 13755-13765.

31 Thallapally, P. K.; Jetti, R. K. R.; Katz, A. K.; Carrell, H. L.; Singh, K.; Lahiri, K.; Kotha, S.; Boese, R.; Desiraju, G. R. *Angew. Chem. Int. Ed.* **2004**, *43*, 1149-1155.

32 Jetti, R. K. R.; Thallapally, P. K.; Nangia, A.; Lam, C.-K.; Mak, T. C. W. *Chem. Commun.* **2002**, 952-953.

acide carboxylique qui devraient dominer entièrement l'assemblage supramoléculaire.[33] Il existe aussi une poignée d'exemples dans lesquels les groupements nitro agissent comme accepteur avec un groupement carbonyle[34] ou le doublet d'électron d'un atome d'azote adjacent (de façon intramoléculaire).[35] Les groupements nitro peuvent donc établir un bon nombre d'interactions non-covalentes aux propriétés distinctes. Toutefois, tous les systèmes étudiés jusqu'à maintenant possédaient un squelette hydrocarboné pouvant établir diverses interactions π-π et C-H···π. De plus, les groupements nitro entraient en compétition avec d'autres groupes fonctionnels pour définir les interactions non-covalentes dominantes de la structure.

Pour documenter le comportement à l'état solide d'une molécule dénudée de ces éléments interférents, nous avons entrepris une étude de l'hexakis(4-nitrophényl)benzène (**4.1**). Le cœur moléculaire hexaphénylbenzène élimine la majeure partie des interactions non-covalentes typiquement issues du squelette hydrocarboné. De plus, les groupements fonctionnels dans ce composé sont limités à des liens C-H (sp^2) et des groupements nitro. On s'attendrait donc à n'observer que des interactions entre ces groupements fonctionnels. Cette approche vise aussi à déterminer le potentiel des groupements nitro en tectonique moléculaire, à savoir s'ils peuvent diriger efficacement les assemblages supramoléculaires en établissant un réseau supramoléculaire d'interactions non-covalentes dominantes. La cristallisation du composé **4.1** dans divers solvants révèle toutefois une histoire plus complexe.

---

[33] Čorić, I.; Milić, D.; Matković-Čalogović, D.; Tomašković, L. *Struct. Chem.* **2009**, *20*, 73-80.

[34] Yin, Z.; Jiang, L.; He, J.; Cheng, J.-P. *Chem. Commun.* **2003**, 2326-2327.

[35] (a) Yap, G. P. A.; Jové, F. A.; Claramunt, R. M.; Sanz, D.; Alkorta, I.; Elguero, J. *Aust. J. Chem.* **2005**, *58*, 817-822. (b) Santa María, M. D.; Claramunt, R. M.; García, M. Á.; Elguero, J. *Tetrahedron* **2007**, *63*, 3737-3744.

4.4 Article 2

The potential of intermolecular N•••O interactions of nitro groups in crystal engineering, as revealed by structures of hexakis(4-nitrophenyl)benzene

Eric Gagnon,[†] Thierry Maris, Kenneth E. Maly,[‡] and James D. Wuest

Tetrahedron **2007**, *63*, 6603-6613

Reprinted from Tetrahedron, 63, Eric Gagnon, Thierry Maris, Kenneth E. Maly and James D. Wuest, *The potential of intermolecular N•••O interactions of nitro groups in crystal engineering, as revealed by structures of hexakis(4-nitrophenyl)benzene*, 6603-6613, Copyright 2007, with permission from Elsevier

Abstract

Like other derivatives of hexaphenylbenzene, hexakis(4-nitrophenyl)benzene (**1**) crystallizes under a variety of conditions as layered structures in which significant quantities of guests are included in spaces between the layers or within them. In structures of nitroarene **1**, multiple intermolecular N···O interactions of NO_2 groups help to hold the layers together and determine how the molecular constituents are positioned. The behavior of nitroarene **1** confirms that N···O interactions can allow crystal engineers to position molecules with a useful degree of predictability, particularly when stronger interactions such as hydrogen bonds are absent, and when competition with other weak interactions is limited.

Introduction

No current methods allow the structures and properties of new molecular crystals to be predicted reliably.[1] This constitutes a significant obstacle to progress in materials science and technology. Developing suitable predictive methods is a key goal of the rapidly growing field of crystal engineering.[2] Although this goal has not yet been reached, the ability to control molecular crystallization is increasing dramatically. In part, this progress has occurred because crystal engineers have taken advantage of impressive new tools, including advanced theoretical approaches, accelerated generation of crystallographic data, perceptive statistical analyses of collections of structures, revolutionary methods for revealing crystalline surfaces at atomic resolution, and powerful modern techniques for designing and synthesizing promising molecules.

A productive strategy for engineering new crystals is based on treating them as supramolecular constructs held together by particular intermolecular forces. If each molecular component participates in multiple interactions that are strong and directional, then subsequent association will favor the creation of networks in which each component is positioned predictably with respect to its neighbors. In this strategy of programmed molecular construction, proper choice of the individual components (which

have been called tectons[3]) and their patterns of interaction (which have been called supramolecular synthons[4]) allows crystal engineers to come very close to the goal of producing new structures with predetermined features.[5] This strategy is expected to be most effective when (1) the tectons have well-defined structures, such as those provided by relatively rigid molecular cores and (2) reliable supramolecular synthons are used, such as those involving multiple classical hydrogen bonds. Nevertheless, useful degrees of control can be attained even when the tectons have significant flexibility[6] or when the intermolecular interactions are weaker and less directional.[7]

In exploring the potential of weaker supramolecular synthons, crystal engineers and structural chemists have begun to pay special attention to interactions of the NO_2 group.[8-20] In part, this interest reflects the central role of nitro compounds in molecular synthesis, their significant electron-withdrawing electronic effects, and the variety of supramolecular synthons in which they can engage. Figures 1 and 2 present selected intermolecular interactions observed in structures of simple nitroarenes. In motifs **I–III** (Fig. 1), the NO_2 group serves as an acceptor of a C–H···O hydrogen bond;[7] in motifs **IV–VI** (Fig. 2), N···O interactions involving two or more NO_2 groups are present;[11–16] and in motif **VII** (Fig. 2), dispersive interactions are involved.[17] Related N···N or N···O interactions involving an NO_2 group and a different partner have also been observed.[18,19] In addition to these selected interactions of NO_2 groups,[20] the aryl groups of nitroarenes can also engage directly in characteristic aromatic interactions.

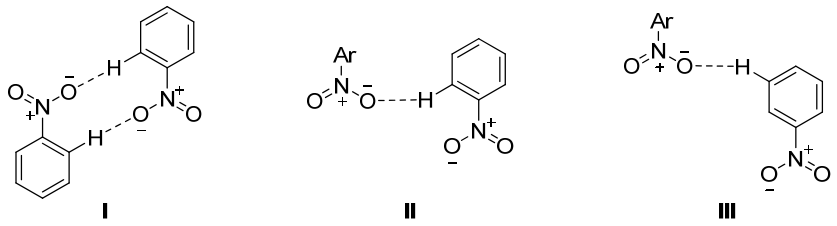

Figure 1. Selected C–H···O interactions involving nitroarenes.

Assessing the relative importance of weak interactions of NO_2 groups is difficult, but several useful guidelines have emerged:

1. NO_2 groups are intrinsically poorer acceptors of hydrogen bonds than related groups with greater electron density on oxygen, such as nitrones or carboxylates.[10,21]
2. The tendency of nitroarenes to adopt conformations with coplanar NO_2 groups and aryl rings can disfavor the in-plane approach of hydrogen–bond donors and lead to distortions in bond angles.[22]
3. Calculations have revealed that N···O interactions of NO_2 groups can be at least as strong as C–H···O hydrogen bonds.[12]
4. Theoretical studies have concluded that dispersive interactions such as motif **VII** (Fig. 2) are stronger than electrostatic attractions involving NO_2 groups.[17]

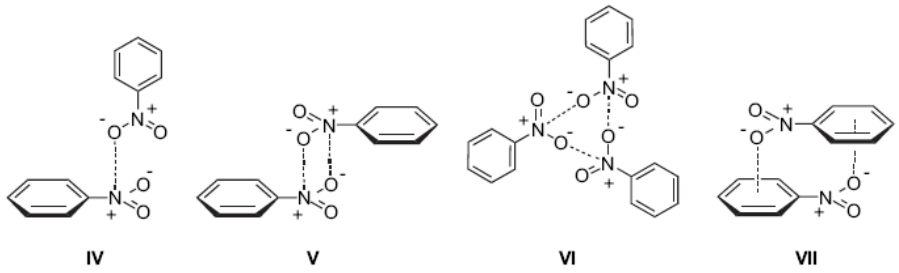

Figure 2. Selected N···O (**IV**–**VI**) or dispersive (**VII**) interactions involving nitroarenes.

These guidelines suggest that N···O interactions of NO_2 groups may play a key role in determining how nitroarenes crystallize when they cannot engage in stronger intermolecular interactions such as classical hydrogen bonds, and when the opportunity to participate in alternative weak interactions is restricted. However, previous studies on the potential of NO_2 groups in crystal engineering have provided few examples in which N···O interactions can be considered to make a dominant contribution to molecular adhesion and organization.[15]

Recent studies of the crystallization of derivatives of hexaphenylbenzene[23–26] led us to examine the behavior of the NO_2 groups of hexakis(4-nitrophenyl)benzene (**1**).[27] Like other hexaphenylbenzenes, nitroarene **1** is expected to favor a chiral propeller conformation and to have a disc-shaped geometry that induces the formation of layered

structures.[23-26] The complex molecular geometry should disfavor extensive intermolecular aromatic interactions, as well as C–H···O interactions of NO_2 groups involving relatively inaccessible meta hydrogens (motif **III**, Fig. 1) or dispersive interactions requiring close contact of hexaphenylbenzene cores (motif **VII**, Fig. 2). Moreover, the tendency to form layered structures assembled from disc-shaped components should inhibit the formation of cyclic doubly hydrogen-bonded motifs in which the ortho hydrogens of nitroaryl groups participate (motif **I**, Fig. 1). Geometric constraints imposed by the hexaphenylbenzene core of nitroarene **1**, together with the absence of groups that can take part in classical hydrogen bonds, therefore suggest that crystallization will be controlled by the following limited set of NO_2 interactions: single C–H···O interactions involving primarily ortho hydrogens (motif **II**, Fig. 1), N•••O interactions (motifs **IV–VI**, Fig. 2), or other cyclic oligomeric motifs analogous to structures **V** and **VI**.

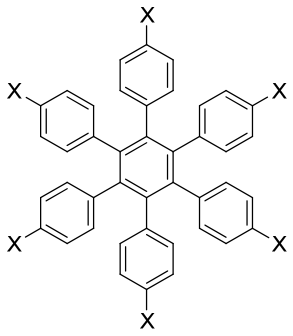

1 (X = NO_2)
2 (X = CN)

In this paper, we report the synthesis of nitroarene **1**, its characterization, and the structure of crystals obtained under six different conditions. Analysis of the structures establishes that (1) compound **1** favors layered structures, as expected, and therefore behaves like a typical hexaphenylbenzene; (2) the dominant intermolecular interactions within the layers are N···O interactions of NO_2 groups; and (3) in certain cases, the layers are joined to adjacent layers of nitroarene **1** by C–H···O interactions according to motifs **I** and **II** (Fig. 1), or they are simply separated by intervening layers of included solvent.

2. Results and discussion

2.1. Synthesis of hexakis(4-nitrophenyl)benzene (1) Nitroarene **1** was first described in 1971 by Bergmann in a brief communication that reported only its decomposition point and elemental analysis.[27] We obtained the compound by the direct nitration of hexaphenylbenzene[28] in fuming HNO_3 containing a catalytic amount of H_2SO_4. Subsequent crystallization of the crude product from DMSO gave purified nitroarene **1** in 60% yield.

2.2. Crystallization of hexakis(4-nitrophenyl)benzene (1) Crystals suitable for structural studies by X-ray diffraction were obtained by allowing vapors of suitable cosolvents to diffuse into solutions of nitroarene **1** in *N,N*-dimethylformamide (DMF). Crystallographic data are summarized in Table 1.

Table 1. Crystallographic data for pseudopolymorphs of hexakis(4-nitrophenyl)benzene (**1**).

Included solvent	7 Benzene	7 Dioxane	2 Acetonitrile	2 Acetone	2 Ethanol	2 DMF
Formula	$C_{84}H_{66}N_6O_{12}$	$C_{70}H_{80}N_6O_{26}$	$C_{46}H_{30}N_8O_{12}$	$C_{48}H_{36}N_6O_{14}$	$C_{46}H_{36}N_6O_{14}$	$C_{48}H_{38}N_8O_{14}$
Crystal system	Triclinic	Triclinic	Monoclinic	Monoclinic	Monoclinic	Monoclinic
Space group	*P*-1	*P*-1	*C*2/*c*	*C*2/*c*	$P2_1/n$	$P2_1$
a (Å)	11.1911(9)	11.533(2)	11.237(2)	11.181(4)	10.7355(10)	11.6772(13)
b (Å)	13.9932(11)	13.037(3)	20.367(5)	20.593(6)	13.9310(14)	17.9809(19)
c (Å)	24.378(2)	14.014(3)	19.002(4)	20.074(5)	14.1161(15)	11.9334(13)
α	84.436(5)	105.10(3)	90	90	90	90
β	83.004(5)	108.37(3)	102.048(11)	104.739(8)	98.039(6)	116.183(6)
γ	68.693(5)	110.42(3)	90	90	90	90
V (Å^3)	3524(5)	1703.7(6)	4253.0(16)	4470(2)	2090.4(4)	2248.5(4)
Z	2	1	4	4	2	2
ρ_{calcd} (g cm^{-3})	1.273	1.385	1.385	1.368	1.425	1.404
T (K)	100(2)	100(2)	100(2)	100(2)	100(2)	100(2)
μ (mm^{-1})	0.697	0.897	0.864	0.862	0.904	0.888
R_1, $I > 2\sigma$ (all)	0.0650	0.0567	0.0568	0.0542	0.0665	0.0567
ωR_2, $I > 2\sigma$ (all)	0.1465	0.1327	0.1292	0.1670	0.1422	0.1442
Measured reflections	11 726	5328	3815	3217	3774	4938
Independent observed reflections	6567	3740	2069	3878	2110	3946

Table 2. Summary of key structural features observed in pseudopolymorphs of hexakis(4-nitrophenyl)benzene (**1**).

Composition	Volume occupied by guests (%)	Number of adjacent molecules of nitroarene **1** engaging in significant N···O interactions[a,b]	Total number of significant N···O interactions per molecule[b]
1 · 7 benzene	54	6	12
1 · 7 dioxane	52	4	8
1 · 2 acetonitrile	18	4	16
1 · 2 acetone	19	4	12
1 · 2 ethanol	14	4	12
1 · 2 DMF	22	4	12

[a] As measured per molecule of nitroarene **1**.
[b] Significant N···O interactions are judged to be those shorter than 3.5 Å.[11,12]

Table 3. Conformations adopted by the hexaphenylbenzene core of nitroarene **1** in different pseudopolymorphs.

Included guest	Angles (°) between the average planes of the 4-nitrophenyl substituents and the central ring of the hexaphenylbenzene core
Benzene	60.99(12), 63.61(12), 63.92(13), 67.91(12), 68.05(12), 70.46(13)
Dioxane	81.81(12) (2×), 84.29(10) (2×), 87.87(11) (2×)
Acetonitrile	60.83(11), 62.61(11), 65.70(9) (2×), 67.80(9) (2×)
Acetone	62.10(8), 63.11(9) (2×), 64.23(9) (2×), 67.64(7)
Ethanol	71.46(17) (2×), 78.99(18) (2×), 79.11(15) (2×)
DMF	73.1(3), 73.9(4), 76.3(3), 82.0(3), 84.8(3), 88.7(3)

2.2.1. Structure of crystals of hexakis(4-nitrophenyl)benzene (1) grown from DMF/benzene. Crystals grown by allowing vapors of benzene to diffuse into solutions of nitroarene **1** in DMF were found to belong to the triclinic space group *P*-1 and to have the composition **1**·7 benzene, as established crystallographically (Table 1). Included benzene occupies 54% of the volume of the crystals, and no included DMF is observed (Table 2). Derivatives of hexaphenylbenzene are known to define a class of compounds with molecular shapes that disfavor efficient packing in crystals, and guests are included in essentially every previously reported structure.[23-26] In crystals in which the inherent difficulties of packing hexaphenylbenzenes have been exacerbated by

forcing them to engage in strong directional intermolecular interactions, the percentage of volume accessible to guests can even exceed 70%.[24] The observed inclusion in crystals of compound **1** is therefore fully consistent with the general behavior of derivatives of hexaphenylbenzene. As expected, molecules of nitroarene **1** lie in well-defined monolayers and adopt a chiral propeller-shaped conformation, as observed in many other derivatives of hexaphenylbenzene.[23-26] The torsional angles between the central and outer rings have values in the range 63-71° (Table 3), and each layer of nitroarene **1** contains an equal number of the two enantiomers. Each molecule is linked to six neighbours within the same layer by multiple N···O interactions of NO_2 groups, which can be considered to be the principle force ensuring adhesion of the layers (Fig. 3). In accord with the criterion adopted by Woźniak et al.,[11,12] N···O interactions are judged to be significant if the distance is less than 3.5 Å. Bonding would normally require an N···O distance of less than 3.07 Å,[29] which corresponds to standard values for the van der Waals radii of oxygen (1.52 Å) and nitrogen (1.55 Å); however, the dipolar character of NO_2 groups allows their N···O interactions to be significantly stabilizing at distances exceeding the sum of the van der Waals radii. In the structure of crystals grown from DMF/benzene, each molecule of nitroarene **1** engages in 12 interactions that satisfy this criterion by lying in the range 3.153(4) – 3.410(4) Å. Of these interactions, six are incorporated in a set of three cyclic trimers (motif **VI**, Fig. 2). Related trimeric aggregates of NO_2 groups were first explicitly recognized as potential supramolecular synthons by Nangia, Mak, and collaborators;[15] however, similar trimeric motifs are present in the structures of many nitroarenes, although they have frequently been overlooked.[30] In the trimeric motif described by Nangia, Mak, and collaborators,[15] both N···O and O···O interactions appear to be significant, but in the trimeric motifs identified in Figure 3, the average N···O distance is much shorter than the average O···O distance. This suggests that trimeric aggregates of NO_2 groups can adopt distinctly different geometries and should not be regarded as particularly reliable supramolecular synthons. In the structure of crystals of nitroarene **1** grown from DMF/benzene, monolayers composed of compound **1** are separated by monolayers of included benzene (Fig. 4). Each molecule of benzene is surrounded by six others in the same layer. The characteristic propeller-shaped conformation of hexaphenylbenzene **1** defines a toroidal

volume with a central indentation on each face that can partially accommodate a molecule of benzene. Two molecules of benzene from different layers are oriented in such a way that each directs a C– H bond toward the center of the toroidal volumes defined by host **1** (Fig. 4), creating C–H···aromatic interactions with H···centroid distances of 2.58(1) and 2.78(1) Å.

There are no important intralayer C–H···O interactions of NO_2 groups, as anticipated, but each molecule of nitroarene **1** engages in multiple C–H···O interactions with molecules of benzene in adjacent layers (H···O distances in the range 2.46(1) – 2.74(1) Å).

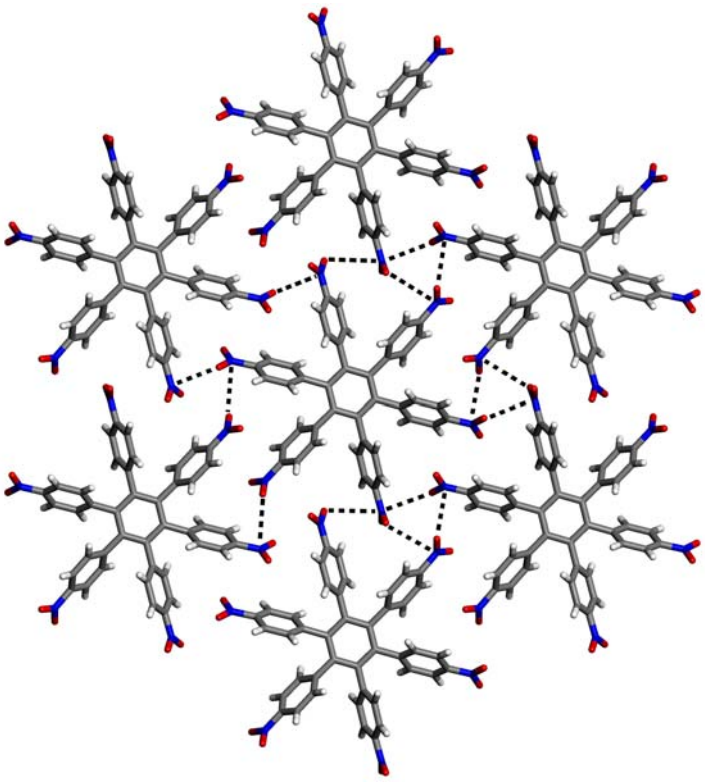

Figure 3. View of the structure of crystals of hexakis(4-nitrophenyl)benzene (**1**) grown from DMF/benzene, showing significant N···O interactions (N···O distances < 3.5 Å) between NO_2 groups of a central molecule of nitroarene **1** and its six coplanar neighbors. The interactions are represented by broken lines. Atoms of hydrogen appear in white, carbon in gray, nitrogen in blue, and oxygen in red.

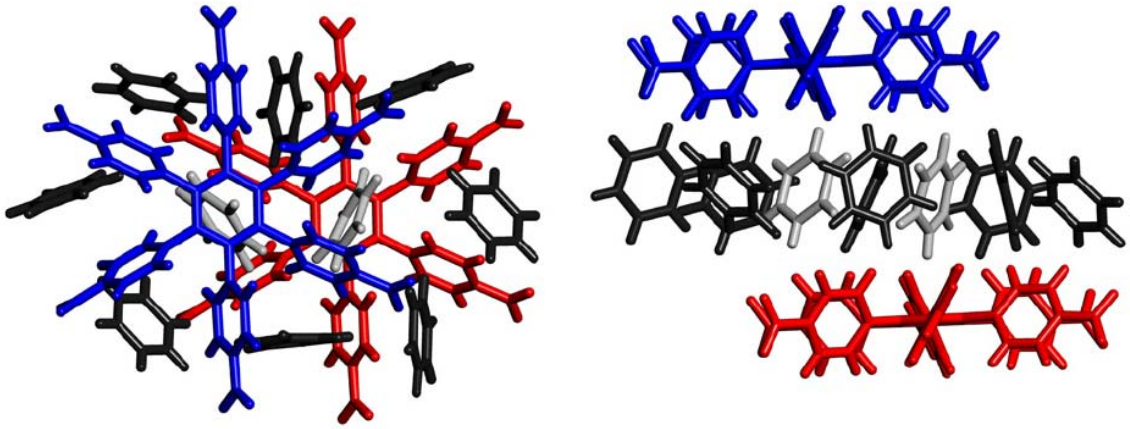

Figure 4. Top view (left) and side view (right) of the alternating monolayers found in crystals of hexakis(4-nitrophenyl)benzene (**1**) grown from DMF/benzene, showing two molecules of nitroarene **1** in different layers (blue and red) separated by a layer consisting of molecules of benzene (black and gray). Each molecule in gray directs a C–H bond toward the center of the hexaphenylbenzene core of a neighboring molecule of nitroarene **1**.

2.2.2. Structure of crystals of hexakis(4-nitrophenyl)benzene (1) grown from DMF/dioxane. Crystals grown by allowing vapors of dioxane to diffuse into solutions of nitroarene **1** in DMF proved to belong to the triclinic space group *P*-1 and to have the composition **1**·7 dioxane, as determined crystallographically (Table 1). Their structure is closely similar to that of crystals grown from DMF/benzene, and it will not be discussed in detail (see the Supplementary data for figure). Dioxane occupies 52% of the volume, and again no DMF is included (Table 2). Molecules of nitroarene **1** lie in well-defined monolayers and adopt a conformation in which the central and outer rings of the hexaphenylbenzene core are essentially orthogonal, with torsional angles in the range 81–88° (Table 3). Each molecule of nitroarene **1** is joined to neighbors within the same layer by eight significant N···O interactions (four N···O distances of 3.396(3) Å and four distances of 3.461(3) Å). These interactions are all of type **IV** (Fig. 2), and they can be considered to play a key role in maintaining the integrity of the layer. In crystals grown from both DMF/benzene and DMF/dioxane, monolayers composed of nitroarene **1** are separated by monolayers of included solvent. Each molecule of included dioxane has six neighbors within the plane, and two molecules of guest are partially accommodated within spaces above and below the central aromatic ring of each molecule of host **1**, creating two C–H···aromatic interactions with H···centroid distances of 2.65(1) Å.

Again, no significant intralayer C–H···O interactions of NO_2 groups are present, but each molecule of nitroarene **1** engages in multiple C–H···O interactions with molecules of dioxane in adjacent layers (H···O distances in the range 2.44(1) – 2.74(1) Å).

2.2.3. Structure of crystals of hexakis(4-nitrophenyl)- benzene (1) grown from DMF/acetonitrile. Crystals grown by allowing vapors of acetonitrile to diffuse into solutions of nitroarene **1** in DMF were found to belong to the monoclinic space group *C*2/*c* and to have the composition **1**·2 acetonitrile, as established crystallographically (Table 1). The ratio of included guests per molecule of host **1** (2:1) is substantially lower than it is in crystals grown from DMF/benzene and DMF/dioxane (7:1), providing immediate evidence of underlying structural differences. Acetonitrile occupies only 18% of the volume of the crystals, and again no DMF is included (Table 2). Molecules of nitroarene **1** lie in well-defined monolayers and adopt a chiral propeller-shaped conformation, with torsional angles between the central and outer rings in the range 60–68° (Table 3). Each layer of nitroarene **1** contains an equal number of the two enantiomers. Unlike the layers in crystals grown from DMF/benzene or DMF/dioxane, which are separated by intervening monolayers of guest, layers of nitroarene **1** in crystals grown from DMF/acetonitrile are in direct contact, and the smaller guests are able to occupy spaces within the layers of host. Again, cohesion within the layers can be attributed to multiple N···O interactions of NO_2 groups, but each molecule of nitroarene **1** is linked to only four neighbors within the same layer (Fig. 5). In addition, each molecule of nitroarene **1** interacts with four neighbors in each of the two adjacent layers by participating in a total 12 significant C–H···O interactions of NO_2 groups, with H···O distances in the range 2.31(1) – 2.75(1) Å (Fig. 6a). Most of these interactions (8) involve hydrogen atoms ortho to NO_2 groups (motif **II**, Fig. 1), and meta hydrogen atoms are engaged in only four interactions (motif **III**, Fig. 1), possibly because the characteristic geometry of the hexaphenylbenzene core of compound **1** makes the meta hydrogen atoms less accessible. In the observed structure, a total of 16 N···O interactions per molecule of nitroarene **1** are shorter than 3.5 Å. No cyclic trimers are observed (motif **VI**, Fig. 2), but eight of the interactions are involved in the formation of cyclic dimers (motif **V**, Fig. 2). N···O distances in the dimeric motifs

(3.366(4) and 3.455(3) Å) are longer than those observed in simple motif **IV**, which lie in the range 3.103(3) – 3.121(1) Å. This may arise from a combination of dipolar attractions and repulsions in the dimeric motif or from constraints introduced by the inherent difficulty of packing hexaphenylbenzene **1**, which may prevent dimeric motif **V** from attaining its optimal geometry. Pairs of guest molecules are included within cages bounded by four molecules of nitroarene **1** in the same layer and capped by two other molecules of host in adjacent layers (Figs. 7a and 8a). Interactions of guests with the host include (1) weak N–O···C interactions (O···C distances of 3.171(4) Å) involving an NO_2 group of the host and the CN groups of two guests (Fig. 5); (2) a C–H···O interaction involving an NO_2 group of the host and the CH_3 group of the guest; and (3) various C–H···N interactions involving aryl groups of the host and the CN group of the guest.

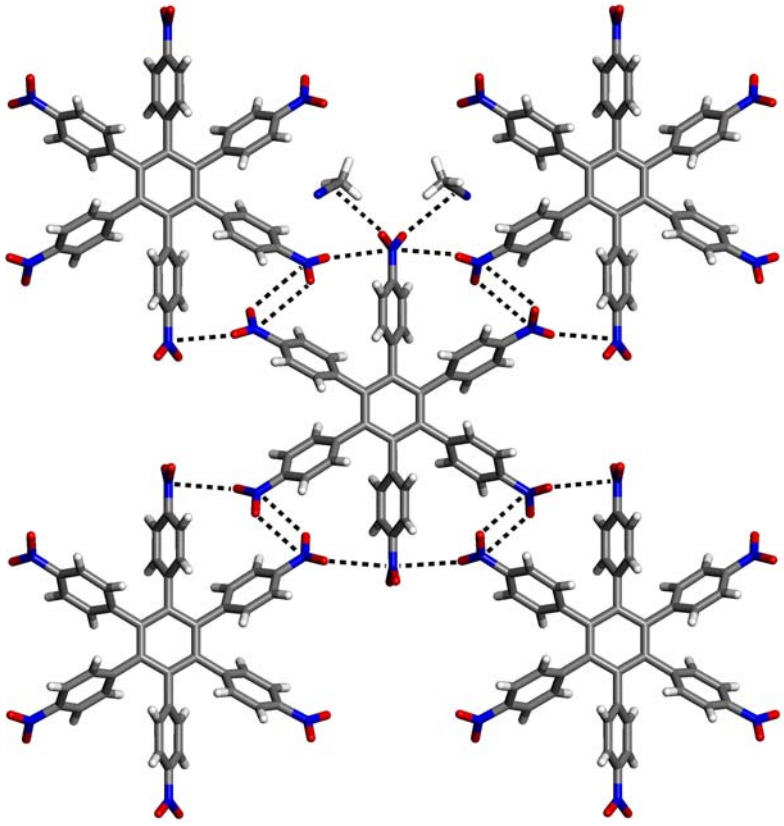

Figure 5. View of the structure of crystals of hexakis(4-nitrophenyl)benzene (**1**) grown from DMF/acetonitrile, showing significant N···O interactions (N···O distances < 3.5 Å) between NO_2 groups of a central molecule of nitroarene **1** and its four coplanar neighbors, as well as C···O interactions with two included molecules of acetonitrile. All interactions are represented by broken lines. Atoms of hydrogen appear in white, carbon in gray, nitrogen in blue, and oxygen in red.

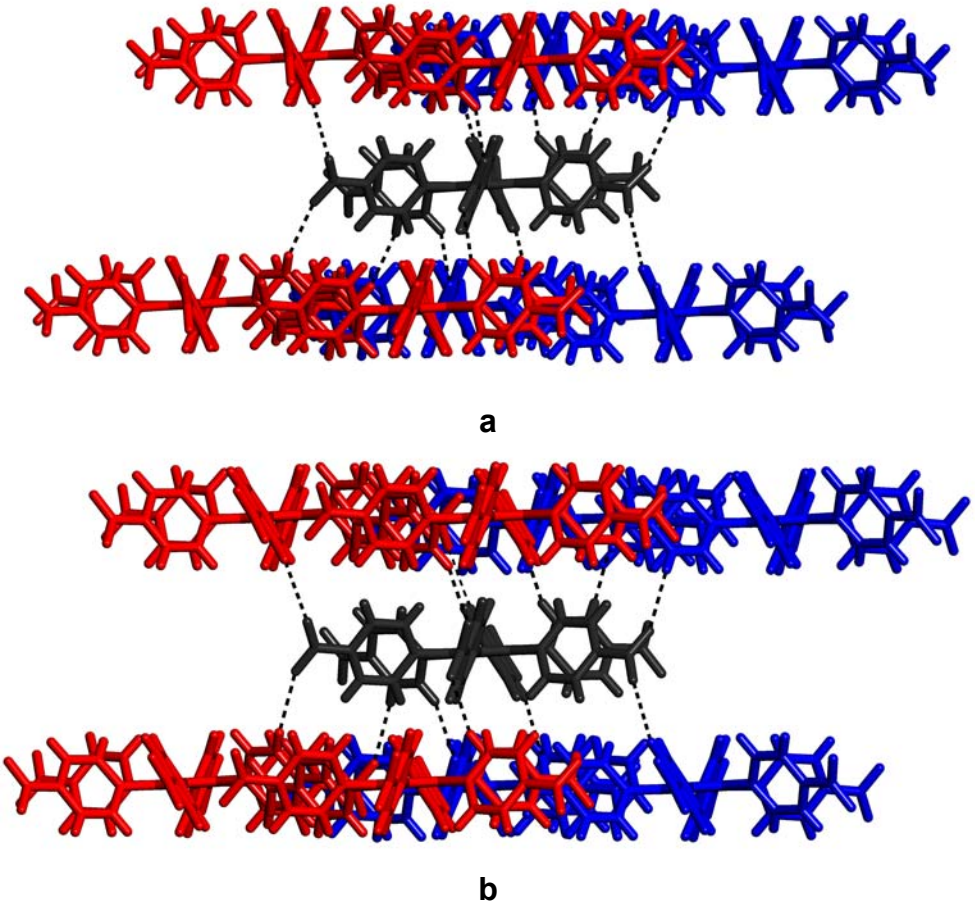

Figure 6. (a) View of the layered structure of crystals of hexakis(4-nitrophenyl)benzene (**1**) grown from DMF/acetonitrile, showing significant interlayer C–H/O interactions (H···O distances less than 2.75 Å) of a central molecule of nitroarene **1** (black). The interactions, which are represented by broken lines, involve four molecules of compound **1** (red and blue) in each of the two adjacent layers. (b) Analogous view of the layered structure of crystals of nitroarene **1** grown from DMF/acetone.

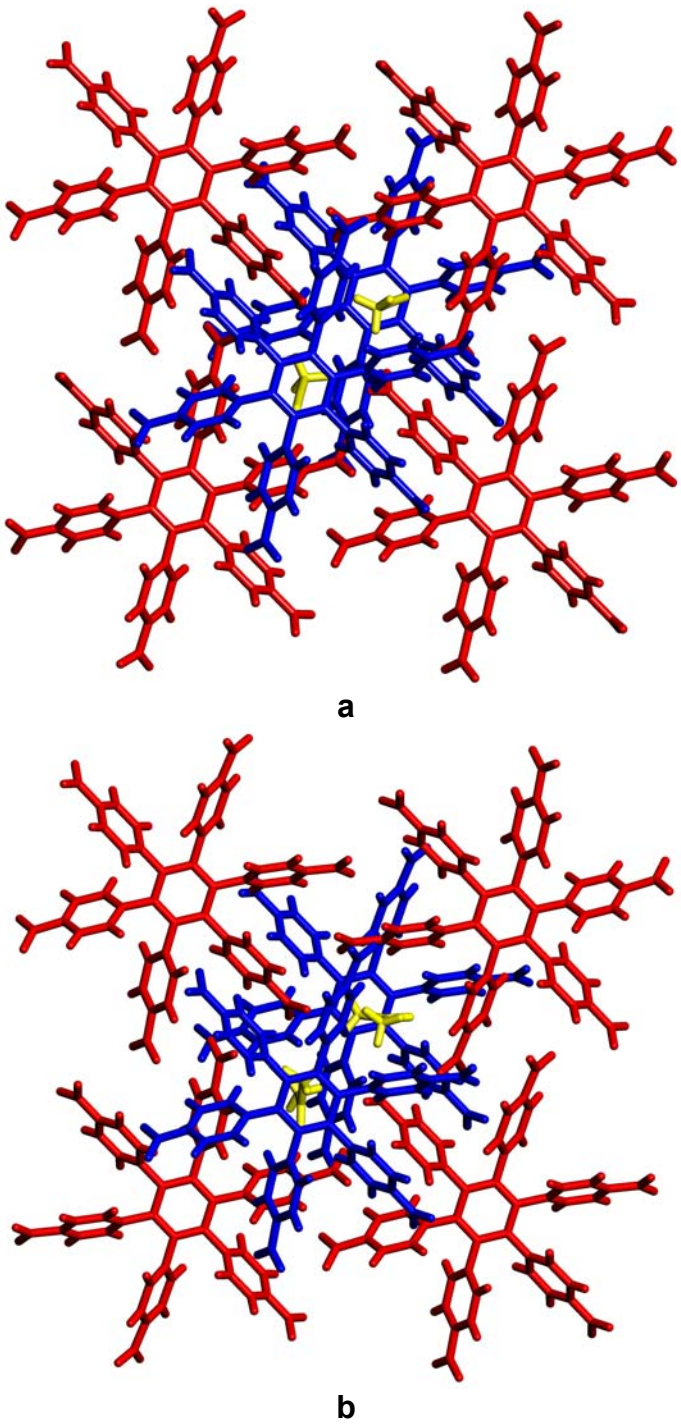

Figure 7. (a) View showing molecules of acetonitrile (yellow) included in crystals of hexakis(4-nitrophenyl)benzene (**1**) grown from DMF/acetonitrile. The guests occupy a cage bounded by four coplanar molecules of host **1** (red) and capped by two other molecules of the host in adjacent layers (blue). (b) Similar view showing the cage in which acetone is included in crystals of host **1** grown from DMF/acetone.

2.2.4. Structure of crystals of hexakis(4-nitrophenyl)benzene (1) grown from DMF/acetone. Crystals grown by allowing vapors of acetone to diffuse into solutions of nitroarene **1** in DMF proved to belong to the monoclinic space group *C*2/*c* and to have the composition **1**·2 acetone, as determined crystallographically (Table 1). The resulting structure is closely similar to that of crystals grown from DMF/acetonitrile. Included acetone occupies 19% of the volume of the crystals, and again no DMF is included (Table 2). Molecules of nitroarene **1** define layers and assume a characteristic chiral propeller-shaped conformation, with torsional angles between the central and outer rings in the range 62-68° (Table 3). Layers of nitroarene **1** incorporate both enantiomers in a 1:1 ratio, and molecules of acetone are included in pairs within each layer in volumes bounded by four coplanar molecules of host and two others in adjacent layers (Figs. 7b and 8b). Again, the individual layers are maintained by multiple N···O interactions of NO_2 groups. Each molecule of nitroarene **1** is joined to four neighbors within the same layer (see the Supplementary data for figure) by a total of 12 significant N···O interactions (distances less than 3.5 Å). Of these interactions, four are present in cyclic dimers (motif **V**, Fig. 2). N···O distances in the dimeric motifs (3.263(3) Å) are similar to those found in simple motif **IV** (3.271(2) – 3.474(2) Å). This supports our suggestion, based on analysis of N···O distances in crystals grown from DMF/acetonitrile, that there is no simple correlation between distance and the number of interactions per NO_2 group. Adjacent layers engage in multiple C–H···O interactions formed by NO_2 groups of the host (Fig. 6b). The included molecules of acetone interact with the host in several ways. Of particular interest are N···O interactions between the carbonyl oxygen atom of the guests and an NO_2 group of the hosts. In these interactions, the N···O distance is 3.051(3) Å and the C–N···O angle is 77.60(12)°. Only one other structure incorporating an N···O interaction beween a carbonyl donor and an NO_2 acceptor has been reported.[19] In the structure of crystals of nitroarene **1** grown from DMF/acetone, included molecules of acetone also serve as donors in one C–H···O interaction in which an NO_2 group of the host acts as acceptor, with an H···O distance of 2.62(1) Å.

2.2.5. Structure of crystals of hexakis(4-nitrophenyl)benzene (1) grown from DMF/ethanol. Crystals grown by allowing vapors of ethanol to diffuse into solutions of nitroarene **1** in DMF were found to belong to the monoclinic space group $P2_1/n$ and to have the composition **1**·2 ethanol, as established crystallographically (Table 1). The resulting structure is closely similar to those of crystals grown from DMF/acetonitrile and DMF/acetone and will be described only briefly. Included ethanol occupies 14% of the volume of the crystals (Table 2). Molecules of nitroarene **1** define layers and adopt an irregular propeller-shaped conformation, with torsional angles in the range 71-80° (Table 3). Layers of nitroarene **1** are composed of both enantiomers in a 1:1 ratio, and paired molecules of ethanol are included within each layer in cages bounded by a total of six molecules of host **1** (Fig. 8c). Again, the individual layers are maintained primarily by multiple N···O interactions of NO_2 groups. Each molecule of nitroarene **1** is linked to four neighbours within the same layer by a total of 12 significant N/O interactions (see the Supplementary data for figure), including four in cyclic dimers (motif **V**, Fig. 2). Adjacent layers engage in multiple C–H···O interactions formed by NO_2 groups of the host and both ortho and meta hydrogen atoms. Ethanol interacts with the host in the following ways: (1) The OH group of each guest donates a hydrogen bond to the oxygen atom of an NO_2 group (H···O distance of 1.95(1) Å , O–H···O angle of 166(1)°); (2) the CH_2 group interacts with an NO_2 group of the host by serving as the donor in a C–H···O hydrogen bond; and (3) the oxygen atom of each guest engages in an N···O interaction with an NO_2 group (N···O distance of 3.366(4) Å). This demonstrates that the ability of groups other than NO_2 to participate in N···O interactions includes not just carbonyl compounds such as acetone (as observed in the structure of crystals of nitroarene **1** grown from DMF/acetone), but also extends to other classes of molecules with functional groups incorporating oxygen.

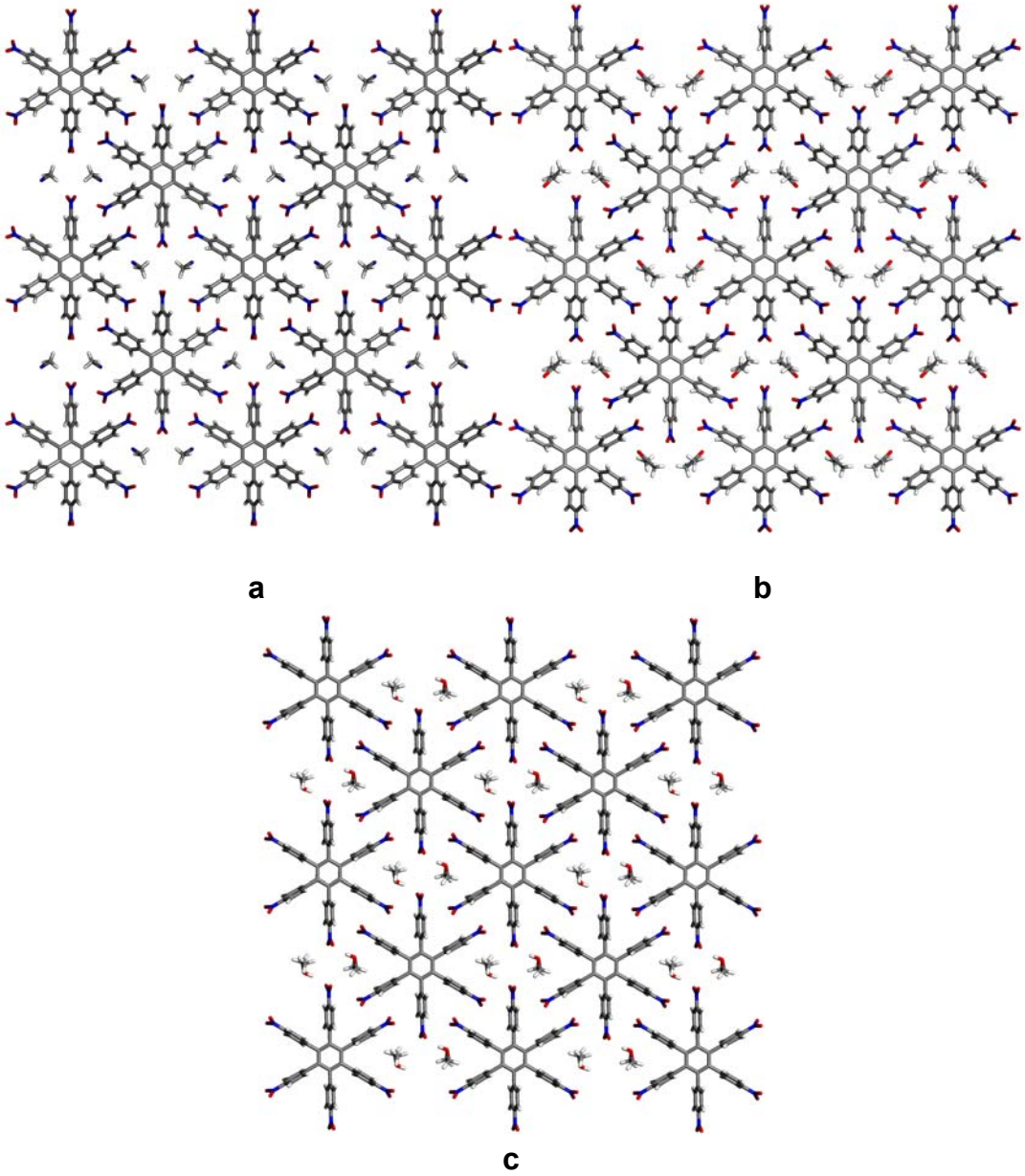

Figure 8. Views of the structure of crystals of hexakis(4-nitrophenyl)benzene (**1**) grown from; DMF/acetonitrile (a), DMF/acetone (b), and DMF/ethanol (c), showing how pairs of guests are included within characteristic layers of host **1** maintained by N···O interactions.

2.2.6. Structure of crystals of hexakis(4-nitrophenyl)benzene (1) grown from DMF/nitrobenzene. All the crystals of nitroarene **1** grown from solutions in DMF containing benzene, dioxane, acetonitrile, acetone, and ethanol have structures that fall into two closely related categories. In crystals of type **I** (obtained from DMF/benzene

and DMF/dioxane), molecules of host **1** form relatively well-packed layers separated by intervening layers of guests, which are a major component of the crystal. Crystals of type **II** are composed exclusively of layers in which smaller quantities of guests occupy spaces between molecules of host **1**, which are less tightly packed than in crystals of type **I**. Surprisingly, no DMF is included in crystals grown under any of these conditions. This suggests that DMF is not readily accommodated by either of the two observed structural types. Further experimentation showed that crystals grown by exposing solutions of nitroarene **1** in DMF to vapors of nitrobenzene belong to the monoclinic space group $P2_1$ and have the composition **1**·2 DMF, as established crystallographically (Table 1). As suggested by the failure of crystals of types **I** and **II** to accommodate DMF, host molecules in crystals of inclusion compound **1**·2 DMF are arranged in a distinctly different way (Figs. 9 and 10). Layers maintained by multiple N···O interactions of NO_2 groups are again present, but they are now corrugated, and the least-squares planes of adjacent molecules of host **1** form an angle of 51° (Fig. 9). As shown in Figure 10, each molecule of host **1** is linked to four neighbors in the same corrugated layer by a total of twelve significant N···O interactions (distances less than 3.5 Å). Of these interactions, four are incorporated in cyclic dimers (motif **V**, Fig. 2). Adjacent corrugated layers engage in multiple C–H···O interactions involving NO_2 groups of the host. In crystals grown from DMF/nitrobenzene, molecules of nitroarene **1** adopt a propeller-shaped conformation, with torsional angles between the central and outer rings in the range 73-89° (Table 3). In DMF/benzene, DMF/acetonitrile, DMF/acetone, and DMF/ethanol, host **1** forms racemic crystals composed of both enantiomers. In contrast, crystals grown from DMF/nitrobenzene are conglomerates, each consisting of a single enantiomer. Included DMF occupies 22% of the volume of the crystals (Table 2), and the guests are paired within cages bounded by six molecules of host **1**. The principal interactions between guest and host are C–H···O hydrogen bonds in which the oxygen atom of DMF serves as an acceptor and the CH_3 groups as donors.

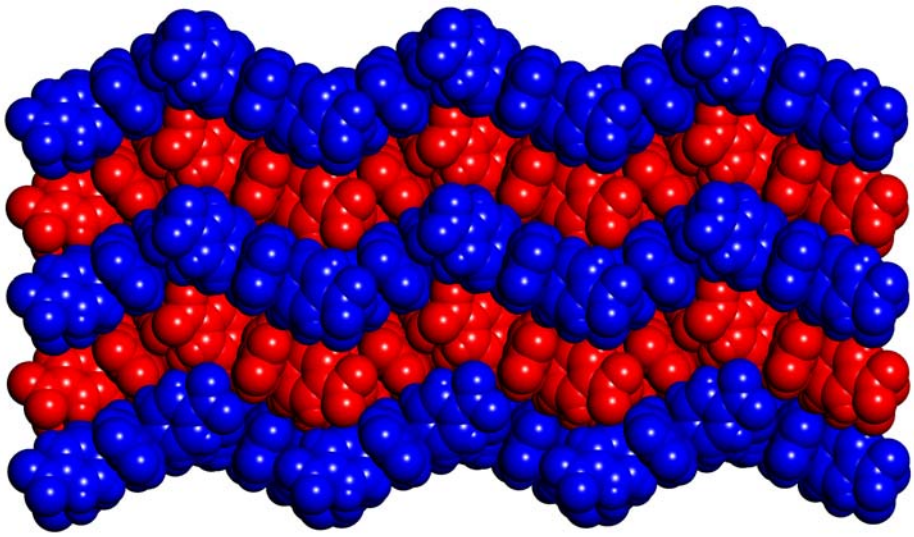

Figure 9. View of the structure of crystals of hexakis(4-nitrophenyl)benzene (**1**) grown from DMF/nitrobenzene, showing adjacent corrugated layers in red and blue.

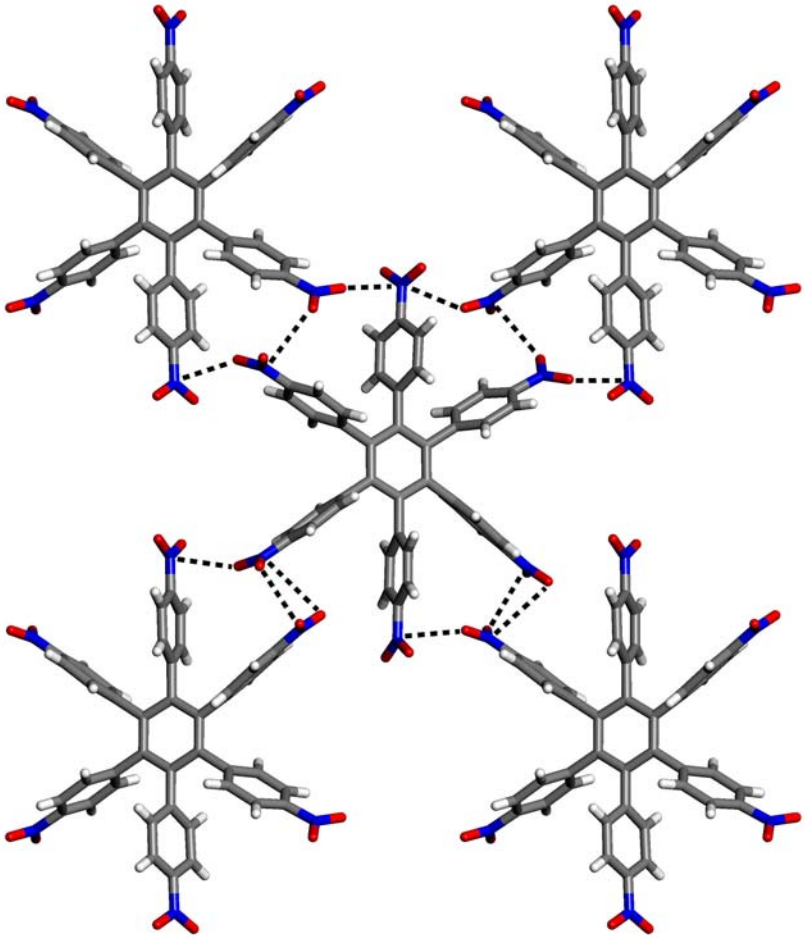

Figure 10. View of the structure of crystals of hexakis(4-nitrophenyl)benzene (**1**) grown from DMF/nitrobenzene, showing significant N···O interactions (N···O distances < 3.5 Å) between NO_2 groups of a central molecule of nitroarene **1** and its four coplanar neighbors. The interactions are represented by broken lines. Atoms of hydrogen appear in white, carbon in gray, nitrogen in blue, and oxygen in red.

3. Conclusions

The behavior of hexakis(4-nitrophenyl)benzene (**1**) confirms that intermolecular N···O interactions of NO_2 groups can help crystal engineers position molecules with a useful degree of predictability, particularly when stronger interactions such as hydrogen bonds are absent, and when competition with other weak interactions is limited. Derivatives of hexaphenylbenzene typically crystallize as layered structures in which significant quantities of guests are included in spaces between the layers or within them. In the case of nitroarene **1**, this tendency is visibly reinforced by multiple intermolecular

N···O interactions of NO_2 groups within the layers, which help to hold the layers together and determine how their molecular constituents are positioned. As a result, nitroarene **1** crystallizes to give six pseudopolymorphs with closely related structures. In contrast, recent studies have established that hexakis(4-cyanophenyl)benzene (**2**), a similar molecule unable to engage in N···O interactions, crystallizes as eight pseudopolymorphs with few shared structural features.[25,26] The different behavior of compounds **1** and **2** underscores the potential of intermolecular N···O interactions of NO_2 groups in crystal engineering.

4. Experimental

4.1. Synthesis of hexakis(4-nitrophenyl)benzene (1) During 5 min, solid hexaphenylbenzene (1.75 g, 3.27 mmol)[28] was added in small portions to a stirred mixture of fuming HNO_3 (40 mL) and concentrated H_2SO_4 (20 drops) kept at 0°C. At the end of the addition, a mixture of CH_3COOH (8 mL) and Ac_2O (4 mL) was added dropwise. The cooling bath was removed, and then the mixture was stirred for 20 h and poured into cold H_2O (150 mL). The resulting precipitate was collected by filtration, washed with acetone, dried, and then crystallized from DMSO. The crystals were isolated by filtration and washed with acetone to give hexakis(4-nitrophenyl)benzene (**1**; 1.57 g, 1.95 mmol, 60%) as a colorless solid. A sample of analytical purity was obtained by recrystallization from DMF: mp > 360 °C (lit.[27] 440–450 °C (dec)); IR (KBr) 1602, 1530, 1350, 860 cm^{-1}; ^1H NMR (400 MHz, DMF-d_7) δ 7.44 (d, ^3J = 8.5 Hz, 12H), 7.92 (d, ^3J = 8.5 Hz, 12H); ^{13}C NMR (75 MHz, DMF-d_7) δ 123.7, 133.7, 140.1, 146.8, 147.4.

4.2. X-ray crystallographic studies. Structures were solved by direct methods using SHELXS-97 and refined with SHELXL-97.[31] All non-hydrogen atoms were refined anisotropically. Hydrogen atoms attached to aromatic rings were placed in ideal positions and refined as riding atoms. The structures have been deposited at the Cambridge Crystallographic Data Centre and assigned the deposition numbers CCDC 634938–634943.

Acknowledgements

We are grateful to the Natural Sciences and Engineering Research Council of Canada, the Ministère de l'Éducation du Québec, the Canada Foundation for Innovation, the Canada Research Chairs Program, and the Université de Montréal for financial support. Supplementary data Additional crystallographic details, including ORTEP drawings and tables of structural data for pseudopolymorphs of hexakis(4-nitrophenyl)benzene (1). Supplementary data associated with this article can be found in the online version, at doi:10.1016/j.tet.2007.03.101.

References and notes

1. Dunitz, J. D. *Chem. Commun.* **2003**, 545–548; Desiraju, G. R. *Nat. Mater.* **2002**, *1*, 77–79; Gavezzotti, A. *Acc. Chem. Res.* **1994**, *27*, 309–314; Maddox, J. *Nature* **1988**, *335*, 201.

2. Braga, D. *Chem. Commun.* **2003**, 2751–2754; Biradha, K. *CrystEngComm* **2003**, *5*, 374–384; Hollingsworth, M. D. *Science* **2002**, *295*, 2410–2413; *Crystal Engineering: From Molecules and Crystals to Materials*; Braga, D., Grepioni, F., Orpen, A. G., Eds.; Kluwer: Dordrecht, The Netherlands, 1999; Desiraju, G. R. *Crystal Engineering: The Design of Organic Solids*; Elsevier: Amsterdam, 1989.

3. Simard, M.; Su, D.; Wuest, J. D. *J. Am. Chem. Soc.* **1991**, *113*, 4696–4697.

4. Nangia, A.; Desiraju, G. R. *Top. Curr. Chem.* **1998**, *198*, 57–95; Desiraju, G. R. *Angew. Chem., Int. Ed. Engl.* **1995**, *34*, 2311–2327.

5. For recent references, see: Sokolov, A. N.;Friščić, T.; MacGillivray, L. R. *J. Am. Chem. Soc.* **2006**, *128*, 2806–2807; Roques, N.; Maspoch, D.; Wurst, K.; Ruiz-Molina, D.; Rovira, C.; Veciana, J. *Chem.–Eur. J.* **2006**, *12*, 9238–9253; Pigge, F. C.; Dighe, M. K.; Rath, N. P. *Cryst. Growth Des.* **2006**, *6*, 2732–2738; Saha, B. K.; Nangia, A.; Nicoud, J.-F. *Cryst. Growth Des.* **2006**, *6*, 1278–1281; Jayaraman, A.; Balasubramaniam, V.; Valiyaveettil, S. *Cryst. Growth Des.* **2006**, *6*, 636–642; Wuest, J. D. *Chem. Commun.* **2005**, 5830–5837; Hosseini, M. W. *Acc. Chem. Res.* **2005**, *38*, 313–323; Suslick, K. S.; Bhyrappa, P.; Chou, J.-H.; Kosal, M. E.;

Nakagaki, S.; Smithenry, D. W.; Wilson, S. R. *Acc. Chem. Res.* **2005**, *38*, 283–291; Aakeröy, C. B.; Desper, J.; Urbina, J. F. *Chem. Commun.* **2005**, 2820–2822; Braga, D.; Brammer, L.; Champness, N. R. *CrystEngComm* **2005**, *7*, 1–19; Sisson, A. L.; del Amo Sanchez, V.; Magro, G.; Griffin, A. M. E.; Shah, S.; Charmant, J. P. H.; Davis, A. P. *Angew. Chem., Int. Ed.* **2005**, *44*, 6878–6881; Malek, N.; Maris, T.; Perron, M.-È.; Wuest, J. D. *Angew. Chem., Int. Ed.* **2005**, *44*, 4021–4025; Voogt, J. N.; Blanch, H. W. *Cryst. Growth Des.* **2005**, *5*, 1135–1144; Lee, S.-O.; Shacklady, D. M.; Horner, M. J.; Ferlay, S.; Hosseini, M. W.; Ward, M. D. *Cryst. Growth Des.* **2005**, *5*, 995–1003; Saied, O.; Maris, T.; Wang, X.; Simard, M.; Wuest, J. D. *J. Am. Chem. Soc.* **2005**, *127*, 10008–10009; Malek, N.; Maris, T.; Simard, M.; Wuest, J. D. *J. Am. Chem. Soc.* **2005**, *127*, 5910–5916; Custelcean, R.; Gorbunova, M. G.; Bonnesen, P. V. *Chem.–Eur. J.* **2005**, *11*, 1459–1466; Moorthy, J. N.; Natarajan, R.; Venugopalan, P. *J. Org. Chem.* **2005**, *70*, 8568–8571; Soldatov, D. V.; Moudrakovski, I. L.; Ripmeester, J. A. *Angew. Chem., Int. Ed.* **2004**, *43*, 6308–6311; Alshahateet, S. F.; Nakano, K.; Bishop, R.; Craig, D. C.; Harris, K. D. M.; Scudder, M. L. *CrystEngComm* **2004**, *6*, 5–10.

6. For representative recent studies, see: Laliberté, D.; Maris, T.; Ryan, P. E.; Wuest, J. D. *Cryst. Growth Des.* **2006**, *6*, 1335–1340; Laliberté, D.; Maris, T.; Wuest, J. D. *J. Org. Chem.* **2004**, *69*, 1776–1787.

7. For example, crystal engineering using C–H bonds as weak donors of hydrogen bonds has been reviewed by: Desiraju, G. R. *Chem. Commun.* **2005**, 2995–3001; Desiraju, G. R. *Acc. Chem. Res.* **2002**, *35*, 565–573; Desiraju, G. R.; Steiner, T. *The Weak Hydrogen Bond in Structural Chemistry and Biology*; Oxford University Press: Oxford, 1999.

8. Laliberté, D.; Maris, T.; Wuest, J. D. *CrystEngComm* **2005**, *7*, 158–160; Demers, E.; Maris, T.; Cabana, J.; Fournier, J.-H.; Wuest, J. D. *Cryst. Growth Des.* **2005**, *5*, 1237–1245.

9. Thaimattam, R.; Xue, F.; Sarma, J. A. R. P.; Mak, T. C. W.; Desiraju, G. R. *J. Am. Chem. Soc.* **2001**, *123*, 4432–4445.

10. Robinson, J. M. A.; Philp, D.; Harris, K. D. M.; Kariuki, B. M. *New J. Chem.* **2000**, *24*, 799–806.

11. Woźniak, K.; Mallinson, P. R.; Wilson, C. C.; Hovestreydt, E.; Grech, E. *J. Phys. Chem. A* **2002**, *106*, 6897–6903; Woźniak, K. *Pol. J. Chem.* **1997**, *71*, 779–791; Woźniak, K.; He, H.; Klinowski, J.; Jones, W.; Grech, E. *J. Phys. Chem.* **1994**, *98*, 13755–13765.

12. Platts, J. A.; Howard, S. T.; Woźniak, K. *Chem. Phys. Lett.***1995**, *232*, 479–485.

13. Glidewell, C.; Low, J. N.; Skakle, J. M. S.; Wardell, J. L. *Acta Crystallogr.* **2006**, *C62*, o1–o4; Sonoda, Y.; Goto, M.; Tsuzuki, S.; Tamaoki, N. *J. Phys. Chem. A* **2006**, *110*, 13379–13387; Sonoda, Y.; Kawanishi, Y.; Goto, M. *Acta Crystallogr.* **2005**, *E61*, o1200–o1202; Zeller, M.; Hunter, A. D. *Acta Crystallogr.* **2004**, *C60*, o415–o417; Szczęsna, B.; Urbańczyk-Lipkowska, Z. *New J. Chem.* **2002**, *26*, 243–249.

14. Thallapally, P. K.; Jetti, R. K. R.; Katz, A. K.; Carrell, H. L.; Singh, K.; Lahiri, K.; Kotha, S.; Boese, R.; Desiraju, G. *Angew. Chem., Int. Ed.* **2004**, *43*, 1149–1155.

15. Jetti, R. K. R.; Thallapally, P. K.; Nangia, A.; Lam, C.-K.; Mak, T. C. W. *Chem. Commun.* **2002**, 952–953.

16. For an overview of multipolar interactions, see: Paulini, R.; Müller, K.; Diederich, F. *Angew. Chem., Int. Ed.* **2005**, *44*, 1788–1805.

17. Tsuzuki, S.; Honda, K.; Uchimaru, T.; Mikami, M. *J. Chem. Phys.* **2006**, *125*, 124304/1–124304/6.

18. Yap, G. P. A.; Jové, F. A.; Claramunt, R. M.; Sanz, D.; Alkorta, I.; Elguero, J. *Aust. J. Chem.* **2005**, *58*, 817–822.

19. Yin, Z.; Jiang, L.; He, J.; Cheng, J.-P. *Chem. Commun.* **2003**, 2326–2327.

20. The NO_2 group also engages in well-established supramolecular synthons involving interactions with halogen atoms bonded to carbon. Low, J. N.; Skakle, J. M. S.; Garden, S. J.; Wardell, J. L.; Glidewell, C. *Acta Crystallogr.* **2006**, *C62*, o441–o443; Saha, B. K.; Nangia, A.; Jask_olski, M. *CrystEngComm* **2005**, *7*,

355–358; Glidewell, C.; Low, J. N.; Skakle, J. M. S.; Wardell, J. L. *Acta Crystallogr.* **2005**, *C61*, o276–o280; Garden, S. J.; Glidewell, C.; Low, J. N.; Skakle, J. M. S.; Wardell, J. L. *Acta Crystallogr.* **2005**, *C61*, o145–o147; Thalladi, V. R.; Goud, B. S.; Hoy, V. J.; Allen, F. H.; Howard, J. A. K.; Desiraju, G. R. *Chem. Commun.* **1996**, 401–402.

21. Allen, F. H.; Baalham, C. A.; Lommerse, J. P. M.; Raithby, P. R.; Sparr, E. *Acta Crystallogr.* **1997**, *B53*, 1017–1024.

22. Holden, J. R.; Dickinson, C. *J. Phys. Chem.* **1977**, *81*, 1505–1514.

23. Kobayashi, K.; Kobayashi, N.; Ikuta, M.; Therrien, B.; Sakamoto, S.; Yamaguchi, K. *J. Org. Chem.* **2005**, *70*, 749–752; Kobayashi, K.; Sato, A.; Sakamoto, S.; Yamaguchi, K. *J. Am. Chem. Soc.* **2003**, *125*, 3035–3045; Kobayashi, K.; Shirasaka, T.; Horn, E.; Furukawa, N. *Tetrahedron Lett.* **2000**, *41*, 89–93; Kobayashi, K.; Shirasaka, T.; Sato, A.; Horn, E.; Furukawa, N. Angew. Chem., Int. Ed. 1999, 38, 3483–3486.

24. Maly, K. E.; Gagnon, E.; Maris, T.; Wuest, J. D. *J. Am. Chem. Soc.* **2007**, *129*, 4306–4322.

25. Maly, K. E.; Maris, T.; Gagnon, E.;Wuest, J. D. *Cryst. Growth Des.* **2006**, *6*, 461–466.

26. Gagnon, E.; Maris, T.; Maly, K. E.; Wuest, J. D. *Acta Crystallogr.* **2007**, *C63*, o4–o6.

27. Bergmann, P. Z. *Chem.* **1971**, *11*, 341–342.

28. Fieser, L. F. *Org. Synth.* **1966**, *46*, 44–48; Fieser, L. F. *Organic Syntheses Collective Volume V*; Wiley: New York, NY, 1973; pp 604–608.

29. Bondi, A. *J. Phys. Chem.* **1964**, *68*, 441–451.

30. For example, in a study of pseudopolymorphs of tetrakis(4-nitrophenyl)methane, Sarma, Mak, Desiraju, and collaborators[9] concluded that the structures are maintained by aromatic interactions and C–H···O interactions of NO_2 groups, but they failed to note that certain pseudopolymorphs incorporate trimeric motifs of

type **VI** (Fig. 2) in which the N···O interactions are shorter than the sum of the van der Waals radii.

31. Sheldrick, G. M. SHELXS-97, *Program for the Solution of Crystal Structures*; Universität Göttingen: Göttingen, Germany, 1997; Sheldrick, G. M. SHELXL-97, *Program for the Refinement of Crystal Structures*; Universität Göttingen: Göttingen, Germany, 1997.

4.5 Conclusions

Tel que démontré au chapitre précédent, l'approche de la tectonique moléculaire permet de créer des réseaux supramoléculaires grâce à la formation de ponts hydrogène. Dans le cas bien particulier de l'hexakis(4-nitrophényl)benzène (**4.1**), les interactions non-covalentes entre groupements nitro sont nettement dominantes et déterminent la structure cristalline de chaque solvate. La clé de ce succès réside dans l'utilisation de l'hexaphénylbenzène en tant que cœur moléculaire puisque celui-ci a une influence très limitée sur les réseaux supramoléculaires obtenus. Le composé **4.1** mérite ainsi d'être qualifié de tecton.

On note aussi que les dérivés nitrés de l'hexaphénylbenzène (**4.1**) et du tétraphénylméthane (**4.9**)[12] forment à eux deux un total de 20 solvates. En effet, les composés **4.1** et **4.9** tendent à former des cavités pouvant inclure des molécules de solvant variées. Par exemple, dans les solvates d'acétonitrile, d'acétone et d'éthanol du composé **4.1**, les molécules invitées sont incluses dans le même type de cavité, avec un ajustement minimal de la structure cristalline. Ce comportement suggère que les interactions non-covalentes qui retiennent ces réseaux sont adéquates pour supporter d'importantes variations d'environnement. En effet, les interactions faibles apportent à la fois un degré de stabilité et de flexibilité permettant ainsi aux réseaux supramoléculaires de s'adapter facilement à la forme de différentes molécules invitées.[36]

En contrepartie, ces résultats suggèrent que les composés nitrés **4.1** et **4.9** s'opposent à cristalliser par eux-mêmes, sans inclure de molécules de solvant. Il serait donc intéressant d'établir à quel point le phénomène de solvatation est important pour ces composés. Par exemple, on pourrait essayer d'obtenir des cristaux par sublimation afin d'éviter l'inclusion de molécules invitées. À l'opposée, un échantillon amorphe pourrait être mis en contact avec des vapeurs de solvants afin de vérifier si un phénomène de solvatation/cristallisation spontané est possible. On note dans cette direction le travail de Desiraju et collaborateurs qui ont démontré que le solvate de THF

[36] Kumar, V. S. S.; Nangia, A. *Chem. Commun.* **2001**, 2392-2393.

du tétrakis(4-nitrophényl)méthane (**4.9**) peut être vidé partiellement de son contenu, puis remplis de nouveau.[12]

Dans un tout autre ordre d'idées, les assemblages de l'hexakis(4-nitrophényl)benzène (**4.1**) nous ont permis d'observer un grand nombre de contacts de type dipôle-dipôle. Ces interactions orthogonales impliquant les groupements nitro sont déjà suffisamment rares pour justifier à elles seules certaines publications. Puisque l'utilisation du cœur moléculaire hexaphénylbenzène permet de mettre en valeur les interactions faibles venant des groupements nitro, il serait donc valable de procéder à l'étude d'autres groupes fonctionnels. En particulier, on note que les groupements nitro et formyle peuvent agir d'isostères.[37] Cet aspect pourrait être mis en valeur par une comparaison de la structure de l'hexakis(4-formylphényl)benzène (**4.20**) avec celle du composé nitro **4.1**.

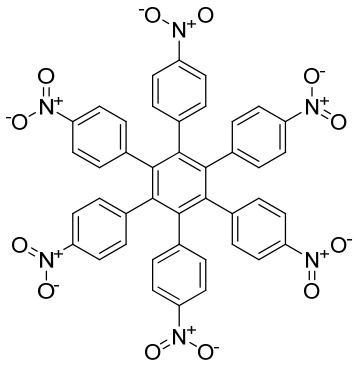

4.1

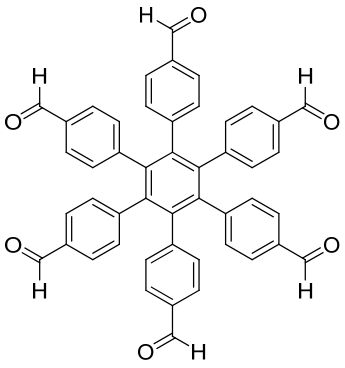

4.20

[37] Taylor, R.; Mullaley, A.; Mullier, G. W. *Pesti. Sci.* **1990**, *29*, 197-213.

Chapitre 5

Utilisation des interactions C–H···π intermoléculaires pour contrôler l'organisation des dérivés d'hexaphénylbenzène

5.1 Introduction

Les deux chapitres précédents ont démontré que l'hexaphénylbenzène peut servir d'unité centrale en tectonique moléculaire. Bien que cette molécule soit entièrement constituée de cycles aromatiques, aucun n'est facilement accessible pour participer dans des interactions intermoléculaires puisque la surface moléculaire est recouverte par des liens C–H pointant vers l'extérieur. C'est en partie pour cette raison que nos approches en tectonique moléculaire ont été si fructueuses : les groupements fonctionnels installés sur la périphérie de l'hexaphénylbenzène, tels que les unités diaminotriazines, les groupements cyano et les groupements nitro ont pu diriger les assemblages supramoléculaires sans interférence majeure provenant des interactions du cœur moléculaire lui-même.

Tel que relevé précédemment, la cristallisation de l'hexakis(4-nitrophényl)benzène (**5.1**) dans des mélanges de DMF/benzène et DMF/dioxane a mené à l'inclusion de molécules de solvant dans les réseaux. Curieusement, les molécules de solvant incluses participent dans des interactions C-H···π avec le cycle aromatique central du cœur moléculaire de l'hexaphénylbenzène (Figure 5.1). Ce comportement est à l'opposé de nos présomptions initiales, basées sur l'inaccessibilité quasi-absolue des cycles aromatiques dans l'hexaphénylbenzène. Lors d'une réinspection de la structure cristalline de l'hexaphénylbenzène, nous avons constaté la présence d'interactions non-covalentes similaires.

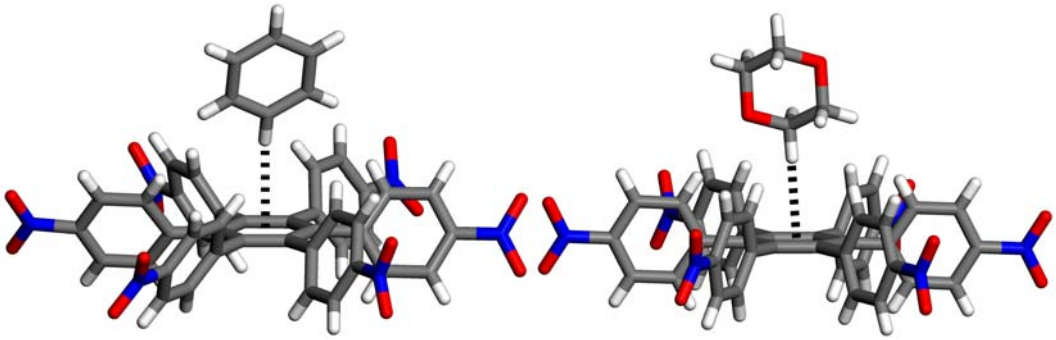

Figure 5.1. Interactions C-H···π avec le cycle aromatique central de l'unité hexaphénylbenzène, tels qu'observées dans les structures cristallines de **5.1** • 7 benzène (gauche) et de **5.1** • 7 dioxane (droite).

Mais quelle est l'importance d'une telle observation? S'agit-il d'une interaction non-covalente fiable ou d'un artéfact dû à l'équilibre des différentes forces intermoléculaires à l'état cristallin? Pour répondre à ces questions, on propose dans un premier temps un survol des liaisons π···π et des interactions C-H···π (Section 5.2). Ensuite, nous présenterons un premier article visant à documenter le comportement à l'état solide de l'hexaphénylbenzène et de ses dérivés afin de déterminer le potentiel des interactions C-H···π en ingénierie cristalline (Section 5.3). Les connaissances acquises lors de cette étude seront ensuite exploitées pour favoriser des assemblages supramoléculaires maintenus par des liens C-H···π (Sections 5.4 et 5.5). Finalement (Section 5.6), on propose une série d'idées exploitant les connaissances accumulées au fil de ce chapitre.

5.2.1 Interactions π···π

Les interactions non-covalentes impliquant deux cycles aromatiques ont souvent été classées dans une seule catégorie: les interactions par empilement-π. C'est en partie grâce à l'article « The Nature of π-π Interactions »[1] qu'une distinction importante s'est opérée entre les interactions π···π et C-H···π. On y présente un modèle simple et intuitif dans lequel le système aromatique est composé d'une charpente de liens σ, chargée positivement, située entre deux nuages d'électrons π, chargés négativement (Figure 5.2)

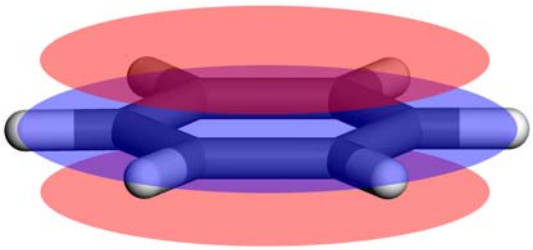

Figure 5.2. Représentation schématisée d'un système aromatique. Le réseau de liens σ de basse densité électronique est représenté en bleu et est situé entre deux nuages d'électrons π illustrés en rouge.

[1] Hunter, C. A.; Sanders, J. K. M. *J. Am. Chem. Soc.* **1990**, *112*, 5525-5534.

D'après le modèle de Hunter et Sanders, il est conclu que si les systèmes aromatiques sont déplacés latéralement l'un par rapport à l'autre (Figure 5.3, **I**), l'interaction est plus stabilisante que dans le cas d'une superposition exacte (Figure 5.3, **II**). Alternativement, les systèmes aromatiques peuvent être perpendiculaires l'un par rapport à l'autre (Figure 5.3, **III**), formant aussi un autre type d'interaction stabilisante. Ces résultats sont expliqués à la fois par la complémentarité des charges et la répulsion des deux nuages électroniques négatifs. Bien que qualitatif, ce modèle s'accorde parfaitement avec des calculs plus récents, tels que pour les énergies de liaison des dimères de benzène (Figure 5.3, **I-III**) qui sont de -2.48, -1.48 et -2.46 kcal mol^{-1}, respectivement.[2]

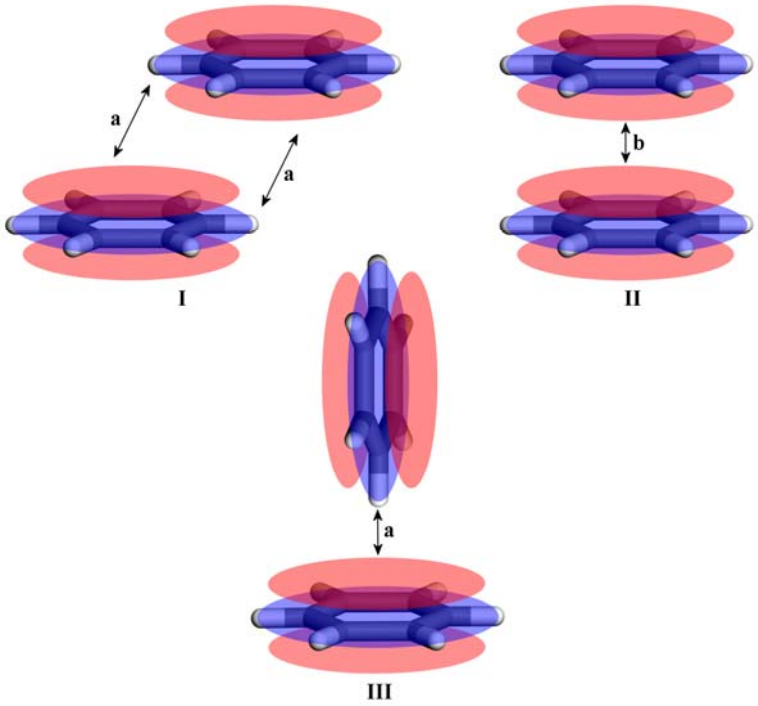

Figure 5.3. Représentations schématisées des interactions π···π et C-H···π dans les dimères de benzène **I-III**. Les flèches identifiées par les caractères « a » et « b » dénotent des interactions stabilisantes et répulsives, respectivement. L'énergie des dimères de benzène avec ces orientations sont -2.48 kcal mol^{-1} (**I**), -1.48 kcal mol^{-1} (**II**) et -2.46 kcal mol^{-1} (**III**).

[2] Tsuzuki, S.; Honda, K.; Uchimaru, T.; Mikami, M.; Tanabe, K. *J. Am. Chem. Soc.* **2002**, *124*, 104-112.

On remarque aussi dans les dimères **I** et **II** que de larges portions des nuages électroniques sont en contact. Ces recouvrements sont typiques des interactions π···π. À l'opposée, le motif **III** origine d'un contact important entre le côté d'un système aromatique et un nuage d'électrons π. Cette association intermoléculaire est souvent nommée *herringbone*, *edge-to-face* ou encore *T-shaped*, mais elle est décrite plus explicitement par le terme « interaction C-H···π ». À cause de la géométrie particulière de l'hexaphénylbenzène, les motifs d'association π···π (**I** et **II**) ne sont pas possibles; on doit donc considérer exclusivement les interactions C-H···π.

5.2.2 Interactions C-H···π

Pauling était très restrictif quant à sa définition de ce qui est ou n'est pas un pont hydrogène.[3] Selon lui, seuls les atomes très électronégatifs (N, O et F) peuvent se partager un atome d'hydrogène. Au fil des ans, la définition du pont hydrogène s'est grandement élargie, et dans ce contexte, Aakeröy et Seddon[4] ont cité Samuel Butler :

> A definition is the enclosing a wilderness of idea within a wall of words.
>
> Samuel Butler, English writer, *Notebooks*, 1912

Bien que la définition du pont hydrogène reste encore au cœur de bien des débats, plusieurs s'accordent maintenant pour le définir par ses propriétés plutôt que par ses éléments constitutifs. Les ponts hydrogène « normaux » sont caractérisés par une série de propriétés géométriques et physiques (Tableau 3.1). De même, les ponts hydrogène faibles, tels que les interactions C-H···O[5,6] et O-H···π[7], possèdent aussi ces propriétés, quoique d'une façon plus limitée.

---

3 Pauling, L. *The Nature of the Chemical Bond and the Structure of Molecules and Crystals - An Introduction to Modern Structural Chemistry, 2nd Edition*, Oxford University Press, London, 1940.
4 Aakeröy, C. B.; Seddon, K. R. *Chem. Soc. Rev.* **1993**, *22*, 397-407.
5 Taylor, R.; Kennard, O. *J. Am. Chem. Soc.* **1982**, *104*, 5063-5070.
6 Desiraju, G. R. *J. Chem. Soc., Chem. Commun.* **1990**, 454-455.
7 Viswamitra, M. A.; Radhakrishnan, R.; Bandekar, J.; Desiraju, G. R. *J. Am. Chem. Soc.* **1993**, *115*, 4868-4869.

Mais qu'en est-il de la combinaison d'un donneur faible tel qu'un lien C-H et d'un accepteur faible comme un cycle aromatique? À première vue, on pourrait s'imaginer qu'il ne s'agit que d'un cas particulier d'interaction de type van der Waals. Toutefois, les interactions non-covalentes C-H···π possèdent les mêmes caractéristiques géométriques que les ponts hydrogène,[8] contrairement aux contacts van der Waals de type C-H···H-C.[9] De plus, la spectroscopie infrarouge a aussi été utilisée pour mesurer la différence des fréquences de vibration d'élongation ($\Delta\nu_s$) d'alcynes entre des solutions et l'état cristallin.[10] Des variations faibles mais significatives des $\Delta\nu_s$ des liens C-H (*sp*) ont été observées dans tous les cas étudiés lorsqu'un lien C-H···π était établi à l'état cristallin. D'après ces résultats, on peut qualifier les liens C-H···π de ponts hydrogène faibles.

Tout comme pour un pont hydrogène « normal », l'énergie des liens C-H···π varie en fonction du donneur et de l'accepteur. On observe dans les ponts hydrogène faibles C-H···O/N et C-H···π une gradation de la force des interactions en fonction de l'acidité du lien C-H impliqué (Figure 5.4).[11] Similairement, les interactions C-H···π sont plus fortes lorsque la densité électronique au niveau du cycle aromatique accepteur est élevée.[12] L'énergie de l'interaction a été calculée pour plusieurs donneurs différents[2,13] et tous les résultats soulignent que l'énergie des plus fortes interactions C-H···π est de l'ordre de 12-16 kJ mol^{-1}.

---

8 Takahashi, O.; Kohno, Y.; Iwasaki, S.; Saito, K.; Iwaoka, M.; Tomoda, S.; Umezawa, Y.; Tsuboyama, S.; Nishio, M. *Bull. Chem. Soc. Jpn.* **2001**, *74*, 2421-2430.

9 Steiner, T.; Desiraju, G. R. *Chem. Commun.* **1998**, 891-892.

10 (a) Steiner, T. *J. Chem. Soc., Chem. Commun.* **1995**, 95-96. (b) Steiner, T.; Starikov, E. B.; Amado, A. M.; Teixeira-Dias, J. J. C. *J. Chem. Soc., Perkin Trans. 2* **1995**, 1321-1326. (c) Steiner, T.; Starikov, E. B.; Tamm, M. *J. Chem. Soc., Perkin Trans. 2* **1995**, 67-71. (d) Steiner, T.; Tamm, M.; Lutz, B.; van der Maas, J. *Chem. Commun.* **1996**, 1127-1128.

11 (a) Allerhand, A.; Schleyer, P. v. R. *J. Am. Chem. Soc.* **1963**, *85*, 1715-1723. (b) Pedireddi, V. R.; Desiraju, G. R. *J. Chem. Soc., Chem. Commun.* **1992**, 988-990. (c) Steiner, T.; Desiraju, G. R. *Chem. Commun.* **1998**, 891-892. (d) Takahashi, O.; Kohno, Y.; Iwasaki, S.; Saito, K.; Iwaoka, M.; Tomoda, S.; Umezawa, Y.; Tsuboyama, S.; Nishio, M. *Bull. Chem. Soc. Jpn.* **2001**, *74*, 2421-2430. (e) Jeffrey, G. A. *Crystallography Reviews* **2003**, *9*, 135-176. (f) Nishio, M. *CrystEngComm* **2004**, *6*, 130-158.

12 (a) Lee, E. C.; Hong, B. H.; Lee, J. Y.; Kim, J. C.; Kim, D.; Kim, Y.; Tarakeshwar, P.; Kim, K. S. *J. Am. Chem. Soc.* **2005**, *127*, 4530-4537. (b) Suewaza, H.; Hashimoto, T.; Tsuchinaga, K.; Yoshida, T.; Yuzuri, T.; Sakakibara, K.; Hirota, M.; Nishio, M. *J. Chem. Soc., Perkin Trans. 2* **2000**, 1243-1249.

13 (a) Tsuzuki, S.; Honda, K.; Uchimaru, T.; Mikami, M.; Tanabe, K. *J. Am. Chem. Soc.* **2000**, *122*, 3746-3753. (b) Tsuzuki, S.; Honda, K.; Uchimaru, T.; Mikami, M.; Takahashi, O. *J. Phys. Chem. A* **2002**, *106*, 4423-4428.

$$\underset{\text{acidité du lien CH}\\ \text{force du lien CH}\cdots\pi}{\xleftarrow{\qquad\qquad}} \quad \text{sp-CH} > \text{sp}^2\text{-CH} > \text{sp}^3\text{-CH}$$

Figure 5.4. Augmentation de la force des liens C-H···π selon l'hybridation.

Sans l'ombre d'un doute, les interactions C-H···π possèdent les caractéristiques d'une interaction non-covalente stabilisante et directionnelle. Par contre, son utilisation en chimie supramoléculaire est compliquée par l'omniprésence des liens C-H et des accepteurs-π dans les composés organiques. Ce point est aisément illustré par la molécule de phénylacétylène (**5.2**). Malgré une structure très simple consistant de seulement 14 atomes, cette molécule possède à la fois quatre liens C-H différents et deux accepteurs-π (Figure 5.5). De plus, ces accepteurs sont diffus et recouvrent la quasi-totalité de la molécule. Ces observations contrastent fortement avec les ponts hydrogène « normaux », dont les interactions non-covalentes impliquent des donneurs et accepteurs ponctuels et beaucoup moins nombreux.

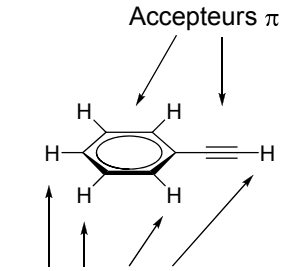

5.2

Figure 5.5. La structure du phénylacétylène (**5.2**). L'omniprésence des donneurs et accepteurs de liens C-H···π rend l'utilisation de cette interaction difficile à contrôler.

L'utilisation de benzènes substitués par plusieurs cycles aromatiques élimine deux des problèmes cités ci-haut. Premièrement, l'encombrement stérique au niveau des cycles aromatiques périphériques limite leur capacité à agir comme accepteur-π, ne laissant seulement que le cycle aromatique central pour établir une telle interaction. Cette affirmation est supportée par les structures des solvates de benzène et de dioxane de l'hexakis(4-nitrophényl)benzène (**5.1**, Figure 5.1). Ensuite, l'approche des liens C-H vers le cycle aromatique central de l'hexaphénylbenzène est limitée par l'encombrement

stérique, de sorte que l'atome d'hydrogène doit se situer juste au-dessus du centre de l'accepteur-π. On élimine ainsi le caractère diffus de ce type d'accepteur et on s'approche davantage d'une interaction ponctuelle. Afin de vérifier ce potentiel particulier de l'hexaphénylbenzène, nous avons préparé plusieurs dérivés que nous avons étudiés à l'état cristallin. On espère ainsi confirmer la tendance des (polyphényl)benzènes à s'engager dans des interactions C-H···π, et leur ouvrir la porte vers la chimie supramoléculaire. Ces résultats sont présentés dans l'article 3 qui suit.

5.3 Article 3

Structural Features in Crystals of Derivatives of Benzene with Multiple Contiguous Phenyl Substituents

Eric Gagnon, Thierry Maris, Pierre-Marc Arseneault,
Kenneth E. Maly, and James D. Wuest

Crystal Growth and Design, **2010**, *10*, 648-657

Reproduced with permission from *Crystal Growth and Design*
Copyright 2010 American Chemical Society

Abstract

Hexaphenylbenzene and related derivatives of benzene with multiple contiguous phenyl substituents have well-defined non-planar topologies. Their structures limit conjugation and disfavor intermolecular π-π and C-H···π interactions. Such compounds therefore show higher HOMO-LUMO gaps, lower degrees of self-association, less efficient packing, and higher solubilities than planar analogues. These characteristic properties underlie the growing utility of non-planar phenyl-substituted benzenes in science and technology. Surprisingly, no systematic structural analysis of compounds of this type has been reported. We have now examined structural features in crystals of hexaphenylbenzene, 1,2,4,5-tetraphenylbenzene, 1,4-dimethyl-2,3,5,6-tetraphenylbenzene, pentaphenylbenzene, 1-methyl-2,3,4,5,6-pentaphenylbenzene, and an octaphenyl-*p*-quinquephenyl. These compounds tend to crystallize in sheets held together by van der Waals contacts and small numbers of C-H···π interactions. Although the non-planar topologies of these compounds do not eliminate C···H contacts entirely, the ratios of H···H contacts to C···H contacts greatly exceed those found in analogous aromatic compounds that can assume planar structures. Our structural analyses promise to help explain the characteristic behavior of non-planar aryl-substituted arenes and to accelerate the discovery of new applications.

Introduction

Derivatives of benzene with multiple aryl substituents have special properties that make them useful in many areas of science and technology.[3] Such compounds can be formally divided into two broad classes: 1) Conjugated polynuclear aromatic hydrocarbons, typified by hexa-*peri*-hexabenzocoronene (**1** = HBC), and 2) structures with more limited conjugation, represented by hexaphenylbenzene (**2a** = HPB), in which the aryl substituents are not constrained by additional bonds to lie in the plane of the aromatic core. Compounds in both classes typically show high thermal stability, but other properties of interest differ substantially.

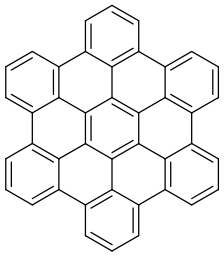

1 (HBC)

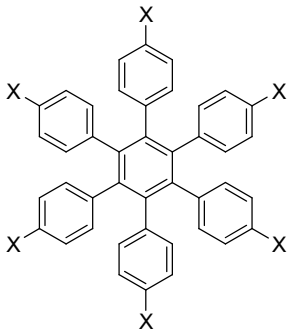

2a (X = H; HPB)
2b (X = OH)
2c (X = COOH)
2d (X = $CONH_2$)
2e (X = CN)
2f (X = NO_2)
2g (X = DAT)

DAT = 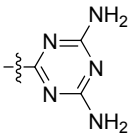

Planar polynuclear aromatic hydrocarbons related to HBC (**1**) have been studied intensively for many years. In particular, classic early work by Clar and others helped established basic correlations between molecular structure and electronic properties.[4] A recent resurgence of interest in these compounds, due in large part to studies carried out by Müllen and coworkers,[3] has focused on their use in materials science as molecular models of graphene[5] and as components of discotic liquid crystals.[6,7] Benzene itself, as well as extended analogues such as HBC (**1**), have topologically simple disk-shaped structures that can easily engage in aromatic π-π and C-H···π interactions.[8,9] As established by Desiraju and Gavezzotti,[10] such compounds crystallize in four distinct ways, depending predictably on the relative contribution of carbon and hydrogen atoms in defining the molecular surface. When polynuclear aromatic hydrocarbons are small

and their C/H ratio is relatively low, C-H···π interactions dominate in molecular association, and packing therefore favors a herringbone motif. In the case of larger analogues, however, π-π interactions play an increasingly important role, leading to structures that favor π-stacking or combinations of stacking and herringbone interactions.[11] As a result of these various studies, the use of analogues of HBC (**1**) in materials science is now guided by a relatively clear understanding of the relationship between their molecular structures and properties, including their organization in crystals and other ordered phases.

In contrast, the more complex non-planar topologies of HPB (**2a**) and related compounds limit conjugation and disfavor extensive aromatic π-π and C-H···π interactions. In general, compounds of this type can therefore be expected to show higher HOMO-LUMO gaps, lower degrees of self-association, less efficient packing, and higher solubilities than planar analogues such as HBC (**1**). Indeed, these characteristic properties underlie the broad and growing utility of non-planar phenyl-substituted benzenes in science and technology.

In macromolecular chemistry, for example, the distinctive properties of highly aryl-substituted poly(*p*-phenylenes) were noted independently in the 1960's by Stille, Ried, and their collaborators,[12,13] who prepared the compounds by Diels-Alder reactions of aryl-substituted bis(cyclopentadienones) with bis(acetylenes), followed by the elimination of CO.[14] The resulting aryl-substituted poly(phenylenes) showed much higher solubility than unsubstituted models, yet they retained similarly high thermal stability. These initial observations have led to the incorporation of phenyl-substituted phenylenes in the backbones or side chains of a wide range of polymers,[15] typically yielding new materials with low degrees of molecular association, high glass-transition temperatures (T_g), an ability to form transparent films, and retention of many of the useful properties of the original unmodified polymers. In particular, poly(fluorenes) encapsulated within a sheath of phenyl-substituted phenylene side chains proved to retain the characteristic blue emission of simpler poly(fluorenes) but yielded more stable thin-film electroluminescent devices, without undesirable red shifts and reduced

luminance attributed to the aggregation of simpler poly(fluorenes).[16] Similarly, poly(arylene ethers) incorporating phenyl-substituted phenylene units were shown to have high solubility and to produce amorphous thin films with high values of T_g that can be adjusted by choosing 1,2,3,4-tetraphenyl-, pentaphenyl-, or hexaphenylbenzene moieties as the phenylene units.[17]

Using aryl-substituted arenes to engineer materials is not limited to the field of polymers. New applications have been stimulated by recent work of Müllen and coworkers,[3] who have used aryl-substituted arenes as precursors for the synthesis of shape-persistent dendrimers, as well as for the preparation of analogues of graphene by intramolecular Scholl reactions.[18] Related compounds have proven to yield molecular glasses for use as photoresists[19] and to be effective components of molecular devices such as light-emitting diodes.[20] Most small molecules crystallize readily, making them inherently unsuited for constructing amorphous films.[21] In addition, the association of luminescent compounds can broaden their emission bands, shift the frequencies emitted, and cause quenching. Arenes with contiguous aryl substituents can help circumvent all of these problems by resisting aggregation and crystallization, thereby allowing thin films to be processed from solution as long-lived amorphous phases with high values of T_g, excellent thermal stability, efficient luminescence, and other attractive properties. For these reasons, aryl-substituted arenes are promising compounds for engineering thin-film devices.

Aryl-substituted arenes have also found important applications outside the field of bulk materials. In particular, their well-defined geometries make them useful as templates for directing supramolecular assembly,[22] components of molecular machines,[23] and agents for nanopatterning surfaces.[24] Their special steric properties can also be exploited in catalysis. For example, ligands derived from aryl-substituted arenes have been shown to yield catalysts that can 1) suppress the formation of palladium black in the aerobic oxidation of alcohols,[25] 2) kinetically resolve chiral derivatives of BINOL,[26] and 3) promote efficient Suzuki, Heck, and silylation reactions of unactivated

aryl chlorides[27] and α,β-unsaturated ketones.[28] The useful behavior of such ligands in catalysis has been attributed to their well-defined shape, bulk, and rigidity.[29]

Collectively, these diverse applications suggest that the utility of analogues of HPB (**2a**) results in part from a well-defined non-planar topology that inhibits efficient molecular packing and disfavors typical intermolecular aromatic interactions. Surprisingly, however, no systematic structural analysis of simple compounds of this type has been reported. Related studies of the structures of selected derivatives of HPB (**2a**) have recently been published by Kobayashi, Wuest, and their coworkers.[30-32] In particular, they examined the structures of hexaphenylbenzenes **2b-g**, which bear various substituents that engage in characteristic directional intermolecular interactions. In all cases, the compounds were found to crystallize as open networks that define significant volumes for the inclusion of guests, thereby underscoring the intrinsic inability of such compounds to pack effectively. These results encouraged us to examine the structures of simpler phenyl-substituted benzenes that lack functional groups able to engage in strong intermolecular interactions. We now report a systematic study of structural features found in crystals of HPB (**2a**), 1,2,4,5-tetraphenylbenzene (**3** = TPB), 1,4-dimethyl-2,3,5,6-tetraphenylbenzene (**4** = DMTPB), pentaphenylbenzene (**5** = PPB), 1-methyl-2,3,4,5,6-pentaphenylbenzene (**6** = MPPB), and a more complex analogue, 2',2''',3',3''',5',5''',6',6'''-octaphenyl-*p*-quinquephenyl (**7** = OPQP). By probing the structures and intermolecular interactions of aryl-substituted arenes, our study promises to help explain their behavior and accelerate the discovery of new applications.

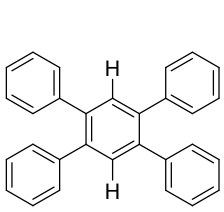

3 (TPB)

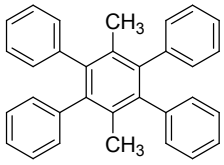

4 (DMTPB)

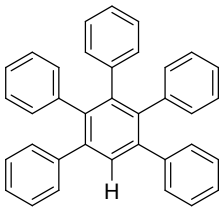

5 (PPB)

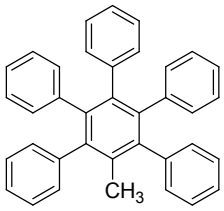

6 (MPPB)

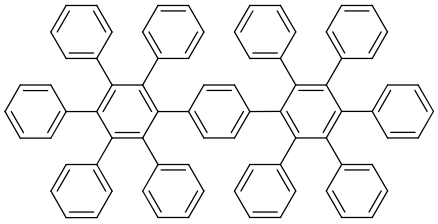

7 (OPQP)

Results and Discussion

Synthesis of Compounds 2a and 3-7. HPB (**2a**),[33] DMTPB (**4**),[31] PPB (**5**),[31] and OPQP (**7**)[34] were synthesized by published methods. TPB (**3**) was prepared in 84% yield from 1,2,4,5-tetrabromobenzene by standard Suzuki coupling, and MPPB (**6**) was obtained in 89% yield by heating tetraphenylcyclopentadienone with 1-phenylpropyne.

Structure of Crystals of HPB (2a). HPB (**2a**) has been reported to crystallize from CH_2Cl_2 or CH_2Br_2 as two orthorhombic polymorphs A and B.[35] The structure of polymorph B was disclosed in 1968,[35] and a newer and more highly refined structure of polymorph A is available in the Cambridge Structural Database.[36] The high symmetry of HPB (**2a**) makes it a logical starting point for the systematic analysis of benzenes with multiple adjacent phenyl substituents. For the sake of brevity, only the structure of polymorph A will be reviewed. With six contiguous phenyl substituents, HPB (**2a**) is forced to adopt a conformation with large torsional angles (65.1-88.6°) between the central and peripheral aromatic rings (Table 1). Similar values are found in crystals of derivatives **2b-g**.[30-32] No twisting is observed in the fully substituted central aromatic ring of HPB (**2a**) or related compounds.[37] Topologically, molecules of HPB (**2a**) can be described as having a chiral propeller-shaped framework of carbon atoms with an exposed surface rich in hydrogen atoms. Each molecule of HPB (**2a**) engages in two C-

H···π interactions with two neighbors (C-H···centroid distances of 3.00 Å) to define chains (Figure 1a),[38,39] which pack to form corrugated sheets. Adjacent sheets are joined by four additional C-H···π interactions per molecule (C-H···centroid distances of 2.80 Å and 2.85 Å), with each central aromatic ring of HPB (**2a**) serving as a double acceptor (Figure 1b). It is noteworthy that C-H···π interactions are present in crystals of HPB (**2a**), even though the unique topology of the compound appears to set severe limits on access to the faces of all seven aromatic rings.

Table 1. Torsional Angles Between the Peripheral Phenyl Groups and the Central Aromatic Rings in HPB (**2a**), TPB (**3**), DMTPB (**4**), PPB (**5**), MPPB (**6**), and OPQP (**7**).

Compound	**Torsional angles (°)**
HPB (**2a**)/Polymorph A	65.14(10), 75.53(10), 76.50(10), 82.17(11), 87.95(12), 88.59(10)
TPB (**3**)/Polymorph TPB-1	2 × 39.84(5), 2 × 66.19(5)
TPB (**3**)/Polymorph TPB-2	2 × 51.08(6), 2 × 62.21(7)
TPB (**3**)/Polymorph TPB-3	2 × 40.30(5), 2 × 65.36(5)
DMTPB (**4**)	2 × 68.89(5), 2 × 75.34(5)
PPB (**5**)/Polymorph PPB-1	56.09(7), 57.18(7), 58.12(7), 58.13(7), 72.92(7)
PPB (**5**)/Pseudopolymorph PPB-2	49.83(8), 60.35(8), 61.33(9), 62.78(9), 63.93(8)
MPPB (**6**)	60.49(9), 60.66(9), 66.41(10), 71.68(8), 72.81(10), 78.87(9), 82.67(9), 85.82(9), 89.88(10), 89.97(9)
OPQP (**7**)	2 × 61.26(5), 2 × 77.36(6), 2 × 80.79(8), 2 × 85.67(6), 2 × 69.19(6), 2 × 85.59(6)

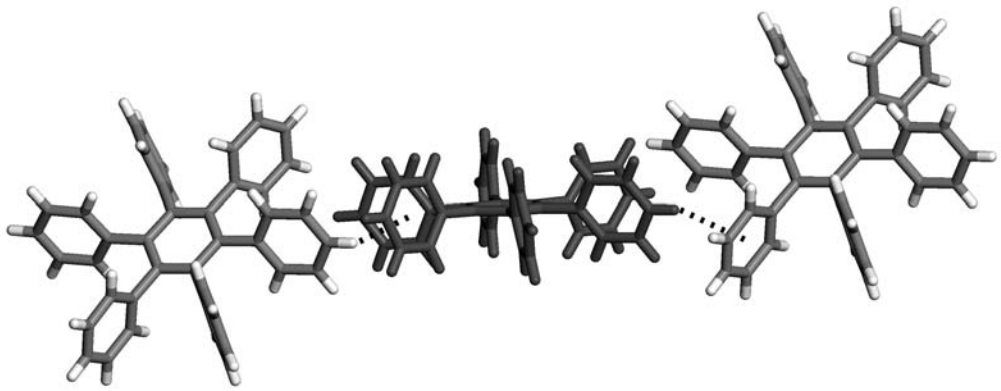

a

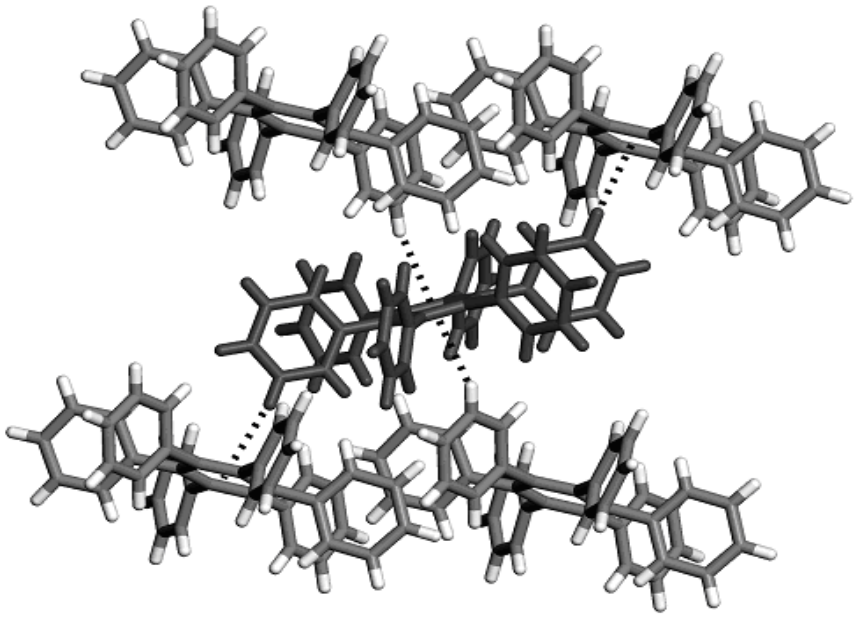

b

Figure 1. Views of the structure of polymorph A of HPB (**2a**) showing C-H···π interactions (a) within the corrugated sheets and (b) between adjacent sheets. In both views, the central molecule of HPB (**2a**) is dark gray, and the neighboring molecules with which it interacts are represented normally, with carbon atoms in light gray and hydrogen atoms in white. C-H···π interactions are shown as broken lines.

Structure of Crystals of TPB (3) Grown from Hexanes (Polymorph TPB-1).[40,41] Colorless crystals of TPB (**3**) were obtained by cooling a solution in hexanes. Selected crystals proved to belong to the triclinic space group *P-1*. Other crystallographic data are provided in Table 2. Only four phenyl groups are attached to the central aromatic ring of TPB (**3**), and the other positions are occupied by atoms of hydrogen, so the average torsional angles between the central and peripheral aromatic rings (Table 2) are much smaller than those observed in the structure of HPB (**2a**). As shown in Figure 2a, each molecule of TPB (**3**) interacts with two neighbors by engaging in a total of four characteristic C-H···π interactions (C-H···centroid distances of 2.76 Å). These interactions define a distinctive embrace, in which peripheral phenyl groups occupy clefts created by the unsubstituted positions of the central aromatic ring of TPB (**3**). The resulting chains then pack to create sheets, and adjacent sheets are joined by additional C-H···π interactions (Figure 3a). Each molecule of TPB (**3**) participates in a total of eight inter-sheet interactions, four involving peripheral phenyl groups as acceptors (C-H···centroid distances of 2.97 Å) and four involving central rings as acceptors (C-H···centroid distances of 2.98 Å). As in the case of HPB (**2a)**, C-H···π interactions contribute to the cohesion of crystals of TPB (**3**), despite the crowded molecular topology. It is noteworthy that the central aromatic ring again serves as an acceptor of two C-H···π interactions, one on each face.

Table 2. Crystallographic Data for TPB (**3**), DMTPB (**4**), PPB (**5**), MPPB (**6**), and OPQP (**7**).

structure	TPB-1	TPB-2	TPB-3	DMTPB
compound	**3**	**3**	**3**	**4**
formula	$C_{30}H_{22}$	$C_{30}H_{22}$	$C_{30}H_{22}$	$C_{32}H_{26}$
included solvent	-	-	-	-
crystal system	triclinic	triclinic	monoclinic	monoclinic
space group	*P*-1	*P*-1	$P2_1/c$	$P2_1/c$
a (Å)	5.8530(2)	6.0881(1)	5.8975(1)	11.1336(2)
b (Å)	7.4229(3)	8.4119(2)	23.7474(4)	8.8786(1)
c (Å)	11.8341(5)	10.6561(2)	7.4116(1)	11.5617(2)
α (°)	83.800(2)	104.517(1)	90	90
β (°)	89.608(2)	91.259(1)	98.052(1)	95.395(1)
γ (°)	81.588(2)	92.359(1)	90	90
V (Å^3)	505.62(3)	527.560(18)	1027.76(3)	1137.82(3)
Z	1	1	2	2
ρ_{calcd} (g cm^{-3})	1.256	1.204	1.236	1.198
T (K)	100(2)	150(2)	150(2)	100(2)
μ (mm^{-1})	0.536	0.514	0.528	0.509
R_1, $I > 2\sigma(I)$ (%)	4.08	4.14	3.41	3.76
R_1, all data (%)	4.18	4.32	3.56	3.79
ωR_2, $I > 2\sigma(I)$ (%)	9.81	11.60	9.50	10.05
ωR_2, all data (%)	9.83	11.84	9.69	10.07
measured reflections	6012	8354	15942	18301
independent reflections	1911	1659	1761	1810
observed reflections, $I > 2\sigma(I)$	1615	1565	1669	1780

Table 2 (continued). Crystallographic Data for TPB (**3**), DMTPB (**4**), PPB (**5**), MPPB (**6**), and OPQP (**7**).

structure	PPB-1	PPB-2	MPPB	OPQP
compound	**5**	**5**	**6**	**7**
formula	$C_{36}H_{26}$	$C_{39}H_{29}$	$C_{77}H_{59}$	$C_{78}H_{54}$
included solvent	-	benzene	benzene	-
crystal system	triclinic	triclinic	orthorhombic	orthorhombic
space group	*P*-1	*P*-1	*Pbcn*	*Pccn*
a (Å)	10.1713(3)	10.0353(12)	38.2531(7)	16.1583(5)
b (Å)	12.1167(4)	12.2584(14)	11.7127(2)	27.9471(8)
c (Å)	13.0185(5)	13.5290(15)	24.2180(4)	12.0443(3)
α (°)	63.194(1)	65.724(5)	90	90
β (°)	68.387(2)	71.255(5)	90	90
γ (°)	65.645(1)	79.740(6)	90	90
V (Å^3)	1271.35(8)	1434.6(3)	10850.8(3)	5438.9(3)
Z	2	2	8	4
ρ_{calcd} (g cm^{-3})	1.198	1.152	1.205	1.210
T (K)	100(2)	150(2)	150(2)	200(2)
μ (mm^{-1})	0.512	0.491	0.513	0.518
R_1, $I > 2\sigma(I)$ (%)	3.40	4.54	4.72	4.55
R_1, all data (%)	3.69	4.92	6.73	4.71
ωR_2, $I > 2\sigma(I)$ (%)	9.44	13.09	13.09	13.03
ωR_2, all data (%)	9.63	13.60	13.98	13.33
measured reflections	20093	23597	176960	74206
independent reflections	4199	4564	9435	5063
observed reflections, $I > 2\sigma(I)$	3826	4044	6780	4757

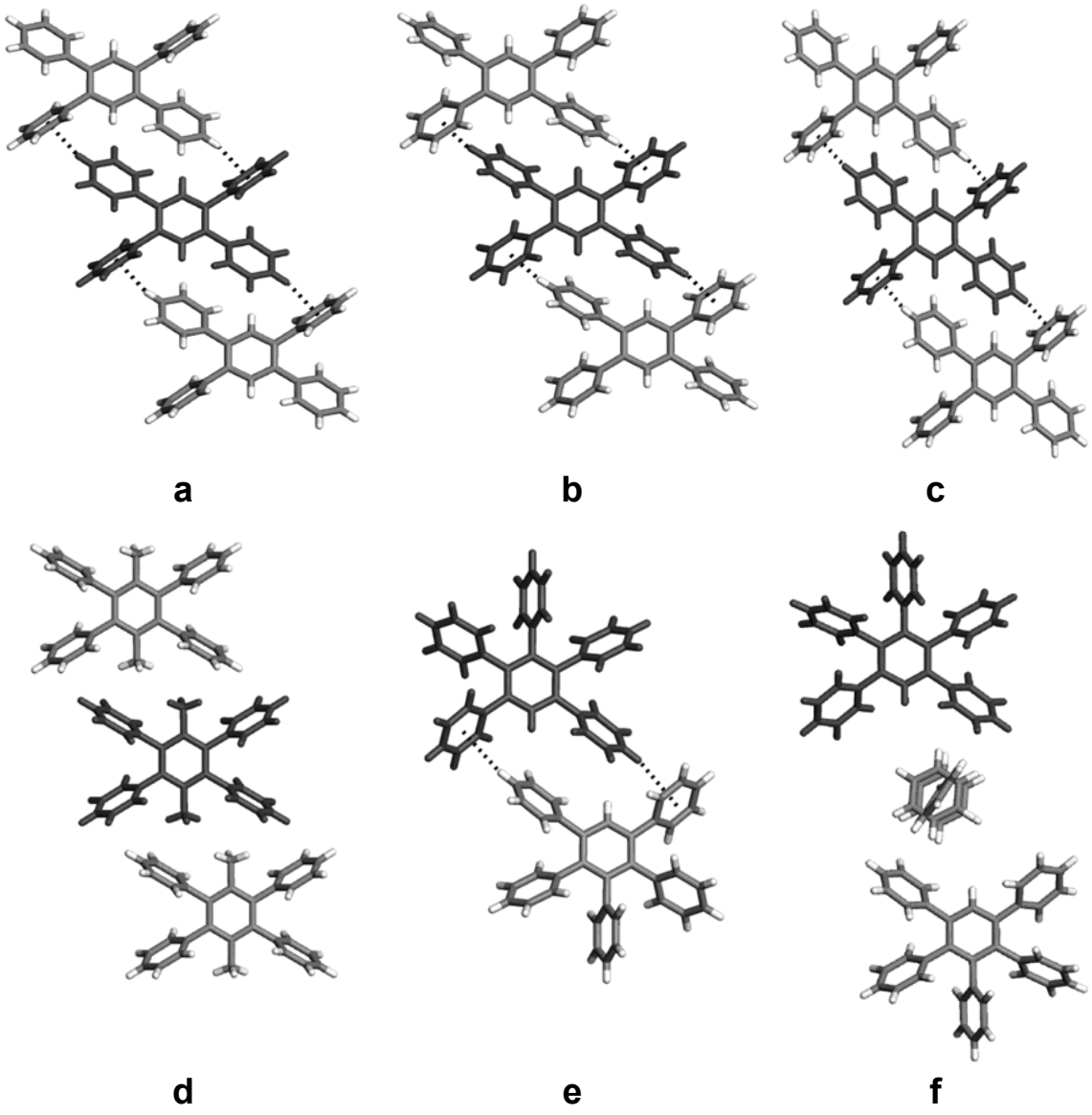

Figure 2. Molecular packing within sheets observed in crystals of selected derivatives of benzene with multiple adjacent phenyl substituents. When C-H···π interactions are present (distances ≤ 3.05 Å), they are represented by broken lines. In each drawing, one molecule appears in dark gray, and key neighbors in the same sheet are represented normally, with carbon atoms in light gray and hydrogen atoms in white. (a) Polymorph TPB-1 of TPB (**3**), obtained by crystallization from hexanes (C-H···centroid distances of 2.76 Å). (b) Polymorph TPB-2 of TPB (**3**), obtained by crystallization from benzene (C-H···centroid distances of 2.81 Å). (c) Polymorph TPB-3 of TPB (**3**), obtained by crystallization from hexanes (C-H···centroid distances of 2.81 Å). d) DMTPB (**4**), obtained by crystallization from xylenes. e) Polymorph PPB-1 of PPB (**5**), obtained by crystallization from hexanes (C-H···centroid distances of 3.02 Å). f) Pseudopolymorph PPB-2 of PPB (**5**), obtained by crystallization from benzene.

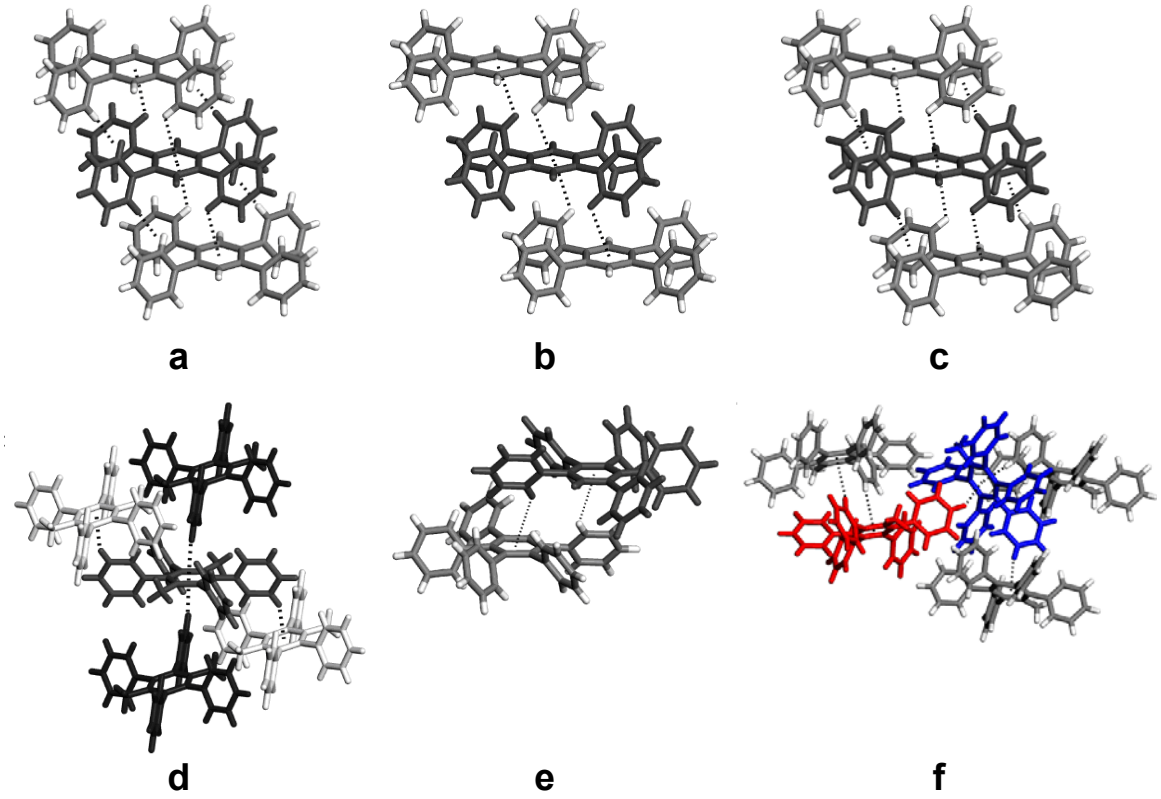

Figure 3. Other C-H···π interactions observed in crystals of selected derivatives of benzene with multiple adjacent phenyl substituents. C-H···π interactions are represented by broken lines. In drawings (a)-(c), a central molecule appears in dark gray, and key neighbors in adjacent sheets are represented normally, with carbon atoms in light gray and hydrogen atoms in white. (a) Polymorph TPB-1 of TPB (**3**), obtained by crystallization from hexanes (C-H···centroid distances of 2.98 Å involving the central aromatic ring and C-H···centroid distances of 2.97 Å involving the peripheral phenyl groups). (b) Polymorph TPB-2 of TPB (**3**), obtained by crystallization from benzene (C-H···centroid distances of 3.01 Å). (c) Polymorph TPB-3 of TPB (**3**), obtained by crystallization from hexanes (C-H···centroid distances of 3.02 Å involving the central aromatic ring and C-H···centroid distances of 2.95 Å involving the peripheral phenyl groups). d) Structure of DMTPB (**4**), obtained by crystallization from xylenes, showing a central molecule (dark gray) interacting with two neighbors (black and white for clarity) in each of the two adjacent sheets (C-H···centroid distances of 2.63 Å). e) Pseudopolymorph PPB-2 of PPB (**5**), obtained by crystallization from benzene, showing a molecule in dark gray paired with a neighbor represented normally, with carbon atoms in light gray and hydrogen atoms in white (C-H···centroid distances of 2.99 Å). f) MPPB (**6**), obtained by crystallization from benzene, with the two molecules of the asymmetric unit shown in red and blue. The central aromatic ring of the molecule in red engages in one C-H···π interaction (C-H···centroid distance of 2.99 Å), and the central aromatic ring of the molecule in blue engages in two C-H···π interactions (C-H···centroid distances of 2.63 Å and 2.92 Å). In Figures 3e and 3f, guest molecules are omitted for clarity.

Structure of Crystals of TPB (3) Grown from Benzene (Polymorph TPB-2). Colorless crystals of a second polymorph of TPB (**3**) were grown by slowly cooling a concentrated solution in benzene. The crystals were found to belong to the triclinic space group *P-1*, and other crystallographic data are compiled in Table 2. In this structure, molecules of TPB (**3**) adopt a conformation in which the average torsional angles are slightly larger than those in polymorph TPB-1 (Table 1). As shown in Figure 2b, TPB (**3**) again forms sheets built from chains held together by characteristic embraces (C-H···centroid distances of 2.81 Å). The altered conformation increases the separation of the sheets (Figure 3b), thereby decreasing the number of inter-sheet C-H···π interactions to four per molecule and increasing their length (C-H···centroid distances of 3.01 Å). Again, the central aromatic ring of each molecule accepts two C-H···π interactions, one on each face.

Structure of Crystals of TPB (3) Grown from Hexanes (Polymorph TPB-3). Careful examination of crystals of TPB (**3**) grown from hexanes revealed the presence of a third polymorph (TPB-3), which proved to belong to the monoclinic space group $P2_1/c$. Other crystallographic data are presented in Table 2. In polymorph TPB-3, the conformation of TPB (**3**) is almost identical to the one observed in polymorph TPB-1 (Table 1), and the resulting structure (Figure 2c) consists of sheets with embraces closely similar to those found in polymorphs TPB-1 and TPB-2 (C-H···centroid distances of 2.81 Å). Adjacent sheets are linked by eight additional C-H···π interactions per molecule (Figure 3c), four involving peripheral phenyl groups as acceptors and four involving central aromatic rings as acceptors (C-H···centroid distances of 2.95 Å and 3.02 Å, respectively).

Further Analysis of the Polymorphs of TPB (3). As underscored by the close similarity of Figures 2a-c and 3a-c, polymorphs TPB-1, TPB-2, and TPB-3 share many key features. To better reveal the small differences, we constructed Hirshfeld surfaces for the three polymorphs.[42-44] Analysis of such surfaces can help summarize all intermolecular contacts in unique 2D fingerprint plots (Figure 4). A cursory examination

of the three plots reveals that polymorph TPB-2 is distinctly different from the other two. In particular, the presence of a diffuse area of contacts at large values of d_i and d_e suggests that packing is less efficient in polymorph TPB-2 (Figure 4b). In addition, non-bonded H···H contacts in TPB-2 are less abundant and slightly longer (values of $d_i \approx d_e = 1.2$). These conclusions are corroborated by the lower calculated density of TPB-2 (Table 2). In contrast, the 2D fingerprint plots of polymorphs TPB-1 and TPB-3 are strikingly similar, both in shape and in intensity (Figures 4a and 4c). A small but significant difference of intensity is found in the areas of H···H contacts ($d_i \approx d_e = 1.2$). To further confirm that polymorphs TPB-1 and TPB-3 are in fact different, we created a superimposed image of the two structures, with one molecule in each occupying essentially the same position (Figure 5). The resulting offset, as well as the presence of a screw axis in polymorph TPB-3, establishes that the polymorphs are not identical.

Subsequent crystallizations of TPB (**3**) from hexanes, toluene, benzene, and xylenes yielded samples that were analyzed by powder X-ray diffraction.[45] The analyses showed various ratios of polymorphs TPB-1 and TPB-3, but no TPB-2 could be detected. We conclude that polymorph TPB-2 is present in only minute amounts or has disappeared.[46] Indeed, its low density (Table 2) and inefficient packing (Figure 4b) suggest that it is less stable than polymorphs TPB-1 and TPB-3.

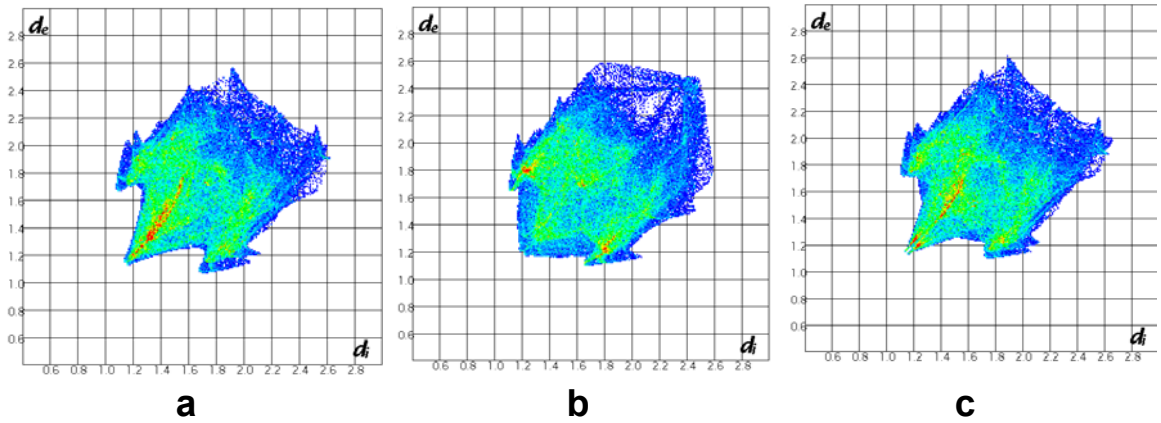

Figure 4. 2D fingerprint plots obtained by analyzing Hirshfeld surfaces corresponding to the structures of three polymorphs of TPB (**3**).[43-44] (a) Polymorph TPB-1. (b) Polymorph TPB-2. (c) Polymorph TPB-3. In the plots, d_e and d_i represent the distance (in Å) from the Hirshfeld surface to the nearest external or internal atom, respectively. The colors used range from blue to green to red in order of increasing frequency of the corresponding values of d_e and d_i.

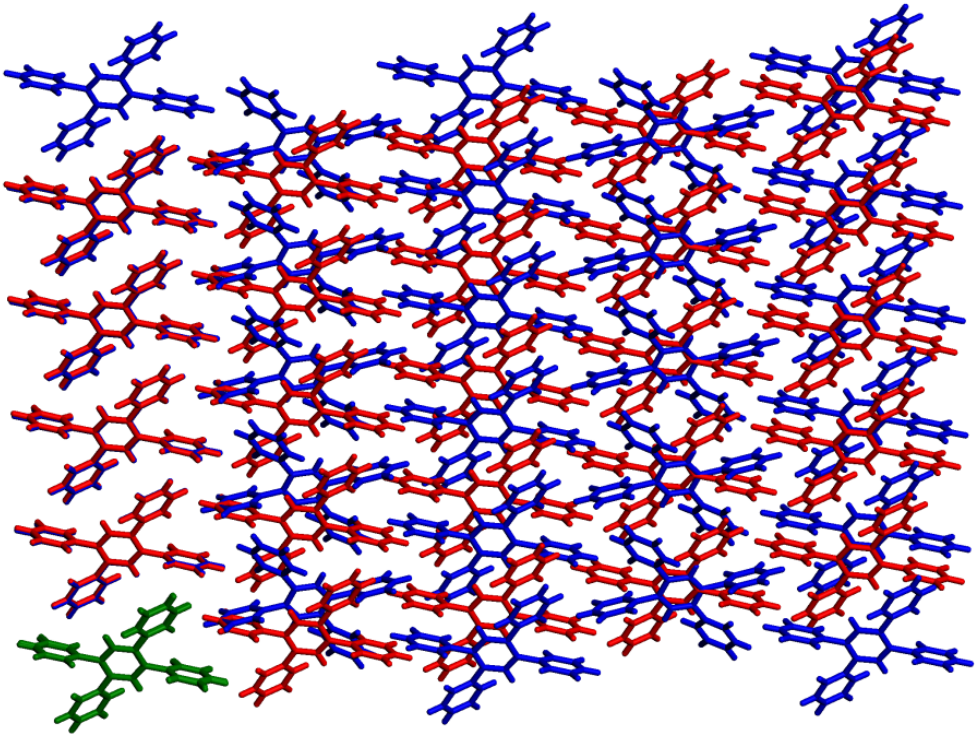

Figure 5. Comparison of the structures of polymorphs TPB-1 and TPB-3 of TPB (**3**) crystallized from hexanes. A sheet of TPB-1 (in red) is superimposed on a sheet of TPB-3 (in blue), with one molecule (in green) in essentially the same position, shared by both sheets.

Structure of Crystals of DMTPB (4). Colorless crystals of DMTPB (**4**) could be grown by cooling hot concentrated solutions in benzene, toluene, or xylenes. The resulting crystals proved to have identical structures and to belong to the monoclinic space group $P2_1/c$. Additional crystallographic data are provided in Table 2. As expected, the introduction of two methyl groups at the unsubstituted positions of TPB (**3**) markedly increases the torsional angles between the central aromatic ring and the peripheral phenyl groups (Table 1). As in the case of TPB (**3**), the structure of DMTPB (**4**) can be described as consisting of sheets, but the methyl groups prevent the close molecular proximity needed to form the characteristic embraces found in the polymorphs of TPB (**3**). As a result, short intra-sheet C-H···π interactions are absent (Figure 2d). Nevertheless, the packing is closely related and makes similarly effective use of molecular clefts. Adjacent sheets are connected by four C-H···π interactions per molecule (C-H···centroid distances of 2.63 Å) in which two peripheral phenyl groups of DMTPB (**4**) serve as donors, and the central aromatic ring acts as a double acceptor (Figure 3d).

Structure of Crystals of PPB (5) Grown from Hexanes or Hexanes/Toluene (Polymorph PPB-1). Cooling a hot concentrated solution of PPB (**5**) in hexanes or allowing hexanes to diffuse into a solution in toluene yielded colorless crystals belonging to the triclinic space group *P-1*. Other crystallographic data are presented in Table 2. As expected, the average torsional angles between the central aromatic ring and the peripheral phenyl groups of PPB (**5**) are lower than those in HPB (**2a**) and DMTPB (**4**), in which all positions of the central ring are substituted (Table 1). As in the case of all polymorphs of TPB (**3**), PPB (**5**) forms sheets with prominent embraces (Figure 2e), which define dimers joined by two C-H···π interactions (C-H···centroid distances of 3.02 Å). No inter-sheet C-H···π interactions are present in polymorph PPB-1, and the shortest intermolecular distance in the structure between an atom of hydrogen and the centroid of a central aromatic ring is 3.44 Å.

Structure of Crystals of PPB (5) Grown from Benzene (Pseudopolymorph PPB-2). Slow evaporation of a solution of PPB (**5**) in benzene produced a crystalline sample containing a pseudopolymorph of composition PPB • 0.5 benzene (PPB-2). In addition, powder X-ray diffraction revealed the simultaneous presence of polymorph PPB-1. Crystals of pseudopolymorph PPB-2 were found to belong to the triclinic space group *P*-1. Additional crystallographic data are provided in Table 2. Pseudopolymorph PPB-2 is stable in air at 25 °C, and thermogravimetric analysis showed that included benzene is lost only near its boiling point.[45] The guest is included in the molecular cleft created by the unsubstituted position of PPB (**5**), thereby interrupting the typical embraces observed in polymorph PPB-1 and related structures (Figure 2f). The guest is disordered over three positions and does not take part in any C-H···π interactions. As shown in Figure 3e, molecules of PPB (**5**) in adjacent sheets form pairs held together in part by two C-H···π interactions involving the central aromatic ring (C-H···centroid distances of 2.99 Å).

Structure of Crystals of MPPB (6) Grown from Benzene/Methanol. Compounds **3**-**5** were found to crystallize readily, but many attempts were required to obtain crystals of analogue **6** suitable for analysis by X-ray diffraction. Crystallization from acetic acid has been reported, but it failed in our hands to yield a sample suitable for structural analysis.[47] Finally, we were able to grow satisfactory crystals of MPPB (**6**) by allowing methanol to diffuse slowly into a solution in benzene. This procedure yielded crystals that proved to have the composition MPPB • 0.25 benzene and to belong to the orthorhombic space group *Pbcn*. Other crystallographic data are presented in Tables 1 and 2. Unlike analogues TPB (**3**), DMTPB (**4**), and PPB (**5**), MPPB (**6**) failed to crystallize as sheets with prominent embraces. Instead, two crystallographically independent molecules each engage in three C-H···π interactions with C-H···centroid distances of 2.63 Å, 2.92 Å, and 2.99 Å (Figure 3f). Presumably, molecules of MPPB (**6**) can achieve closer packing by foregoing the formation of sheets with normal embraces. The observed packing involves H···H contacts as short as 2.22 Å, which is 0.18 Å lower than the sum of the van der Waals radii. Such short contacts are not seen in

any of the other phenyl-substituted benzenes we have studied.[48] The included benzene is ordered and does not participate in C-H···π or π···π interactions. The behavior of HPB (**2a**) and DMTPB (**4**), which crystallize readily from various solvents, yield structures without included guests, and form typical sheets, is distinctly unlike that of their close relative MPPB (**6**), which is reluctant to crystallize, includes guests, and fails to form sheets. In all three compounds, the central aromatic ring is fully substituted, thereby producing similar highly non-planar topologies. As a result, it is likely that the observed differences arise in part from the lowered symmetry of MPPB (**6**). This suggests that derivatives of alkyl-substituted pentaphenylbenzenes may be particularly effective in enhancing solubility and resisting crystallization.

Structure of Crystals of OPQP (7) Grown from Diphenyl Ether. Comparison of the structures of HPB (**2a**), TPB (**3**), DMTPB (**4**), PPB (**5**), and MPPB (**6**) reveals certain shared features, including an absence of π···π interactions and a general tendency to form sheets that incorporate a small number of C-H···π interactions. To see if these features are also present in the structures of more complex relatives, we examined the behavior of OPQP (**7**).[49] Colorless crystals were obtained by slowly cooling a solution in hot diphenyl ether. The crystals were found to belong to the orthorhombic space group *Pccn*. Additional crystallographic data are compiled in Tables 1 and 2. As shown in Figure 6, the structure consists of rippled sheets in which each molecule of OPQP (**7**) shares a total of eight bifurcated C-H···π interactions with four neighbors in the same sheet (C-H···centroid distances of 2.61 Å and 2.92 Å). Adjacent sheets are linked by a total of eight C-H···π interactions per molecule (C-H···centroid distances of 2.74 Å and 2.97 Å), all involving the two fully substituted aromatic rings of OPQP (**7**) as acceptors (Figure 7). The resulting motif defines columns aligned with the *c* axis. OPQP (**7**) has a non-planar topology that hinders close packing, yet each molecule in the structure nevertheless engages in a total of sixteen intermolecular C-H···π interactions. Particularly noteworthy is the ability of the most highly substituted aromatic rings to engage as π-donors in such interactions, both in the structure of OPQP (**7**) and in those of its simpler analogues HPB (**2a**), TPB (**3**), DMTPB (**4**), PPB (**5**), and MPPB (**6**).[50]

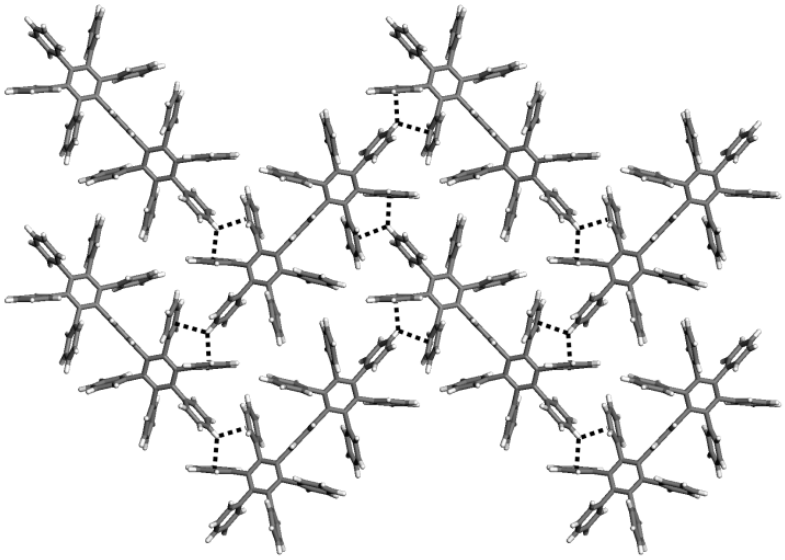

Figure 6. View of the structure of crystals of OPQP (**7**) grown from diphenyl ether, showing part of a sheet held together by multiple bifurcated intermolecular C-H···π interactions. The interactions are represented by broken lines, and the C-H···centroid distances are 2.61 and 2.92 Å.

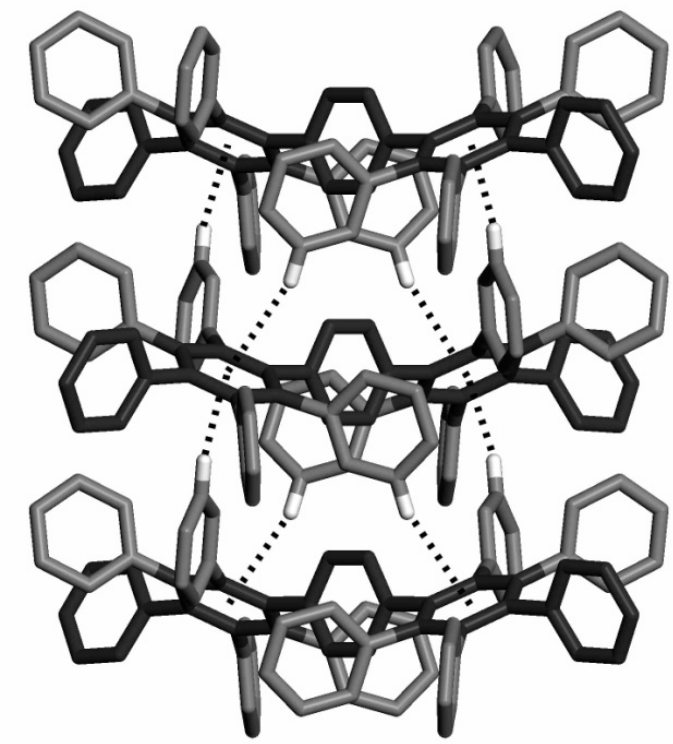

Figure 7. View of the structure of crystals of OPQP (**7**) grown from diphenyl ether, showing inter-sheet C-H···π interactions. The interactions are represented by broken lines, and the C-H···centroid distances are 2.74 and 2.97 Å. For clarity, hydrogen atoms not involved in C-H···π interactions are omitted, and the *p*-quinquephenyl core is highlighted in black.

Comparison of Intermolecular Interactions in the Structures of Derivatives of Benzene with Multiple Phenyl Substituents. The relative importance of non-bonded C···C, C···H, and H···H contacts in the structures of planar aromatic hydrocarbons, represented by HBC (**1**), should be dramatically different from that found in non-planar analogues, represented by HPB (**2a**). Specifically, the characteristic topology of HPB (**2a**) and related compounds should essentially eliminate C···C contacts and increase the importance of H···H contacts relative to C···H contacts. To test this assertion, we have used Hirshfeld surfaces to analyze C···C, C···H, and H···H contacts in the structures of HPB (**2a**), TPB (**3**), DMTPB (**4**), PPB (**5**), MPPB (**6**), and OPQP (**7**), as well as those in the structures of related phenyl-substituted derivatives of benzene drawn from the Cambridge Structural Database. The results of this analysis are presented in the form of a bar graph in Figure 8. Key conclusions are summarized below:

- ***p*-Phenylenes.** In the homologous series of *p*-phenylene compounds ranging from benzene to *p*-septiphenyl, the percentage of C···H contacts increases monotonically with molecular length, from 35% in benzene to 61% in *p*-septiphenyl.
- ***o*-Diphenyl substitution.** As illustrated by the cases of *o*-terphenyl and *p*-terphenyl, *o*-substitution by phenyl groups prevents planarity and thereby leads to marked increases in the ratio of H···H contacts to C···H contacts (63:37 for *o*-terphenyl versus 48:51 for *p*-terphenyl).
- **Higher degrees of phenyl substitution.** The ratio of H···H to C···H contacts increases with the degree of substitution, as shown by comparing the behavior of triphenyl-, tetraphenyl-, pentaphenyl-, and hexaphenylbenzene.
- **Branching.** In linear *p*-phenylenes, C···H contacts are much more important than in branched isomers, as shown by comparing *p*-quinquephenyl with TPB (**3**), *p*-sexiphenyl with PPB (**5**), and *p*-septiphenyl with HPB (**2a**).

Together, these results reveal how the intermolecular interactions of non-planar derivatives of benzene with multiple contiguous phenyl substituents, typified by HPB (**2a**), differ significantly from those of planar isomers, represented by HBC (**1**).

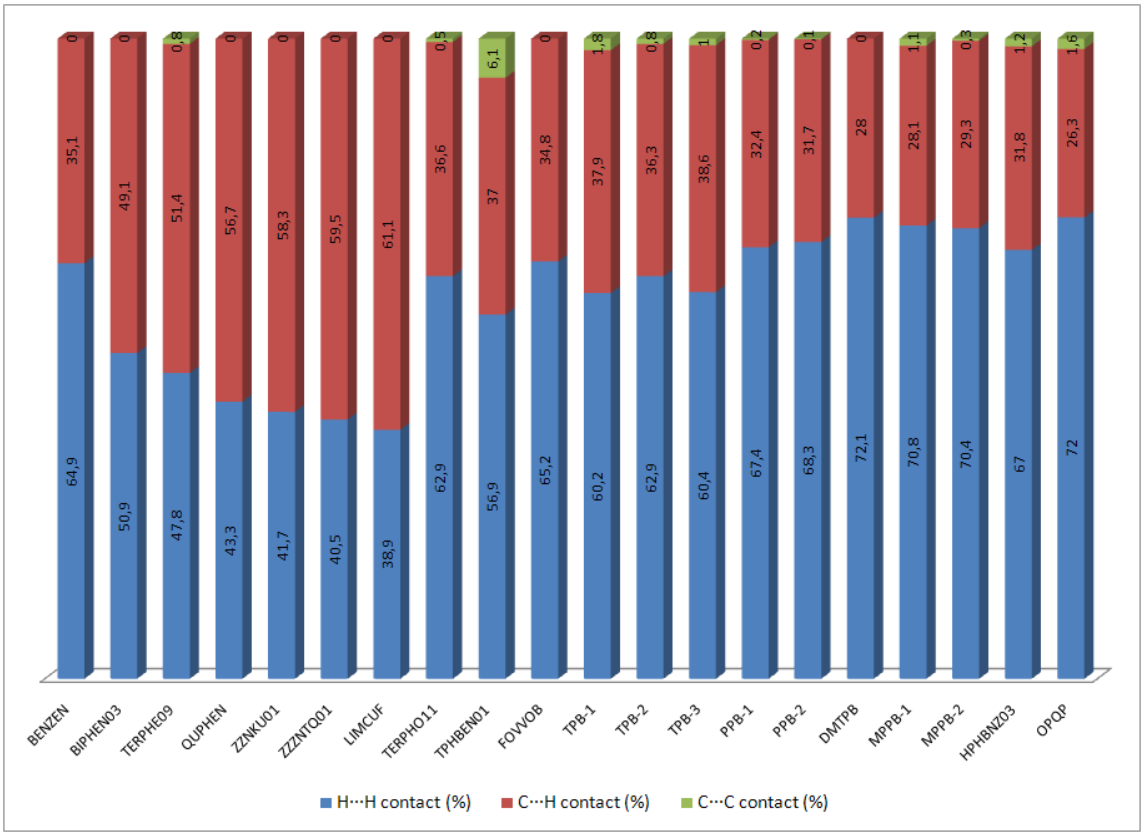

Figure 8. Bar graph showing the nature of intermolecular contacts in crystals of derivatives of benzene with multiple phenyl substituents, as determined by analysis of Hirshfeld surfaces. Previously reported structures are identified by reference codes assigned by the Cambridge Structural Database, which appear below the bars. New structures are identified by the names defined in the present paper. Compounds analyzed include benzene (BENZEN), biphenyl (BIPHEN03), *p*-terphenyl (TERPHO09), *p*-quaterphenyl (QUPHEN), *p*-quinquephenyl (ZZZNKU01), *p*-sexiphenyl (ZZZNTQ01), *p*-septiphenyl (LIMCUF), *o*-terphenyl (TERPHO11), 1,3,5-triphenylbenzene (TPHBNZ01), 1,2,3,4-tetraphenylbenzene (FOVVOB), 1,2,4,5-tetraphenylbenzene (TPB-1, TPB-2, and TPB-3), pentaphenylbenzene (PPB-1 and PPB-2), 1,4-dimethyl-2,3,5,6-tetraphenylbenzene (DMTPB), 1-methyl-2,3,4,5,6-pentaphenylbenzene (MPPB), hexaphenylbenzene (HPHBNZ03), and 2',2''',3',3''',5',5''',6',6'''-octaphenyl-*p*-quinquephenyl (OPQP).

Conclusions

Producing new molecular materials by design requires careful consideration of the behavior of the components, both as individual molecules and as aggregates. Recent work has underscored the utility of derivatives of benzene with multiple contiguous aryl substituents as components of molecular materials. Their usefulness arises in part from their high thermal stability and their characteristic non-planar topologies, which limit conjugation and disfavor aromatic π-π and C-H···π interactions. As a result, such compounds exhibit higher HOMO-LUMO gaps, lower degrees of self-association, less efficient packing, and higher solubilities than planar analogues. To provide a deeper understanding of this behavior, we have systematically analyzed the structure of crystals of HPB (**2a**) and a series of related derivatives of benzene with multiple adjacent phenyl substituents. Our observations reveal a general tendency for these compounds to crystallize in sheets. Despite having non-planar topologies that appear to obstruct access to the faces of the aromatic rings, HPB (**2a**) and its analogues typically engage in small numbers of intermolecular C-H···π interactions, both within sheets and between them. Of special note in the structures of these compounds is the ability of the central aromatic rings, which are highly substituted and poorly accessible, to serve as acceptors in C-H···π interactions, sometimes even on both faces. Although C···H contacts are not entirely eliminated in the structures of HPB (**2a**) and its analogues, the ratio of H···H contacts to C···H contacts is far higher than that observed in the case of related aromatic compounds able to adopt planar structures. Together, these observations help explain the distinctive behavior of non-planar aryl-substituted arenes and may lead to new applications of these useful compounds.

Experimental Section

All reagents and solvents were purchased from commercial sources and used without further purification unless otherwise indicated. 1,2,4,5-Tetrabromobenzene was recrystallized from ethyl acetate prior to use. $Pd(PPh_3)_4$ was prepared by reducing $PdCl_2$ with hydrazine in the presence of PPh_3 according to a known procedure.[51]

Tetraphenylcyclopentadienone,[52] HPB (**2a**),[33] DMTPB (**4**),[31] pentaphenylbenzene (**5**),[31] and 2',2''',3',3''',5',5''',6',6'''-octaphenyl-*p*-quinquephenyl (**7**)[34] were prepared by reported methods. Anhydrous and oxygen-free solvents were obtained by passage through columns packed with activated alumina and supported copper catalyst (Glass Contour, Irvine, CA). NMR spectra were recorded using a Bruker AV400 spectrometer, and high-resolution mass spectra were obtained using an Agilent LC-MSD TOF spectrometer. Thermogravimetric analyses were carried out using a TA Instruments high-resolution TGA 2950 apparatus. Elemental analyses were performed at the Université de Montréal.

1,2,4,5-Tetraphenylbenzene (3). 1,2,4,5-Tetrabromobenzene (1.97 g, 5.00 mmol), phenylboronic acid (3.66 g, 30.0 mmol), and $Pd(PPh_3)_4$ (0.289 g, 0.252 mmol) were suspended in a mixture of 95% ethanol (30 mL), aqueous K_2CO_3 (2 M, 30 mL), and toluene (60 mL). The mixture was purged thoroughly with a stream of N_2 for 1 h, heated at reflux overnight, and cooled to 25 °C. Toluene (500 mL) was then added, and the resulting mixture was stirred in the air for 1 h. The aqueous phase was discarded, and the organic layer was washed with 1 M aqueous NaOH (2 × 50 mL) and brine. The solution was dried with anhydrous $MgSO_4$ and filtered through silica, using toluene as the eluent. Volatiles were then removed by evaporation under reduced pressure. The colorless residue was recrystallized from hexanes (1.2 L) to give 1,2,4,5-tetraphenylbenzene (**3**; 1.61 g, 4.21 mmol, 84%) as colorless needles. Spectroscopic data matched those reported earlier.[53] ^{1}H NMR (400 MHz, $CDCl_3$) δ 7.24-7.30 (m, 20H), 7.57 (s, 2H); ^{13}C NMR (100 MHz, $CDCl_3$) δ 126.8, 128.1, 130.1, 133.1, 139.8, 141.1; HRMS (ESI-TOF) calcd for $C_{30}H_{22}$ + H *m/z* 383.17943, found 383.17865; calcd for $C_{30}H_{22}$ + Na *m/z* 405.16137, found 405.16001.

1-Methyl-2,3,4,5,6-pentaphenylbenzene (6). 1-Methyl-2,3,4,5,6-pentaphenylbenzene was prepared by a modification of a method reported previously.[47,54] Tetraphenylcyclopentadienone (7.78 g, 20.2 mmol) and 1-phenylpropyne (2.48 g, 21.3 mmol) were combined in diphenyl ether (15 mL) and heated overnight at reflux under N_2. The solution was then cooled to 25 °C and diluted with ethanol. The resulting precipitate was separated by filtration and washed with

ethanol to give 1-methyl-2,3,4,5,6-pentaphenylbenzene (**6**; 8.45 g, 17.9 mmol, 89%) as a colorless powder. ^{1}H NMR spectroscopic data matched those reported earlier.[54] ^{1}H NMR (400 MHz, $CDCl_3$) δ 1.92 (s, 3H), 6.80-6.85 (m, 15H), 7.09-7.18 (m, 10H); ^{13}C NMR (100 MHz, $CDCl_3$) δ 19.8, 125.2, 125.3, 126.1, 126.6, 126.6, 127.6, 130.5, 131.3, 131.5, 133.6, 138.7, 140.3, 140.7, 140.8, 141.1, 141.4; HRMS (ESI-TOF) calcd for $C_{37}H_{28}$ + H *m/z* 473.22638, found 473.22569; calcd for $C_{37}H_{28}$+Na *m/z* 495.20832, found 495.20789.

X-ray crystallographic studies. Data were collected using a Bruker SMART 2000 diffractometer, a Bruker SMART 6000 CCD diffractometer equipped with an FR591 rotating anode generator, or a Bruker Microstar diffractometer with Cu Kα radiation. Details related to the collection of data are summarized in Table 2. The structures were solved by direct methods, using SHELXS-97[55,56] or SIR97,[57] and were refined with SHELXL-97.[55,56] All non-hydrogen atoms were refined anisotropically, whereas hydrogen atoms were placed in ideal positions and refined as riding atoms.

Experimental X-ray powder diffraction patterns were recorded at 25 °C in reflection mode and in Bragg-Brentano geometry, using a Bruker D8 ADVANCE diffractometer with Ge-monochromatized Cu $K\alpha_1$ radiation generated at 40 kV and 40 mA. The diffractometer was equipped with a VÅNTEC-1 linear position-sensitive detector. Calculated X-ray powder diffraction patterns were generated from structural data with the aid of the program Mercury Version 2.0.[58]

Acknowledgments. We are grateful to the Natural Sciences and Engineering Research Council of Canada, the Ministère de l'Éducation du Québec, the Canada Foundation for Innovation, the Canada Research Chairs Program, and Université de Montréal for financial support.

Supporting Information Available: Representative thermogravimetric analysis and additional crystallographic details, including ORTEP drawings and tables of

structural data in CIF format. This material is available free of charge via the Internet at http://pubs.acs.org.

Notes and References

1. Fellow of the Natural Sciences and Engineering Research Council of Canada (2003-2009).

2. Fellow of the Natural Sciences and Engineering Research Council of Canada (2003-2004).

3. For reviews, see: Zhi, L.; Müllen, K. *J. Mater. Chem.* **2008**, *18*, 1472-1484. Bauer, R. E.; Grimsdale, A. C.; Müllen, K. *Top. Curr. Chem.* **2005**, *245*, 253-286. Watson, M. D.; Fechtenkötter, A.; Müllen, K. *Chem. Rev.* **2001**, *101*, 1267-1300. Wiesler, U.-M.; Weil, T.; Müllen, K. *Top. Curr. Chem.* **2001**, *212*, 1-40. Berresheim, A. J.; Müller, M.; Müllen, K. *Chem. Rev.* **1999**, *99*, 1747-1785.

4. For references, see: Clar, E.; Schmidt, W. *Tetrahedron* **1979**, *35*, 2673-2680.

5. For recent reviews, see: Geim, A. K. *Science* **2009**, *324*, 1530-1534. Wu, J.; Pisula, W.; Müllen, K. *Chem. Rev.* **2007**, *107*, 718-747.

6. Tomović, Ž.; Watson, M. D.; Müllen, K. *Angew. Chem., Int. Ed.* **2004**, *43*, 755-758.

7. For recent reviews, see: Chen, Z.; Lohr, A.; Saha-Möller, C. R.; Würthner, F. *Chem. Soc. Rev.* **2009**, 38, 564-584. Sergeyev, S.; Pisula, W.; Geerts, Y. H. *Chem. Soc. Rev.* **2007**, *36*, 1902-1929. Laschat, S.; Baro, A.; Steinke, N.; Giesselmann, F.; Hägele, C.; Scalia, G.; Judele, R.; Kapatsina, E.; Sauer, S.; Schreivogel, A.; Tosoni, M. *Angew. Chem., Int. Ed.* **2007**, *46*, 4832-4887.

8. For recent reviews of the subject of C-H···π interactions, see: Tsuzuki, S.; Fujii, A. *Phys. Chem. Chem. Phys.* **2008**, *10*, 2584-2594. Nishio, M. *CrystEngComm.* **2004**, *6*, 130-158.

9. A database related to C-H···π interactions, maintained by Professor Motohiro Nishio, is available via the Internet at http://www.tim.hi-ho.ne.jp/dionisio.

10. Desiraju, G. R.; Gavezzotti, A. *Acta Crystallogr.* **1989,** *B45*, 473-482. Desiraju, G. R.; Gavezzotti, A. *J. Chem. Soc., Chem. Commun.* **1989,** 621-623. Gavezzotti, A.; Desiraju, G. R. *Acta Crystallogr.* **1988,** *B44*, 427-434.

11. For example, see: Kübel, C.; Eckhardt, K.; Enkelmann, V.; Wegner, G.; Müllen, K. *J. Mater. Chem.* **2000**, *10*, 879-886.

12. Stille, J. K.; Noren, G. K. *Macromolecules* **1972**, *5*, 49-55. Stille, J. K. *Makromol. Chem.* **1972**, *154*, 49-61. Schilling, C. L., Jr.; Reed, J. A.; Stille, J. K. *Macromolecules* **1969**, *2*, 85-88. Stille, J. K.; Noren, G. K. *J. Polymer Sci., Part B* **1969**, *7*, 525-527. Stille, J. K.; Rakutis, R. O.; Mukamal, H.; Harris, F. W. *Macromolecules* **1968**, *1*, 431-436. Mukamal, H.; Harris, F. W.; Stille, J. K. *J. Polymer Sci., Part A-1* **1967**, *5*, 2721-2729. Stille, J. K.; Harris, F. W.; Rakutis, R. O.; Mukamal, H. *J. Polymer Sci., Part B*, **1966**, *4*, 791-793.

13. Ried, W.; Freitag, D. *Angew. Chem., Int. Ed.* **1968**, *7*, 835-902. Ried, W.; Freitag, D. *Naturwissenschaften*, **1966**, *53*, 306.

14. For an early example of the use of Diels-Alder reactions of aryl-substituted cyclopentadienones with acetylenes to form aryl-substituted arenes, see: Dilthey, W.; Schommer, W.; Trösken, O. *Ber. Dtsch. Chem. Ges.* **1933**, *66*, 1627-1628.

15. For example, see: Morgenroth, F.; Müllen, K. *Tetrahedron* **1997**, *45*, 15439-15366. Kumar, U.; Neenan, T. X. *Macromolecules* **1995**, *28,* 124-130.

16. Pogantsch, A.; Wenzl, F. P.; List, E. J. W.; Leising, G.; Grimsdale, A. C.; Müllen, K. *Adv. Mater.* **2002**, *14*, 1061-1064. Setayesh, S.; Grimsdale, A. C.; Weil, T.; Enkelmann, V.; Müllen, K.; Meghdadi, F.; List, E. J. W.; Leising, G. *J. Am. Chem. Soc.* **2001**, *123*, 946-953.

17. Liaw, B. R.; Huang, W. Y.; Huang, P. T.; Chang, M. Y.; Han, Y. K. *Polymer* **2007**, *48*, 7087-7097.

18. Rempala, P.; Kroulík, J.; King, B. T. *J. Org. Chem.* **2006**, *71*, 5067-5081.

19. De Silva, A.; Ober, C. K. *J. Mater. Chem.* **2008**, *18*, 1903-1910.

20. For representative recent references, see: Sun, X.; Xu, X.; Qiu, W.; Yu, G.; Zhang, H.; Gao, X.; Chen, S.; Song, Y.; Liu, Y. *J. Mater. Chem.* **2008**, *18*, 2709-2715. Bera, R. N.; Cumpstey, N.; Burn, P. L.; Samuel, I. D. W. *Adv. Funct. Mater.* **2007**, *17*, 1149-1152. Watanabe, S.; Kido, J. *Chem. Lett.* **2007**, *36*, 590-591. Tong, Q.-X.; Lai, S.-L.; Chan, M.-Y.; Lai, K.-H.; Tang, J.-X.; Kwong, H.-L.; Lee, C.-S.; Lee, S.-T. *Chem. Mater.* **2007**, *19*, 5851-5855. Kuo, W.-J.; Chen, Y.-H.; Jeng, R.-J.; Chan, L.-H.; Lin, W.-P.; Yang, Z.-M. *Tetrahedron* **2007**, *63*, 7086-7096. Huang, C.; Zhen, C.-G.; Su, S. P.; Loh, K. P.; Chen, Z.-K. *Org. Lett.* **2005**, *7*, 391-394. Thomas, K. R. J.; Velusamy, M.; Lin, J. T.; Sun, S.-S.; Tao, Y.-T.; Chuen, C.-H. *Chem. Commun.* **2004**, 2328-2329. Chen, C.-T.; Chiang, C.-L.; Lin, Y.-C.; Chan, L.-H.; Huang, C.-H.; Tsai, Z.-W.; Chen, C.-T. *Org. Lett.* **2003**, *5,* 1261-1264. Wu, I.-Y.; Lin, J.-T.; Tao, Y.-T.; Balasubramaniam, E. *Adv. Mater.* **2000**, *12*, 668-669.

21. For reviews, see: Shirota, Y. *J. Mater. Chem.* **2005**, *15*, 75-93. Strohriegel, P.; Grazulevicius, J. V. *Adv. Mater.* **2002**, *14*, 1439-1452.

22. Hoffmann, M.; Kärnbratt, J.; Chang, M.-H.; Herz, L. M.; Albinsson, B.; Anderson, H. L. *Angew. Chem., Int. Ed.* **2008**, *47*, 4993-4996. Alam, M. A.; Kim, Y.-S.; Ogawa, S.; Tsuda, A.; Ishii, N.; Aida, T. *Angew. Chem., Int. Ed.* **2008**, *47*, 2070-2073.

23. Chiaravalloti, F.; Gross, L.; Rieder, K.-H.; Stojkovic, S. M.; Gourdon, A.; Joachim, C.; Moresco, F. *Nature Mater.* **2007**, *6*, 30-33.

24. Xiao, W.; Feng, X.; Ruffieux, P.; Gröning, O.; Müllen, K.; Fasel, R. *J. Am. Chem. Soc.* **2008**, *130*, 8910-8912.

25. Iwasawa, T.; Tokunaga, M.; Obora, Y.; Tsuji, Y. *J. Am. Chem. Soc.* **2004**, *126*, 6554-6555.

26. Aoyama, H.; Tokunaga, M.; Kiyosu, J.; Iwasawa, T.; Obora, Y.; Tsuji, Y. *J. Am. Chem. Soc.* **2005**, *127*, 10474-10475.

27. Iwasawa, T.; Kamei, T.; Watanabe, S.; Nishiuchi, M.; Kawamura, Y. *Tetrahedron Lett.* **2008**, *49*, 7430-7433. Iwasawa, T.; Komano, T.; Tajima, A.; Tokunaga, M.; Obora, Y.; Fujihara, T.; Tsuji, Y. *Organometallics* **2006**, *25*, 4665-4669.

28. Sato, H.; Fujihara, T.; Obora, Y.; Tokunaga, M.; Kiyosu, J.; Tsuji, Y. *Chem. Commun.* **2007**, 269-271.

29. For reviews, see: Tsuji, Y.; Fujihara, T. *Inorg. Chem.* **2007**, *46,* 1895-1902. Tsuji, Y.; Fujihara, T. *Chem. Lett.* **2007**, *36,* 1296-1301.

30. Kobayashi, K.; Sato, A.; Sakamoto, S.; Yamaguchi, K. *J. Am. Chem. Soc.* **2003**, *125*, 3035-3045. Kobayashi, K.; Shirasaka, T.; Horn, E.; Furukawa, N. *Tetrahedron Lett.* **2000**, *41*, 89-93. Kobayashi, K.; Shirasaka, T.; Sato, A.; Horn, E.; Furukawa, N. *Angew. Chem., Int. Ed*. **1999**, *38*, 3483-3486.

31. Maly, K. E.; Gagnon, E.; Maris, T.; Wuest, J. D. *J. Am. Chem. Soc.* **2007**, *129*, 4306-4322.

32. Gagnon, E.; Maris, T.; Maly, K. E.; Wuest, J. D. *Tetrahedron* **2007**, *63*, 6603-6613. Gagnon, E.; Maly, K. E.; Maris, T.; Wuest, J. D. *Acta Crystallogr.* **2007**, *C63*, o4-o6. Maly, K. E.; Maris, T.; Gagnon, E.; Wuest, J. D. *Cryst. Growth Des.* **2006**, *6*, 461-466.

33. Fieser, L. F. *Org. Synth.* **1966**, *46*, 44. Fieser, L. F. *Organic Syntheses*; Wiley: New York, 1973; Collect. Vol. V, p 604.

34. Müller, M.; Iyer, V. S.; Kübel, C.; Enkelmann, V.; Müllen, K. *Angew. Chem., Int. Ed.* **1997**, *36*, 1607-1610.

35. Bart, J. C. J. *Acta Crystallogr.* **1968**, *B24*, 1277-1287.

36. Lutz, M.; Spek, A. L.; Bonnet, S.; Klein Gebbink, R. J. M.; van Koten, G., private communication, 2006 (CCDC 609800, Refcode: HPHBNZ03).

37. For a review of twisted acenes, see: Pascal, R. A., Jr. *Chem. Rev.* **2006**, *106*, 4809-4819.

38. The existence of significant intermolecular C-H···π aromatic interactions can be assessed in various ways. In the case of HPHBNZ03,[36] for example, the central aromatic ring engages in an intermolecular C-H···π interaction that can be characterized by various geometric parameters, including 1) the distance of the hydrogen atom to the mean-square plane of the central aromatic ring (2.76 Å); 2) the distance of the same hydrogen atom to the nearest carbon atom of the central aromatic ring (2.91 Å); and 3) the corresponding C-H···centroid distance (3.00 Å). To avoid ambiguity, we consider that an intermolecular C-H···π aromatic interaction is present only when the C-H···centroid distance is ≤ 3.05 Å, which is 1.05 times greater than the sum of the accepted van der Waals radii of hydrogen (1.20 Å) and carbon (1.70 Å). Similar criteria have been used previously in other studies of C-H···π interactions.[39]

39. Umezawa, Y.; Tsuboyama, S.; Takahashi, H.; Uzawa, J.; Nishio, M. *Tetrahedron* **1999**, *55*, 10047-10056. Umezawa, Y.; Tsuboyama, S.; Honda, K.; Uzawa, J.; Nishio, M. *Bull. Chem. Soc. Jpn.* **1998**, *71*, 1207-1213.

40. The structure of polymorph TPB-1 of TPB (**3**) has been reported previously but not analyzed in detail.[41]

41. Hua, G.; Li, Y.; Slawin, A. M. Z.; Woollins, J. D. *Dalton Trans.* **2007**, 1477-1480.

42. For a recent review of the analysis of Hirshfeld surfaces, see: Spackman, M. A.; Jayatilaka, D. *CrystEngComm* **2009**, *11*, 19-32.

43. Analyses of Hirshfeld surfaces were carried out using the program Crystal Explorer Version 2.1.[44]

44. Wolff, S. K.; Grimwood, D. J.; McKinnon, J. J.; Jayatilaka, D.; Spackman, M. A. *Crystal Explorer 2.1*; University of Western Australia: Perth, 2007 (http://hirshfeldsurface.net/CrystalExplorer).

45. See the Supporting Information for details.

46. Dunitz, J. D.; Bernstein, J. *Acc. Chem. Res.* **1995**, *28*, 193-200.

47. Dudkowski, J. J.; Becker, E. I. *J. Org. Chem.* **1952**, *17*, 201-206.

48. For a discussion of unusually short intermolecular H···H contacts, see: Bombicz, P.; Czugler, M.; Tellgren, R.; Kálmán, A. *Angew. Chem., Int. Ed.* **2003**, *42*, 1957-1960.

49. For related structural studies of albatrossenes, see: Tong, L.; Ho, D. M.; Vogelaar, N. J.; Schutt, C. E.; Pascal, R. A., Jr. *J. Am. Chem. Soc.* **1997**, *119*, 7291-7302.

50. Further theoretical and experimental analysis of the unusual ability of the central aromatic ring of hexaphenylbenzenes to engage in C-H···π interactions will be the subject of a future paper.

51. Coulson, D. *Inorg. Synth.* **1972**, *13*, 121.

52. Johnson, J. R.; Grummitt, O. *Org. Synth.* **1943**, *23*, 92. Johnson, J. R.; Grummitt, O. *Organic Syntheses*; Wiley: New York, 1955; Collect. Vol. III, p 806.

53. Yoshikai, N.; Matsuda, H.; Nakamura, E. *J. Am. Chem. Soc.* **2009**, *131*, 9590-9599.

54. Woolsey, N. F.; Radonovich, L. J.; Saad, F. M.; Koch, F. J. *J. Org. Chem.* **1979**, *44*, 2483-2487.

55. Sheldrick, G. M. *SHELXS-97, Program for the Solution of Crystal Structures* and *SHELXL-97, Program for the Refinement of Crystal Structures*; Universität Göttingen: Germany, 1997.

56. Sheldrick, G. M. *Acta Crystallogr.* **2008**, *A64*, 112-122.

57. Altomare, A.; Burla, M. C.; Camalli, M.; Cascarano, G. L.; Giacovazzo, C.; Guagliardi, A.; Moliterni, A. G. G.; Polidori, G.; Spagna, R. *J. Appl. Crystallogr.* **1999**, *32*, 115-119.

58. Macrae, C. F.; Bruno, I. J.; Chisholm, J. A.; Edgington, P. R.; McCabe, P.; Pidcock, E.; Rodriguez-Monge, L.; Taylor, R.; van de Streek, J.; Wood, P. A. *J. Appl. Crystallogr.* **2008**, *41*, 466-470.

5.4 Vers un nouveau système supramoléculaire

Les résultats présentés dans l'article précédent forment une base de données très utile quant au comportement à l'état cristallin de benzènes substitués par plusieurs cycles aromatiques. Ces résultats démontrent sans équivoque que les (polyphényl)benzènes créent autour d'eux un environnement particulier, qui évoque une carapace hérissée de liens C-H. Ainsi, la majeure partie des interactions intermoléculaires proviennent de contacts entre atomes d'hydrogène. Par contre, l'étude minutieuse des structures par diffraction des rayons-X suggère qu'un motif d'association par interactions C-H···π avec le benzène central de ces molécules est privilégié. Les détracteurs de cette conclusion peuvent répliquer aisément en s'appuyant sur des arguments purement stériques; la complémentarité des surfaces convexes et concaves des molécules[14] ou tout simplement le besoin de combler le vide interstitiel[15] sont toutes deux des explications plausibles pour expliquer ce phénomène (Figure 5.6).

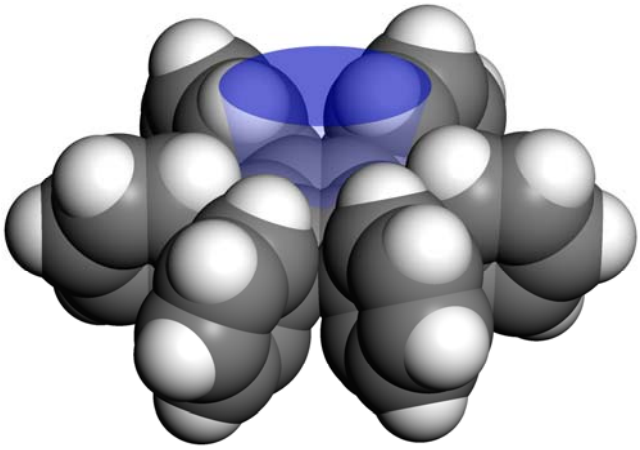

Figure 5.6. Cavité près du cycle aromatique central de l'hexaphénylbenzène (en bleu), telle que définie par l'encombrement stérique. Cette cavité doit être remplie à l'état solide pour respecter le principe de l'empilement compact.

Par contre, plusieurs indices supportent l'idée que les interactions C-H···π observées dans les structures cristallines de l'hexaphénylbenzène et ses dérivés sont fortes et directionnelles. Premièrement, tous les composés étudiés voient leur cycle

[14] Pauling, L.; Delbrück, M. *Science* **1940**, *92*, 77-79.
[15] Kitaigorodskii, A. I. *Organic Chemical Crystallography*; Consultants Bureau: New York, 1961.

aromatique central impliqué dans cette interaction non-covalente. Deuxièmement, les liens C(sp^2)-H sont de relativement bons donneurs dans le cadre de ces interactions non-covalentes (Figure 5.4). Finalement, les distances H···$\pi_{centroïde}$ sont souvent sous la somme des rayons de van der Waals. Ces résultats démontrent que le cycle aromatique central de l'hexaphénylbenzène constitue un partenaire idéal pour former des liens C-H···π.

Ainsi, nous avons décidé d'explorer la chimie supramoléculaire de ce type de système. Pour y arriver, nous avons jumelé notre accepteur à un meilleur donneur : le lien C(*sp*)-H. En se basant sur les règles d'Etter (normalement applicables qu'aux ponts hydrogène),[16] on s'attend effectivement à une association sélective entre le meilleur donneur et le meilleur accepteur présents. Grâce à cette association, on espère démontrer 1) que le cycle aromatique central de l'hexaphénylbenzène est un accepteur de liens C-H···π efficace, 2) que l'on peut appliquer le concept des règles d'Etter aux liens C-H···π, qui sont des ponts hydrogène faibles et 3) que ces interactions non-covalentes peuvent servir à construire des édifices supramoléculaires selon des motifs d'association prévisibles.

[16] Etter, M. C. *Acc. Chem. Res.* **1990**, *23*, 120-126.

5.5 Article 4

Hexaphenylbenzenes as Acetylene Sponges

Eric Gagnon,[†,‡] Alain Rochefort,[§] Valérie Métivaud,[†] and James D. Wuest[†]

Organic Letters, **2010**, *12*, 380-383

Reproduced with permission from *Organic Letters*
Copyright 2010 American Chemical Society

Non-planar aromatic compounds with multiple contiguous aryl substituents, represented by hexaphenylbenzene (**1a** = HBP), have special properties that make them widely useful in science and technology.[1] In particular, their complex topologies limit conjugation and disfavor extensive intermolecular π-π and C-H···π interactions.[2,3] As a result, these compounds can be expected to show higher HOMO-LUMO gaps, lower degrees of self-association, less efficient packing, and higher solubilities than planarized analogues such as hexa-peri-hexabenzocoronene (**2**) or linear analogues such as *p*-septiphenyl (**3**). These marked differences have been underscored by the results of a recent systematic crystallographic analysis of the structures of HPB (**1a**) and its relatives.[4] For example, the ratio of H···H contacts to C···H contacts in the structure of compound **1a** (67:32) greatly exceeds the ratio observed in the structure of linear isomer **3** (39:61).

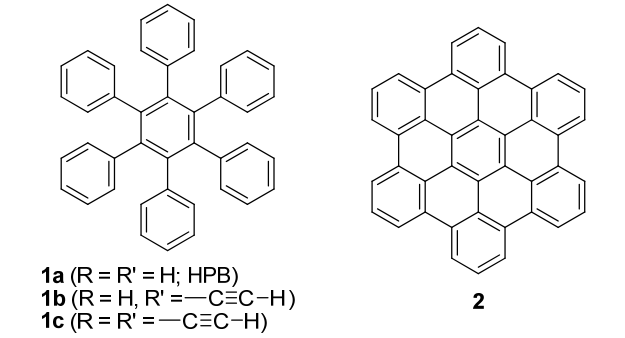

Even though the characteristic non-planar topology of HPB (**1a**) appears to set severe limits on access to the faces of all seven aromatic rings, intermolecular C-H···π interactions are not entirely eliminated in the structure of its crystals.[4,5] Surprisingly, the fully substituted central aromatic ring serves as a double acceptor of C-H···π interactions, one on each face (Figure 1a). This unexpected feature is also found in the structures of many related compounds with multiple contiguous phenyl groups.[4] We now report the results of an integrated experimental and theoretical study that reveals the particularly strong tendency of hexaphenylbenzenes to form C-H···π interactions with alkynes. Their association defines a new supramolecular synthon that can be used predictably to engineer molecular crystals.[6]

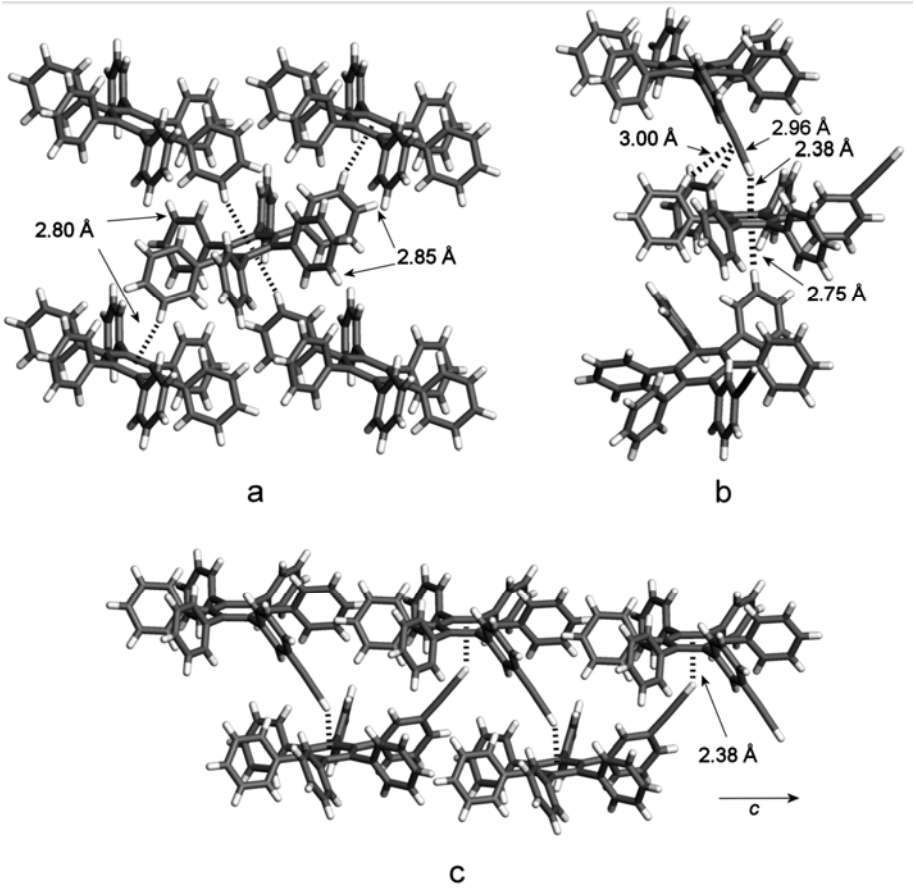

Figure 1. (a) View of the structure of crystals of HPB (**1a**) grown from CH_2Cl_2 or CH_2Br_2.[5] (b) View of the structure of crystals of analogue **1b** grown from CH_2Cl_2. (c) View of molecules of analogue **1b** enchained along the *c* axis by multiple C-H···π interactions. In all views, carbon atoms are shown in light gray and hydrogen atoms in white. C-H···π interactions are represented by broken lines, with key distances indicated.. In Figure 1c, only the primary C(*sp*)-H···π interactions are shown.

By the route summarized in Scheme 1,[7] we made compound **1b**, in which a hexaphenylbenzene core and an ethynyl group are present within a single molecule. Compound **1b** was crystallized by slow evaporation of a solution in CH_2Cl_2. Routine analysis of disorder in the ethynyl group yielded a structure with noteworthy features.[7,8] As expected, the core adopts a non-planar conformation similar to those of other derivatives of HPB (**1a**), with large torsional angles between the central and peripheral aromatic rings.[4,9,10] As shown in Figure 1b, one face of the central aromatic ring serves as acceptor in an unusually short C(*sp*)-H···π interaction involving the ethynyl group as donor (2.38 Å/140°).[11] The other face engages in a C(sp^2)-H···π interaction with a

second neighboring molecule (2.75 Å/164°). A special feature in the structure is reinforcement of the primary C(*sp*)-H···π interaction by secondary C(sp^2)-H···π interactions in which the ethynyl group acts as acceptor (2.96 Å/140° and 3.00 Å/153°).[12] Overall, the resulting structure consists of supramolecular chains along the *c* axis maintained by multiple C-H···π interactions (Figure 1c).

Scheme 1.

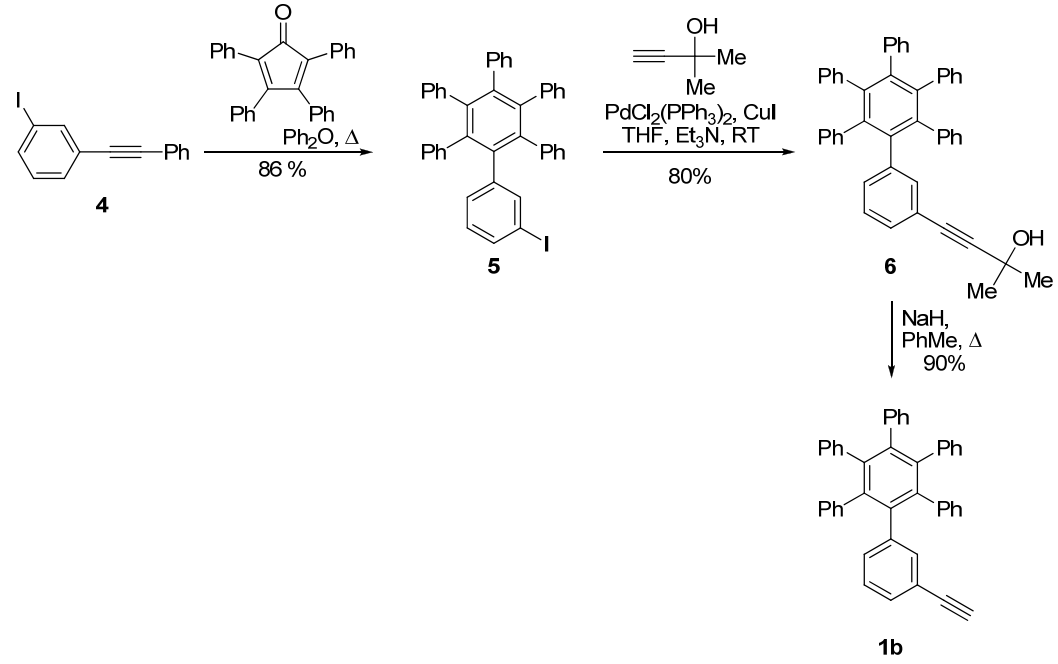

Scheme 2.

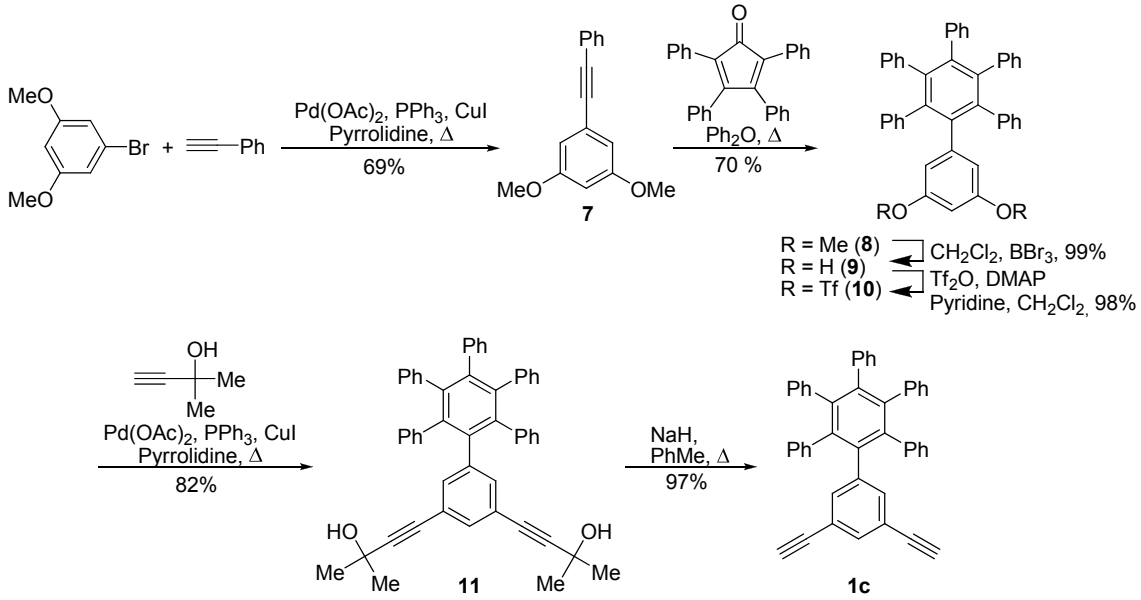

In the structure of compound **1b**, the acetylenic C-H bond competes successfully with a total of 29 other C-H bonds for access to the faces of the central aromatic ring. We reasoned that supramolecular organization could be better controlled in analogue **1c**, in which two C(*sp*)-H donors are available for both faces of the central ring. Compound **1c** was synthesized as shown in Scheme 2,[7] and crystals of composition **1c** • 1 toluene were grown from toluene/hexanes.[8,13] As planned, the molecules are linked exclusively by short C(*sp*)-H···π interactions (2.47 Å/135° and 2.46 Å/138°), creating chains along the *c* axis reinforced by additional C(sp^2)-H···π interactions in which the ethynyl groups serve as acceptors (Figure 2).

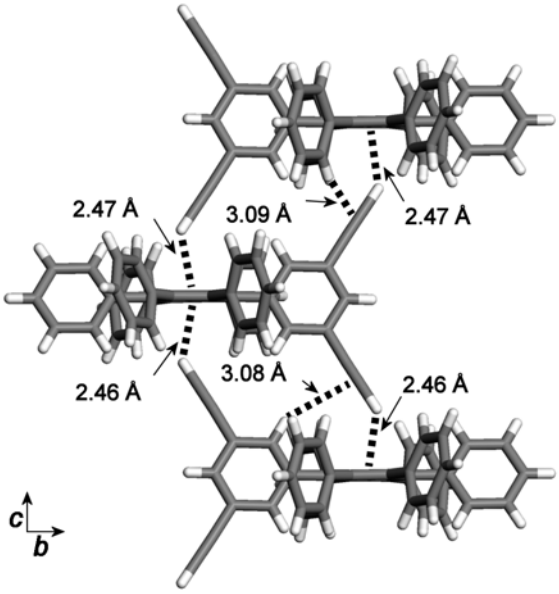

Figure 2. View of the structure of crystals of compound **1c** grown from toluene/hexanes, with guest molecules of toluene omitted for clarity. Carbon atoms are shown in light gray and hydrogen atoms in white. C-H···π interactions are represented by broken lines, with key distances indicated.

Surprisingly, reinforced C-H···π interactions of the type observed in the structures of compounds **1b** and **1c** are strong enough to force the co-crystallization of suitable hexaphenylbenzenes and acetylenes.[14] Cooling a hot solution of HPB (**1a**) in PhC≡CH produced crystals that proved to belong to the monoclinic space group *Cc* and to have the composition **1a** • 0.5 PhC≡CH.[14] The resulting structure is maintained by multiple C-H···π interactions (Figure 3), including the expected reinforced C(*sp*)-H···π interaction involving PhC≡CH and the central aromatic ring of HPB (**1a**). In the

structure of the co-crystals of HPB (**1a**) and PhC≡CH, as well as in the crystals of hexaphenylbenzenes **1b** and **1c**, the thermal parameters of the -C≡C-H group are reduced,[7] presumably because the group is bound in a pocket and engages in strong C(*sp*)-H···π interactions.[15]

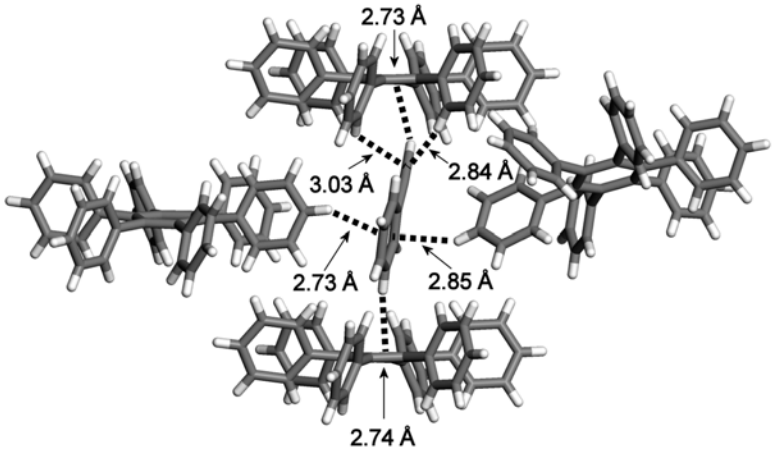

Figure 3. View of the structure of 2:1 co-crystals of HPB (1a) and PhC≡CH. Carbon atoms are shown in light gray and hydrogen atoms in white. C-H···π interactions are represented by broken lines, with key distances indicated.

The pronounced tendency of hexaphenylbenzenes to engage in reinforced C(*sp*)-H···π interactions whenever possible suggests that such compounds can serve as sponges for acetylenes. To test this notion, we used DFT calculations to evaluate the association of acetylene with benzene, HPB (**1a**), and 1,3,5-triphenylbenzene held in three distinct conformations. The geometries were fully optimized at the B3LYP/6-31G* level, including corrections for van der Waals interactions and basis set superposition error.[7] The results are summarized in Figure 4. The complex of acetylene and benzene is calculated to favor an orthogonal geometry, with a short C(*sp*)-H···π interaction (2.31 Å), and the energy of interaction is estimated to be 3.5 kcal/mol, in good agreement with the conclusions of previous studies.[15,16] The addition of three phenyl groups does not not increase this energy when they are forced to remain in the plane of the central ring; however, when they are orthogonal, the energy increases to 5.0 kcal/mol. Finally, the complex of acetylene with HPB (**1a**) is estimated to be stabilized by 6.4 kcal/mol, and the C(*sp*)-H···π interaction is linear and very short (2.18 Å/180°).

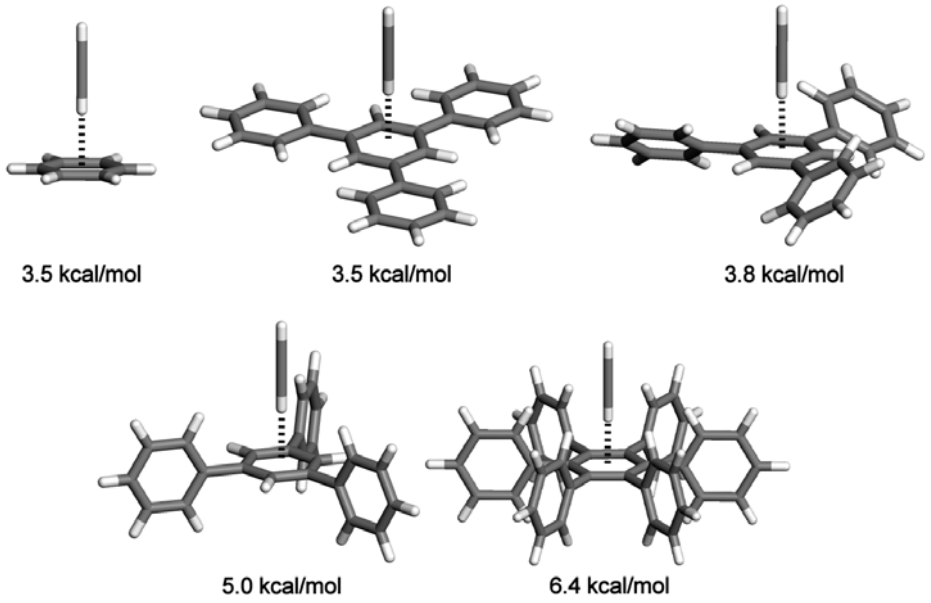

Figure 4. Energy of interaction between acetylene and benzene, between acetylene and 1,3,5-triphenylbenzene (in three conformations), and between acetylene and HPB (1a), as estimated by DFT calculations.

Together, these results suggest that the central C(*sp*)-H···π interaction contributes 3.5 kcal/mol, and each co-facial *ortho* C-H bond of an orthogonal phenyl group adds a reinforcing C(sp^2)-H···π interaction worth 0.5 kcal/mol. Simple C(*sp*)-H···π interactions are well known, but they account for only about half of the overall stabilization of the acetylene-HPB (**1a**) complex. Moreover, the reinforcing secondary interactions draw the bound acetylene much closer to the π-acceptor. For both reasons, it is clear that acetylene-hexaphenylbenzene complexes have unique features not previously observed. Careful examination of electron densities in the calculated acetylene-HPB (**1a**) complex shows reductions on the cofacial *ortho* hydrogens,[7] thereby confirming the importance of the secondary reinforcing interactions. Moreover, these interactions appear to be strong enough to slightly distort the geometry of HPB (**1a**) in a way that brings the *ortho* hydrogens closer to the bound acetylene.[7] Although theory suggests that the reinforced C(*sp*)-H···π interactions of hexaphenylbenzenes should be linear, competing intermolecular interactions and geometric constraints in crystals can induce significant deformations, as observed in the structures formed by compounds **1a-c**.

The characteristic non-planar topology of hexaphenylbenzenes creates sites on both faces of the central aromatic ring that are ideal for binding acetylenes by C(*sp*)-H···π interactions reinforced by secondary C(sp^2)-H···π interactions. The importance of this new associative motif is revealed by its widespread presence in the structures of crystals. Moreover, calculations show that its strength is nearly twice that of normal C(*sp*)-H···π interactions, making it similar to hydrogen bonds in its ability to direct molecular association with predictable directionality. If so, it should be possible to observe the binding of acetylenes by hexaphenylbenzenes in solution; however, compounds **1a-c** are too poorly soluble in suitable solvents to permit such tests, and we are currently preparing derivatives with higher solubility. We believe that such compounds can be engineered for new applications in supramolecular chemistry, such as the creation of sponges for the selective sorption of acetylene itself.[17]

Acknowledgments.

We are grateful to the Natural Sciences and Engineering Research Council of Canada, the Ministère de l'Éducation du Québec, the Canada Foundation for Innovation, the Canada Research Chairs Program, and Université de Montréal for financial support. We also thank Dr. Thierry Maris for his help in analyzing crystallographic data.

Supporting Information Available.

Detailed experimental procedures, spectroscopic data for all new compounds, and additional crystallographic and computational details. This material is available free of charge via the Internet at http://pubs.acs.org.

Notes and References

† Université de Montréal.

‡ Fellow of the Natural Sciences and Engineering Research Council of Canada (2003-2009).

§ École Polytechnique.

1. Zhi, L.; Müllen, K. *J. Mater. Chem.* **2008**, *18*, 1472-1484. Bauer, R. E.; Grimsdale, A. C.; Müllen, K. *Top. Curr. Chem.* **2005**, *245*, 253-286. Watson, M. D.; Fechtenkötter, A.; Müllen, K. *Chem. Rev.* **2001**, *101*, 1267-1300. Wiesler, U.-M.; Weil, T.; Müllen, K. *Top. Curr. Chem.* **2001**, *212*, 1-40. Berresheim, A. J.; Müller, M.; Müllen, K. *Chem. Rev.* **1999**, *99*, 1747-1785.

2. For recent reviews of the subject of C-H···π interactions, see: Tsuzuki, S.; Fujii, A. *Phys. Chem. Chem. Phys.* **2008**, *10*, 2584-2594. Nishio, M. *CrystEngComm* **2004**, *6*, 130-158.

3. A database related to C-H···π interactions, maintained by Professor Motohiro Nishio, is available via the Internet at http://www.tim.hi-ho.ne.jp/dionisio.

4. Gagnon, E.; Maris, T.; Arseneault, P.-M.; Maly, K. E.; Wuest, J. D. *Cryst. Growth Des.* **2009**, in press (DOI: 10.1021/cg9010746).

5. Lutz, M.; Spek, A. L.; Bonnet, S.; Klein Gebbink, R. J. M.; van Koten, G., as communicated in 2006 to the Cambridge Crystallographic Data Centre (CCDC 609800, Refcode: HPHBNZ03).

6. Nangia, A.; Desiraju, G. R. *Top. Curr. Chem.* **1998**, *198*, 57-95. Desiraju, G. R. *Angew. Chem., Int. Ed.* **1995**, *34*, 2311-2327.

7. See the Supporting Information for details.

8. Only the structure of the major component of the disordered model is described in detail.[7]

9. Maly, K. E.; Gagnon, E.; Maris, T.; Wuest, J. D. *J. Am. Chem. Soc.* **2007**, *129*, 4306-4322.

10. Kobayashi, K.; Sato, A.; Sakamoto, S.; Yamaguchi, K. *J. Am. Chem. Soc.* **2003**, *125*, 3035-3045. Kobayashi, K.; Shirasaka, T.; Horn, E.; Furukawa, N. *Tetrahedron Lett.* **2000**, *41*, 89-93. Kobayashi, K.; Shirasaka, T.; Sato, A.; Horn, E.; Furukawa, N. *Angew. Chem., Int. Ed.* **1999**, *38*, 3483-3486.

11. The values correspond to the H···centroid distance and the C-H···centroid angle, respectively.

12. The values correspond to 1) the distance from the hydrogen atom to the midpoint of the triple bond and 2) the C-H···midpoint angle, respectively.

13. The composition was determined by X-ray diffraction.

14. For a related crystallographic and theoretical study of the co-crystallization of benzene and acetylene, see: Boese, R.; Clark, T.; Gavezzotti, A. *Helv. Chim. Acta* **2003**, *86*, 1085-1100.

15. Steiner, T. *Chem. Commun.* **1994**, 101-102.

16. Singh, N. J.; Min, S. K.; Kim, D. Y.; Kim, K. S. *J. Chem. Theory Comput.* **2009**, *5*, 515-529. Shibasaki, K.; Fujii, A.; Mikami, N.; Tsuzuki, S. *J. Phys. Chem. A* **2007**, *111*, 753-758. Tekin, A.; Jansen, G. *Phys. Chem. Chem. Phys.* **2007**, *9*, 1680-1687. Sundararajan, K.; Viswanathan, K. S.; Kulkarni, A. D.; Gadre, S. R. *J. Mol. Struct.* **2002**, *613*, 209-222. Takahashi, O.; Kohno, Y.; Iwasaki, S.; Saito, K.; Iwaoka, M.; Tomoda, S.; Umezawa, Y.; Tsuboyama, S.; Nishio, M. *Bull. Chem. Soc. Jpn.* **2001**, *74*, 2421-2430. Jemmis, E. D.; Subramanian, G.; Nowek, A.; Gora, R. W.; Sullivan, R. H.; Leszczynski, J. *J. Mol. Struct.* **2000**, *556*, 315-320. Novoa, J. J.; Mota, F. *Chem. Phys. Lett.* **2000**, *318*, 345-354.

17. For recent related work, see: Xiang, S.; Zhou, W.; Gallegos, J. M.; Liu, Y.; Chen, B. *J. Am. Chem. Soc.* **2009**, *131*, 12415-12419.

5.6 Conclusions et projets connexes

Les résultats rapportés dans l'article 3 (section 5.3) démontrent que le cycle aromatique central de l'hexaphénylbenzène et de ses dérivés est un excellent accepteur de liens C-H···π. Cette caractéristique a été exploitée pour créer des assemblages supramoléculaires en introduisant dans le même environnement des groupements éthynyles possédant des liens C(*sp*)-H, qui sont de meilleurs donneurs que les liens C(sp^2)-H. Ainsi, les molécules **5.3** et **5.4** peuvent être qualifiées de tectons puisqu'elles en possèdent les qualités requises : les ponts hydrogène C-H···π sont les interactions non-covalentes dominantes des assemblages obtenus et les composés **5.3** et **5.4** établissent des réseaux supramoléculaires selon des motifs prévisibles. En effet, la formation de liens C-H···π impliquant un lien C(*sp*)-H et le cycle aromatique central de l'hexaphénylbenzène se fait de façon sélective, respectant les règles d'Etter. Finalement, nos calculs théoriques suggèrent que l'hexaphénylbenzène pourrait se lier à une molécule d'acétylène efficacement.

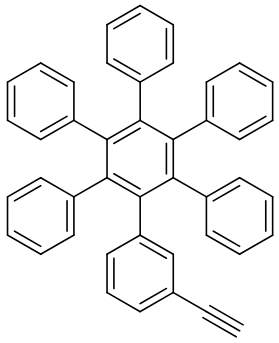

5.3

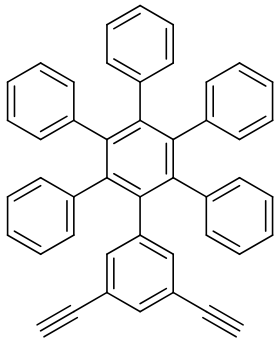

5.4

Suite à l'obtention de ces résultats, plusieurs projets connexes sont envisageables. Premièrement, on peut imaginer qu'une molécule d'acétylène serait fortement complexée par un système judicieusement conçu, tel que le composé **5.5** (Figure 5.7). Le design de ce composé repose sur deux éléments-clés dus à des conformations privilégiées. Premièrement, on note l'obligation des cycles aromatiques périphériques des hexaarylbenzènes à être (quasi)-perpendiculaires au cycle aromatique central à cause des interactions stériques. Deuxièmement, les 2,2';6',6''-terpyridines ont une forte tendance à adopter une conformation transoïde et coplanaire lorsqu'elles ne

sont pas complexées à des métaux.[17] Globalement, ces deux conditions conformationnelles placeraient le récepteur dans une position idéale pour accueillir des molécules invitées. La petite poche hydrophobe créée posséderait un fort potentiel d'association avec l'acétylène via la formation de deux liens C-H···π. La cavité formée par la superposition des deux unités hexaarylbenzène pourrait aussi accommoder d'autres petites molécules, telles que CO_2 ou N_2. Ainsi, il serait intéressant de vérifier la sélectivité de l'inclusion de divers gaz par ce récepteur. Un modèle du complexe **5.5** · C_2H_2 est illustré à la Figure 5.7.

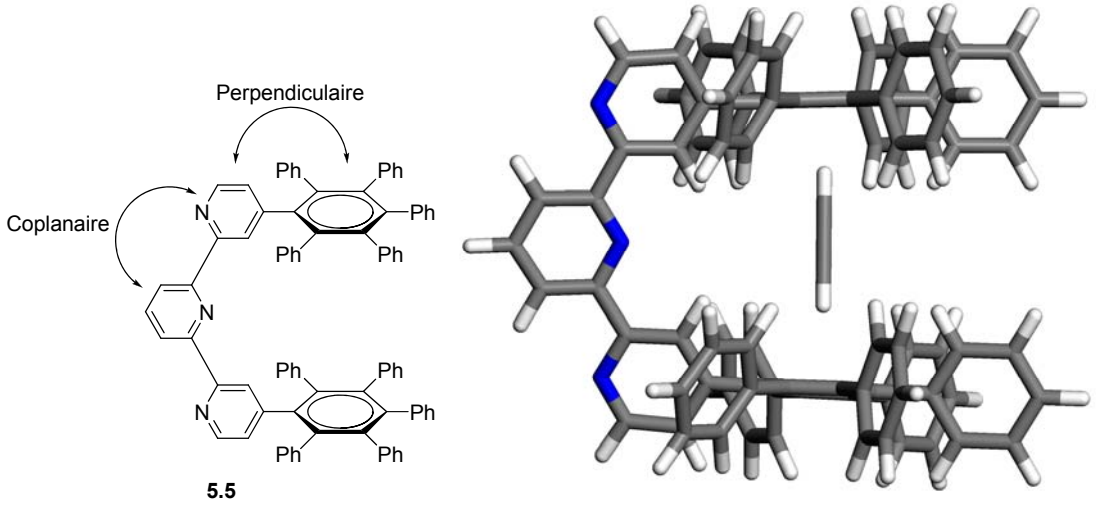

Figure 5.7. Structure de la molécule hôte **5.5** (gauche) et modèle du complexe **5.5** · acétylène (droite). Les atomes sont identifiés par la couleur comme suit : carbone, gris; azote, bleu; hydrogène, blanc.

Un second projet à aborder serait l'étude des interactions C-H···π dans un système dynamique. Plus particulièrement, on s'intéresserait à la formation de ces liens en solution. Toutefois, la molécule d'hexaphénylbenzène est trop peu soluble pour étudier des phénomènes d'association par résonance magnétique nucléaire ^{1}H.[18] De plus, les interactions de type C-H···π étant de nature majoritairement dispersives,[19] il s'ensuit que n'importe quel solvant utilisé pourrait entrer en compétition pour interagir avec l'hexaphénylbenzène. Il serait donc préférable d'élaborer de nouveaux dérivés de

[17] Fallahpour, R.-A.; Neuburger, M.; Zehnder, M. *New J. Chem.* **1999**, *23*, 53-61.
[18] Nous avons tenté l'expérience avec l'hexaphénylbenzène et l'hexakis(4-*t*-butylphényl)benzène dans différents solvants organiques.
[19] Nishio, M. *CrystEngComm* **2004**, *6*, 130-158.

l'hexaphénylbenzène solubles en phase aqueuse afin de favoriser une complexation grâce à l'effet hydrophobe. On propose d'ajouter des groupements reconnus pour augmenter la solubilité en phase aqueuse, tels que des chaînes polyéthylène glycol (**5.6**), des phénolates (**5.7**) ou encore des acides sulfoniques (**5.8)**, tous illustrés à la Figure 5.8. De plus, si une association par lien C-H···π se produit, il serait intéressant de comparer la solubilité de l'acétylène en solution aqueuse, avec et sans les composés **5.6-5.8**.

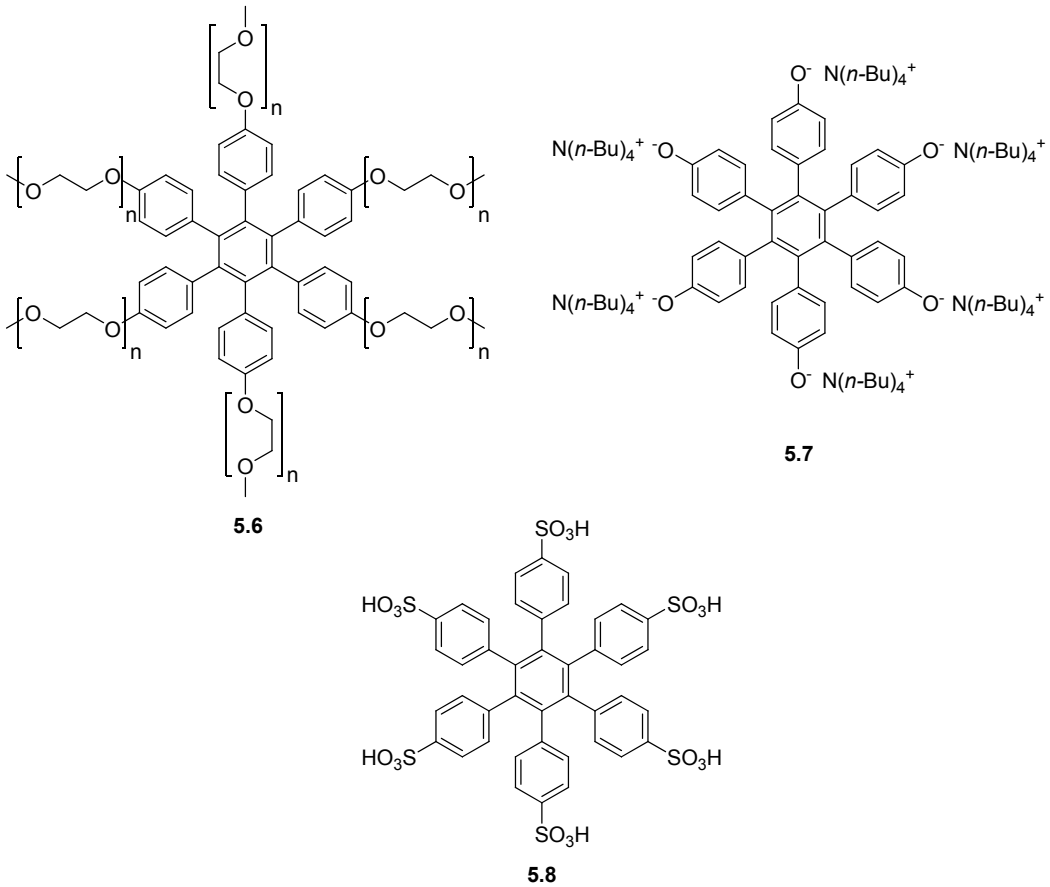

Figure 5.8. Composés solubles en phase aqueuse, permettant une analyse par RMN ^{1}H d'une complexation avec un groupement acétylène.

Finalement, il est bien connu que les systèmes-π peuvent interagir avec des cations métalliques ou ammonium (Figure 1.4).[20] Il serait donc intéressant de vérifier si le benzène central de l'hexaphénylbenzène pourrait participer dans ces types d'interactions non-covalentes. Des travaux dans cette direction ont été rapportés

[20] Ma, J. C.; Dougherty, D. A. *Chem. Rev.* **1997**, *97*, 1303-1324.

récemment. L'introduction d'un éther-couronne autour d'une des faces de l'hexaphénylbenzène permet de créer le récepteur **5.9** (Figure 5.9). Lorsque ce composé est cristallisé en présence de KBF_4, l'atome de potassium est complexé à la fois par des liens ions-dipôle avec l'éther-couronne et par la formation d'un lien cation-π.[21] Ainsi, les auteurs affirment que la complexation du cation potassium dépend fortement de la présence de l'éther-couronne.

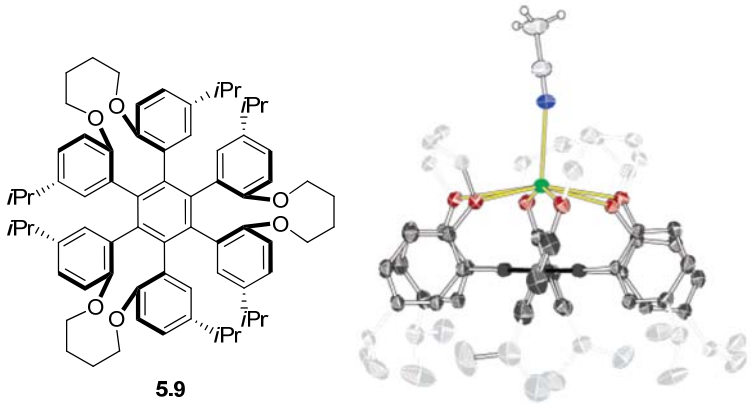

5.9

Figure 5.9. Structure moléculaire de l'hexaphénylbenzène/éther-couronne **5.9** (gauche) et structure par diffraction des rayons-X du complexe **5.9** • KBF_4 • MeCN. L'ion BF_4^- est omis pour des raisons de clarté. Les atomes sont identifiés par la couleur comme suit : carbone, gris et noir; azote, bleu; potassium, vert; oxygène, rouge.

Toutefois, nous croyons que l'éther-couronne n'est pas nécessaire pour former efficacement ce type de complexe. En effet, au cours de la caractérisation de nos dérivés de l'hexaphénylbenzène, nous avons remarqué la présence en spectrométrie de masse de plusieurs adduits différents. Notamment, les adduits d'ammonium, $[M+NH_4]^+$, et de sodium, $[M+Na]^+$, étaient souvent plus abondants que l'ion moléculaire protoné, $[M+H]^+$. Ceci laisse présager que l'hexaphénylbenzène lui-même pourrait interagir fortement avec des cations métalliques ou ammonium.

On propose donc un troisième projet connexe, visant à exploiter les liaisons cation···π. Pour étudier le potentiel de l'hexaphénylbenzène comme partenaire dans ces interactions, deux composés sont proposés : l'amine **5.13** et l'acide carboxylique **5.17** (Schémas 5.1 et 5.2). Leurs synthèses sont rapides et les réactions proposées sont bien

[21] Shukla, R.; Lindeman, S. V.; Rathore, R. *J. Am. Chem. Soc.* **2006**, *128*, 5328-5329.

documentées. De plus, à partir des composés **5.13** et **5.17**, une grande variété de sels d'ammonium (**5.14**, Schéma 5.1) et de carboxylates (**5.18**, Schéma 5.2) seraient disponibles, permettant de cribler une grande quantité de composés en peu de temps.

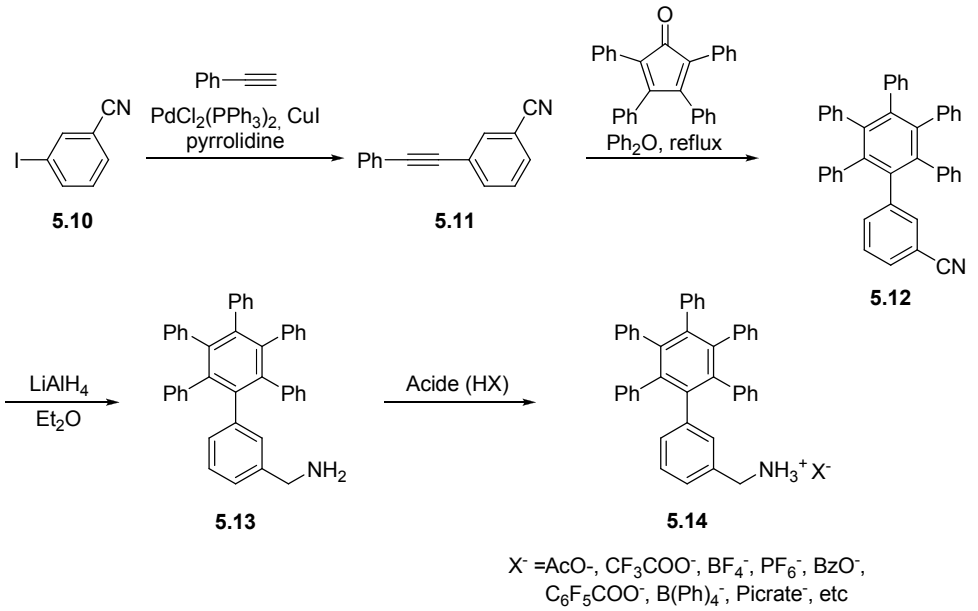

Schéma 5.1. Préparation proposée des sels d'ammonium **5.14**. Ces composés auraient le potentiel de s'associer de façon analogue au composé **5.3**, via la formation d'interactions ammonium···π.

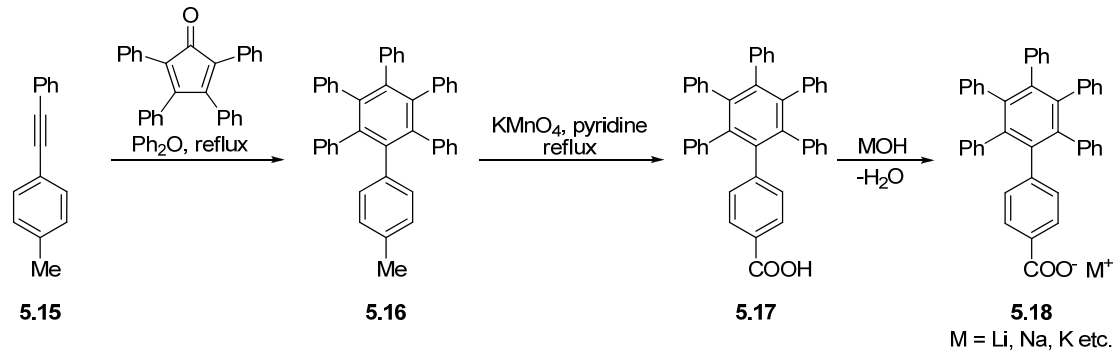

Schéma 5.2. Préparation proposée des carboxylates **5.18**. Ces composés auraient le potentiel de s'associer via la formation d'interactions M^+···π.

Ces trois projets soulignent la versatilité des interactions dans lesquelles un cycle aromatique peut prendre part. Ils exploitent l'encombrement stérique autour d'un cycle aromatique pour diriger une molécule invitée vers celui-ci, afin de former une interaction directionnelle. On croit que cette approche pourrait trouver une application plus générale dans la chimie des matériaux. Par exemple, le remplacement d'un groupement *p*-phénylène (tel que dans le composé **5.19**) par un groupement durène

(**5.20**) est connu pour ajouter beaucoup d'encombrement stérique et du fait même, limiter la rotation des groupements en position 1,4. Toutefois, il est aussi possible que des interactions différentes aient lieu. Ainsi, on peut imaginer des polymères contenant cette unité, qui interagirait avec des cations en solution ou encore, pourrait agir de filtre échangeur d'ion.

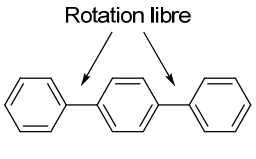

5.19

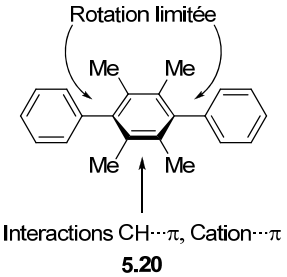

5.20

Alternativement, on peut penser à modifier un hydrocarbone polyaromatique tel que le pyrène, fréquemment utilisé comme sonde fluorescente, pour favoriser les interactions avec sa surface π. En installant plusieurs groupements phényles sur sa périphérie (**5.21**), on aurait la possibilité de modifier les propriétés de fluorescence, mais surtout les types de molécules pouvant être détectés. Les interactions de type π···π seraient défavorisées avec des molécules moindrement volumineuses, au profit des autres interactions présentées dans ce chapitre. Ces idées additionnelles démontrent bien la transposition que nous pouvons faire entre nos résultats, ciblés sur l'étude de l'hexaphénylbenzène, et la chimie des matériaux en général.

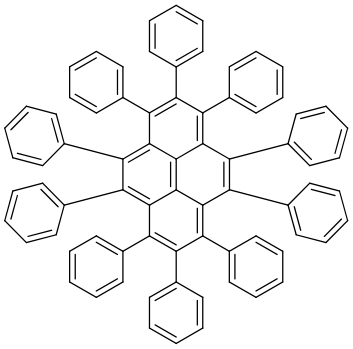

5.21

Chapitre 6

Inhibition des interactions C–H···π dans les hexaphénylbenzènes

6.1 Introduction

Comme nous l'avons vu au chapitre précédent, l'hexaphénylbenzène (**6.1**) et ses dérivés établissent des interactions C-H···π entre eux à l'état cristallin. On note en particulier le rôle du cycle aromatique central: malgré l'encombrement stérique autour de celui-ci, il agit constamment comme accepteur de liens C-H···π. Cette observation a mené au développement des tectons **6.2** et **6.3** (Figure 6.1). Les assemblages supramoléculaires produits par ces derniers démontrent clairement l'importance que peuvent revêtir les interactions C-H···π dans les dérivés de l'hexaphénylbenzène.

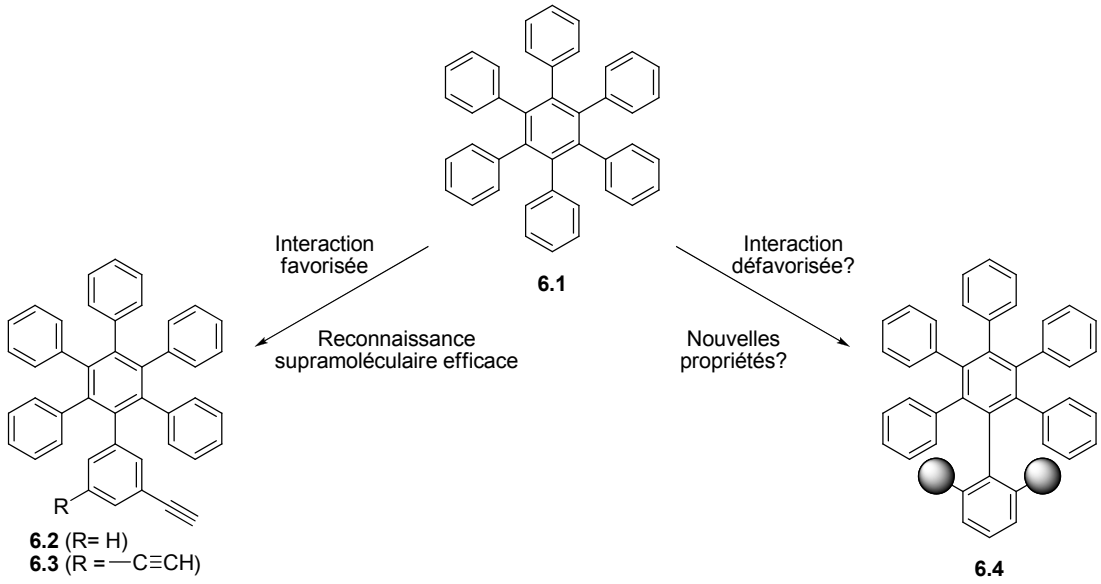

Figure 6.1. À partir de l'hexaphénylbenzène **6.1**, deux projets ont été envisagés. Le premier vise à favoriser les interactions C-H···π et a mené au développement des composés **6.2** et **6.3** dans lesquels on observe des motifs de reconnaissance fiables (gauche). Dans le chapitre présent, on tente de défavoriser ces interactions afin de générer de nouvelles propriétés (droite).

Mais qu'adviendrait-il si nous tentions l'expérience inverse? En éliminant la possibilité de s'associer par des liens C-H···π, seuls des contacts non-directionnels de type C-H···H-C pourraient avoir lieu.[1] En conséquence, l'association de deux molécules judicieusement conçues pourrait n'avoir aucune orientation préférentielle. Afin de défavoriser les interactions C-H···π impliquant le cycle aromatique central de

[1] Steiner, T.; Desiraju, G. R. *Chem. Commun.* **1998**, 891-892.

l'hexaphénylbenzène, nous avons préparé quatre dérivés possédant des groupements alkyles de grosseurs variées à proximité du centre de la molécule (**6.4**, Figure 6.1).

Ce chapitre sera débuté par la présentation de l'article 5, qui contient une analyse détaillée des hexaphénylbenzènes alkylés représentés schématiquement par la molécule **6.4** (section 6.2). Cet article sera suivi d'une discussion sur les applications potentielles de nos découvertes, notamment en vue du développement de nouveaux verres moléculaires (section 6.3) et de matériaux à basse cohésion moléculaire (section 6.4), puis le chapitre sera terminé par une courte conclusion (section 6.5).

6.2 Article 5

Tampering with Molecular Cohesion in Crystals of Hexaphenylbenzenes

Eric Gagnon,[†,1] Shira D. Halperin,[‡] Valérie Métivaud,[†] Kenneth E. Maly,[‡,2] and James D. Wuest[†]

Journal of Organic Chemistry, **2010**, *75*, 399-406

Reproduced with permission from *Journal of Organic Chemistry*
Copyright 2010 American Chemical Society

Abstract

Hexaphenylbenzene (HPB) and analogous compounds have properties of broad utility in science and technology, including conformationally well-defined molecular structures, high thermal stability, high HOMO-LUMO gaps, little self-association, inefficient packing, and high solubilities. Previous structural studies of HPB and its analogues have revealed persistent involvement of the central aromatic ring in strong C-H···π interactions. These interactions can be blocked by adding simple *ortho* alkyl substituents to the peripheral phenyl groups. Comparison of the structures of HPB and a series of *ortho*-substituted derivatives has shown systematic changes in molecular cohesion and packing, as measured by packing indices, densities, solubilities, temperatures of sublimation, melting points, and ratios of H···H, C···H, and C···C contacts. These results illustrate how crystal engineering can guide the search for improved materials by identifying small but telling molecular alterations that thwart established patterns of association.

Introduction

Specialized aromatic compounds have found a niche in modern materials science and molecular electronics.[3] Their properties permit the fabrication of various devices, including light-emitting diodes, photovoltaic cells, field-effect transistors, lasers, sensors, RFID tags, and photorefractive systems. Among the most promising classes of aromatic compounds are acenes such as pentacene (**1**),[4,5] which are notable for high charge-carrier mobilities, and polynuclear aromatics such as hexa-*peri*-hexabenzocoronene (HBC, **2**),[6] which feature large π-surfaces. Unfortunately, compounds **1** and **2** cannot easily be used in thin-film molecular devices without significant structural modification. For example, the use of pentacene (**1**) itself is hampered by its ease of crystallization and by the existence of multiple polymorphic forms with different electronic properties.[7] Moreover, molecular packing in these polymorphs is guided by extensive C-H···π interactions, and the preferred structures have herringbone arrangements with minimal π···π overlap, which are considered

unfavorable for conductivity. To increase orbital overlap in acenes, various strategies have been devised to favor π···π interactions at the expense of C-H···π interactions, such as by adding substituents or by modifying the surfaces on which thin films are grown.[4,5] Similarly, substituents have been attached to the periphery of HBC (**2**) to control the extent of π-stacking, increase solubility, and produce new functional materials.[8,9]

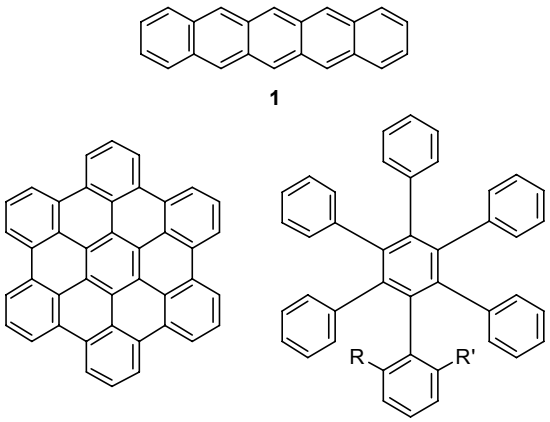

1

2 (HBC)

3a (R = R' = H; HPB)
3b (R = H, R' = Me)
3c (R = R' = Me)
3d (R = R' = Et)
3e (R = R' = *i*-Pr)

These examples show that many compounds with inherently attractive molecular properties, such as pentacene (**1**) and HBC (**2**), cannot achieve their full potential as components of materials without modifications specifically introduced to control packing and cohesion. Of particular value in the cases of compounds **1** and **2** are structural changes designed to alter the importance of C···H contacts (resulting from C-H···π interactions)[10,11] relative to C···C contacts (created by π-stacking). Identifying effective structural alterations requires insights about molecular packing and cohesion best drawn from the field of crystal engineering,[12] which is therefore poised to play a growing role in guiding the search for new functional materials. In particular, crystal engineering can reveal how classes of compounds prefer to crystallize and why those patterns are favored, thereby providing a blueprint for making subtle structural alterations that change how crystallization occurs or even prevent it from happening.[13]

A useful class of compounds related to acenes and polynuclear aromatics is defined by analogues of hexaphenylbenzene (**3a**, HPB), in which multiple contiguous

aryl groups are attached to an aromatic core. Systematic structural studies of HPB (**3a**) and similar compounds have established that they are forced to adopt characteristic non-planar conformations, with large torsional angles between the central and peripheral aromatic rings.[14] The resulting topology is propeller-shaped and toroidal. Its surface is rich in exposed C-H bonds, and access to the π-faces of the constituent aromatic rings is severely restricted. These conformational preferences have the predictable effect of limiting conjugation and disfavoring extensive intermolecular π-π and C-H···π interactions,[14] leading to higher HOMO-LUMO gaps, lower degrees of self-association, less efficient packing, and higher solubilities than observed in planarized analogues such as HBC (**2**). These characteristic properties make derivatives of HPB (**3a**) increasingly useful in various areas of science and technology, particularly when poor molecular cohesion and inefficient packing are beneficial.[14]

Analysis of the Hirshfeld surface derived from the structure of HPB (**3a**) suggests that cohesion is maintained primarily by diffuse H···H contacts, and well-defined directional forces such as C-H···π and π···π interactions are less important.[15-18] Specifically, the ratio of H···H to C···H contacts is 67:32, and C···C contacts are essentially absent. Close examination of C-H···π interactions in the structure of HPB (**3a**) reveals that none of the hindered peripheral phenyl groups serves as an acceptor, but both faces of the central aromatic ring are used in this way (Figure 1a).[14] This is not merely because potential pockets for binding are created above and below the central ring by the characteristic toroidal topology of HPB (**3a**). In fact, a primary driving force for association appears to be the ability of the central ring to act as an acceptor in C-H···π interactions, which can be reinforced by secondary interactions involving the *ortho* hydrogen atoms of the peripheral phenyl groups. This phenomenon is illustrated by the binding of a terminal acetylene in structure **4** (for clarity, only two of the six equivalent secondary C-H···π interactions are drawn).[19] DFT calculations have established that reinforced C-H···π interactions of this type can be as strong as normal hydrogen bonds, so they can make an important contribution to molecular cohesion.[19]

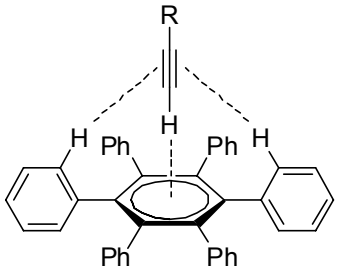

4

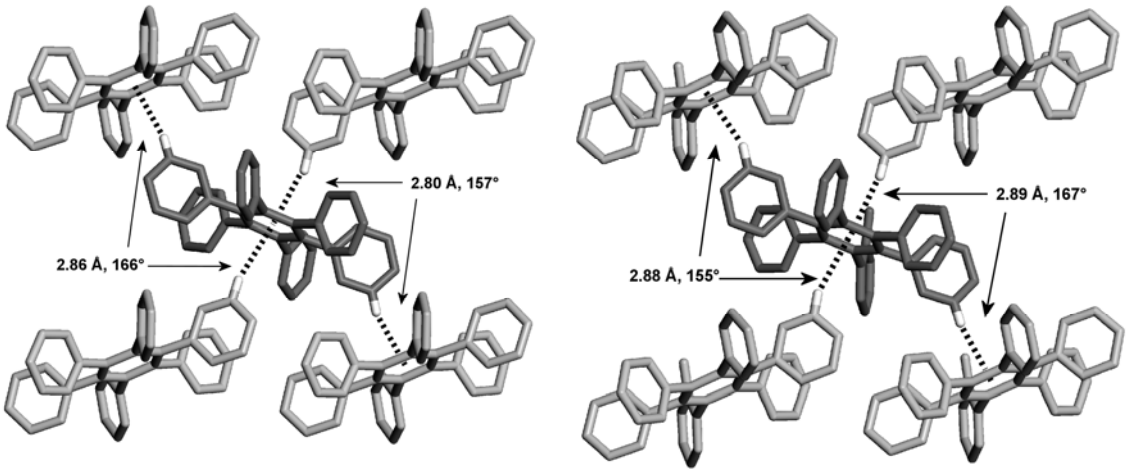

a **b**

Figure 1. (a) View of the structure of crystals of HPB (**3a**) grown from CH_2Cl_2 or CH_2Br_2.[15] (b) View of the structure of crystals of monomethyl derivative **3b** grown from chlorobenzene. Both views show a central molecule (dark gray) and its primary neighbors (light gray). Carbon atoms are shown in gray, hydrogen atoms involved in C-H···π interactions appear in white, and the interactions are represented by broken lines. C-H···$\pi_{centroid}$ distances and angles are indicated.

Detailed understanding of cohesion and packing in the structures of HPB (**3a**) and related compounds allows crystal engineers to devise subtle yet potent structural alterations that can obstruct established preferences. We reasoned that preventing the central aromatic ring of HPB (**3a**) from engaging in reinforced C-H···π interactions would increase the ratio of H···H to C···H contacts and possibly lead to reduced molecular cohesion, increased volatility, and higher solubility. In principle, the C-H···π

interactions of HPB (**3a**) can be blocked by adding suitable *ortho* substituents to the peripheral phenyl groups. In this paper, we describe the syntheses and structures of *ortho*-substituted derivatives **3b-e**. As planned, these compounds show substantial increases in the ratio of H···H to C···H contacts, as well as other properties that suggest decreased molecular cohesion.

Results and Discussion

Synthesis of *ortho*-Substituted Hexaphenylbenzenes 3b-e. The targets were prepared by an established general method for making hexaphenylbenzenes, using Diels-Alder reactions of suitably substituted tetraphenylcyclopentadienones with diphenylacetylenes, followed by extrusion of carbon monoxide (eq. 1).[20] The required substituted diphenylacetylenes **5**[21] and **6**[22] were prepared by reported methods, and known compounds **7**[23] and **8**[24] were made by straightforward new procedures (Scheme 1). Diphenylacetylene **7** was synthesized in 71% yield by Sonogashira coupling of 1,3-diethyl-2-iodobenzene[25] with phenylacetylene, using Pd_2dba_3/PPh_3 and CuI as catalysts.[26] Compound **8** was prepared from 2,6-diisopropylaniline by the following two steps. A one-pot diazotization-iodination developed by Knochel and co-workers[25] provided the known 2-iodo-1,3-diisopropylbenzene (**9**)[24,27] in 57% yield, and then Sonogashira coupling[26] of intermediate **9** with phenylacetylene gave diphenylacetylene **8** in 71% yield. Diphenylacetylenes **5-8** were then allowed to react with tetraphenylcyclopentadienone to generate the desired *ortho*-substituted hexaphenylbenzenes **3b-e** in yields ranging from 52 to 77%. It is noteworthy that the high-temperature Diels-Alder reactions leading to hexaphenylbenzenes **3d** and **3e** were efficient despite very significant steric congestion. The success of these reactions demonstrates the broad scope of the methodology employed, as well as the inherently high thermal stability of hexaphenylbenzenes.

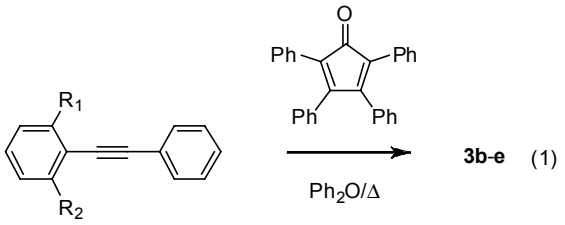

5 (R_1= Me, R_2 = H)
6 (R_1= R_2 = Me)
7 (R_1= R_2 = Et)
8 (R_1= R_2 = *i*-Pr)

Scheme 1

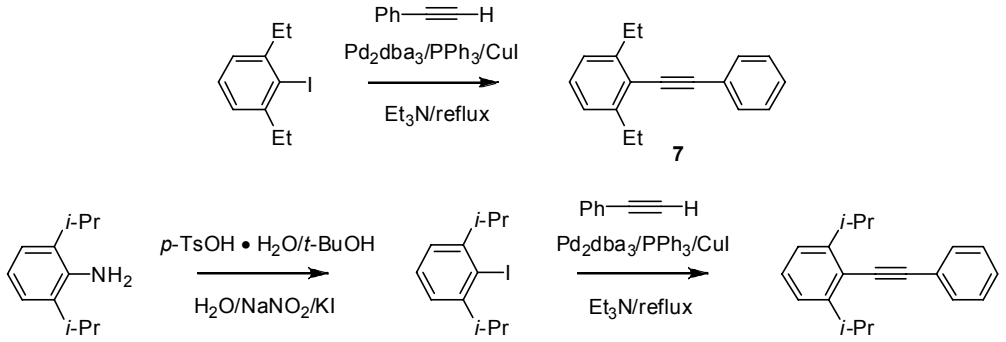

Structure of Crystals of Monomethyl Derivative 3b of HPB (3a). After substantial effort, we found that monomethyl derivative **3b** of HPB (**3a**) could be crystallized by slow evaporation of a solution in chlorobenzene. The resulting crystals proved to belong to the orthorhombic space group $Pna2_1$, and other crystallographic data are summarized in Table 1. The observed structure is essentially identical to that of HPB (**3a**), which has the same space group and closely similar unit cell parameters.[15,28] Comparison of Figures 1a and 1b reveals the striking overall similarity of the two structures. The failure of an added methyl group to alter the structure radically may result in part from inefficiencies in the packing of HPB (**3a**) itself. Its Kitaigorodskii packing index (67.1%)[29,30] and density (1.208 g cm^{-3}) are slightly lower than those of monomethyl derivative **3b** (67.3% and 1.212 g cm^{-3}), suggesting that the substituent simply fits into previously unoccupied voids, without disrupting the original lattice appreciably. Although the added methyl group does not eliminate C-H···π interactions, it makes them weaker, and the two C-H···$\pi_{centroid}$ distances rise from 2.80 and 2.85 Å in HPB (**3a**) to 2.88 and 2.89 Å in substituted derivative **3b**.[31,32]

Table 1. Crystallographic Data for *ortho*-Substituted Hexaphenylbenzenes **3b-e.**

compound	**3b**	**3c**	**3d**	**3e**
formula	$C_{43}H_{32}$	$C_{44}H_{34}$	$C_{46}H_{38}$	$C_{48}H_{42}$
crystal system	orthorhombic	orthorhombic	monoclinic	monoclinic
space group	*Pna*2$_1$	*Pna*2$_1$	*P*2$_1$/*n*	*P*2$_1$
a (Å)	12.3269(3)	12.3809(4)	12.3918(2)	12.8715(2)
b (Å)	11.6835(3)	11.7357(3)	11.7268(2)	10.8218(2)
c (Å)	20.8753(5)	21.3061(5)	23.2394(5)	13.1831(2)
α (Å)	90	90	90	90
β (Å)	90	90	98.217(1)	102.061(1)
γ (Å)	90	90	90	90
V (Å^3)	3006.49(13)	3095.74(15)	3342.39(11)	1795.78(5)
Z	4	4	4	2
ρ_{calcd} (g cm^{-3})	1.212	1.207	1.174	1.144
T (K)	150	150	150	150
μ (mm^{-1})	0.517	0.514	0.498	0.484
R_1, $I > 2\sigma$ (%)	4.85	6.42	5.29	3.22
R_1, *all data* (%)	4.99	6.49	5.54	3.23
ωR_2, $I > 2\sigma$ (%)	14.57	17.20	14.60	8.45
ωR_2, *all data* (%)	14.75	17.32	14.85	8.46
measured reflections	46644	49197	55091	29219
independent reflections	5275	5511	5529	5704
observed reflections, $I > 2\sigma(I)$	5078	5426	5193	5685

Structure of Crystals of Dimethyl Derivative 3c of HPB (3a). Cooling a hot saturated solution of compound **3c** in toluene gave colorless crystals belonging to the orthorhombic space group *Pna*2$_1$, as previously observed for both HPB (**3a**) and monomethyl derivative **3b**. Additional crystallographic data are presented in Table 1, and the structure is shown in Figure 2a. The unit cell parameters are very similar to those of analogues **3a** and **3b**, with a slight increase in the lengths of the axes to accommodate the two methyl groups. In addition, the packing index (67.5%) and density (1.207 g cm^{-3}) are also close to those observed for compounds **3a** and **3b**. Molecular packing in the structure of dimethyl derivative **3c** (Figure 2a) resembles that of less-substituted analogues **3a** and **3b** (Figure 1). However, addition of a second

methyl group allows the central aromatic ring to accept only one C-H···π interaction, instead of one on each face. In addition, the C-H···$\pi_{centroid}$ distance in the surviving interaction rises to 2.98 Å, whereas the average values in HPB (**3a**) and monomethyl derivative **3b** are 2.82 and 2.88 Å, respectively. These results 1) confirm that *ortho* substituents can alter the association of hexaphenylbenzenes by interfering with normal C-H···π interactions and 2) suggest that cohesion can be reduced to even lower levels by introducing larger *ortho* substituents.

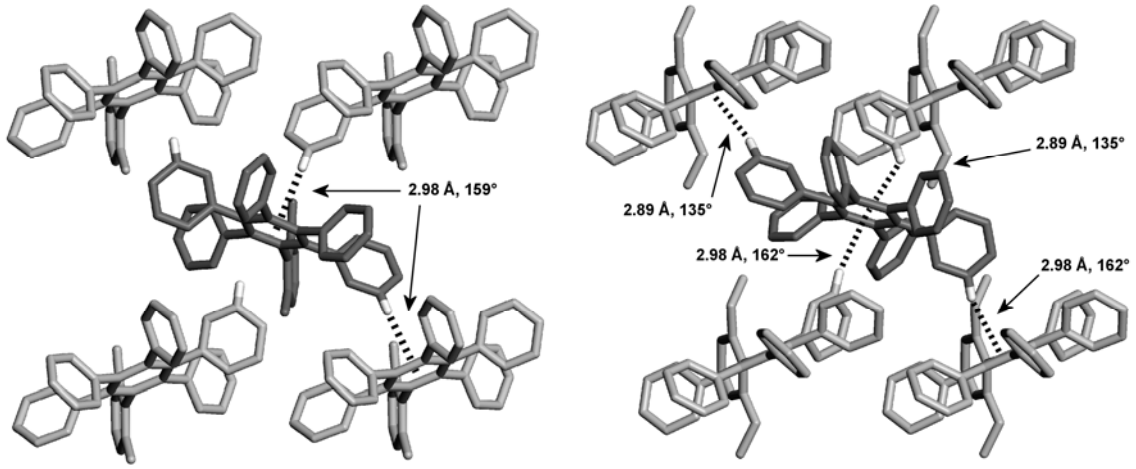

a **b**

Figure 2. (a) View of the structure of crystals of dimethyl derivative **3c** grown from toluene. (b) View of the structure of crystals of diethyl derivative **3d** grown from toluene/hexanes. Both views show a central molecule (dark gray) and its primary neighbors (light gray). Carbon atoms are shown in gray, hydrogen atoms involved in C-H···π interactions appear in white, and the interactions are represented by broken lines. C-H···$\pi_{centroid}$ distances and angles are indicated.

Structure of Crystals of Diethyl Derivative 3d of HPB (3a). Hexaphenylbenzene **3d**, with two added ethyl groups, was significantly more soluble in typical organic solvents than less-substituted analogues **3a-c**. Crystals grown by cooling a hot saturated solution in toluene/hexanes were found to belong to the monoclinic space group $P2_1/n$, and additional crystallographic data are provided in Table 1. The introduction of two ethyl groups had the desired effect of lowering both the packing index (66.3%) and density (1.174 g cm^{-3}) relative to the values observed for analogues **3a-c**. Despite these differences, molecular organization in the structure remains largely

unaltered (Figure 2b). The space group is different from those of the structures of less-substituted analogues **3a-c**, but the unit cell dimensions are still very similar, and the β angle remains close to 90° (Table 1). Comparison of the unit cell parameters observed for the structures of hexaphenylbenzenes **3b-d** (Table 1) shows nearly monotonic evolution in response to the increasing size of the *ortho* substituents. Despite evidence of poorer cohesion in the structure of diethyl derivative **3d**, both faces of the central aromatic ring engage in C-H···π interactions, with an average C-H···$\pi_{centroid}$ distance of 2.94 Å. The average distance is significantly longer than those observed in the crystal structures of HPB (**3a**) and monomethyl derivative **3b** (2.82 Å and 2.88 Å, respectively), but slightly shorter than that found in dimethyl derivative **3c** (2.98 Å).

Structure of Crystals of Diisopropyl Derivative 3e of HPB (3a). Like diethyl analogue **3d**, diisopropyl derivative **3e** showed higher solubility than less-substituted hexaphenylbenzenes **3a-c**. Crystals grown from toluene/hexanes proved to belong to the monoclinic space group $P2_1$, and additional crystallographic data are presented in Table 1. As expected, further decreases are observed in the packing index (65.1%) and density (1.144 g cm^{-3}). Moreover, the bulky substituents induce a major change in packing, and the consistent pattern observed in compounds **3a-d** is no longer favored by analogue **3e** (Figure 3). Only one face of the central aromatic ring participates in a C-H···π interaction, and the C-H···$\pi_{centroid}$ distance is 2.76 Å, the shortest observed in the series of compounds **3a-e**. The unexpected observation of the shortest C-H···$\pi_{centroid}$ distance in the most hindered derivative (**3e**) of HPB underscores the special difficulty of engineering predictable molecular crystals when no strong directional interactions are present. However, it is important to note that the unusually short contact appears to come at the cost of foregoing any C-H···π interaction involving the other face of the central ring. Indeed, no C-H···π contact involving the second face is shorter than 5.06 Å, and an empty pocket with a volume of approximately 13 $Å^3$ lies directly above the face.[33]

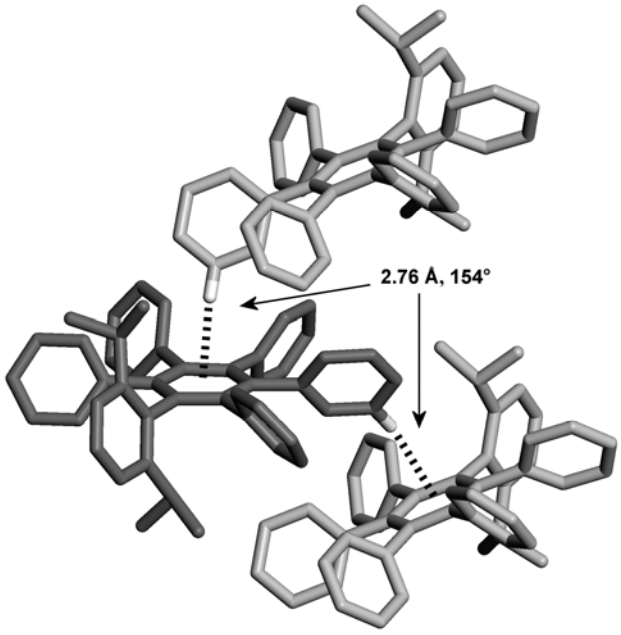

Figure 3. View of the structure of crystals of diisopropyl derivative **3e** grown from toluene/hexanes, showing a central molecule (dark gray) and its principal neighbors (light gray). Carbon atoms are shown in gray, hydrogen atoms involved in C-H···π interactions appear in white, and the interactions are represented by broken lines. C-H···$\pi_{centroid}$ distances and angles are indicated.

Comparison of Structural Features Exhibited by Hexaphenylbenzenes 3a-e. Analysis of the structures of compounds **3a-e** confirms that the central aromatic ring of hexaphenylbenzenes is strongly predisposed to engage in intermolecular C-H···π interactions. However, the number and strength of these interactions can be controlled rationally by the simple expedient of placing alkyl groups at the *ortho* positions of a single peripheral phenyl group. As planned, adding substituents of increasing size reduces the efficiency of packing, as demonstrated by progressively lower packing indices, lower densities, and longer average C-H···$\pi_{centroid}$ distances. When the substituents reach a critical size, the characteristic packing observed in HPB (**3a**) and simple derivatives can no longer be sustained.

The series of compounds **3a-e** is designed to show increasing resistance to the formation of intermolecular C-H···π interactions, so the ratio of H···H to C···H contacts should increase systematically. To test this hypothesis, we used standard analyses of

Hirshfeld surfaces to decipher and quantify intermolecular contacts in the structures of hexaphenylbenzenes **3a-e** (Figure 4).[16-18] These analyses confirm that progressively larger *ortho* substituents cause a monotonic increase in H···H contacts at the expense of C···H and C···C contacts. HPB (**3a**) itself has an impressively high ratio of H···H to C···H contacts (67:32), but the value reaches an even higher level in diisopropyl derivative **3e** (83:17).

It is remarkable that the cohesion of compounds with largely aromatic surfaces can be so thoroughly dominated by diffuse H···H contacts. The growing utility of hexaphenylbenzenes in science and technology is based in part on properties associated with poor molecular cohesion, such as inefficient packing and high solubility. Our results suggest that these valuable properties can be enhanced by astute structural alterations, without simultaneously changing other useful features of hexaphenylbenzenes, such as their well-defined topologies and high HOMO-LUMO gaps.

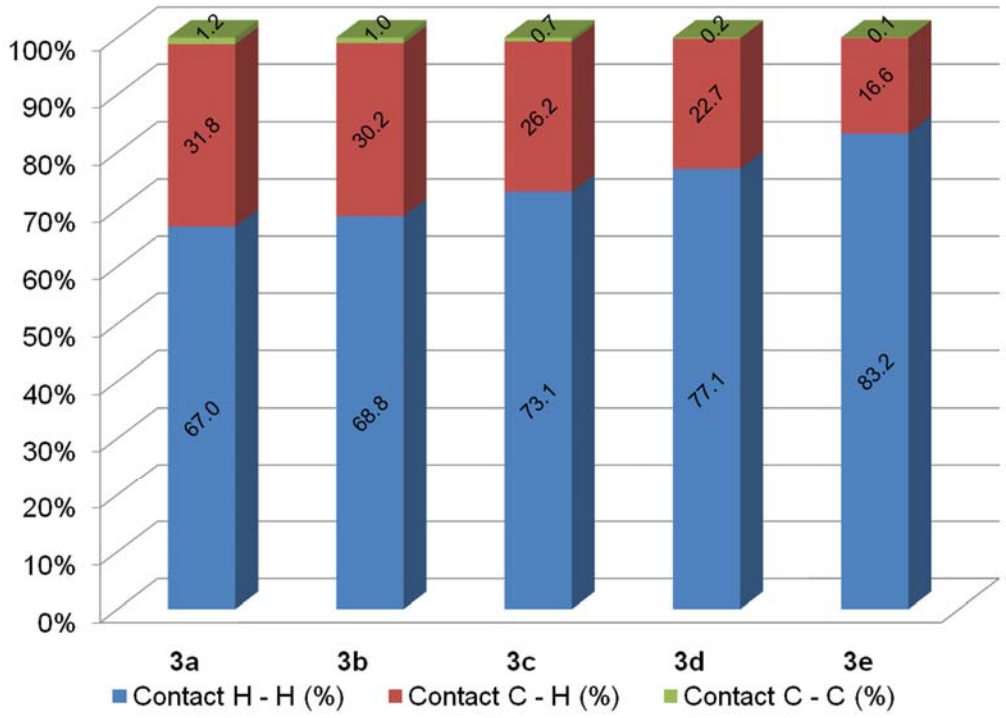

Figure 4. Bar graph showing the nature of intermolecular contacts in crystals of hexaphenylbenzenes **3a-e**, as determined by analyses of Hirshfeld surfaces.

Thermal Analyses of Hexaphenylbenzenes 3a-e. Thermogravimetric analyses of crystalline samples of hexaphenylbenzenes **3a-e** demonstrated that all five compounds have high thermal stability (Figure 5). Heating the samples above 250 °C led to a 100% weight loss due to complete sublimation, as confirmed visually. It is noteworthy that the temperatures at which sublimation begins decrease as the size of the *ortho* substituents increases. This observation is consistent with the notion that the substituents decrease overall molecular cohesion by increasing diffuse H···H contacts at the expense of directional C···H contacts. In the case of diisopropyl derivative **3e**, subsequent loss of weight is less rapid than in the cases of analogues **3a-d**, possibly because their packing is markedly different.

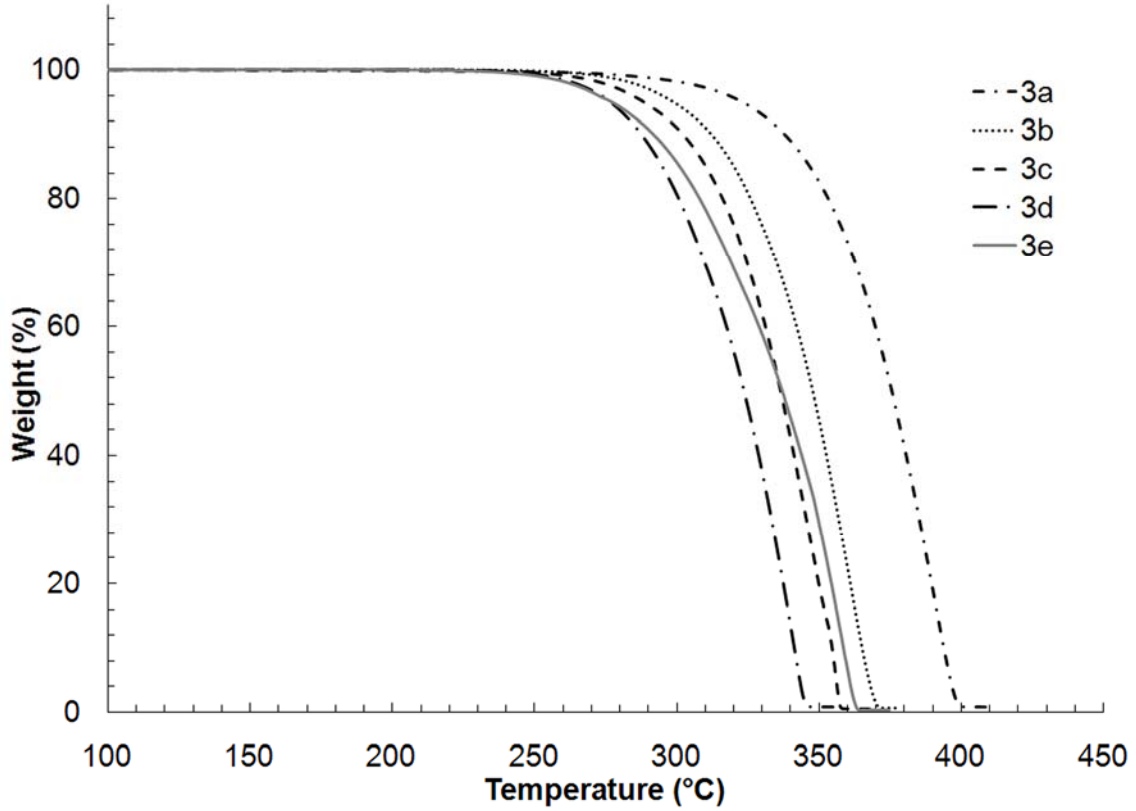

Figure 5. Thermogravimetric analyses of crystalline samples of hexaphenylbenzenes **3a-e**, carried out under N_2 at a rate of heating of 10 °C/min.

Hexaphenylbenzenes **3a-e** also show systematic differences in their melting points, which tend to decrease as the *ortho* substituents increase in size. HPB (**3a**) is reported to melt at 454-456 °C,[34] and monomethyl derivative **3b** also melts above 400

°C; however, dimethyl, diethyl, and diisopropyl derivatives **3c-e** melt at 364-365 °C, 282-283 °C, and 285-287 °C, respectively. Enthalpies of sublimation and lattice energies are directly related,[35] but melting points do not provide a reliable measure of molecular cohesion; nevertheless, the observed values are consistent with the notion that *ortho* substituents reduce cohesion as they increase in size.

Conclusions

A traditional pursuit of crystal engineers is the systematic structural analysis of series of related compounds to discern characteristic patterns of crystallization, which then allow the behavior of other compounds to be predicted. An exciting new thrust in crystal engineering is to use accumulated structural knowledge in a contrary way, by identifying small but telling molecular alterations that can foil established patterns of association, thereby preventing crystallization or forcing it to occur in different ways. We have tested the power of this strategy by examining the representative case of hexaphenylbenzenes, which have properties of broad utility in science and technology, including conformationally well-defined molecular structures, high thermal stability, high HOMO-LUMO gaps, low degrees of self-association, inefficient packing, and high solubilities.

Previous structural studies of hexaphenylbenzene (**3a**) and related compounds have revealed persistent involvement of the central aromatic ring in strong C-H···π interactions.[14,19] In principle, these key cohesive forces can be blocked by adding simple *ortho* substituents to the peripheral phenyl groups. Comparison of the structures of HPB (**3a**) and *ortho*-substituted derivatives **3b-e** has shown systematic changes in molecular cohesion and packing, as measured by packing indices, densities, solubilities, temperatures of sublimation, melting points, and ratios of H···H, C···H, and C···C contacts. As planned, adding *ortho* substituents to hexaphenylbenzene (**3a**) has the beneficial effect of altering molecular cohesion without necessarily changing other properties of value.

Our work has focused on the particular case of hexaphenylbenzenes, but it illustrates a potentially general strategy for using principles of crystal engineering to guide the search for improved molecular materials. At the core of this strategy is the ability to control association by making astute molecular alterations based rationally on systematic crystallographic analyses.

Experimental Section

2,6-Diisopropylaniline was purified by distillation from CaH_2 prior to use. 2-Methyl-(1-phenylethynyl)benzene (**5**),[21] 1,3-dimethyl-2-(phenylethynyl)benzene (**6**),[22] tetraphenylcyclopentadienone,[36] and 1,3-diethyl-2-iodobenzene[25] were prepared according to reported procedures. Anhydrous and oxygen-free solvents were obtained by passage through columns packed with activated alumina and supported copper catalyst (Glass Contour, Irvine, CA). All other reagents and solvents were purchased from commercial sources and used without further purification unless otherwise indicated.

In studies of single crystals by X-ray diffraction, data were collected at 150 K using a Bruker Microstar diffractometer with Cu Kα radiation. The structures were solved by direct methods using SHELXS-97 and refined with SHELXL-97.[37,38] Non-hydrogen atoms were refined anisotropically, whereas hydrogen atoms were placed in ideal positions and refined as riding atoms. In all structural studies, calculated X-ray powder diffraction patterns closely matched those obtained experimentally by analysis of bulk crystalline samples.[39]

1,3-Diethyl-2-(phenylethynyl)benzene (7).[23] Pd_2dba_3 (0.352 g, 0.384 mmol), CuI (0.073 g, 0.38 mmol), and PPh_3 (0.403 g, 1.54 mmol) were combined under N_2. Triethylamine (10 mL) was added, followed by 1,3-diethyl-2-iodobenzene (1.00 g, 3.84 mmol) and phenylacetylene (0.84 mL, 0.78 g, 7.6 mmol), and a stream of N_2 was bubbled through the mixture for 10 min. The mixture was heated at reflux for 18 h under N_2 and then allowed to cool to 25 °C. Removal of volatiles by evaporation under

reduced pressure left a dark residue, which was dissolved in CH_2Cl_2 (75 mL). The solution was washed with 1 N aqueous HCl, saturated aqueous $NaHCO_3$, and brine. The organic phase was dried with anhydrous $MgSO_4$ and filtered through a small pad of silica gel, using CH_2Cl_2 as eluent. Removal of volatiles from the eluent by evaporation under reduced pressure left a residue, which was purified by flash chromatography (silica gel, hexanes) to give 1,3-diethyl-2-(phenylethynyl)benzene (**7**; 0.64 g, 2.7 mmol, 71%) as a colorless liquid: ^{1}H NMR ($CDCl_3$, 400 MHz) δ 7.57-7.53 (m, 2H), 7.41-7.31 (m, 3H), 7.23 (AK_2 system,[40] 1H, ^3J = 7.6 Hz), 7.11 (AK_2 system,[40] 2H, ^3J = 7.6 Hz), 2.92 (q, 4H, ^3J = 7.6 Hz), 1.33 (t, 6H, ^3J = 7.6 Hz); ^{13}C NMR ($CDCl_3$, 100 MHz) δ 146.7, 131.5, 128.5, 128.4, 128.2, 125.5, 124.1, 121.6, 97.0, 86.8, 28.3, 15.0; HRMS (APCI-TOF) calcd for $[C_{18}H_{18} + H]^+$ *m/e* 235.14812, found 235.14768.

2-Iodo-1,3-diisopropylbenzene (9).[24,27] 2,6-Diisopropylaniline (15.1 mL, 14.2 g, 80.1 mmol) was added to a suspension of *p*-TsOH • H_2O (68.5 g, 360 mmol) in a mixture of *t*-BuOH (480 mL) and water (20 mL), and the mixture was cooled to 10 °C. A solution of sodium nitrite (16.6 g, 240 mmol) and potassium iodide (49.8 g, 300 mmol) in water (70 mL) was then added dropwise during 2.5 h, without allowing the temperature of the mixture to rise above 10-15 °C. The temperature was then allowed to rise to 25 °C, and the mixture was stirred for an additional 1.5 h. Solid $NaHCO_3$ (~30 g) was then added to bring the mixture to pH 9-10, followed by solid $Na_2S_2O_3$ (79 g). The resulting mixture was stirred vigorously for 30 min, giving rise to an orange solution that was poured into water (2.0 L). The mixture was extracted with Et_2O (4 × 100 mL), and the combined extracts were washed with water and brine, dried with anhydrous $MgSO_4$, and filtered. Removal of volatiles by evaporation under reduced pressure left a residue of dark red liquid, which was purified by distillation to give a slightly pink fraction boiling at 100-105 °C/1.5 mm Hg. The pink color was removed by passing the product through a plug of silica gel, using hexanes as eluent. Removal of solvent from the eluent by evaporation under reduced pressure gave 2-iodo-1,3-diisopropylbenzene (**9**; 13.1 g, 45.5 mmol, 57%) as a colorless liquid: ^{1}H NMR ($CDCl_3$, 400 MHz) δ 7.25 (t, 1H, ^3J = 7.7 Hz), 7.08 (d, 2H, ^3J = 7.7 Hz), 3.41 (septet, 2H, ^3J = 6.8 Hz), 1.24 (d, 12H, ^3J = 6.8 Hz); ^{13}C NMR ($CDCl_3$, 100 MHz) δ 151.2, 128.5, 123.9, 109.3, 39.5, 23.5;

HRMS (ESI-TOF) calcd for $[C_{12}H_{17}I + H]^+$ *m/e* 289.04477, found 289.04513. Anal. Calcd for $C_{12}H_{17}I$: C, 50.02; H, 5.95. Found: C, 49.85; H, 5.90.

1,3-Diisopropyl-2-(phenylethynyl)benzene (8).[24] Pd_2dba_3 (0.636 g, 0.695 mmol), CuI (0.132 g, 0.693 mmol), and PPh_3 (0.728 g, 2.78 mmol) were combined under N_2. Triethylamine (20 mL) was added, followed by 2-iodo-1,3-diisopropylbenzene (**9**; 2.00 g, 6.94 mmol) and phenylacetylene (1.52 mL, 1.41 g, 13.8 mmol), and a stream of N_2 was bubbled through the mixture for 10 min. The mixture was then heated at reflux for 24 h under N_2 and allowed to cool to 25 °C. Volatiles were removed by evaporation under reduced pressure, and the residue was partitioned between CH_2Cl_2 (50 mL) and 1 N aqueous HCl (50 mL). The aqueous phase was discarded, and the organic phase was further washed with 1 N aqueous HCl, saturated aqueous $NaHCO_3$, and brine. The solution was then dried with anhydrous $MgSO_4$ and filtered. Removal of volatiles by evaporation under reduced pressure left a residue that was purified by flash chromatography (silica gel, hexanes) to afford 1,3-diisopropyl-2-(phenylethynyl)benzene (**8**; 1.29 g, 4.92 mmol, 71%) as a colorless liquid: ^{1}H NMR ($CDCl_3$, 400 MHz) δ 7.57-7.53 (m, 2H), 7.41-7.32 (m, 3H), 7.29 (t, 1H, ^3J = 7.7 Hz), 7.16 (d, 2H, ^3J = 7.7 Hz), 3.62 (septet, 2H, ^3J = 6.9 Hz), 1.32 (d, 12H, ^3J = 6.9 Hz); ^{13}C NMR ($CDCl_3$, 100 MHz) δ 150.9, 131.4, 128.6, 128.5, 128.2, 124.2, 122.3, 121.0, 97.5, 86.8, 32.0, 23.4; HRMS (ESI-TOF) calcd for $[C_{20}H_{22} + H]^+$ *m/e* 263.17943, found 263.17871.

1-(2-Methylphenyl)-2,3,4,5,6-pentaphenylbenzene (3b). Tetraphenylcyclopentadienone (2.00 g, 5.20 mmol) and 2-methyl-(1-phenylethynyl)benzene (**5**; 1.00 g, 5.20 mmol) were combined in diphenyl ether (4 mL), and the mixture was heated at reflux for 4 days. The mixture was allowed to cool to 25 °C, and the resulting yellow crystalline precipitate was separated by filtration and washed with EtOH and hexanes. Recrystallization from *o*-xylene yielded 1-(2-methylphenyl)-2,3,4,5,6-pentaphenylbenzene (**3b**; 1.49 g, 2.72 mmol, 52%) as a colorless solid. A sample for thermal analysis was prepared by crystallization from dioxane: mp (sealed capillary) > 400 °C; ^{1}H NMR (400 MHz, $CDCl_3$) δ 6.95-6.70 (m,

29H), 2.03 (s, 3H); ^{13}C NMR (175 MHz, CDCl3) δ 140.79, 140.52, 140.43, 140.39, 140.35, 140.18, 139.84, 135.85, 132.15, 131.71, 131.62, 131.59, 131.50, 130.49, 128.95, 126.71, 126.65, 126.55, 126.43, 126.27, 125.42, 125.27, 124.08, 20.87;[41] HRMS (ESI-TOF) calcd for $[C_{43}H_{32} + H]^+$ *m/e* 549.25768, found 549.25640. Anal. Calcd for $C_{43}H_{32}$: C, 94.12; H, 5.88. Found: C, 94.01; H, 5.72.

1-(2,6-Dimethylphenyl)-2,3,4,5,6-pentaphenylbenzene (3c). 1,3-Dimethyl-2-(phenylethynyl)benzene (**6**; 0.568 g, 2.75 mmol) and tetraphenylcyclopentadienone (1.06 g, 2.76 mmol) were combined in diphenyl ether (2 mL), and the mixture was heated at reflux for 44 h. The mixture was allowed to cool to 25 °C and diluted with MeOH (5 mL). The resulting precipitate was separated by filtration and dried to give 1-(2,6-dimethylphenyl)-2,3,4,5,6-pentaphenylbenzene (**3c**; 1.19 g, 2.11 mmol, 77%) as an off-white solid. A sample for thermal analysis was prepared by crystallization from toluene: mp (sealed capillary) 364-365 °C; ^{1}H NMR ($CDCl_3$, 400 MHz) δ 6.89-6.78 (m, 25H), 6.75 (AK_2 system,[40] 1H, ^3J = 7.6 Hz), 6.64 (AK_2 system,[40] 2H, ^3J = 7.6 Hz), 2.10 (6H, s); ^{13}C NMR (benzene-d_6, 175 MHz) δ 141.58, 141.35, 141.33, 141.27, 140.87, 140.77, 140.36, 139.34, 136.10, 132.12, 132.06, 130.85, 127.28, 127.26, 127.23, 127.09, 126.90, 126.22, 125.80, 125.78, 21.79; HRMS (ESI-TOF) calcd for $[C_{44}H_{34} + H]^+$ *m/e* 563.27333, found 563.27245. Anal. Calcd for $C_{44}H_{34}$: C, 93.91; H, 6.09. Found: C, 93.81; H, 5.97.

1-(2,6-Diethylphenyl)-2,3,4,5,6-pentaphenylbenzene (3d). 1,3-Diethyl-2-(phenylethynyl)benzene (**8**; 0.500 g, 2.13 mmol), tetraphenylcyclopentadienone (0.820 g, 2.13 mmol), and diphenyl ether (2 mL) were combined, and the mixture was heated at reflux for 48 h under N_2. The mixture was allowed to cool to 25 °C and diluted with MeOH (30 mL). The resulting precipitate was collected by filtration, washed with a small amount of MeOH, and dried to yield 1-(2,6-diethylphenyl)-2,3,4,5,6-pentaphenylbenzene (**3d**; 0.828 g, 1.40 mmol, 66%) as a colorless solid. A sample for thermal analysis was prepared by crystallization from toluene: mp (sealed capillary) 282-283 °C; ^{1}H NMR ($CDCl_3$, 400 MHz) δ 6.92 (t, 1H, ^3J = 7.6 Hz), 6.88-6.74 (m, 27H), 2.46 (q, 4H, ^3J = 7.5 Hz), 1.06 (t, 6H, ^3J = 7.5 Hz); ^{13}C NMR ($CDCl_3$, 175 MHz) δ

140.99, 140.90, 140.84, 140.73, 140.40, 140.34, 140.28, 139.14, 138.26, 131.76, 131.73, 130.74, 126.86, 126.66, 126.65, 126.33, 125.57, 125.22, 125.20, 123.33, 26.13, 13.36; HRMS (ESI-TOF) calcd for $[C_{46}H_{38} + H]^+$ *m/e* 591.30463, found 591.30381. Anal. Calcd for $C_{46}H_{38}$: C, 93.52; H, 6.48. Found: C, 93.46; H, 6.35.

1-(2,6-Diisopropylphenyl)-2,3,4,5,6-pentaphenylbenzene (3e). 1,3-Diisopropyl-2-(phenylethynyl)benzene (**8**; 0.750 g, 2.86 mmol) and tetraphenylcyclopentadienone (1.10 g, 2.86 mmol) were combined in diphenyl ether (2 mL), and the mixture was heated at reflux for 24 h under N_2. The mixture was allowed to cool to 25 °C and diluted with MeOH (30 mL). The resulting precipitate was collected by filtration, washed with MeOH (20 mL), and dried to give 1-(2,6-diisopropylphenyl)-2,3,4,5,6-pentaphenylbenzene (**3e**; 1.37 g, 2.21 mmol, 77%) as a colorless solid. A sample for thermal analysis was prepared by crystallization from toluene/hexanes: mp (sealed capillary) 285-287 °C; ^{1}H NMR ($CDCl_3$, 400 MHz) δ 7.09 (t, 1H, ^3J = 7.7 Hz), 6.89-6.73 (m, 27H), 2.83 (septet, 2H, ^3J = 6.7 Hz), 0.86 (d, 12H, ^3J = 6.7 Hz); ^{13}C NMR (benzene-d_6, 175 MHz) δ 146.89, 141.96, 141.84, 141.65, 141.55, 141.30, 140.44, 138.16, 137.26, 132.77, 132.43, 132.01, 128.72, 127.27, 127.22, 126.94, 126.16, 125.74, 125.69, 123.44, 30.76, 25.13; HRMS (ESI-TOF) calcd for $[C_{48}H_{42} + H]^+$ *m/e* 619.33593, found 619.33432. Anal. Calcd for $C_{48}H_{42}$: C, 93.16; H, 6.84. Found: C, 93.16; H, 6.70.

Acknowledgments. We are grateful to the Natural Sciences and Engineering Research Council of Canada, the Ministère de l'Éducation du Québec, the Canada Foundation for Innovation, the Canada Research Chairs Program, and Université de Montréal for financial support. In addition, we thank Dr. Thierry Maris for his help in analyzing crystallographic data and Sylvain Essiembre for his assistance in carrying out thermal analyses.

Supporting Information Available: ^{1}H and ^{13}C NMR spectra of compounds **3b-e** and **7-9**; additional crystallographic details, including ORTEP views, X-ray powder

diffraction patterns, and tables of structural data in CIF format. This material is available free of charge via the Internet at http://pubs.acs.org.

Notes and References

† Département de Chimie, Université de Montréal, Montréal, Québec H3C 3J7 Canada.

‡ Department of Chemistry, Wilfrid Laurier University, Waterloo, Ontario N2L 3C5 Canada.

1. Fellow of the Natural Sciences and Engineering Research Council of Canada (2003-2009).

2. Fellow of the Natural Sciences and Engineering Research Council of Canada (2003-2004).

3. Roncali, J.; Leriche, P.; Cravino, A. *Adv. Mater.* **2007**, *19*, 2045-2060. Forrest, S. R. *Nature* **2004**, *428*, 911-918.

4. For recent reviews, see: Anthony, J. E. *Angew. Chem., Int. Ed.* **2008**, *47*, 452-483. Anthony, J. E. *Chem. Rev.* **2006**, *106*, 5028-5048.

5. Sele, C. W.; Kjellander, B. K. C.; Niesen, B.; Thornton, M. J.; van der Putten, J. B. P. H.; Myny, K.; Wondergem, H. J.; Moser, A.; Resel, R.; van Breemen, A. J. J. M.; van Aerle, N.; Heremans, P.; Anthony, J. E.; Gelinck, G. H. *Adv. Mater.* **2009**, *21*, in press (DOI: 10.1002/adma.200901548). Lee, S. S.; Kim, C. S.; Gomez, E. D.; Purushothaman, B.; Toney, M. F.; Wang, C.; Hexemer, A.; Anthony, J. E.; Loo, Y.-L. *Adv. Mater.* **2009**, *21*, 3605-3609. Hamilton, R.; Smith, J.; Ogier, S.; Heeney, M.; Anthony, J. E.; McCulloch, I.; Veres, J.; Bradley, D. D. C.; Anthopoulos, T. D. *Adv. Mater.* **2009**, *21*, 1166-1171. Lim, Y.-F.; Shu, Y.; Parkin, S. R.; Anthony, J. E.; Malliaras, G. G. *J. Mater. Chem.* **2009**, *19*, 3049-3056. Chen, J.; Subramanian, S.; Parkin, S. R.; Siegler, M.; Gallup, K.; Haughn, C.; Martin, D. C.; Anthony, J. E. *J. Mater. Chem.* **2008**, *18*, 1961-1969.

6. For recent reviews, see: Zhi, L.; Müllen, K. *J. Mater. Chem.* **2008**, *18*, 1472-1484. Wu, J.; Pisula, W.; Müllen, K. *Chem. Rev.* **2007**, *107*, 718-747.

7. Siegrist, T.; Besnard, C.; Haas, S.; Schiltz, M.; Pattison, P.; Chernyshov, D.; Batlogg, B.; Kloc, C. *Adv. Mater.* **2007**, *19*, 2079-2082.

8. For a recent example, see: Feng, X.; Marcon, V.; Pisula, W.; Hansen, M. R.; Kirkpatrick, J.; Grozema, F.; Andrienko, D.; Kremer, K.; Müllen, K. *Nature Mater.* **2009**, *8*, 421-426.

9. For recent reviews, see: Sergeyev, S.; Pisula, W.; Geerts, Y. H. *Chem. Soc. Rev.* **2007**, *36*, 1902-1929. Laschat, S.; Baro, A.; Steinke, N.; Giesselmann, F.; Hägele, C.; Scalia, G.; Judele, R.; Kapatsina, E.; Sauer, S.; Schreivogel, A.; Tosoni, M. *Angew. Chem., Int. Ed.* **2007**, *46*, 4832-4887.

10. For recent reviews of the subject of C-H···π interactions, see: Tsuzuki, S.; Fujii, A. *Phys. Chem. Chem. Phys.* **2008**, *10*, 2584-2594. Nishio, M. *CrystEngComm.* **2004**, *6*, 130-158.

11. A database related to C-H···π interactions, maintained by Professor Motohiro Nishio, is available via the Internet at http://www.tim.hi-ho.ne.jp/dionisio.

12. Braga, D. *Chem. Commun.* **2003**, 2751-2754. Biradha, K. *CrystEngComm* **2003**, *5*, 374-384. Hollingsworth, M. D. *Science* **2002**, *295*, 2410-2413. *Crystal Engineering: From Molecules and Crystals to Materials*; Braga, D.; Grepioni, F.; Orpen, A. G., Eds.; Kluwer: Dordrecht, Netherlands, 1999. Desiraju, G. R. *Crystal Engineering: The Design of Organic Solids*; Elsevier: Amsterdam, 1989.

13. Lebel, O.; Maris, T.; Perron, M.-È.; Demers, E.; Wuest, J. D. *J. Am. Chem. Soc.* **2006**, *128*, 10372.

14. Gagnon, E.; Maris, T.; Arseneault, P.-M.; Maly, K. E.; Wuest. J. D. *Cryst. Growth Des.*, in press (DOI: 10.1021/cg9010746).

15. Bart, J. C. J. *Acta Crystallogr.* **1968**, *B24*, 1277-1287. Lutz, M.; Spek, A. L.; Bonnet, S.; Klein Gebbink, R. J. M.; van Koten, G., as communicated in 2006 to

the Cambridge Crystallographic Data Centre (CCDC 609800, Refcode: HPHBNZ03).

16. For a recent review of the analysis of Hirshfeld surfaces, see: Spackman, M. A.; Jayatilaka, D. *CrystEngComm* **2009**, *11*, 19-32.

17. Analyses of Hirshfeld surfaces were carried out using the program Crystal Explorer Version 2.1.[18]

18. Wolff, S. K.; Grimwood, D. J.; McKinnon, J. J.; Jayatilaka, D.; Spackman, M. A. *Crystal Explorer 2.1*; University of Western Australia: Perth, 2007 (http://hirshfeldsurface.net/CrystalExplorer).

19. Gagnon, E.; Rochefort, A.; Métivaud, V.; Wuest. J. D. *Org. Lett.*, submitted for publication.

20. For an early example of the use of Diels-Alder reactions of aryl-substituted cyclopentadienones with acetylenes to form aryl-substituted arenes, see: Dilthey, W.; Schommer, W.; Trösken, O. *Ber. Dtsch. Chem. Ges.* **1933**, *66*, 1627-1628.

21. Rubin, M.; Trofimov, A.; Gevorgyan, V. *J. Am. Chem. Soc.* **2005**, *127*, 10243-10249.

22. Hundertmark, T.; Littke, A. F.; Buchwald, S. L.; Fu, G. C. *Org. Lett.* **2000**, *2*, 1729-1731.

23. Motti, E.; Rossetti, M.; Bocelli, G.; Catellani, M. *J. Organomet. Chem.* **2004**, *689*, 3741-3749.

24. Li, Z.; Dong, Y.; Mi, B.; Tang, Y.; Häussler, M.; Tong, H.; Dong, Y.; Lam, J. W. Y.; Ren, Y.; Sung, H. H. Y.; Wong, K. S.; Gao, P.; Williams, I. D.; Kwok, H. S.; Tang, B. Z. *J. Phys. Chem. B* **2005**, *109*, 10061-10066.

25. Krasnokutskaya, E. A.; Semenischeva, N. I.; Filimonov, V. D.; Knochel, P. *Synthesis* **2007**, 81-84.

26. Li, G. R.; Wang, X. H.; Li, J.; Zhao, X. J.; Wang, F. S. *Chin. Chem. Lett.* **2005**, *16*, 719-722.

27. Quiroga Norambuena, V. F.; Heeres, A.; Heeres, H. J.; Meetsma, A.; Teuben, J. H.; Hessen, B. *Organometallics* **2008**, *27*, 5672-5683.

28. To facilitate comparison of the structures of hexaphenylbenzenes **3a**-**e**, all crystallographic data were collected at 150 K.

29. Kitaigorodskii, A. I. *Organic Chemical Crystallography*; Consultants Bureau: New York, 1961.

30. Spek, A. L. *PLATON, A Multipurpose Crystallographic Tool*; Utrecht University: Utrecht, The Netherlands, 2003. Spek, A. L. *J. Appl. Cryst.* **2003**, *36*, 7-13.

31. The existence of significant intermolecular C-H···π aromatic interactions can be assessed in various ways. In the case of the structure of HPB (**3a**) itself (Refcode HPHBNZ03),[15] for example, the central aromatic ring engages in an intermolecular C-H···π interaction that can be characterized by various geometric parameters, including 1) the distance of the hydrogen atom to the mean-square plane of the central aromatic ring (2.76 Å); 2) the distance of the same hydrogen atom to the nearest carbon atom of the central aromatic ring (2.91 Å); and 3) the corresponding C-H···$\pi_{centroid}$ distance (3.00 Å). To avoid ambiguity, we consider that an intermolecular C-H···π aromatic interaction is present only when the C-H···$\pi_{centroid}$ distance is ≤ 3.05 Å, which is 1.05 times greater than the sum of the accepted van der Waals radii of hydrogen (1.20 Å) and carbon (1.70 Å). Similar criteria have been used previously in other studies of C-H···π interactions.[32]

32. Umezawa, Y.; Tsuboyama, S.; Takahashi, H.; Uzawa, J.; Nishio, M. *Tetrahedron* **1999**, *55*, 10047-10056. Umezawa, Y.; Tsuboyama, S.; Honda, K.; Uzawa, J.; Nishio, M. *Bull. Chem. Soc. Jpn.* **1998**, *71*, 1207-1213.

33. The value was obtained by using the command VOID in the program PLATON.[30]

34. Fieser, L. F. *Org. Synth.* **1966**, *46*, 44-48. Fieser, L. F. *Organic Syntheses*; Wiley: New York, 1973; Collect. Vol. V, pp 604-608.

35. Ouvrard, C.; Mitchell, J. B. O. *Acta Crystallogr.* **2003**, *B59*, 676-685.

36. Johnson, J. R.; Grummitt, O. *Org. Synth.* **1943**, *23*, 92-93. Johnson, J. R.; Grummitt, O. *Organic Syntheses*; Wiley: New York, 1955; Collect. Vol. III, pp 806-807.

37. Sheldrick, G. M. *SHELXS-97, Program for the Solution of Crystal Structures* and *SHELXL-97, Program for the Refinement of Crystal Structures*; Universität Göttingen: Germany, 1997.

38. Sheldrick, G. M. *Acta Crystallogr.* **2008**, *A64*, 112-122.

39. See the Supporting Information for details.

40. Friebolin, H. *Basic One- and Two-Dimensional NMR Spectroscopy*; Wiley-VCH: Weinheim, Germany, 1998.

41. In hexaphenylbenzene **3b**, rotation of the *o*-tolyl group about the biphenyl bond is expected to be slow at 25 °C.[42] As a result, compound **3b** possesses 28 aromatic carbon atoms that are unique but spectroscopically very similar. We could not entirely resolve these signals by ^{13}C NMR, even at 175 MHz using a cryoprobe.

42. Gust, D. *J. Am. Chem. Soc.* **1977**, *99*, 6980-6982.

6.3.1 Vers de nouveaux matériaux amorphes

Les résultats présentés dans l'article précédent démontrent que le cycle aromatique central de l'hexaphénylbenzène a une tendance marquée envers la formation de liens C-H···π. Même dans le cas du composé le plus substitué (**6.8**), on observe encore des interactions C-H···π, quoique en quantité très réduite. Malgré l'omniprésence des interactions C-H···π dans ces composés, le ratio de contacts H···H par rapport aux contacts C···H varie graduellement au travers de la série, allant de 67.0 : 31.8 pour l'hexaphénylbenzène (**6.1**) à 83.2 : 16.6 pour l'hexaphénylbenzène **6.8**. Ainsi, l'augmentation remarquable de la proportion des contacts non-directionnels de type C-H···H-C suggère que plus les groupements alkyles sont volumineux, moins l'ensemble des interactions intermoléculaires ont une composante directionnelle.

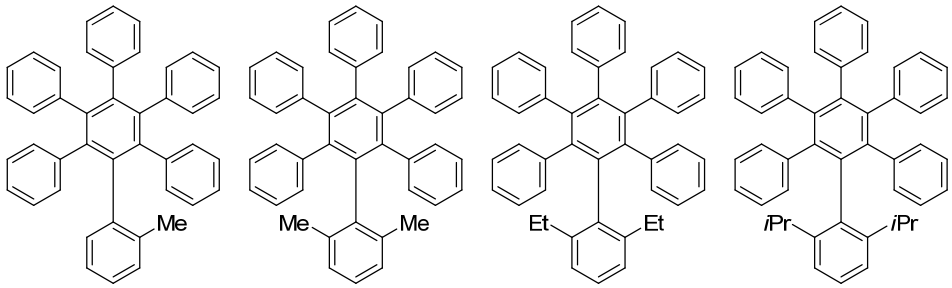

6.5 **6.6** **6.7** **6.8**

La diminution globale des contacts directionnels dans les dérivés hautement encombrés de l'hexaphénylbenzène laisse présager qu'ils peuvent être utiles pour certaines applications. En particulier, lorsqu'on scrute attentivement la littérature, on remarque que certains dérivés de l'hexaphénylbenzène sont aussi intimement liés à la formation de matériaux amorphes. Ce type de matériau possède des applications dans plusieurs domaines dont l'industrie alimentaire,[2] l'industrie pharmaceutique,[3] la conservation de protéines[4] et plus particulièrement en électronique organique.[5] En effet, les verres moléculaires, petites molécules résistantes à la cristallisation, sont de plus en

[2] Hartel, R. W. *Crystallization in Foods*; Springer: Boston, 2001.

[3] a) Hancock, B. C.; Zografi, G. *J. Pharm. Sci.* **1997**, *86*, 1-12. b) Yu, L. *Adv. Drug Delivery Rev.* **2001**, *48*, 27-42.

[4] (a) Carpenter, J. F.; Crowe, J. H. *Biochemistry* **1989**, *28*, 3916-3922. (b) Dirama, T. E.; Carri, G. A.; Sokolov, A. P. *J. Chem. Phys.* **2005**, *122*, 114505.

[5] a) Strohriegl, P.; Grazulevicius, J. V. *Adv. Mater.* **2002**, *14*, 1439-1452. (b) Shirota, Y. *J. Mater. Chem.* **2005**, *15*, 75-93. (c) Shirota, Y.; Kageyama, H. *Chem. Rev.* **2007**, *107*, 953-1000.

plus fréquemment exploités dans ce domaine. On note leur présence dans divers dispositifs dont les diodes électroluminescentes organiques,[6] les transistors à effet de champ,[5c] les cellules photovoltaïques organiques,[7] les photoresists[8] ou encore les dispositifs photochromiques.[9] Toutes ces applications tirent avantage de l'état amorphe qu'adopte un verre moléculaire. Afin de bien comprendre les subtilités liées à cet état de la matière, on se propose de faire un rapide survol de ses caractéristiques, avec une emphase particulière sur l'électronique organique.

6.3.2 L'état amorphe

Une phase amorphe est caractérisée par le désordre, autant dans les distances intermoléculaires que dans l'orientation des molécules les une par rapport aux autres.[5a] De façon plus imagée, c'est une phase solide dans laquelle les molécules sont dispersées comme dans l'état liquide. On y observe souvent la présence de volume libre due à un mauvais empilement des molécules. Les propriétés du matériau sont isotropes, tout comme celles d'un liquide.

Par extension, on comprend aussi qu'une des façons d'obtenir une phase amorphe consiste à piéger la structure désordonnée d'un liquide. Cette approche est fréquemment utilisée pour préparer des phases amorphes : un composé fondu, à l'état liquide, est refroidi rapidement, souvent en le plongeant dans l'azote liquide.[3] Similairement, on peut condenser le produit en phase gazeuse sur une surface froide. Finalement, on arrive à obtenir des films amorphes en utilisant un *spin-coater*; ce dispositif permet de déposer un verre moléculaire en solution sur une surface en rotation rapide. Si les paramètres sont bien ajustés, le solvant s'évapore rapidement et laisse un

---

6 Tang, C. W.; Van Slyke, S. A. *Appl. Phys. Lett.* **1987**, *51*, 913-915.

7 Kinoshita, M.; Fujii, N.; Tsuzuki, T.; Shirota, Y. *Synth. Met.* **2001**, *121*, 1571-1572.

8 a) Dai, J.; Chang, S. W.; Hamad, A.; Yang, D.; Felix, N.; Ober, C. K. *Chem. Mater.* **2006**, *18*, 3404-3411. b) Yang, D.; Chang, S. W.; Ober, C. K. *J. Mater. Chem.* **2006**, *16*, 1693-1696. c) De Silva, A.; Felix, N. M.; Ober, C. K. *Adv. Mater.* **2008**, *20*, 3355-3361.

9 a) Shirota, Y.; Moriwaki, K.; Yoshikawa, S.; Ujike, T.; Nakano, H. *J. Mater. Chem.* **1998**, *8*, 2579-2581. b) Utsumi, H.; Nagahama, D.; Nakano, H.; Shirota, Y. *J. Mater. Chem.* **2000**, *10*, 2436-2437. c) Yamaguchi, T.; Nomiyama, K.; Isayama, M.; Irie, M. *Adv. Mater.* **2004**, *16*, 643-645. d) Tomari, A.; Yamaguchi, T.; Sakamoto, N.; Fujita, Y.; Irie, M. *Chem. Lett.* **2004**, *33*, 1380-1381.

film amorphe. Ces trois méthodes agissent de la même façon : à partir d'une phase liquide, d'une phase gazeuse ou d'une solution du verre moléculaire, on doit former une phase solide le plus rapidement possible afin d'éviter qu'un réarrangement structurel intensif mène à une cristallisation.

Ces trois approches décrivent des manipulations physiques permettant d'obtenir des phases amorphes. Celles-ci peuvent par contre être combinées à une approche centrée sur les aspects moléculaires des composés étudiés. Au fil des ans, des dizaines de verres moléculaires ont été rapportés. Ces études ont permis de faire ressortir des éléments structurels favorisant l'obtention d'une phase amorphe.[10,5b] Ceux-ci sont : 1) une non-planarité des molécules, 2) un nombre élevé de conformations possibles, possédant des énergies similaires, 3) une grande structure moléculaire, 4) l'addition de groupements volumineux et encombrants, 5) l'addition de fragments moléculaires rigides, 6) des structures avec des formes irrégulières ou globulaires et 7) des interactions intermoléculaires faibles. L'objectif de cette approche moléculaire peut se résumer par deux effets : rendre l'empilement des molécules difficile ou encore ralentir la vitesse de réarrangement des molécules à l'état solide. Dans le second cas, on parvient à ralentir la cinétique menant à un état thermodynamiquement plus stable, tel que l'état cristallin. On favorise ainsi la formation et la métastabilité d'une phase amorphe.[11]

Ainsi, l'unité pentaphénylbenzène est particulièrement efficace pour induire la formation d'une phase amorphe. En ligne avec les critères structurels cités ci-haut, cette unité possède une grande structure rigide, non-plane, irrégulière en plus d'avoir suffisamment de flexibilité pour adopter plusieurs conformères d'énergies similaires. Ce dernier point est possible grâce à la présence de seulement cinq substituants sur le cycle aromatique central. Comme nous l'avons vu au courant de l'article 3,[12] les angles dièdres entre les cycles aromatiques périphériques et centraux sont nettement plus petits

---

[10] a) Naito, K.; Miura, A. *J. Phys. Chem.* **1993**, *93*, 6240-6248. b) Alig, I.; Braun, D.; Langendorf, R.; Wirth, H. O.; Voigt, M.; Wendorff, J. H. *J. Mater. Chem.* **1998**, *8*, 847-851.

[11] Naito, K. *Chem. Mater.* **1994**, *6*, 2343-2350.

[12] Gagnon, E.; Maris, T.; Arseneault, P.-M.; Maly, K. E.; Wuest, J. D. *Cryst. Growth Des.* **2009**, (DOI: 10.1021/cg9010746).

dans le pentaphénylbenzène (moyenne : 60.5°) que dans l'hexaphénylbenzène (moyenne : 79.3°). L'addition de ces groupements encombrants permet aussi d'obtenir des températures de transition vitreuse élevées,[13] nécessaires pour une bonne stabilité de la phase amorphe.[10a, 11] Le groupement pentaphénylbenzène a démontré plus d'une fois son potentiel d'inducteur de phase amorphe : une sélection de verres moléculaires basés sur l'unité pentaphénylbenzène est illustrée à la Figure 6.2.

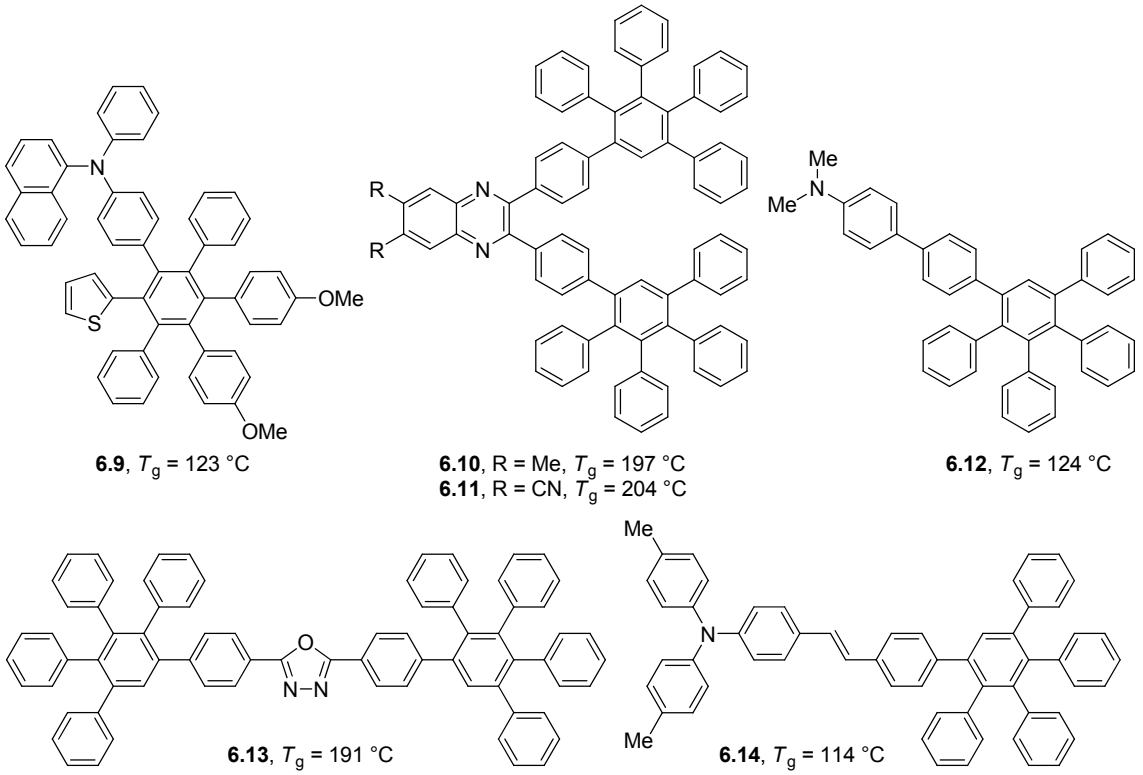

Figure 6.2. Sélection de verres moléculaires possédant une ou plusieurs unités pentaphénylbenzène, avec les valeurs de leur température de transition vitreuse, T_g.[14]

[13] La température de transition vitreuse, T_g, est la température à laquelle certains mouvements moléculaires deviennent permis. Par exemple, dans le cas des dérivés du pentaphénylbenzène, elle peut correspondre au début de la rotation des cycles aromatiques périphériques.

[14] (a) Justin Thomas, K. R.; Velusamy, M.; Lin, J. T.; Sun, S.-S.; Tao, Y.-T.; Chuen, C.-H. *Chem. Commun.* **2004**, 2328-2329. (b) Xu, X.; Chen, S.; Yu, G.; Di, C. a.; You, H.; Ma, D.; Liu, Y. *Adv. Mater.* **2007**, *19*, 1281-1285. (c) Xu, X.; Chen, S.; Di, C. a.; Liu, Y. *J. Mater. Chem.* **2008**, *18*, 299-305. (d) Huang, C.; Zhen, C.-G.; Su, S. P.; Loh, K. P.; Chen, Z.-K. *Org. Lett.* **2005**, *7*, 391-394. (e) Chen, S.; Xu, X.; Liu, Y.; Qiu, W.; Yu, G.; Sun, X.; Zhang, H.; Qi, T.; Lu, K.; Gao, X.; Liu, Y.; Zhu, D. *J. Mater. Chem.* **2007**, *17*, 3788-3795. (f) Chen, C.-T.; Chiang, C.-L.; Lin, Y.-C.; Chan, L.-H.; Huang, C.-H.; Tsai, Z.-W.; Chen, C.-T. *Org. Lett.* **2003**, *5*, 1261-1264.

6.4 Le côté sombre de l'ingénierie cristalline

Comme nous l'avons vu tout au long de cette thèse, l'ingénierie cristalline a comme but de comprendre et de contrôler toutes les étapes reliées au phénomène de la cristallisation. En particulier, pour les composés organiques, de grands efforts ont été faits dans l'objectif de documenter, comprendre et manipuler les interactions non-covalentes en vue d'obtenir des structures cristallines précises. Par contre, ce n'est que depuis peu que le côté « sombre » de l'ingénierie cristalline a été abordé : en effet, en sachant ce qui favorise la cristallisation, nous pouvons aussi travailler à favoriser ce qui s'y oppose.

Récemment, cette approche a été utilisée par Lebel et co-auteurs pour développer de nouveaux verres moléculaires, tels que les composés **6.15** et **6.16**.[15] Bien que ces molécules aient la possibilité de former de nombreux ponts hydrogène, elles résistent fortement à la cristallisation. Les auteurs ont déterminé par spectroscopie infrarouge que ces composés forment des ponts hydrogène, même dans l'état amorphe. L'hypothèse formulée est que ces ponts hydrogène permettent aux molécules de s'associer fortement en de nombreux agrégats peu ordonnés, sans ordre à courte et longue distances. De plus, la présence de ces ponts hydrogène réduit la mobilité moléculaire et la cinétique de cristallisation devient donc extrêmement lente.

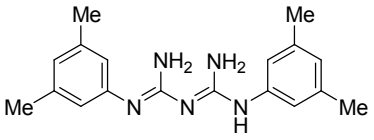

6.15

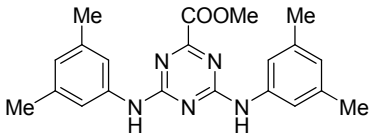

6.16

En vue de développer de nouveaux verres moléculaires, nous pouvons exploiter les nombreuses connaissances acquises lors de nos études cristallographiques de l'hexaphénylbenzène et de ses dérivés. Par exemple, la structure du pentaphénylbenzène révèle deux types d'interactions C-H···π, impliquant dans un cas des cycles aromatiques périphériques et dans le second, le cycle aromatique central (voir article 3, chapitre 5). À

[15] (a) Lebel, O.; Maris, T.; Perron, M.-È.; Demers, E.; Wuest, J. D. *J. Am. Chem. Soc.* **2006**, *128*, 10372-10373. (b) Wang, R.; Pellerin, C.; Lebel, O. *J. Mater. Chem.* **2009**, *19*, 2747-2753. (c) Wuest, J. D.; Lebel, O. *Tetrahedron* **2009**, *65*, 7393-7402.

l'opposée, l'hexaphénylbenzène **6.8** établit un nombre beaucoup plus limité d'interactions C-H···π.

Nous avons donc de bonnes raisons de penser qu'une unité (2,6-diisopropylphényl)pentaphénylbenzène pourrait induire la formation de phases amorphes lorsqu'utilisée judicieusement. En effet, elle possède les mêmes qualités que le pentaphénylbenzène (grande structure rigide, non-plane et irrégulière). Bien que la structure soit moins flexible (nombre de conformations plus limité à cause de l'encombrement stérique), l'unité (2,6-diisopropylphényl)pentaphénylbenzène a une forme plus globulaire et les interactions intermoléculaires dans lesquelles elle peut prendre part ont toutes les chances d'être moins directionnelles.

Afin de vérifier le potentiel du (2,6-diisopropylphényl)pentaphénylbenzène en tant qu'inducteur de phase amorphe, il serait intéressant de préparer des dérivés analogues aux verres moléculaires déjà connus. Ainsi, en se basant sur la structure du composé **6.12**, nous pourrions en quelques étapes préparer son analogue **6.20** (Schéma 6.1), dans lequel un groupement 2,6-diisopropylphényle occupe la position préalablement inoccupée de l'unité pentaphénylbenzène.

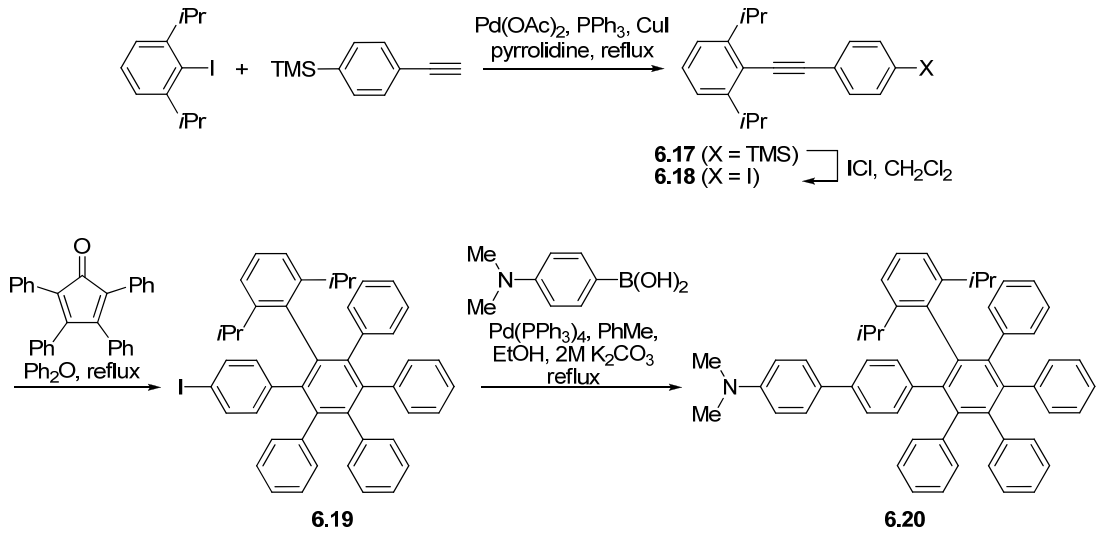

Schéma 6.1. Synthèse proposée du dérivé **6.20**, analogue de l'amine **6.12**.

Alternativement, s'il s'avère qu'il est essentiel de retirer un des six cycles périphériques de l'hexaphénylbenzène pour pouvoir obtenir des verres moléculaires, nous pouvons tenter l'expérience avec un groupement 1-(2,6-diisopropylphényl)-2,3,4,5-tétraphénylbenzène. Cette unité combinerait la flexibilité du pentaphénylbenzène avec l'encombrement stérique additionnel des groupements isopropyles. Encore une fois, une synthèse rapide pourrait mener à un premier analogue pouvant être analysé (**6.24**, Schéma 6.2). On établirait alors rapidement la viabilité d'une telle approche.

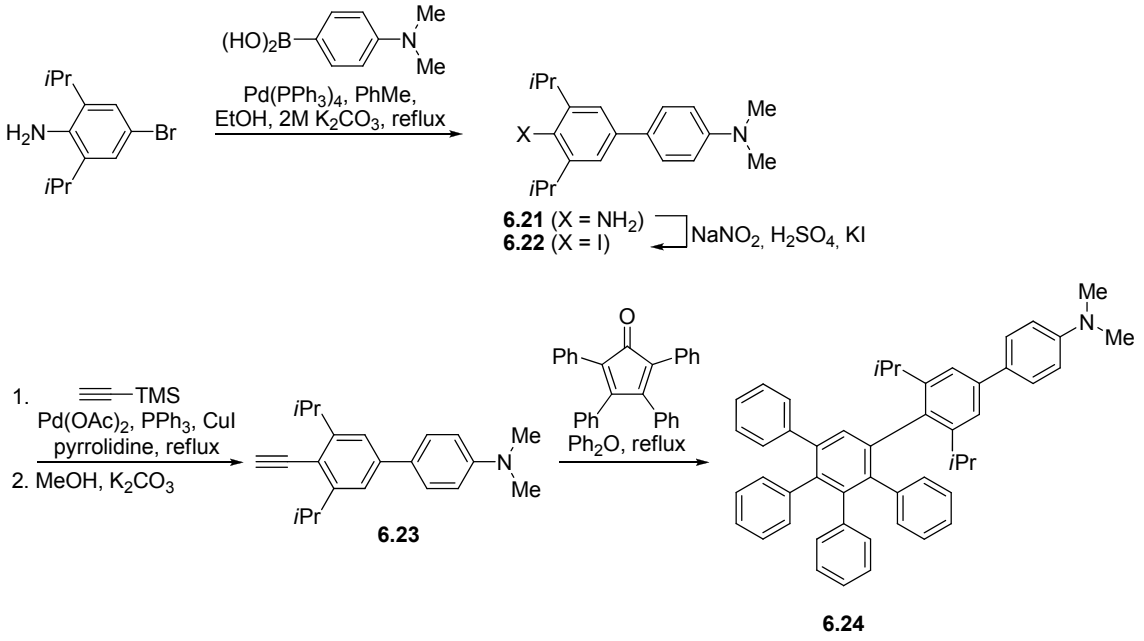

Schéma 6.2. Synthèse proposée du dérivé **6.24**.

6.5 Composés à basse cohésion moléculaire

Un autre aspect frappant du comportement physique des hexaphénylbenzènes **6.1** et **6.5-6.8** est la température à laquelle ils commencent à sublimer (voir l'article 5, Figure 5). En effet, celle-ci diminue de plusieurs dizaines de degrés Celsius en fonction de l'addition de groupements alkyles de plus en plus volumineux. Compte tenu de la relation directe entre l'enthalpie de sublimation et l'énergie réticulaire,[16] il y a lieu de penser qu'une température de sublimation moins élevée serait le signe d'une cohésion moléculaire moindre. En effet, l'enthalpie de sublimation correspond

[16] (a) Ouvrard, C.; Mitchell, J. B. O. *Acta Crystallogr.,* **2003**, B*59*, 676-685. (b) Eckhardt, C. J.; Gavezzotti, A. *J. Phys. Chem. B* **2007**, *111*, 3430-3437.

approximativement à l'énergie requise pour briser toutes les interactions non-covalentes dans un réseau, menant ainsi à des molécules isolées les unes des autres : l'état gazeux.

Ainsi, une mesure de l'enthalpie de sublimation des composés **6.1** et **6.5-6.8** permettrait de souligner davantage le comportement thermique particulier de ces hexaphénylbenzènes substitués. Toutefois, les méthodes typiques pour obtenir cette donnée demandent souvent un montage expérimental élaboré.[17] On peut malgré tout obtenir ces valeurs par des analyses thermogravimétriques isothermes, en autant qu'une substance de référence existe pour la plage de températures étudiée.[18] Les mesures d'enthalpies de sublimation des composés **6.1** et **6.5-6.8** sont actuellement prises en charge par Pr. Kenneth E. Maly de l'université Wilfrid Laurier.

Si les enthalpies de sublimation varient tel qu'espéré, l'utilisation d'une unité (2,6-diisopropylphényl)pentaphénylbenzène au lieu du pentaphénylbenzène permettrait d'obtenir des composés plus volatiles. Ce comportement serait très avantageux lorsque l'on voudrait obtenir des films minces d'un analogue des composés **6.9-6.12** par sublimation; les températures nécessaires seraient plus basses, permettant ainsi de sublimer des molécules contenant des groupements fonctionnels plus sensibles.

6.6 Conclusions

Les analyses cristallographiques des hexaphénylbenzènes substitués **6.5-6.8** démontrent que l'association intermoléculaire peut être fortement influencée par la présence de groupements alkyles. Il est clair que cette étude n'est qu'un point de départ pour plusieurs autres projets; nous avons présenté dans les sections précédentes deux avenues que nous jugeons essentielles d'explorer. De plus, on doit souligner l'approche adoptée : grâce à des résultats issus de l'ingénierie cristalline, nous croyons pouvoir avoir un impact majeur sur les propriétés physiques des matériaux moléculaires

[17] Zielenkiewica, W.; Perlovich, G. L.; Wszelaka-Rylik, M. *J. Therm. Anal. Calorim.* **1999**, *57*, 225-334.
[18] (a) Lähde, A.; Raula, J.; Malm, J.; Kaupinnen, E. I.; Karppinen, M. *Thermochim. Acta* **2009**, *482*, 17-20. (b) Barontini, F.; Cozzani, V. *Thermochim. Acta* **2007**, *460*, 15-21. (c) Focke, W. W. *J. Therm. Anal. Calorim.* **2003**, *74*, 97-107.

amorphes. Ces relations entre structures cristallographiques et propriétés physiques renforcissent l'idée que le vaste domaine des matériaux moléculaires peut grandement bénéficier d'une approche multidisciplinaire.

Chapitre 7

Conclusions et perspectives

7.1 Retour sur la thèse

L'objectif central de cette thèse consistait à explorer l'utilité de l'hexaphénylbenzène et de ses dérivés hautement substitués en chimie des matériaux. Ces molécules peuvent être aisément préparées selon les trois approches distinctes et bien documentées qui sont présentées au chapitre 2. Afin de synthétiser la large gamme de composés inclus dans cette thèse, nous avons exploité la flexibilité de la réaction de Diels-Alder pour contrôler la distribution des substituants sur l'hexaphénylbenzène et ses dérivés.

Le chapitre 3 présente nos efforts centrés sur la préparation d'hexaphénylbenzènes et de ses dérivés comportant des groupements de reconnaissance diaminotriazinyles, bien connus pour former de nombreux ponts hydrogène. Cette étude, impliquant à la fois une variation de la distribution des substituants et une variation de la symétrie du cœur moléculaire, a démontré que la porosité des réseaux supramoléculaires obtenus peut être augmentée en excisant, partie par partie, la molécule-mère **7.1.**

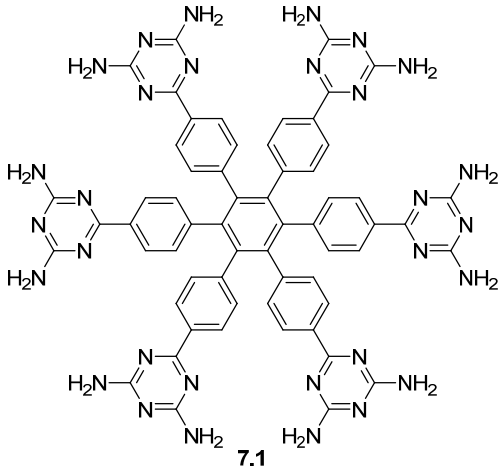

7.1

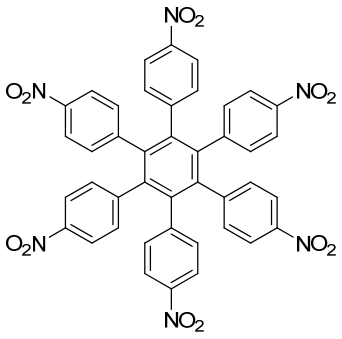

7.2

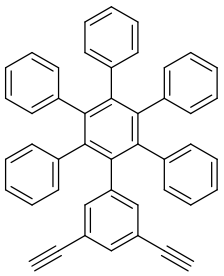

7.3

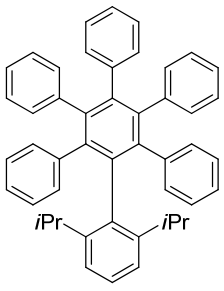

7.4

Ensuite, nous nous sommes attaqués à l'étude des interactions faibles à l'état cristallin, réputées pour être difficiles à manipuler. Au chapitre 4, on s'est intéressé au fait que l'hexaphénylbenzène ne peut établir avec facilité des interactions non-covalentes de type π···π, contrairement aux autres cœurs moléculaires aromatiques typiquement utilisés en science des matériaux tels que le tétraphénylméthane ou le 9,9'-spirobifluorène. Ainsi, la cristallisation de l'hexakis(4-nitrophényl)benzène (**7.2**) a mis à jour des motifs de reconnaissance associés au groupement nitro qui sont normalement obscurcis par la présence d'interactions non-covalentes compétitives.

Au chapitre 5, on s'est intéressé au cœur moléculaire lui-même. Une étude cristallographique approfondie de l'hexaphénylbenzène et de ses dérivés a démontré que, malgré un encombrement stérique élevé, un motif d'association par interaction C-H···π est observé de façon récurrente avec les cycles aromatiques centraux poly-substitués. Cette interaction non-covalente est la force principale d'association directionnelle dans ces composés. Afin d'exploiter la capacité d'accepteur de liens C-H···π de l'hexaphénylbenzène, nous l'avons ensuite mis en présence de l'excellent donneur qu'est le groupement éthynyle, tel qu'illustré par la molécule **7.3**. Ainsi, nous avons pu former des assemblages supramoléculaires uniquement grâce à des interactions C-H···π fortes et directionnelles.

Plus récemment, les connaissances de l'ingénierie cristalline ont été exploitées pour empêcher la cristallisation. Dans cette optique, nous rapportons au chapitre 6 nos travaux visant à défavoriser le motif d'interactions C-H···π précédemment observé dans l'hexaphénylbenzène et ses dérivés. L'introduction de groupements alkyles, tel qu'illustré par le dérivé **7.4**, bloque partiellement l'accès au cycle aromatique central de l'hexaphénylbenzène. Les résultats obtenus par cette approche sont encourageants : on note une grande diminution des interactions non-covalentes directionnelles en faveur des contacts C-H···H-C. On travaille maintenant à introduire ce groupement dans de nouveaux matériaux moléculaires afin de déterminer le potentiel de cette stratégie pour induire la formation de phases amorphes.

7.2 Perspectives finales

Chacun des chapitres contenus dans cette thèse apporte des éléments de réponse quant au contrôle des assemblages supramoléculaires à l'état cristallin. Ces éléments de contrôle ont également le potentiel de pouvoir régir l'organisation moléculaire locale dans d'autres phases solides ou même liquides. Les ponts hydrogène, les interactions entre groupements nitro et les interactions C-H···π que nous avons examinés ne sont que quelques représentants de la grande diversité des interactions non-covalentes pouvant être exploitées. La majorité des molécules que nous avons étudiées fait partie d'une petite famille de structures dérivées de l'hexaphénylbenzène; néanmoins, les implications de notre étude ont une portée plus générale. Nous avons choisi le système hexaphénylbenzène comme point focal de l'étude pour deux raisons : 1) Nous étions motivés par l'intérêt intrinsèque d'explorer une famille de structures peu exploitées et 2) le système hexaphénylbenzène met certaines propriétés optimales à la disposition du chercheur désirant faire une étude systématique de la relation entre la structure d'une molécule individuelle et le comportement des agrégats en phase liquide ou solide. En particulier, les propriétés-clés du système hexaphénylbenzène sont :

- Une haute symétrie et rigidité, formant une structure tridimensionnelle bien définie
- Un nombre de conformations limité et contrôlé par le choix des substituants
- La difficulté pour ses cycles aromatiques d'établir des interactions π···π
- Des facteurs stéréo-électroniques favorisant l'établissement d'interactions C-H···π avec le cycle aromatique central
- La facilité de synthétiser des dérivés portant divers substituants
- Une haute stabilité thermique

Pour ces différentes raisons, le système hexaphénylbenzène permet de mettre en relief des phénomènes qui seraient obscurcis dans d'autres familles de molécules. En même temps, le système que nous avons choisi facilite grandement une approche méthodique

pour explorer la relation structure-propriété. Nos travaux, quoique focalisés sur le système hexaphénylbenzène, illustrent cette stratégie générale et nous amènent à des conclusions de valeur universelle en science des matériaux moléculaires.

Tout au long des chapitres, nous avons discuté des projets connexes qui devraient être abordés, dans le contexte des résultats présentés. On réalise que l'utilisation de l'hexaphénylbenzène en chimie des matériaux n'est qu'entamée tout au plus. Ainsi, en tenant compte des propriétés citées plus haut, on peut penser à accéder à des composés présentant de nouvelles caractéristiques. Notamment, les conformations limitées que peuvent adopter les hexaarylbenzènes en général laissent penser que l'hexakis[(3,5-diphényl)phényl]benzène (**7.5**) et son analogue **7.6** pourraient être des candidats intéressants en chimie supramoléculaire. Les cavités déterminées par les bras aromatiques seraient très grandes et ces composés auraient une porosité intrinsèque élevée pouvant inclure une variété de molécules invitées. La Figure 7.1 souligne l'immensité de la cavité formée par la molécule **7.6**.

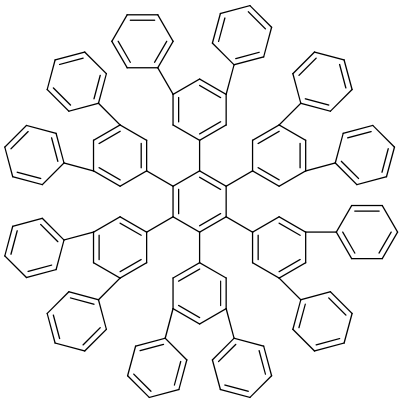

7.5

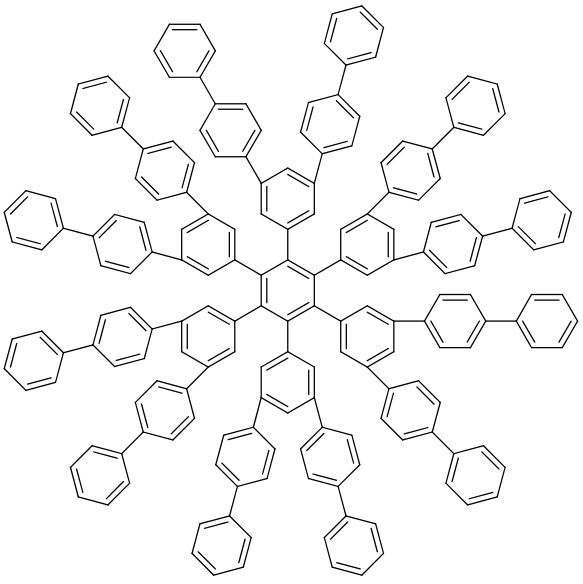

7.6

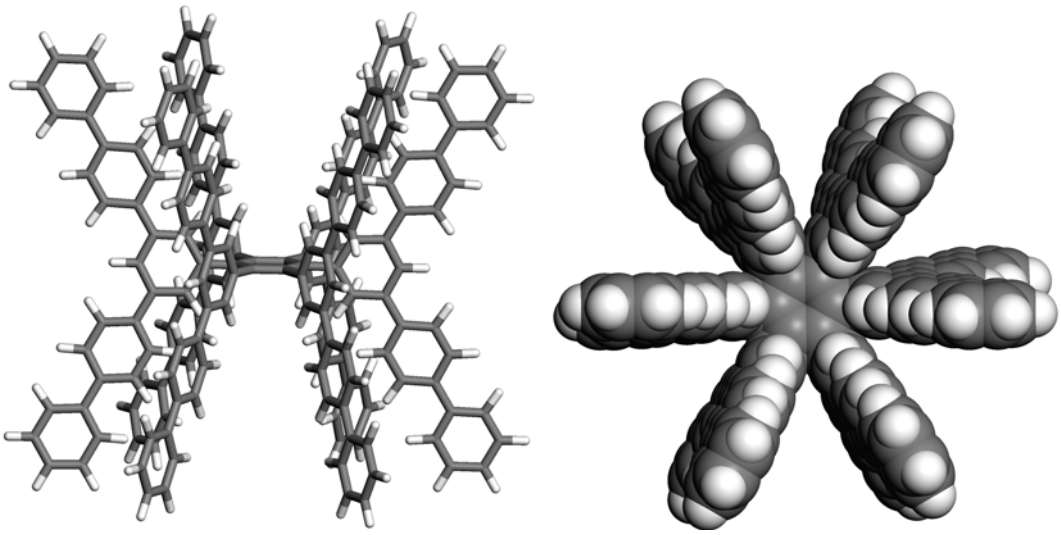

Figure 7.1. Haut : structures des composés **7.5** et **7.6**. Bas, gauche : vue de côté d'un modèle du composé **7.6**, droite : représentation du modèle CPK du composé **7.6** vue du haut.

Un second phénomène qui mériterait une plus grande attention est attribué au fait que l'hexaphénylbenzène peut adopter une conformation en hélice *chirale*, tel qu'illustré à la Figure 7.2. On note toutefois que l'hexaphénylbenzène peut fluctuer facilement entre les deux conformations par de simples rotations partielles autour des liens C-C simples. De plus, on retrouve souvent les deux conformères dans la même structure cristalline, où ils sont reliés par un élément de symétrie.

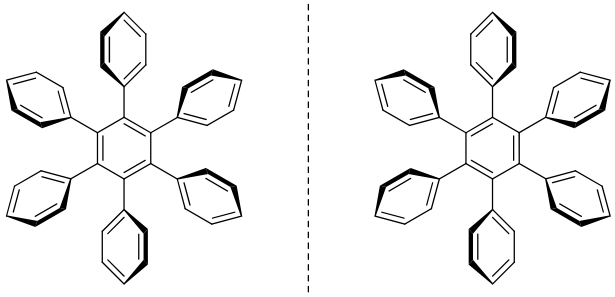

Figure 7.2. Conformations en hélice chirale de l'hexaphénylbenzène.

On peut donc imaginer un système dans lequel un seul groupement chiral pourrait diriger l'orientation de tous les autres cycles périphériques. Ainsi, un composé tel que l'oxazolidinone **7.9**, obtenue par une réaction de Diels-Alder entre l'ynamine

7.7[1] et la tétraphénylcyclopentadiènone **7.8**, pourrait posséder un effet d'amplification chirale important. Ces quelques idées s'ajoutent à toutes celles présentées au fil de cette thèse.

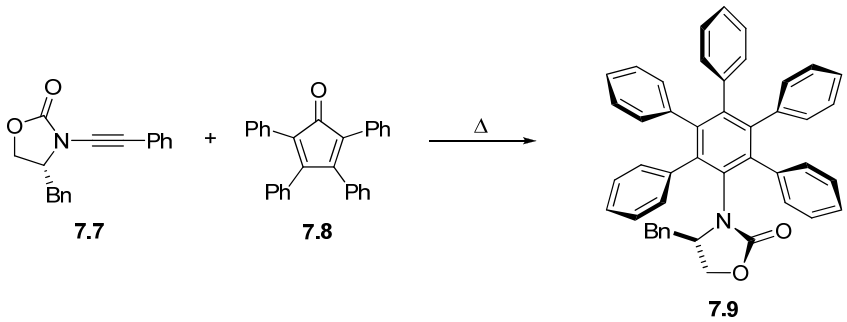

Schéma 7.1. Synthèse proposée de l'oxazolidinone chirale **7.9**.

En conclusion, soulignons que le contrôle de la structure et des propriétés des matériaux moléculaires continue à être un des plus importants défis à relever en science des matériaux. À cause de la présence concomitante de plusieurs forces intermoléculaires, il s'avère encore difficile de déterminer avec certitude le produit d'une association supramoléculaire. Pour y arriver, nous avons utilisé une approche systématique nous permettant de caractériser diverses facettes de ces phénomènes d'association intermoléculaire. L'hexaphénylbenzène a été à la base de notre approche : sa structure moléculaire a pu être modifiée systématiquement afin de déterminer une série de relations entre la structure et les propriétés. Les leçons apprises aux travers de nos travaux démontrent la nécessité de faire des variations méthodiques lors de n'importe quelles études structurelles; c'est grâce aux modifications majeures apportées aux molécules **7.1**, **7.3** et **7.4**, ainsi qu'à l'étude de plusieurs solvates du composé **7.2** que nous avons réussis à apporter une contribution importante à la science des matériaux.

[1] Dunetz, J. R.; Danheiser, R. L. *Org. Lett.* **2003**, *5*, 4011-4014.

Annexe 1

Partie supplémentaire de l'article 3

Supporting Information

Structural Features in Crystals of Derivatives of Benzene with Multiple Contiguous Phenyl Substituents

Eric Gagnon, Thierry Maris, Pierre-Marc Arseneault, Kenneth E. Maly, and James D. Wuest*

Département de Chimie, Université de Montréal Montréal, Québec, H3C 3J7 Canada

Content **Page**

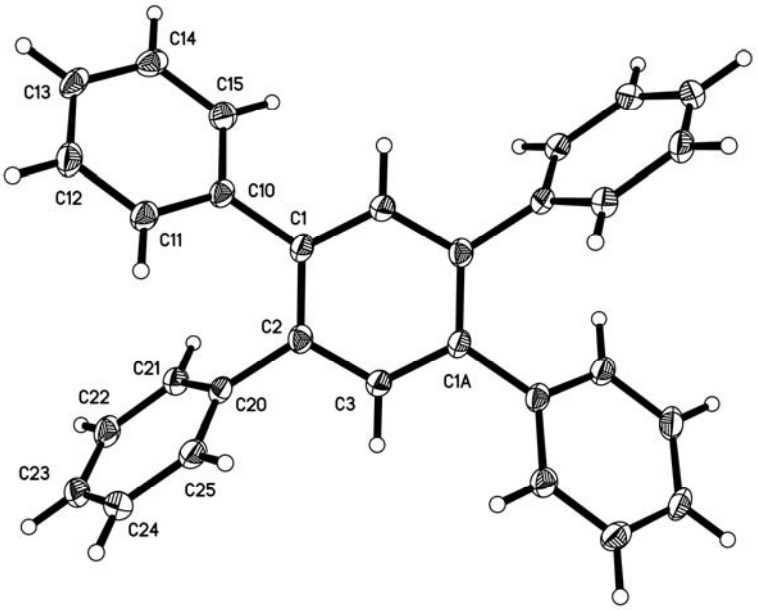

Figure S1. Thermal displacement ellipsoid plot showing the structure of crystals of polymorph TPB-1 of TPB (**3**) at 100 K. The ellipsoids of non-hydrogen atoms are drawn at the 50% probability level, and hydrogen atoms are represented by a sphere of arbitrary size. Unlabeled parts of the molecule are related by the symmetry operation [2-*x*, -*y*, 1-*z*].

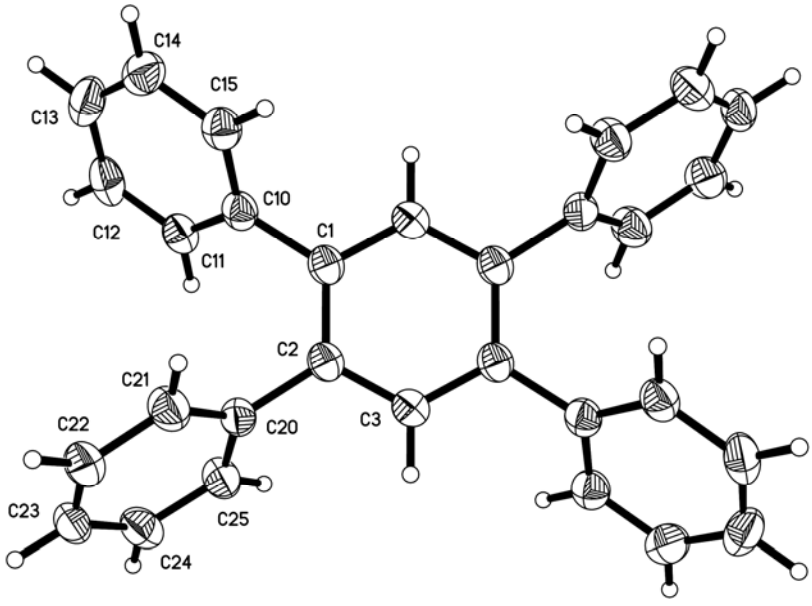

Figure S2. Thermal displacement ellipsoid plot showing the structure of crystals of polymorph TPB-2 of TPB (**3**) at 150 K. The ellipsoids of non-hydrogen atoms are drawn at the 50% probability level, and hydrogen atoms are represented by a sphere of arbitrary size. Unlabeled parts of the molecule are related by the symmetry operation [-*x*, -*y*, -*z*].

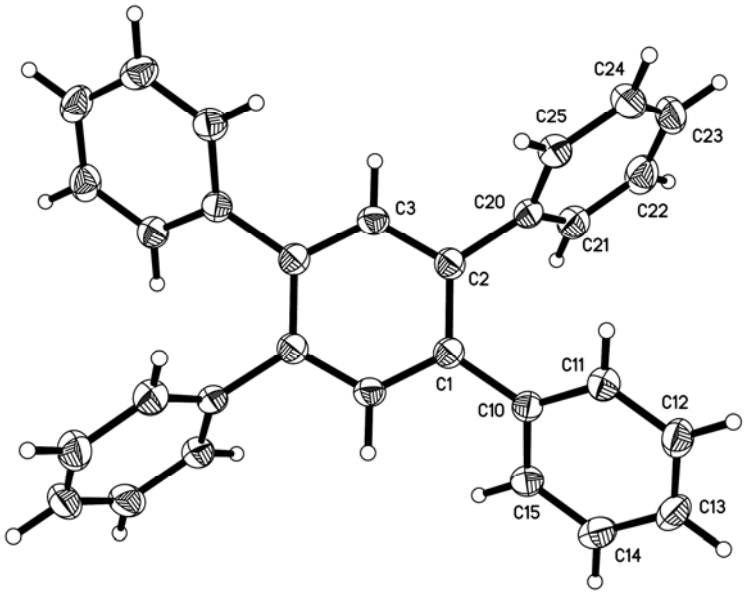

Figure S3. Thermal displacement ellipsoid plot showing the structure of crystals of polymorph TPB-3 of TPB (**3**) at 150 K. The ellipsoids of non-hydrogen atoms are drawn at the 50% probability level, and hydrogen atoms are represented by a sphere of arbitrary size. Unlabeled parts of the molecule are related by the symmetry operation [1-*x*, 1-*y*, 1-*z*].

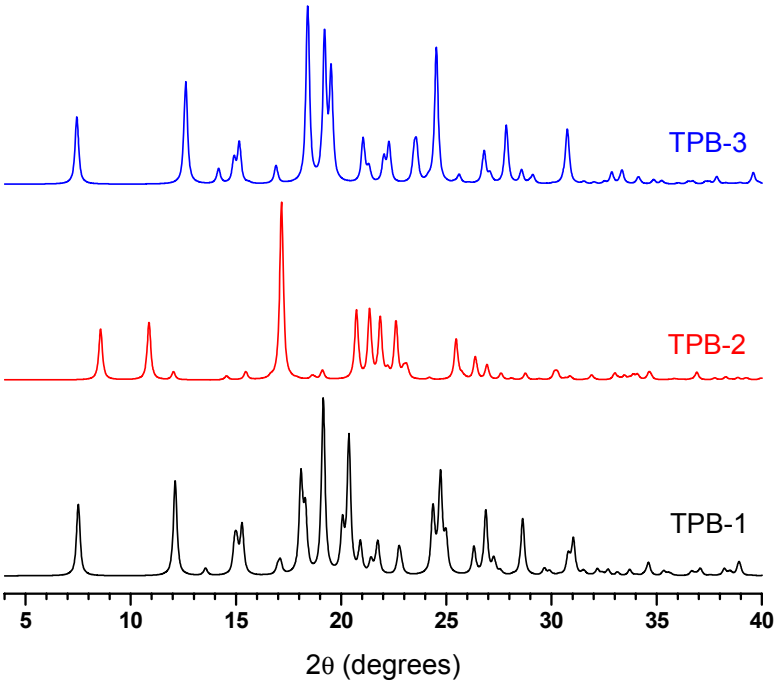

Figure S4. X-ray powder diffraction patterns corresponding to the structures of the three polymorphs of TPB-1, TPB-2, and TPB-3 of TPB (**3**). All patterns were calculated using Mercury 2.2, based on Cu Kα_1 radiation (λ = 1.5406 Å).

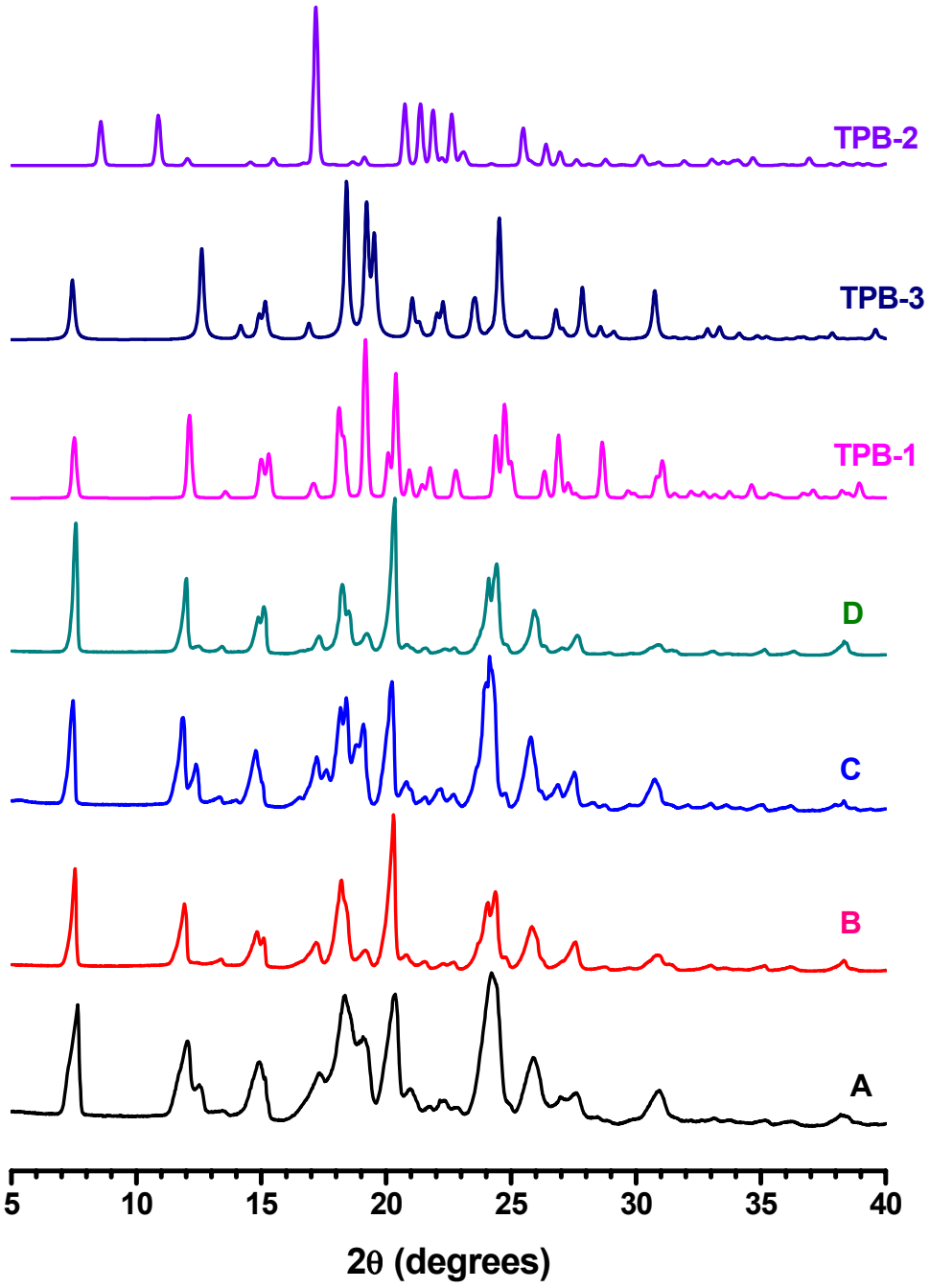

Figure S5. Comparison of X-ray powder diffraction patterns recorded for TPB (**3**) crystallized from hexanes (**A**, black), toluene (**B**, red), benzene (**C**, blue), and xylenes (**D**, green) with the X-ray powder diffraction patterns calculated for pure polymorphs TPB-1 (pink), TPB-3 (dark blue), and TPB-2 (purple).

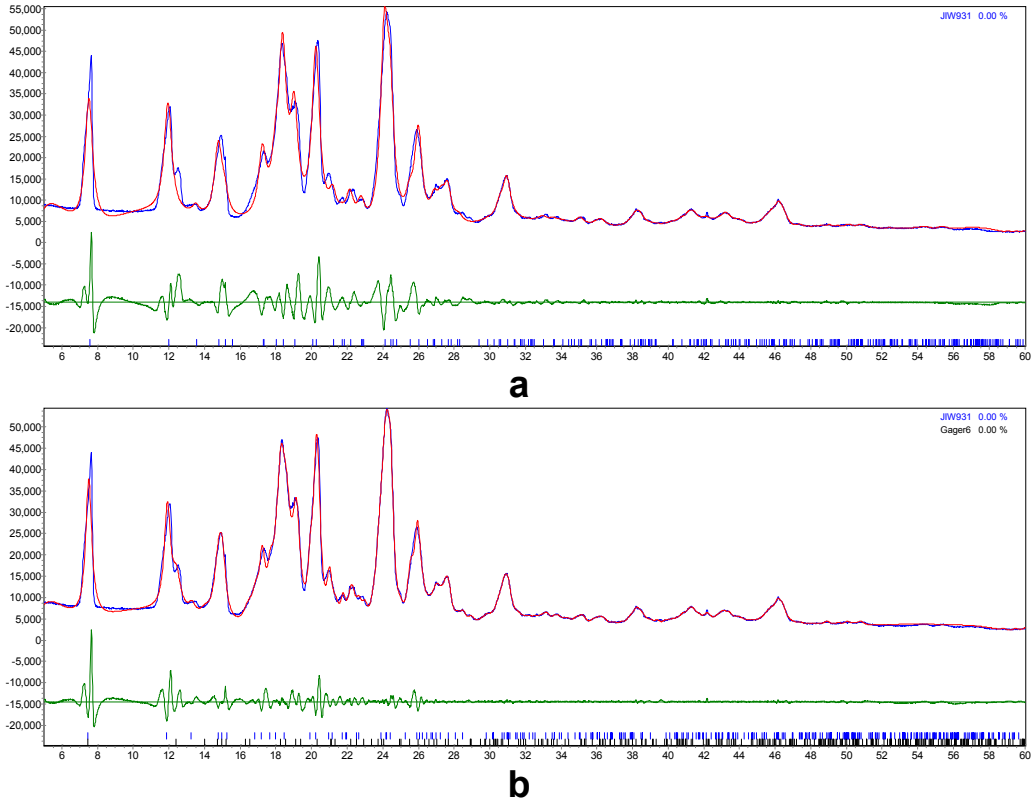

Figure S6. Pawley fits (TOPAZ, Bruker) for the X-ray powder diffraction pattern measured for TPB (**3**) crystallized from hexanes (a) using the unit cell of pure polymorph TPB-1 and (b) using a mixture of polymorphs TPB-1 and TPB-3. Note the better fit in the 2Θ ranges 11°-13° and 16°-22° in (b).

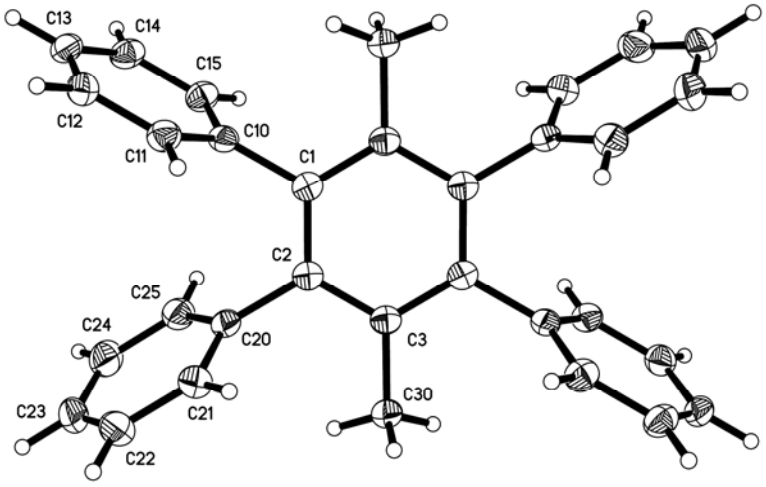

Figure S7. Thermal displacement ellipsoid plot showing the structure of crystals of DMTPB (**4**) at 100 K. The ellipsoids of non-hydrogen atoms are drawn at the 50% probability level, and hydrogen atoms are represented by a sphere of arbitrary size. Unlabeled parts of the molecule are related by the symmetry operation [*x*, 2-*y*, 1-*z*].

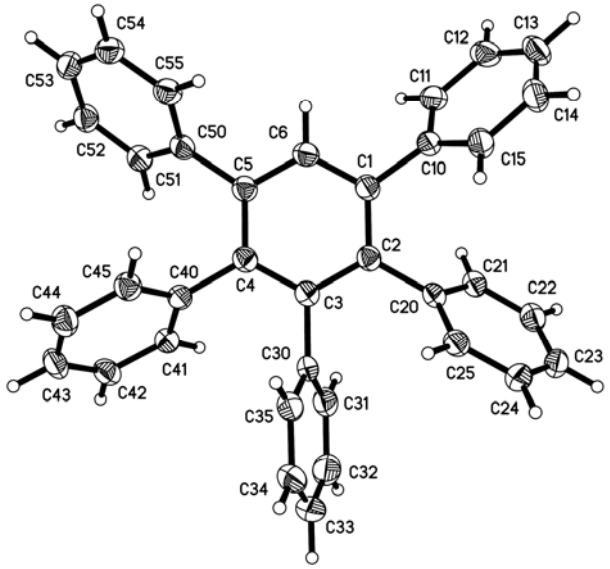

Figure S8. Thermal displacement ellipsoid plot showing the structure of crystals of polymorph PPB-1 of PPB (**5**) at 100 K. The ellipsoids of non-hydrogen atoms are drawn at the 50% probability level, and hydrogen atoms are represented by a sphere of arbitrary size.

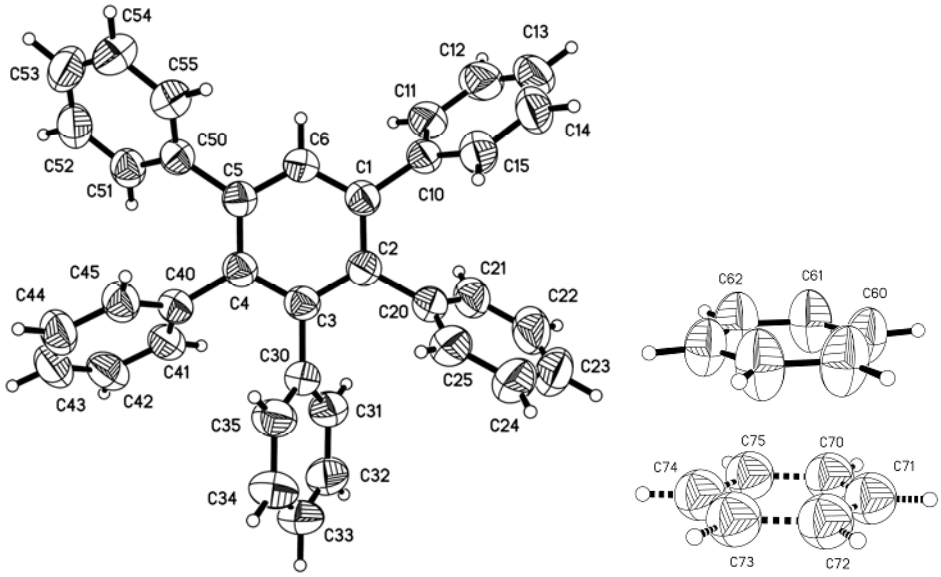

Figure S9. Thermal displacement ellipsoid plot showing the structure of crystals of pseudopolymorph PPB-2 of composition PPB (**5**) • 0.5 benzene at 150 K. The ellipsoids are drawn at the 50% probability level for C1-C55 and at the 30% probability level for C60-C75. Hydrogen atoms are represented by a sphere of arbitrary size. Unlabeled parts of the included molecule of benzene are related by the symmetry operation [-*x*, 2-*y*,1-*z*].

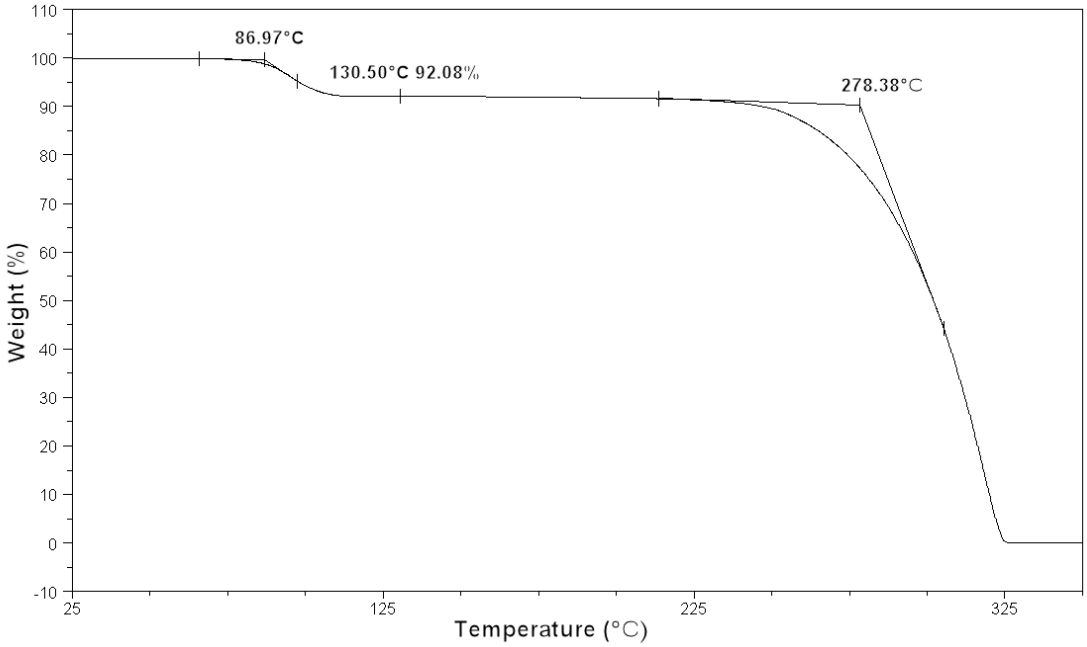

Figure S10. Thermogravimetric analysis of a crystalline sample of pseudopolymorph PPB-2 of composition PPB (**5**) • 0.5 benzene. The initial loss of weight (measured as 7.9%) closely matches the theoretical amount of included benzene (calculated to be 7.85%).

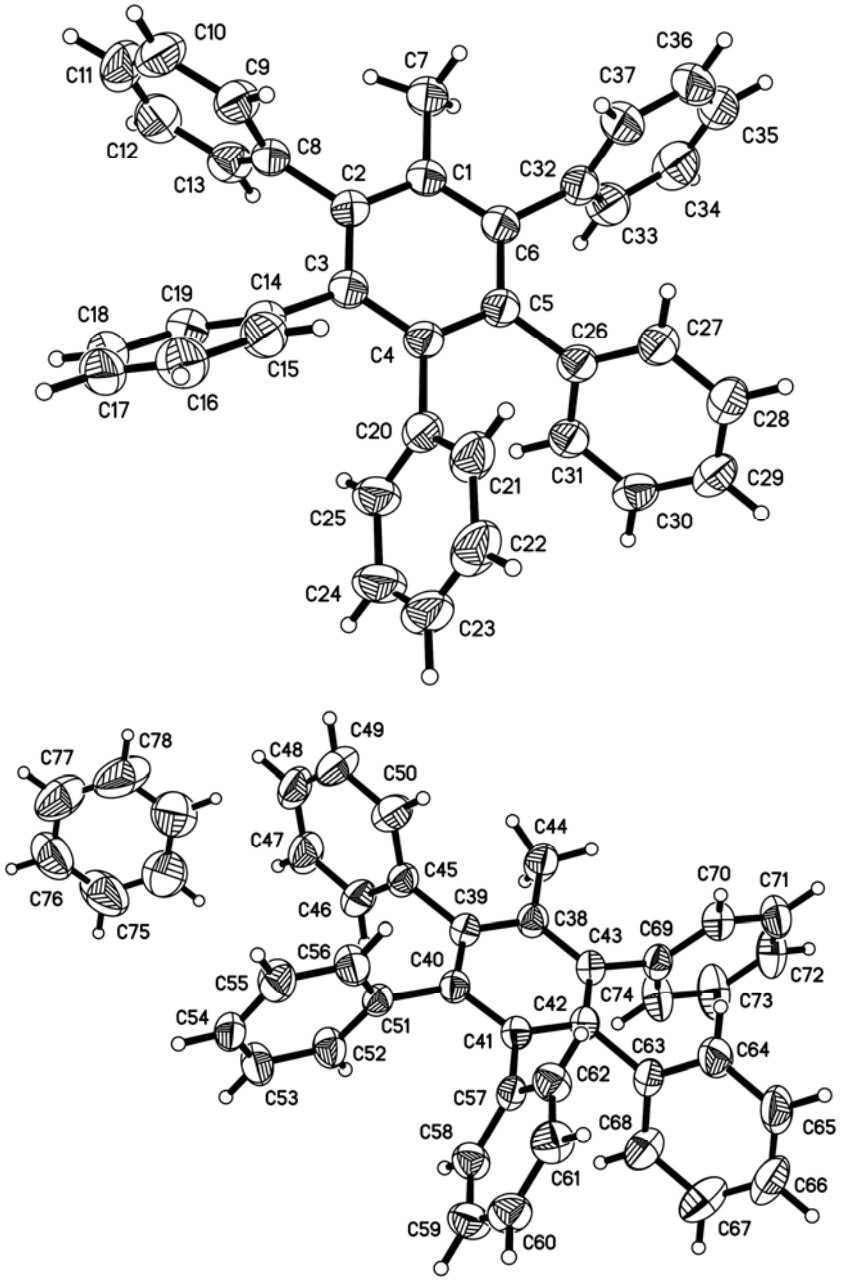

Figure S11. Thermal displacement ellipsoid plot showing the structure of crystals of MPPB (**6**) • 0.25 benzene at 150 K. The ellipsoids of non-hydrogen atoms are drawn at the 50% probability level, and hydrogen atoms are represented by a sphere of arbitrary size. Unlabeled parts of the included molecule of benzene are related by the symmetry operation [-*x*, *y*, 3/2-*z*].

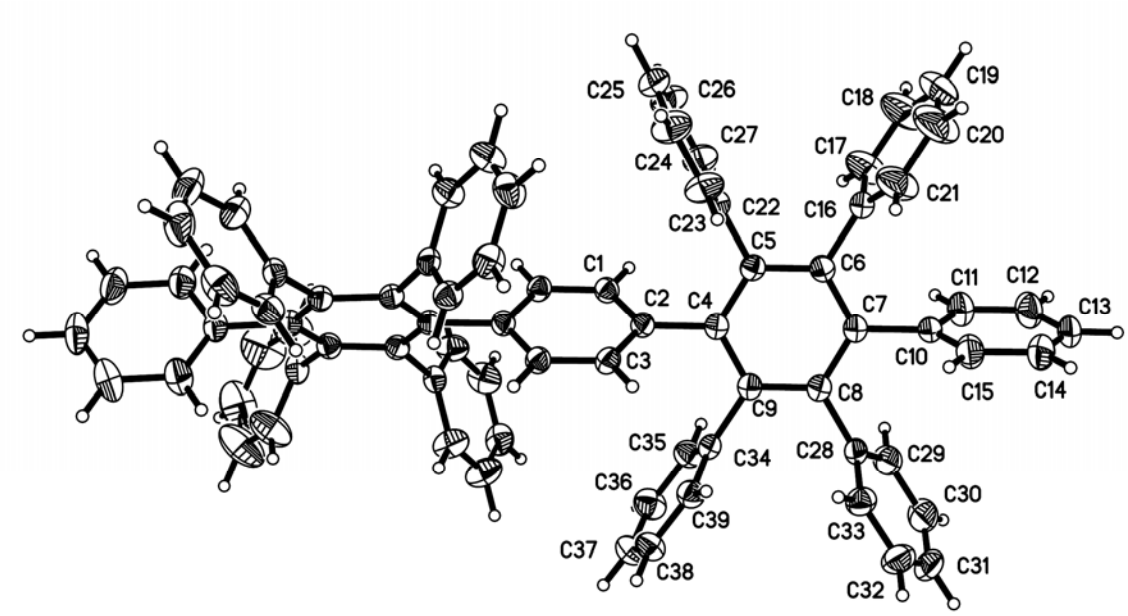

Figure S12. Thermal displacement ellipsoid plot showing the structure of crystals of OPQP (**7**) at 200 K. The ellipsoids of non-hydrogen atoms are drawn at the 50% probability level, and hydrogen atoms are represented by a sphere of arbitrary size. Unlabeled parts of the molecule are related by the symmetry operation [½-*x*, ½-*y*, *z*].

Annexe 2

Partie supplémentaire de l'article 4

Supporting Information

Hexaphenylbenzenes as Acetylene Sponges

Eric Gagnon,[†] Alain Rochefort,[‡] Valérie Métivaud,[†] and James D. Wuest[†]

[†]*Département de Chimie, Université de Montréal, Montréal, Québec H3C 3J7 Canada*

[‡]*Département de génie physique and Regroupement québécois sur les matériaux de pointe (RQMP), École Polytechnique de Montréal, Montréal, Québec H3C 3A7, Canada*

Contents **Page**

I. General Experimental Notes

Solvents and reagents. Triethylamine, THF, toluene, CH_2Cl_2, and pyridine were prepared in anhydrous O_2-free form by passage through columns packed with activated alumina and supported copper catalyst (Glass Contour, Irvine, CA). Tetraphenylcyclopentadienone,[1] hexaphenylbenzene,[2] and triflic anhydride[3] were synthesized according to reported procedures. All other solvents and reagents were purchased from commercial suppliers and used without further purification.

Spectroscopic characterizations, elemental analyses, and thermal analyses. ^{1}H, ^{13}C, and ^{19}F NMR spectra were recorded on a Bruker Avance 400 spectrometer (400 MHz for ^{1}H NMR spectra, 100 MHz for ^{13}C NMR spectra, and 376 MHz for ^{19}F NMR spectra). All peaks are reported in ppm relative to the following internal references: Peaks at δ 7.26 (^{1}H) or δ 77.16 (^{13}C) in $CDCl_3$, δ 54.0 (^{13}C) in CD_2Cl_2, δ 128.06 (^{13}C) in benzene-d_6, δ 25.40 (^{13}C) in THF-d_8, δ 0 (^{13}C) for TMS added to CD_3OD, or δ 2.50 ppm (^{1}H) in DMSO-d_6. High-resolution mass measurements were made with an Agilent Technologies TOF LC/MS spectrometer operated in positive mode by electrospray ionisation (ESI). Protonated molecular ions $[M + H]^+$, silver adducts $[M + Ag]^+$, or sodium adducts $[M + Na]^+$, or ammonium adducts $[M + NH_4]^+$ were used to confirm empirical formulas. Elemental analyses were performed either on a Fisons Instruments EA1108 analyzer or on a Costech ECS 4010 instrument. Melting points were recorded with a Barnstead Electrothermal Digital IA9200 apparatus. Thermogravimetric analysis (TGA) was done on a TA Instruments Hi-Res TGA 2950 analyzer.

X-ray crystallographic studies. Data were collected using a Bruker Microstar diffractometer with Cu Kα radiation at 150 K. The structures were solved by direct methods using SHELXS-97[4,5] and refined with SHELXL-97.[4,5] All non-hydrogen atoms were refined anisotropically, whereas hydrogen atoms were placed in ideal positions and refined as riding atoms.

CCDC 749348-749350 contains the supplementary crystallographic data for this paper. These data can be obtained free of charge from The Cambridge Crystallographic Data Centre via www.ccdc.cam.ac.uk/data_request/cif.

To confirm that single crystals selected for structural analysis were in fact representative of the bulk crystalline sample, experimental powder X-ray diffraction patterns were recorded for each bulk sample and then compared with those calculated from the single-crystal X-ray diffraction data. Experimental powder X-ray diffraction patterns were recorded at room temperature in reflection mode using one of the following two instruments:

1) **Bruker D8 Advance powder X-ray diffractometer equipped with a VÅNTEC-1 linear position-sensitive detector, using Ge-monochromatized Cu Kα_1 radiation generated at 40 kV and 40 mA.** Calibration of the instrument was done with a NIST 1976 corundum sample. For each experiment, the bulk crystalline sample was ground, the resulting powder was placed in a sample holder (PMMA holder ring), and the surface of the powder was flattened with a glass plate. Data were collected in Bragg-Brentano geometry in the range $2° < 2\theta < 60°$ with a step size of 0.025 º and a counting time of 4 s/step.
2) **Bruker D8 Discover diffractometer with GADDS HTS, using graphite monochromatized Cu Kα radiation generated at 40 kV and 40 mA.** The 2D general area detector was positioned at a distance of 15 cm from the powder sample, which was placed on a glass plate. This allowed simultaneous collection of data over an angular domain up to 35° in 2θ. Measurements were carried out in coupled scan mode (θ-θ geometry). Four separate images (diffraction arcs) were collected (scanning time: 5 min/image), and intensity along each arc was integrated to create the 1D powder pattern of intensity versus 2θ, over the angular range $10° < 2\theta < 105°$. Structural data from single-crystal analyses were used to calculate theoretical powder X-ray diffraction patterns with the aid of Mercury software. Peak fitting and the refinement of lattice parameters were carried out using TOPAS software (Bruker), and Pawley fitting was applied to the powder X-ray diffraction patterns.

II. Syntheses

Scheme S1. Synthesis of compound **1b**.

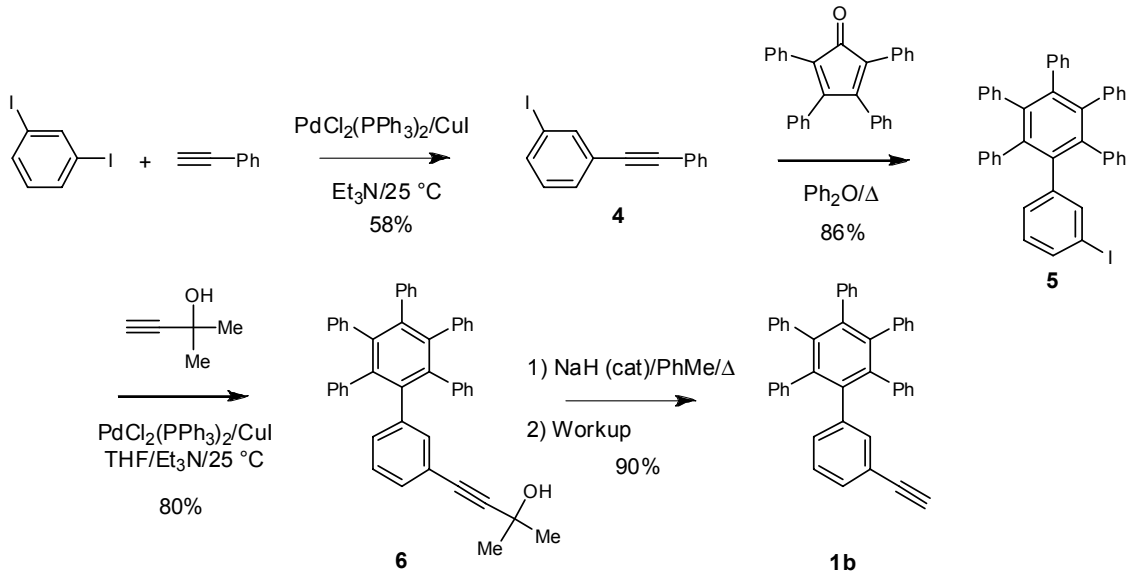

Scheme S2. Synthesis of compound **1c**.

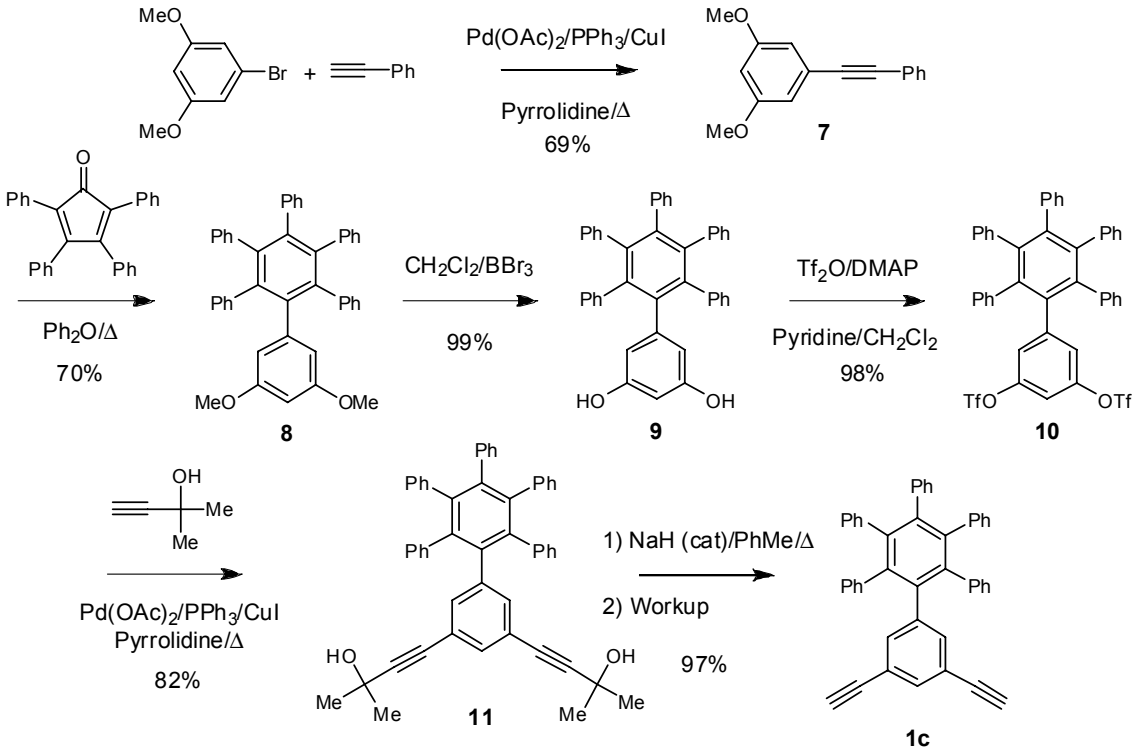

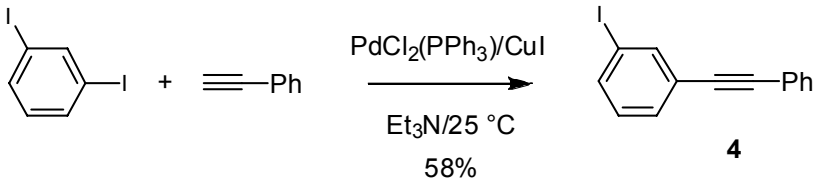

1-Iodo-3-(phenylethynyl)benzene (4). 1,3-Diiodobenzene (10.0 g, 30.3 mmol), $PdCl_2(PPh_3)_2$ (0.212 g, 0.302 mmol), and CuI (0.0576 g, 0.302 mmol) were combined in triethylamine (50 mL), and dry N_2 was bubbled through the mixture for 5 min. Phenylacetylene (3.40 mL, 3.16 g, 30.9 mmol) was then added, and a solid precipitate formed rapidly. The mixture was kept at 25 °C for 18 h. An amount of water sufficient to dissolve the precipitate was added, followed by Et_2O (150 mL). The aqueous phase was discarded, and the organic phase was washed three times with saturated aqueous NH_4Cl and once with brine. The solution was then dried with anhydrous $MgSO_4$. Volatiles were removed by evaporation under reduced pressure, and the residue was purified by flash chromatography (silica gel, 100% hexanes) to give 1-iodo-3-(phenylethynyl)benzene (**4**) as a colorless waxy solid (5.36 g, 17.6 mmol, 58%): mp 45-47 °C (lit. 45-47°C);[6] ^{1}H NMR ($CDCl_3$, 400 MHz) δ 7.91 (ddd, 1H, ^4J = 1.8 Hz, ^4J = 1.5 Hz, ^5J = 0.3 Hz), 7.67 (ddd, 1H, ^3J = 8.0 Hz, ^4J = 1.8 Hz, ^4J = 1.1 Hz), 7.55-7.51 (m, 2H), 7.49 (ddd, 1H, ^3J = 7.7 Hz, ^4J = 1.5 Hz, ^4J = 1.1 Hz), 7.38-7.33 (m, 3H), 7.08 (ddd, ^3J = 8.0 Hz, ^3J = 7.7 Hz, ^5J = 0.3 Hz); ^{13}C NMR ($CDCl_3$, 100 MHz) δ 140.3, 137.3, 131.8, 130.8, 130.0, 128.7, 128.5, 125.5, 122.9, 93.8, 90.8, 87.8; HRMS (ESI) calcd for $[C_{14}H_9I + Ag]^+$ *m/e* 410.87944, found 410.87887.

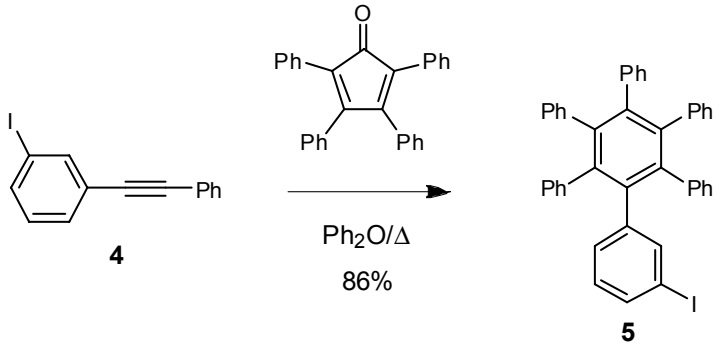

1-(3-Iodophenyl)-2,3,4,5,6-pentaphenylbenzene (5). 1-Iodo-3-(phenylethynyl)benzene (**4**; 2.00 g, 6.58 mmol) and tetraphenylcyclopentadienone (2.53 g, 6.58 mmol) were

combined in diphenyl ether (6 mL). The mixture was heated at reflux for 20 h. It was then cooled to 25 °C and diluted with MeOH (70 mL). The resulting precipitate was collected by filtration, washed twice with MeOH (15 mL portions), and dried in air to give 1-(3-iodophenyl)-2,3,4,5,6-pentaphenylbenzene (**5**) as a slightly pink powder (3.72 g, 5.63 mmol, 86%). A purified sample was obtained by crystallization from toluene/hexanes: mp 376-377 °C; ^{1}H NMR ($CDCl_3$, 400 MHz) δ 7.22 (t, 1H, ^{4}J = 1.8 Hz), 7.15 (ddd, 1H, ^{3}J = 7.8 Hz, ^{4}J = 1.8 Hz, ^{4}J = 1.1 Hz), 6.96-6.75 (m, 26H), 6.59 (t, 1H, ^{3}J = 7.8 Hz); ^{13}C NMR ($CDCl_3$, 100 MHz) δ 142.88, 140.89, 140.68, 140.55, 140.49, 140.34, 140.30, 138.85, 134.28, 131.52, 131.48, 131.44, 131.28, 130.61, 128.37, 127.00, 126.86, 126.78, 126.76, 126.75, 125.66, 125.44, 125.42, 92.53 (C-I);[7] HRMS (ESI) calcd for $[C_{42}H_{29}I + NH_4]^+$ *m/e* 678.16522, found 678.16521. Anal. Calcd for $C_{42}H_{29}I$: C, 76.36; H, 4.43. Found: C, 76.40; H, 4.41.

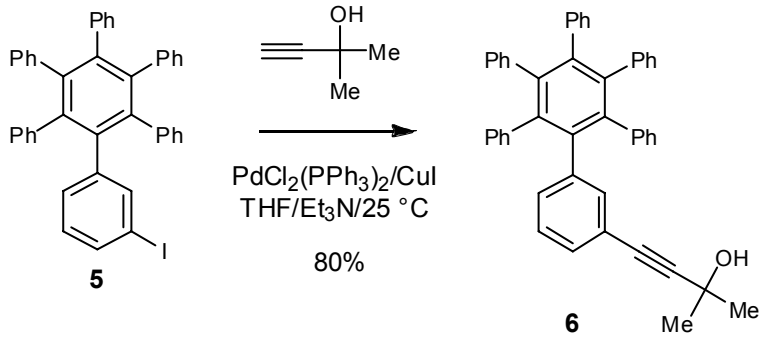

1-[3-[(3-Hydroxy-3-methyl)butynyl]phenyl]-2,3,4,5,6-pentaphenylbenzene (6). 1-(3-Iodophenyl)-2,3,4,5,6-pentaphenylbenzene (**5**; 2.00 g, 3.03 mmol), $PdCl_2(PPh_3)_2$ (0.106 g, 0.151 mmol), and CuI (0.0288 g, 0.151 mmol) were combined, dry THF (100 mL) and 2-methyl-3-butyn-2-ol (1.48 mL, 1.28 g, 15.2 mmol) were added, and the mixture was purged by bubbling a stream of dry N_2 through it for 10 min. Triethylamine (10 mL) was then added, and the mixture was stirred at 25 °C for 24 h under N_2. Volatiles were removed by evaporation under reduced pressure, and the residue was taken up in CH_2Cl_2 (100 mL). The organic phase was washed twice with saturated aqueous NH_4Cl, washed once with brine, and dried with anhydrous sodium sulfate. Removal of volatiles by evaporation under reduced pressure left a residue that was purified by flash chromatography (silica gel, 100% CH_2Cl_2) to give 1-[3-[(3-hydroxy-3-

methyl)butynyl]phenyl]-2,3,4,5,6-pentaphenylbenzene (**6**; 1.49 g, 2.42 mmol, 80%): mp 261-263 °C (dec); IR 3572, 3365 (broad), 3081, 3055, 3024, 2979, 2927, 2866, 2229, 1945, 1874, 1801, 1748, 1599, 1576, 1496, 1479, 1157 cm^{-1}; ^1H NMR ($CDCl_3$, 400 MHz) δ 6.94-6.77 (m, 29H), 1.90 (s, 1H), 1.53 (s, 6H); ^{13}C NMR ($CDCl_3$, 100 MHz) δ 140.82, 140.63, 140.55, 140.51, 140.45, 140.35, 140.30, 139.40, 134.79, 131.45, 131.40, 131.37, 131.23, 128.68, 126.87, 126.74, 126.69, 125.50, 125.34, 121.11, 92.96, 82.33, 65.53, 31.52;[7] HRMS (ESI) calcd for $[C_{47}H_{36}O + Na]^+$ *m/e* 639.26584, found 639.26633.

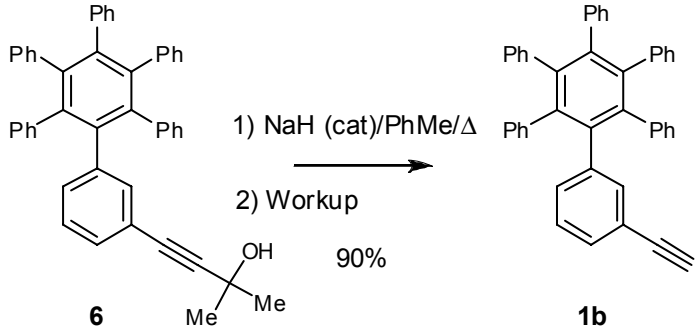

1-(3-Ethynylphenyl)-2,3,4,5,6-pentaphenylbenzene (1b). 1-[3-[(3-Hydroxy-3-methyl)butynyl]phenyl]-2,3,4,5,6-pentaphenylbenzene (**6**; 0.720 g, 1.17 mmol) and a catalytic amount of NaH (10 mg, 60% by weight in oil, 0.25 mmol) were combined in toluene (5 mL), and the mixture was heated at reflux for 100 min. The mixture was then cooled to 25 °C, and water (10 mL) was slowly added, followed by CH_2Cl_2 (75 mL). The aqueous phase was discarded, and the organic phase was washed with water and brine, dried with anhydrous $MgSO_4$, and filtered. Removal of volatiles by evaporation under reduced pressure left a residue that was purified by flash chromatography (silica gel, 25% CH_2Cl_2 in hexanes) to afford 1-(3-ethynylphenyl)-2,3,4,5,6-pentaphenylbenzene (**1b**) as an off-white solid (0.586 g, 1.05 mmol, 90%): mp 354-357 °C (dec); ^1H NMR ($CDCl_3$, 400 MHz) δ 7.00-6.78 (m, 29H), 2.87 (s, 1H); ^{13}C NMR ($CDCl_3$, 100 MHz) δ 141.03, 140.76, 140.62, 140.58, 140.53, 140.41, 140.35, 139.34, 135.22, 132.05, 131.55, 131.51, 131.49, 131.35, 129.28, 126.95, 126.80, 126.78, 126.76, 126.75, 126.73, 125.57, 125.40, 120.47, 83.97, 76.32;[7] HRMS (ESI) calcd for $[C_{44}H_{30} + H]^+$ *m/e* 559.24203, found 559.24432.

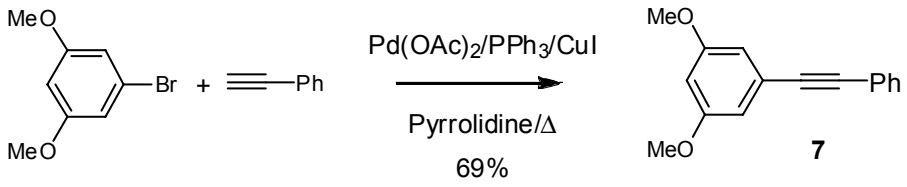

1,3-Dimethoxy-5-(phenylethynyl)benzene (7).[8] 1-Bromo-3,5-dimethoxybenzene (2.00 g, 9.21 mmol), $Pd(OAc)_2$ (0.0413 g, 0.184 mmol), PPh_3 (0.0970 g, 0.370 mmol), and CuI (0.0350 g, 0.184 mmol) were combined in a 25 mL round-bottomed flask. Pyrrolidine (5 mL) and phenylacetylene (1.06 mL, 0.984 g, 9.63 mmol) were added, and N_2 was bubbled through the mixture for 10 min. The mixture was heated at reflux for 1 h, cooled to 25 °C, and diluted with CH_2Cl_2 (100 mL). The organic phase was washed once with water, twice with saturated aqueous NH_4Cl, and once with brine. The organic phase was then dried with anhydrous $MgSO_4$ and filtered. Removal of volatiles by evaporation under reduced pressure left a residue that was purified by flash chromatography (silica gel, 30% CH_2Cl_2 in hexanes) to give 1,3-dimethoxy-5-(phenylethynyl)benzene (**7**) as a slightly orange liquid (1.52 g, 6.38 mmol, 69%): ^{1}H NMR ($CDCl_3$, 400 MHz) δ 7.62-7.56 (m, 2H) 7.43-7.36 (m, 3H), 6.76 (d, 2H, ^4J = 2.3 Hz), 6.52 (t, 1H, ^4J = 2.3 Hz), 3.84 (s, 6H); ^{13}C NMR (benzene-d_6, 100 MHz) δ 161.3, 132.0, 128.7, 128.5, 125.3, 123.9, 109.9, 102.5, 90.5, 89.7, 54.9; HRMS (ESI) calcd for $[C_{16}H_{14}O_2 + H]^+$ *m/e* 239.10666, found 239.10775.

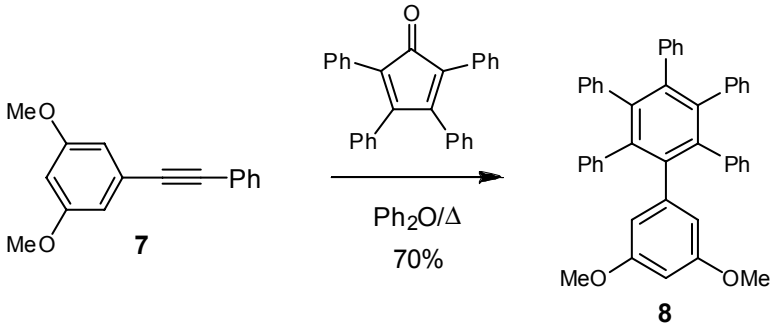

1-(3,5-Dimethoxyphenyl)-2,3,4,5,6-pentaphenylbenzene (8). 1,3-Dimethoxy-5-(phenylethynyl)benzene (**7**; 2.50 g, 10.5 mol) and tetraphenylcyclopentadienone (4.03 g, 10.5 mol) were combined in diphenyl ether (5 mL). The mixture was heated at reflux for 48 h under N_2. The resulting dark mixture was cooled to 25 °C and poured into MeOH

(120 mL). The precipitate was collected by filtration and washed with additional MeOH (30 mL). The solid was purified by flash chromatography (silica gel, 40% CH_2Cl_2 in hexanes) to provide 1-(3,5-dimethoxyphenyl)-2,3,4,5,6-pentaphenylbenzene (**8**) as an off-white solid (4.40 g, 7.40 mmol, 70%). An analytically pure sample was obtained by crystallization from toluene/hexanes: mp 323-324 °C; ^{1}H NMR ($CDCl_3$, 400 MHz) δ 6.93-6.79 (m, 25H), 6.01 (d, 2H, ^4J = 2.3 Hz), 5.98 (t, 1H, ^4J = 2.3 Hz), 3.40 (s, 6H); ^{13}C NMR (CD_2Cl_2, 100 MHz) δ 159.76, 142.94, 141.35, 141.26, 141.24, 140.95, 140.91, 140.63, 140.61, 131.93, 131.90, 131.77, 127.13, 127.08, 127.06, 125.89, 125.76, 125.75, 110.47, 98.88, 55.62; HRMS (ESI) calcd $[C_{44}H_{34}O_2 + H]^+$ *m/e* 595.26316, obtained: 595.26402. Anal. Calcd for $C_{44}H_{34}O_2$: C, 88.86; H, 5.76. Found: C, 88.94; H, 5.87.

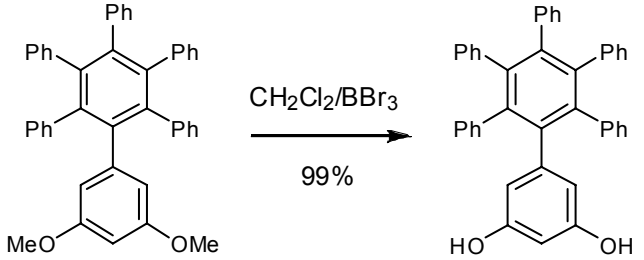

8 **9**

1-(3,5-Dihydroxyphenyl)-2,3,4,5,6-pentaphenylbenzene (9). A stirred solution of 1-(3,5-dimethoxyphenyl)-2,3,4,5,6-pentaphenylbenzene (**8**; 3.00 g, 5.04 mmol) in dry CH_2Cl_2 (50 mL) was cooled to -78 °C under N_2, and a solution of BBr_3 in CH_2Cl_2 (1.0 M, 20 mL, 20 mmol) was added dropwise. The cooling bath was removed, and the temperature of the mixture was allowed to rise to 25 °C overnight. Water (20 mL) was added slowly, followed by AcOEt (300 mL) to dissolve the precipitate. The aqueous phase was discarded, and the organic phase was washed successively with water, 5% (w/v) aqueous $NaHCO_3$, and brine. The washed organic phase was then dried with anhydrous $MgSO_4$ and filtered through a pad of silica gel, using AcOEt to elute the product. Removal of volatiles by evaporation under reduced pressure left a residue of 1-(3,5-dihydroxyphenyl)-2,3,4,5,6-pentaphenylbenzene (**9**; 2.85 g, 5.03 mmol, 99%). A purified sample was obtained by flash chromatography (silica gel, 5% AcOEt in CH_2Cl_2): mp > 400 °C; ^{1}H NMR (DMSO-d_6, 400 MHz) δ 8.67 (s, 2H), 6.92-6.73 (m, 25H), 5.76 (d, 2H, ^4J = 2.2 Hz), 5.64 (t, 1H, ^4J = 2.2 Hz); ^{13}C NMR (THF-d_8, 100 MHz)

δ 158.31, 143.01, 141.97, 141.93, 141.87, 141.81, 141.31, 141.22, 141.14, 132.46, 132.43, 132.19, 127.37, 127.36, 127.32, 125.94, 125.87, 125.84, 111.23, 101.03; HRMS (ESI) calcd for $[C_{42}H_{30}O_2 + H]^+$ *m/e* 567.23186, found 567.23188. Anal. Calcd for $C_{42}H_{30}O_2$: C, 89.02; H, 5.34. Found: C, 88.63; H, 5.42.

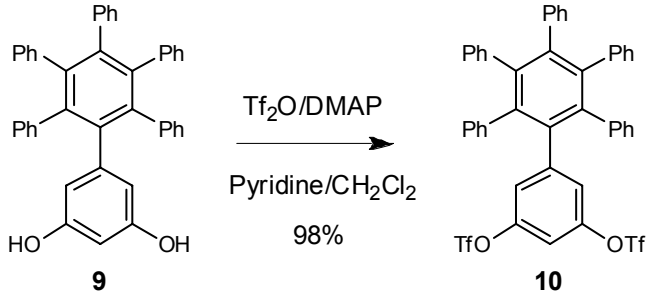

9 **10**

1-[3,5-Bis(trifluoromethanesulfonyloxy)phenyl]-2,3,4,5,6-pentaphenylbenzene (10): 1-(3,5-Dihydroxyphenyl)-2,3,4,5,6-pentaphenylbenzene (**9**; 1.31 g, 2.31 mmol) was dissolved in CH_2Cl_2 (50 mL) and pyridine (0.940 mL, 11.7 mmol). A catalytic amount of DMAP (~5 mg) was added, and the mixture was stirred and cooled to 0 °C under N_2. Triflic anhydride (1.96 mL, 3.29 g, 11.7 mmol) was added dropwise during 5 min. The mixture was kept at 0 °C for 30 minutes, and then 1 N aqueous HCl (20 mL) was added slowly. The aqueous phase was discarded, and the organic phase was washed with 1 N aqueous HCl, 5% (w/v) aqueous $NaHCO_3$, and brine. The washed phase was dried with anhydrous $MgSO_4$ and filtered through a pad of silica gel, using CH_2Cl_2 as eluent. Volatiles were then removed by evaporation under reduced pressure to yield 1-[3,5-bis(trifluoromethanesulfonyloxy)phenyl]-2,3,4,5,6-pentaphenylbenzene (**10**; 1.89 g, 2.27 mmol, 98%). Purification by flash chromatography (silica gel, 30% CH_2Cl_2 in hexanes) yielded a colorless solid: mp 221-222 °C; ^{1}H NMR ($CDCl_3$, 400 MHz) δ 6.95-6.79 (m, 27H), 6.75 (t, 1H, ^4J = 2.2 Hz); ^{13}C NMR ($CDCl_3$, 100 MHz) δ 148.26, 146.10, 142.06, 140.92, 140.14, 140.09, 139.86, 139.18, 136.65, 131.29, 131.28, 131.01, 127.39, 126.92, 126.88, 126.27, 125.73, 125.68, 124.18, 118.62 (quartet, $^1J_{C\text{-}F}$ = 320 Hz), 112.17; ^{19}F NMR ($CDCl_3$, 376 MHz) δ -73.5; HRMS (ESI) calcd for $[C_{44}H_{28}F_6O_6S_2 + Na]^+$ *m/e* 853.11237, found 853.10970. Anal. Calcd for $C_{44}H_{28}F_6O_6S_2$: C, 63.61; H, 3.40; S, 7.72. Found: C, 63.65; H, 3.34; S, 7.53.

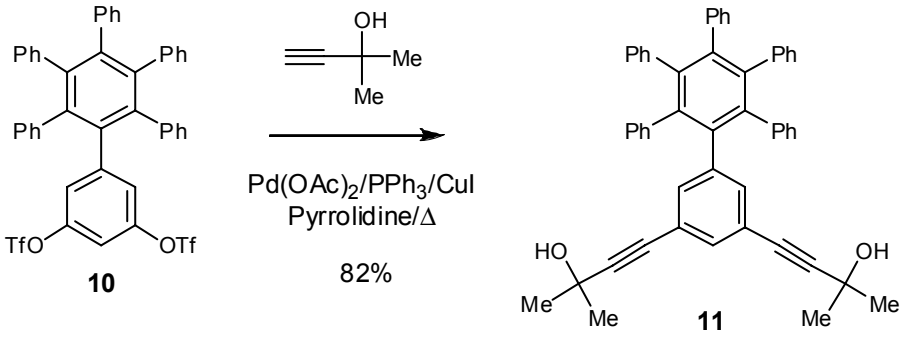

1-[3,5-Bis[(3-hydroxy-3-methyl)butynyl]phenyl]-2,3,4,5,6-pentaphenylbenzene (11). For 5 min, a stream of N_2 was bubbled through a mixture of 1-[3,5-bis(trifluoromethanesulfonyloxy)phenyl]-2,3,4,5,6-pentaphenylbenzene (**10**; 1.00 g, 1.20 mmol), $Pd(OAc)_2$ (0.0135 g, 0.0601 mmol), PPh_3 (0.0316 g, 0.120 mmol), and CuI (0.0115 g, 0.0604 mmol) in pyrrolidine (5 mL). 2-Methyl-3-butyn-2-ol (1.18 mL, 1.02 g, 12.1 mmol) was subsequently added, and the mixture was heated at reflux for 80 min. The resulting mixture was cooled to 25 °C, diluted with CH_2Cl_2 (50 mL), and washed three times with saturated aqueous NH_4Cl, once with water, and once with brine. The organic phase was then dried with anhydrous $MgSO_4$ and filtered. Volatiles were removed by evaporation under reduced pressure, and the residue was purified by flash chromatography (silica gel, 5% AcOEt in CH_2Cl_2) to provide 1-[3,5-bis[(3-hydroxy-3-methyl)butynyl]phenyl]-2,3,4,5,6-pentaphenylbenzene (**11**) as a nearly colorless solid (0.686 g, 0.982 mmol, 82%): mp 269-270 °C (dec); ^{1}H NMR ($CDCl_3$, 400 MHz) δ 6.95 (t, 1H, ^4J = 1.6 Hz), 6.93-6.79 (m, 27H), 1.91 (s, 2H), 1.51 (s, 12H); ^{13}C NMR (CD_3OD/TMS, 100 MHz) δ 142.76, 142.35, 142.97, 141.84, 141.78, 141.68, 141.50, 140.04, 135.15, 132.70, 132.57, 132.56, 132.48, 127.88, 127.70, 127.68, 126.72, 126.41, 126.39, 123.22, 95.19, 81.70, 65.79, 31.62; HRMS (ESI) calcd for $[C_{52}H_{42}O_2 + Na]^+$ *m/e* 721.30770, found 721.30776.

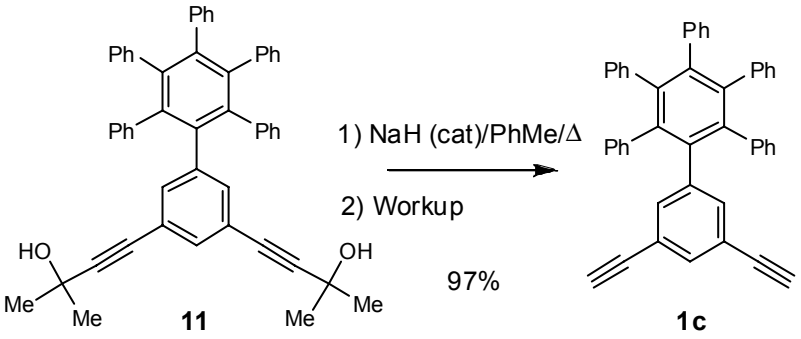

1-(3,5-Diethynylphenyl)-2,3,4,5,6-pentaphenylbenzene (1c): 1-[3,5-Bis[(3-hydroxy-3-methyl)butynyl]phenyl]-2,3,4,5,6-pentaphenylbenzene (**11**; 0.150 g, 0.215 mmol) and NaH (10 mg, 60% by weight in oil, 0.25 mmol) were combined in toluene (10 mL). The mixture was stirred at reflux for 75 min, cooled to 25 °C, and diluted with CH_2Cl_2 (75 mL). The resulting mixture was washed with 1 N aqueous HCl and brine, and then it was dried over anhydrous $MgSO_4$. Purification by column chromatography (silica gel, 40% CH_2Cl_2 in hexanes) afforded 1-(3,5-diethynylphenyl)-2,3,4,5,6-pentaphenylbenzene (**1c**) as a colorless solid (0.121 g, 0.208 mmol, 97%): ^{1}H NMR ($CDCl_3$, 400 MHz) δ 7.10 (t, 1H, ^4J = 1.5 Hz), 6.97 (d, 2H, ^4J = 1.5 Hz), 6.94-6.80 (m, 25H), 2.88 (s, 2H); ^{13}C NMR (CD_2Cl_2, 100 MHz) δ 142.05, 141.48, 141.07, 141.00, 140.99, 140.70, 140.62, 138.71, 135.76, 133.19, 131.83, 131.82, 131.76, 127.32, 127.11, 127.09, 126.16, 125.86, 125.84, 121.33, 82.85, 77.70; HRMS (ESI) calcd for $[C_{46}H_{30} + H]^+$ *m/e* 583.24203, found 583.24290. Anal. Calcd for $C_{53}H_{38}$ [**1c** + PhMe]: C, 94.32; H, 5.68. Found: C, 94.43; H, 5.65.

III. Thermal Analysis

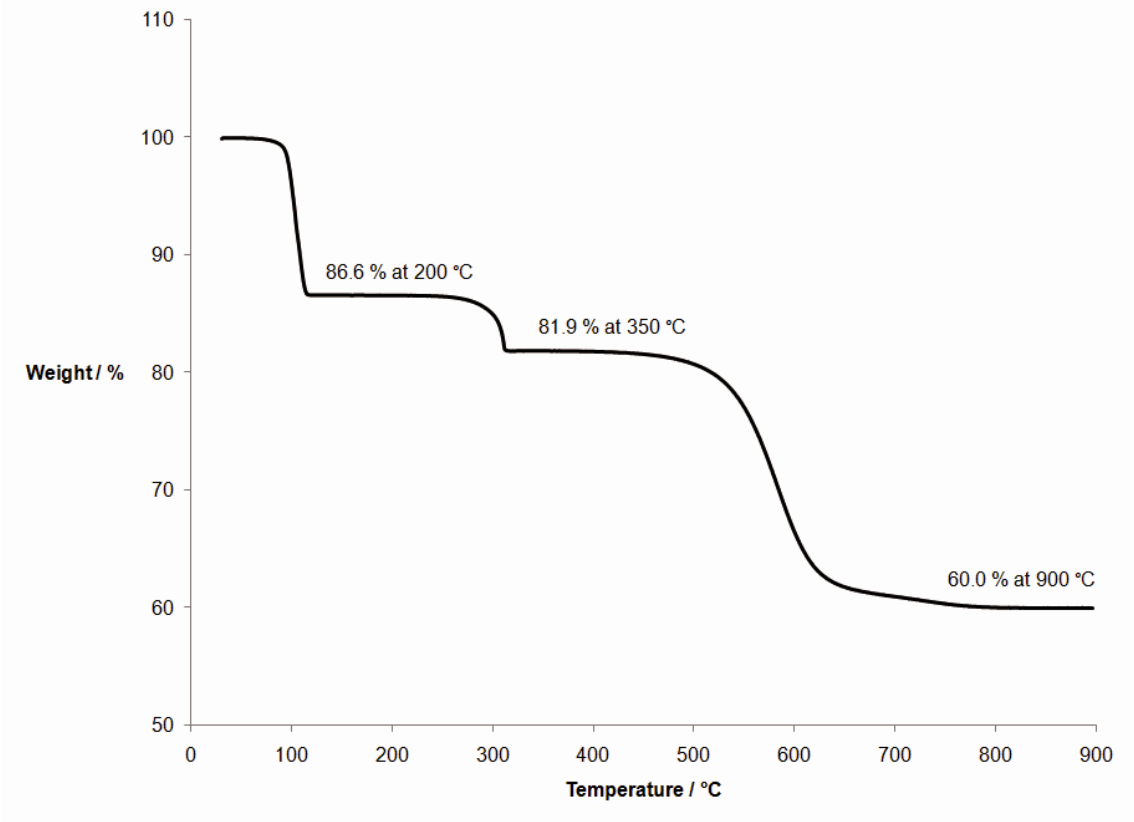

Figure S1. Thermogravimetric analysis of co-crystals of composition **1c** • 1 toluene, carried out under N_2 using a rate of heating of 10 °C/min. The first weight loss (13.4%) corresponds to a quantitative loss of included toluene, within experimental error (theoretical value of 13.7%).

IV. Crystallographic Details

Table S1. Crystallographic Data for Compounds **1a** • 0.5 PhC≡CH, **1b**, and **1c** • 1 toluene.

Compound	**1a** • 0.5 PhC≡CH	**1b**	**1c** • 1 toluene
formula	$C_{92}H_{66}$	$C_{44}H_{30}$	$C_{53}H_{38}$
crystal system	monoclinic	orthorhombic	triclinic
space group	*Cc*	*Pna*21	*P*-1
a (Å)	12.3608(7)	11.5889(5)	11.9507(6)
b (Å)	45.744(3)	21.2681(9)	12.4620(6)
c (Å)	11.5273(7)	12.6708(6)	13.2343(7)
α (°)	90	90	91.379(2)
β (°)	100.850(2)	90	98.081(2)
γ (°)	90	90	95.229(2)
V (Å^3)	6401.3(7)	3123.0(2)	1941.93(17)
Z	4	4	2
ρ_{calcd} (g cm^{-3})	1.216	1.188	1.154
T (K)	150	150	150
μ (mm^{-1})	0.520	0.509	0.493
R_1, $I > 2\sigma(I)$ (%)	3.12	4.79	4.35
R_1, *all data* (%)	3.15	5.18	4.60
ωR_2, $I > 2\sigma(I)$ (%)	8.51	13.60	11.74
ωR_2, *all data* (%)	8.54	14.06	12.03
measured reflections	68698	66558	42170
independent reflections	5832	2961	6998
observed reflections, $I > 2\sigma(I)$	5778	1734	6454

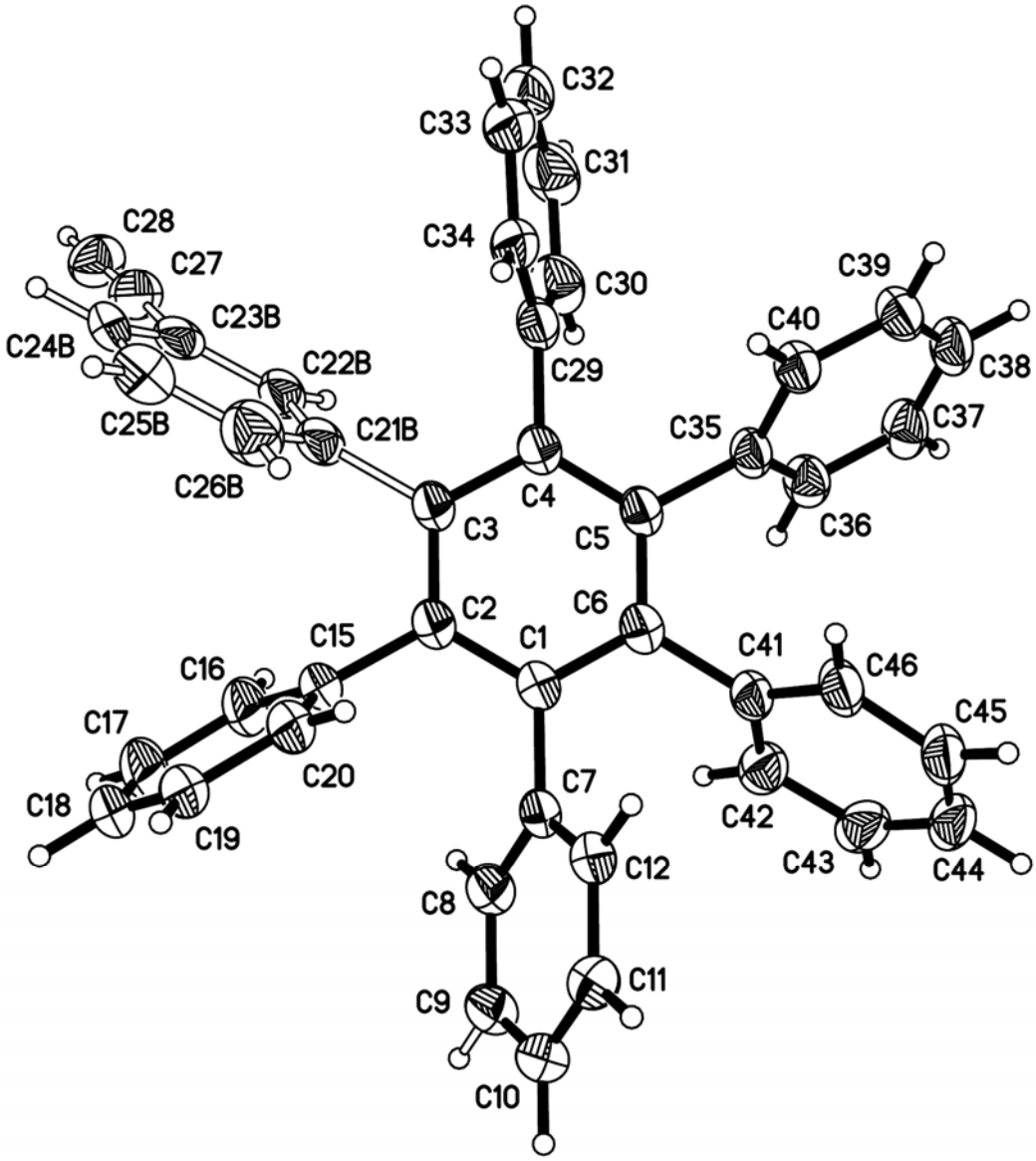

Figure S2. ORTEP view of the structure of crystals of 1-(3-ethynylphenyl)-2,3,4,5,6-pentaphenylbenzene **(1b)** grown from CH_2Cl_2. The ellipsoids of non-hydrogen atoms are drawn at the 30% probability level, and hydrogen atoms are represented by a sphere of arbitrary size.

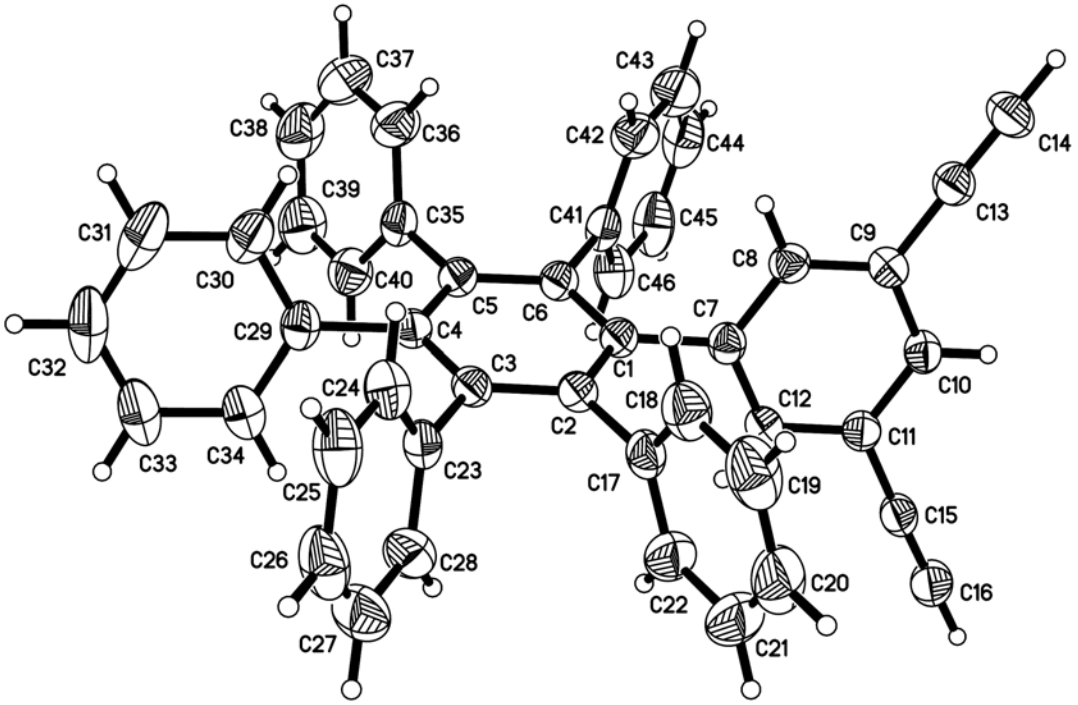

Figure S3. ORTEP view of the structure of crystals of 1-(3,5-diethynylphenyl)-2,3,4,5,6-pentaphenylbenzene **(1c)** grown from toluene/hexanes. The ellipsoids of non-hydrogen atoms are drawn at the 50% probability level, and hydrogen atoms are represented by a sphere of arbitrary size. Guest molecules are omitted for clarity.

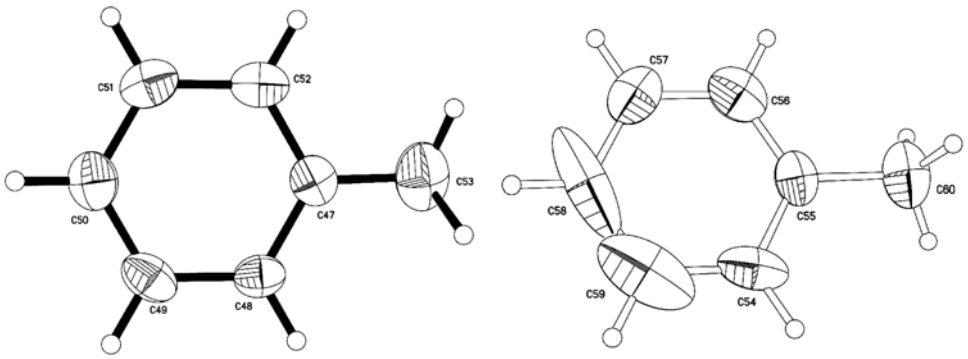

Figure S4. ORTEP view of disordered toluene included in the structure of crystals of 1-(3,5-diethynylphenyl)-2,3,4,5,6-pentaphenylbenzene **(1c)** grown from toluene/hexanes. The major disordered component is shown on the left (C47-C53) and the minor component on the right (C55-C60). The ellipsoids of non-hydrogen atoms are drawn at the 30% probability level, and hydrogen atoms are represented by a sphere of arbitrary size.

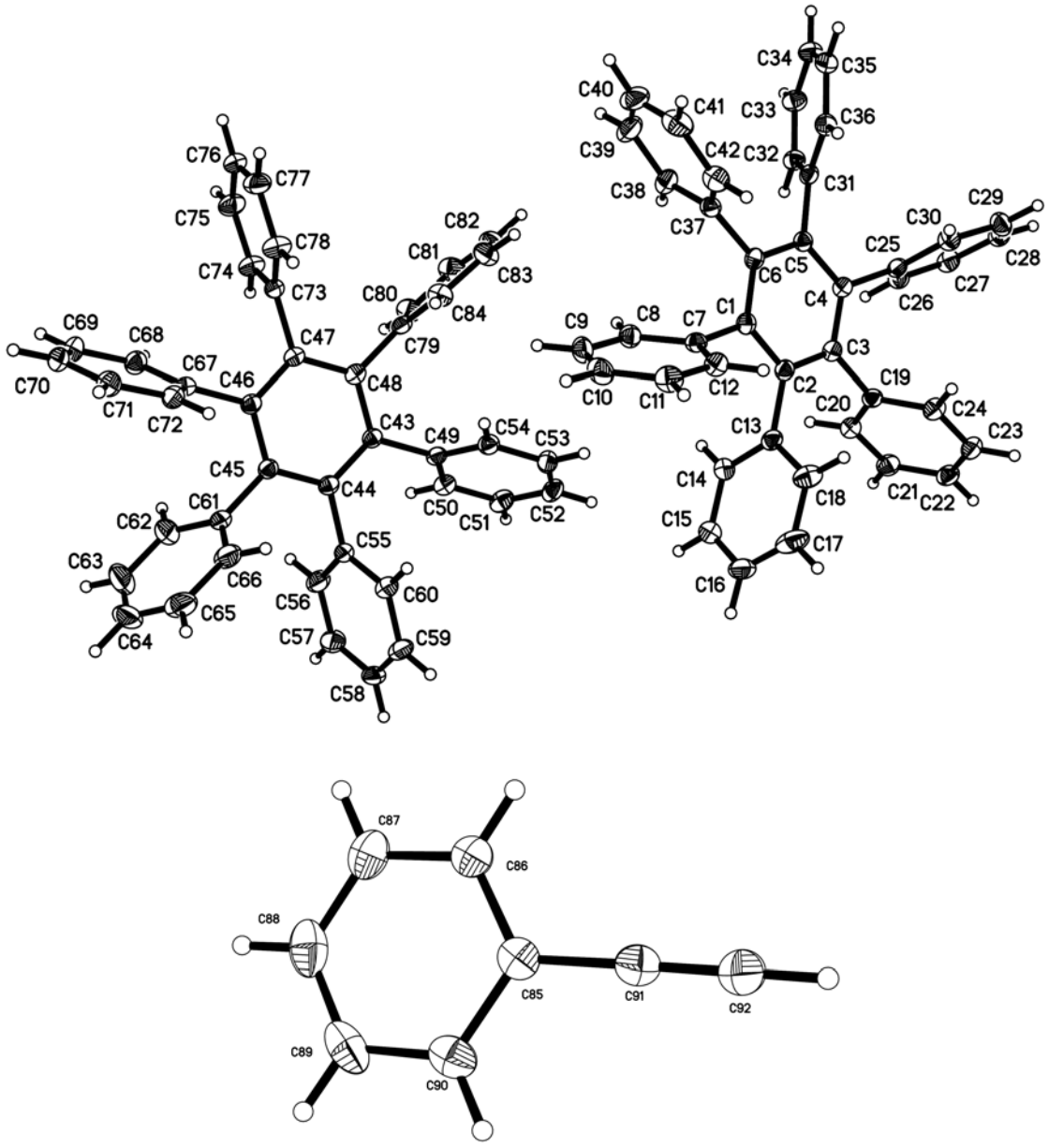

Figure S5. ORTEP view of the structure of co-crystals of hexaphenylbenzene **(1a)** • 0.5 PhC≡CH. The ellipsoids of non-hydrogen atoms are drawn at the 30% probability level, and hydrogen atoms are represented by a sphere of arbitrary size.

Table S2. Evidence for Strong C-H···π Interactions Based on Reduced Thermal Vibrations of R-C_1≡C_2-H Groups.

Compound		$U_{eq}(C_1)$	$U_{eq}(C_2)$	$U_{eq}(C_2)/U_{eq}(C_1)$[a]
1a • 0.5 PhC≡CH		0.0427(4)	0.0553(5)	1.30
1b		0.0361(2)	0.0450(3)	1.25
		0.0368(3)	0.0467(3)	1.27
1c • toluene	minor part	0.0711(16)	0.0811(19)	1.14
	major part	0.072(2)	0.086(3)	1.19

[a]When a terminal C(*sp*)–H bond participates in an intermolecular C(*sp*)-H···π interaction, the quantity defined by $U_{eq}(C_2)/U_{eq}(C_1)$ is expected to fall below 1.4.[9]

Powder X-ray diffraction

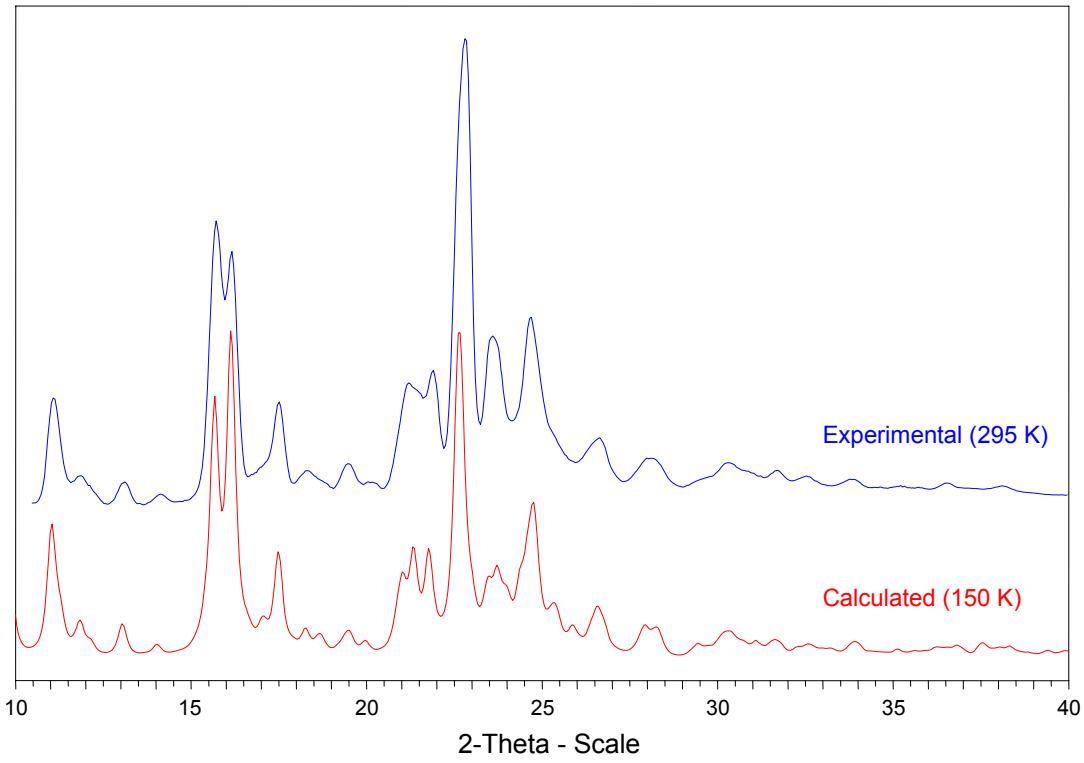

Figure S6. Comparison between experimental (collected using D8 Discover) and calculated powder X-ray diffraction patterns for crystals of compound **1a** • 0.5 PhC≡CH. The *x*-axis of the experimental pattern was shifted to minimize the slight angular shift due to the effect of temperature. The two diffractograms are closely similar, confirming that the bulk crystalline sample consists of a single phase.

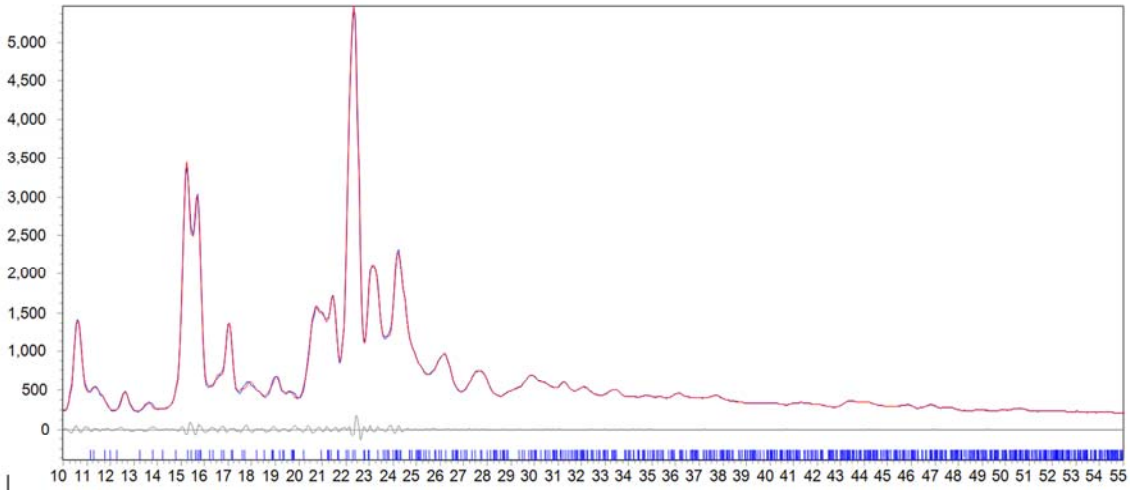

Figure S7. (a) Simulated powder X-ray diffraction pattern of crystals of compound **1a** • 0.5 phenylacetylene (red curve) as determined by Pawley fitting of the experimental powder X-ray diffraction pattern (nearly superimposed blue curve). (b) Difference between experimental and calculated intensities. (c) Position of calculated reflections.

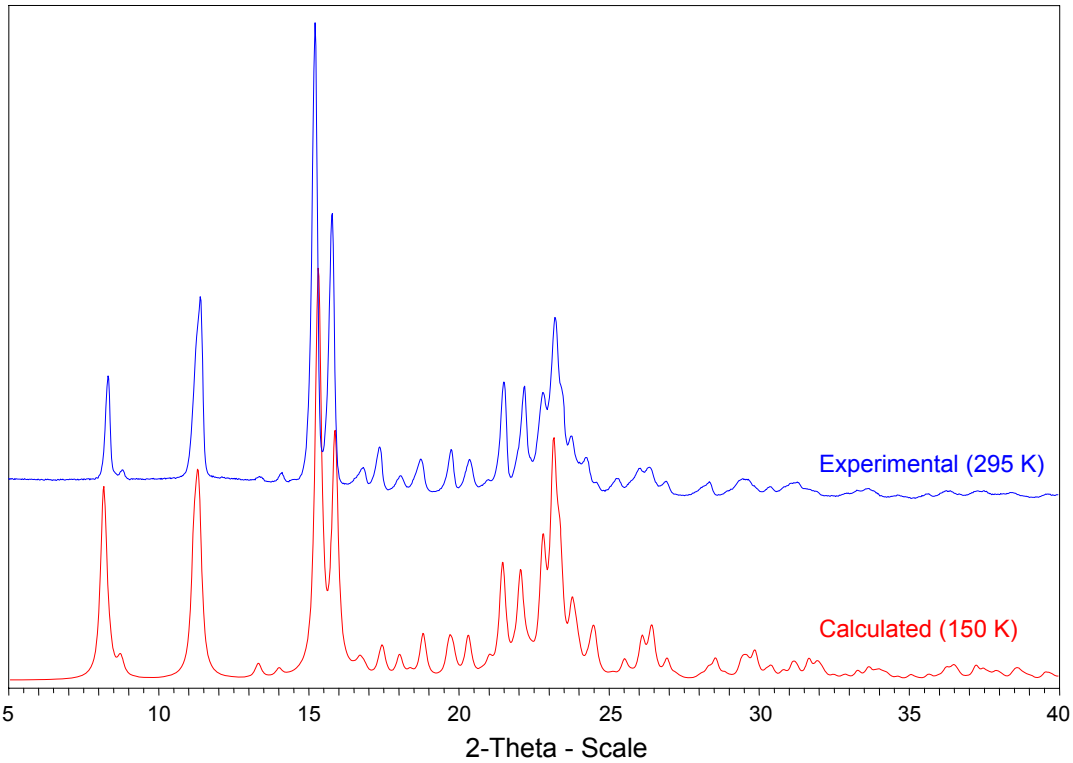

Figure S8. Comparison between experimental (collected using D8 Advance) and calculated powder X-ray diffraction patterns for crystals of compound **1b**. The *x*-axis of the experimental pattern was shifted to minimize the slight angular shift due to the effect of temperature. The two diffractograms are closely similar, demonstrating that the bulk crystalline sample is homogeneous.

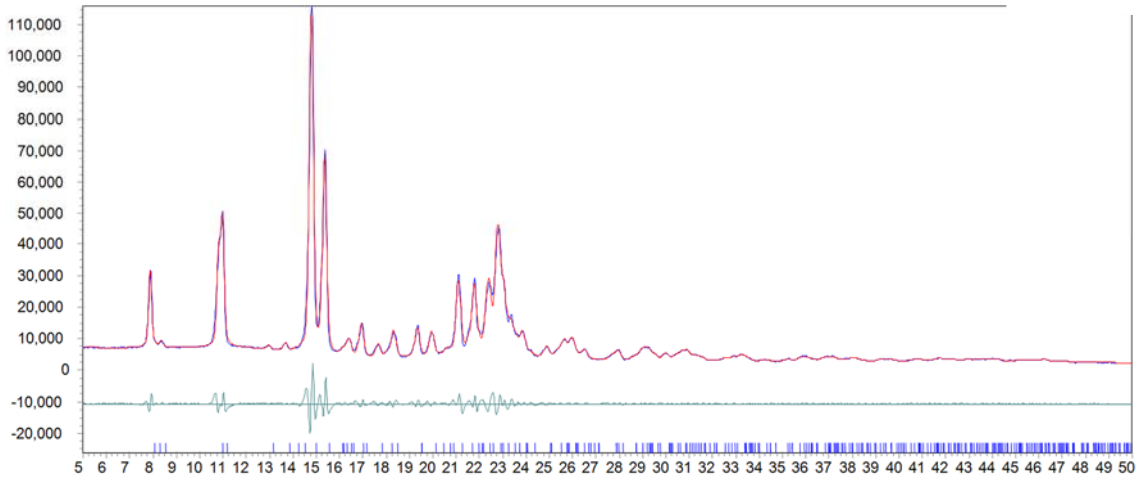

Figure S9. (a) Simulated powder X-ray diffraction pattern of compound **1b** (red curve) as determined by Pawley fitting of the experimental powder X-ray diffraction pattern (nearly superimposed blue curve). (b) Difference between experimental and calculated intensities. (c) Position of calculated reflections.

Table S3. Crystallographic Data for Compounds **1a** • 0.5 PhC≡CH and **1b** as Determined by Pawley Fitting of Powder X-Ray Diffraction Data at 295 K.

Compound	**1a** • 0.5 PhC≡CH	**1b**
composition	$C_{92}H_{66}$	$C_{44}H_{30}$
temperature (K)	295	295
crystal system	monoclinic	orthorhombic
space group	*Cc*	$Pna2_1$
a (Å)	12.246 (66)	11.8160 (20)
b (Å)	45.04 (30)	21.3097 (47)
c (Å)	11.407 (65)	12.7551 (20)
α (°)	90	90
β (°)	101.64 (26)	90
γ (°)	90	90
V (Å^3)	6162.3 (9)	3211.7 (10)
Z	4	4

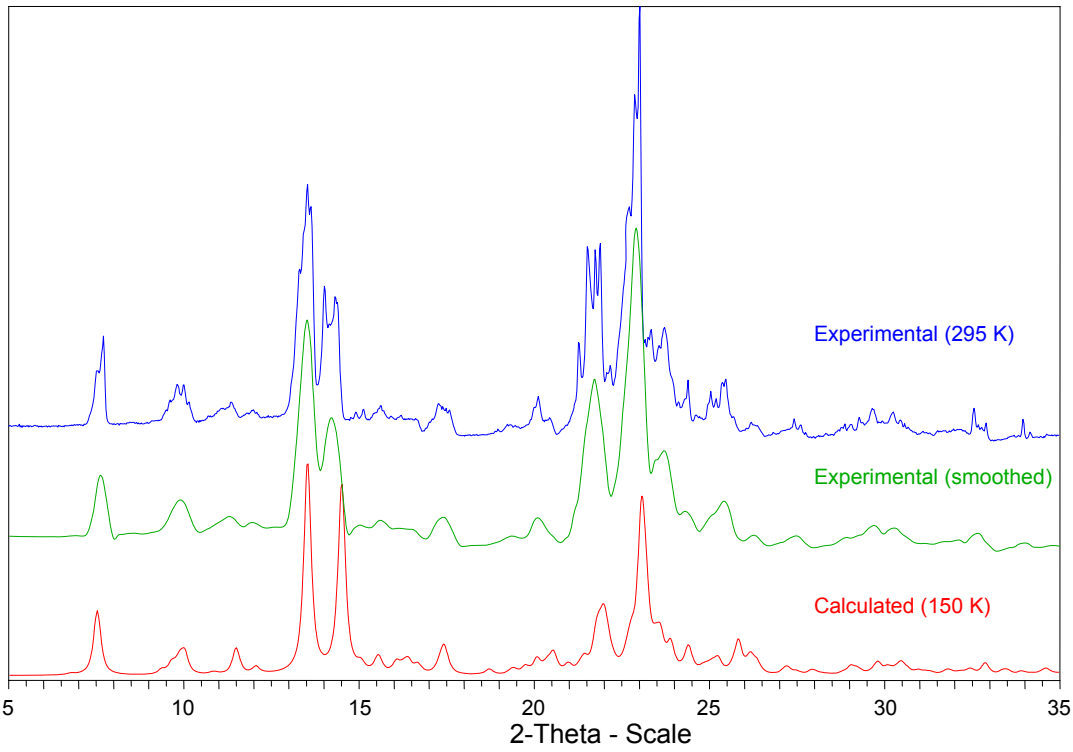

Figure S10. Comparison between experimental (collected using D8 Advance) and calculated powder X-ray diffraction patterns for compound **1c** • toluene. The relatively poor quality of the experimental pattern is due to the small amount of material available. For a better comparison, the pattern was smoothed, and the *x*-axis was shifted to minimize the slight angular shift due to the effect of temperature. The two diffractograms are in good agreement, confirming that the bulk crystalline sample is essentially homogeneous.

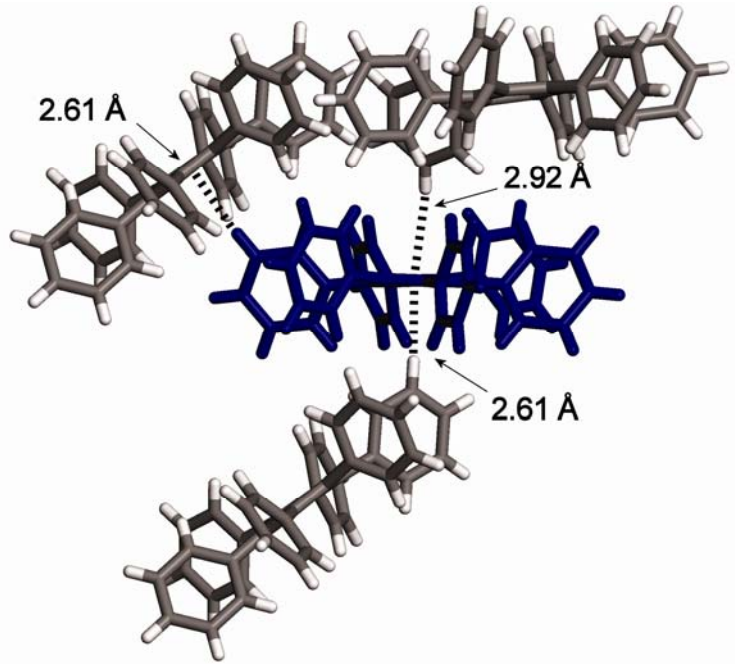

Figure S11. C–H···π interactions between molecules of hexaphenylbenzene (**1a**) in the structure of the co-crystal **1a** • 0.5 PhC≡CH. The central molecule (blue) participates in three interactions with neighbors (C-H···centroid distances/angles are 2.61 Å/171° (2×) and 2.92 Å/153°). The molecule of hexaphenylbenzene shown in blue also interacts with a molecule of PhC≡CH, which is not shown for clarity. This interaction is described in Figure 3 of the manuscript.

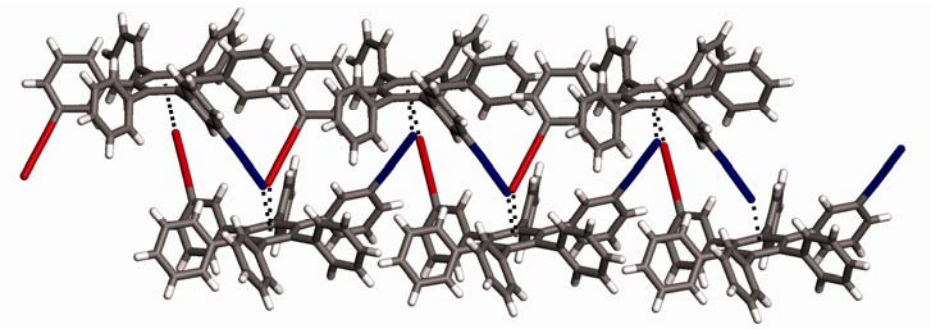

Figure S12. Packing of the two disordered components in crystals of hexaphenylbenzene **1b** grown from CH_2Cl_2. The major component (ethynyl group in blue, 56%) and the minor component (ethynyl group in red, 44%) form very similar patterns of C-H···π interactions. Both lead to a supramolecular chain maintained by C-H···π interactions between the ethynyl C(*sp*)-H and the central aromatic ring of a hexaphenylbenzene unit.

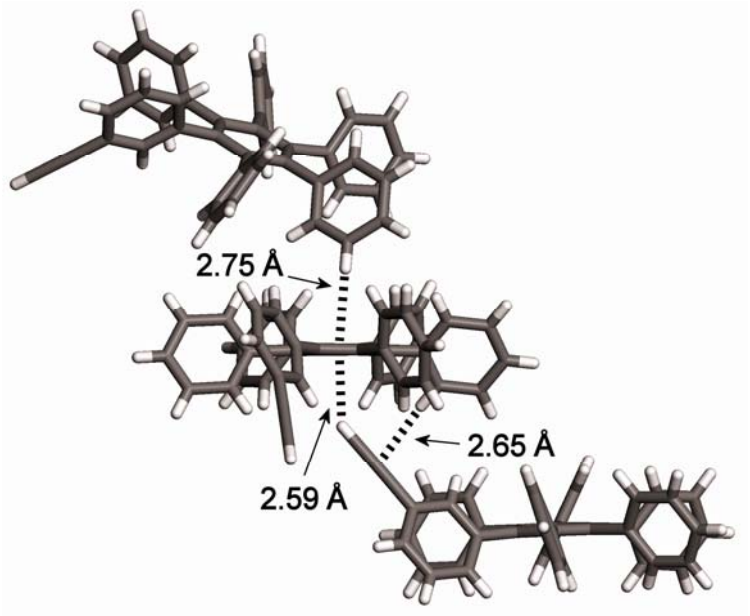

Figure S13. View showing intermolecular C-H···π interactions involving the minor component in the disordered structure of crystals of compound **1b** grown from CH_2Cl_2. A C(sp^2)-H···π interaction is formed between the top molecule and the central aromatic ring of the middle molecule (C-H···$\pi_{centroid}$ distance/angle = 2.75 Å/164°), a C(*sp*)-H···π interaction is formed between the central aromatic ring of the middle molecule and the ethynyl group of the bottom molecule (2.59 Å/142°), and a C(sp^2)-H···π interaction involves the middle molecule and the acetylenic π-electrons of the bottom molecule as the acceptor (2.59 Å/139°).

V. DFT Calculations

Quantum chemical density functional theory (DFT) calculations were performed with the NWChem software package.[10] We used the 6-31G* basis set for carbon and hydrogen atoms in conjunction with the LDA and B3LYP functional. The use of LDA was motivated by its good performance in describing both equilibrium geometries and total energies of π-stacked complexes.[11,12] In the case of B3LYP calculations, the approach used to calculate the π-complexes was similar to the one employed by Grimme[13] to evaluate van der Waals (dispersion) interactions (vdW). Structures were fully optimized without symmetry constraints using the quasi-Newton method until a gradient convergence factor better than 10^{-5} hartree/bohr was reached. Basis set superposition errors (BSSE) were evaluated for the B3LYP + vdW complexes according to the standard counterpoise correction method. The binding energies of acetylene to the aromatic moieties were evaluated with respect to the appropriate isolated and unrelaxed asymptote species. The relative stability of the triphenylbenzene conformations was calculated with respect to the ground-state geometry, in which the phenyl substituents are tilted by approximately 34° from the central benzene plane.

Table S4. Geometric Parameters for the Interaction of Acetylene with Benzene, 1,3,5-Triphenylbenzene, and Hexaphenylbenzene, Obtained by Optimization with Different Methods of Calculation.[a]

Molecule interacting with acetylene	LDA	B3LYP + vdW	B3LYP + vdW – BSSE
Benzene	2.19 Å	2.31 Å	2.31 Å
TPB-planar[b,c]	2.18 Å	2.22 Å	2.22 Å
TPB-twisted[b,d]	2.17 Å	2.28 Å	2.28 Å
TPB-perpendicular[b,e]	2.11 Å	2.24 Å	2.24 Å
HPB-perpendicular[f]	2.06 Å	2.18 Å	2.18 Å

[a]Acetylene is placed perpendicular to the plane of the interacting aromatic ring. The geometric values correspond to the optimized hydrogen-plane distance.

[b]TPB = 1,3,5-triphenylbenzene

[c]The dihedral angles between the peripheral phenyl rings and the central aromatic ring are 0°.

[d]The dihedral angles between the peripheral phenyl rings and the central aromatic ring are 34°.

[e]The dihedral angles between the peripheral phenyl rings and the central aromatic ring are 90°.

[f]HPB = hexaphenylbenzene. The peripheral phenyl rings are perpendicular to the central aromatic ring.

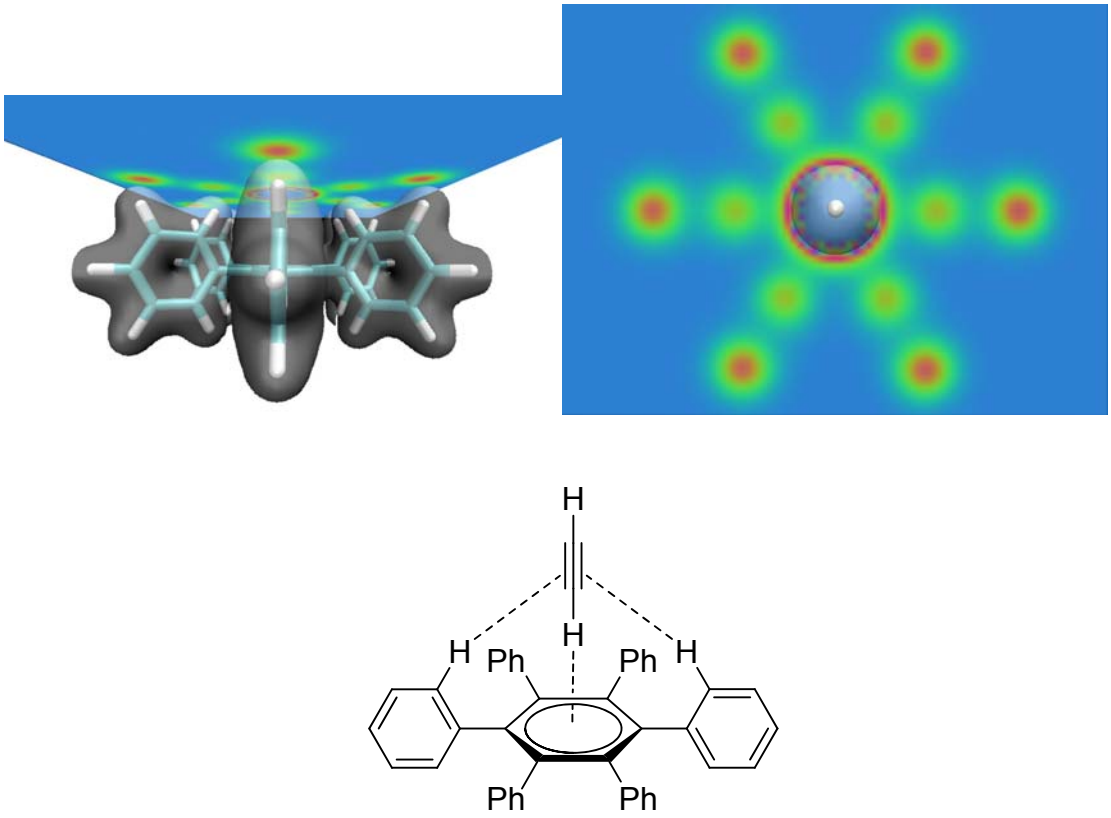

Figure S14. Plots of total charge density, showing the calculated acetylene-hexaphenylbenzene complex viewed from the side (top left) or the top (top right). The red regions correspond to high electron density. The apparent depleted electron density of the hydrogen atoms in the *ortho* positions of the peripheral phenyl groups is due to their participation in C-H···π interactions involving the π electrons of acetylene, as illustrated schematically for two of the six *ortho* hydrogen atoms (bottom). The other four equivalent interactions are omitted for clarity.

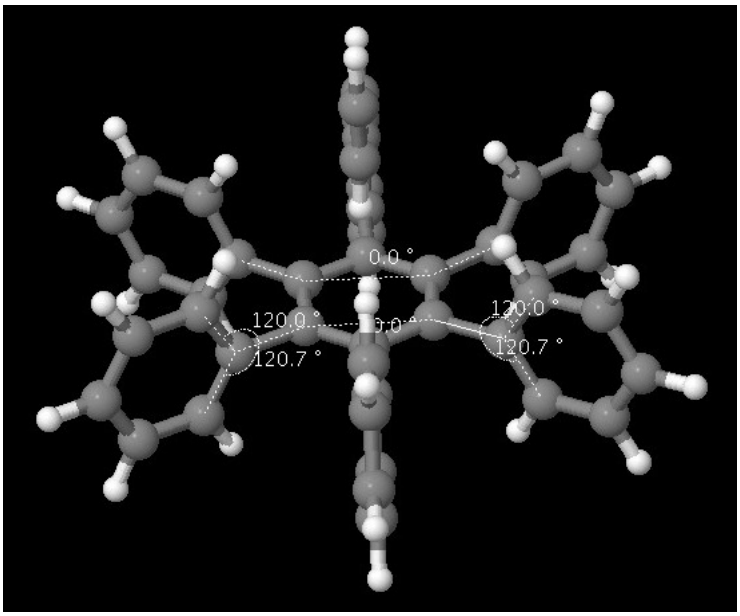

a

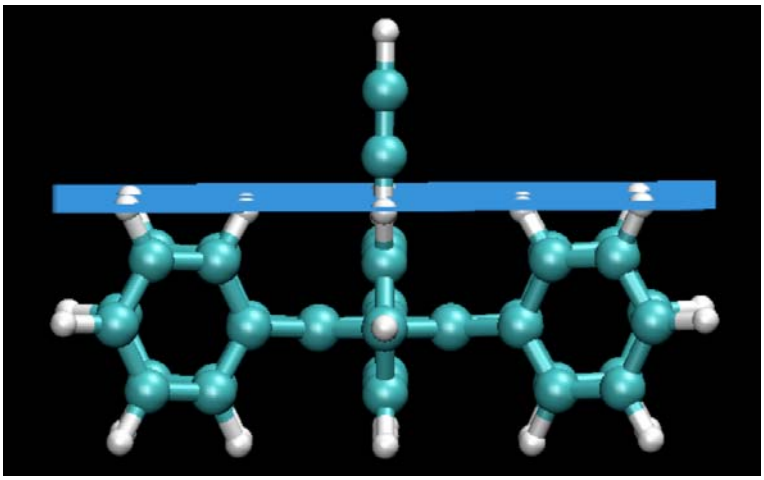

b

Figure S15. (a) Representation of geometric deformations in the calculated acetylene-hexaphenylbenzene complex showing that the aromatic core remains planar, but the *ortho* hydrogen atoms of the phenyl substituents are drawn slightly toward the bound acetylene. (b) View showing how the *ortho* and *meta* hydrogen atoms are positioned relative to a common plane (blue).

VI. Notes and References

1. J. R. Johnson, O. Grummitt, *Org. Synth.* **1943**, *23*, 92-93. J. R. Johnson, O. Grummitt, *Organic Syntheses*; Wiley: New York, 1955; Collect. Vol. III, pp 806-807.
2. L. F. Fieser, *Org. Synth.* **1966**, *46*, 44-48. L. F. Fieser, *Organic Syntheses*; Wiley: New York, 1973; Collect. Vol. V, pp 604-608.
3. J. Burdon, I. Farazmand, M. Stacey, J. C. Tatlow, *J. Chem. Soc.* **1957**, 2574-2578.
4. G. M. Sheldrick, *SHELXS-97, Program for the Solution of Crystal Structures* and *SHELXL-97, Program for the Refinement of Crystal Structures*; Universität Göttingen: Germany, 1997.
5. G. M. Sheldrick, *Acta Crystallogr.* **2008**, *A64*, 112-122.
6. A. Orita, H. Taniguchi, J. Otera, *Chem. Asian J.* **2006**, *1*, 430-437.
7. Signals for multiple aromatic carbon atoms are superimposed or form shoulders on other peaks.
8. S. K. Akubathini, E. Biehl, *Tetrahedron Lett.* **2009**, *50*, 1809-1811. A. Fürstner, A, Leitner, *Synlett* **2001**, 290-292.
9. T. Steiner, *J. Chem. Soc., Chem. Commun.* **1994**, 101-102.
10. E. J. Bylaska, W. A. de Jong, N. Govind, K. Kowalski, T. P. Straatsma, M. Valiev, D. Wang, E. Apra, T. L. Windus, J. Hammond, P. Nichols, S. Hirata, M. T. Hackler, Y. Zhao, P.-D. Fan, R. J. Harrison, M. Dupuis, D. M. A. Smith, J. Nieplocha, V. Tipparaju, M. Krishnan, A. Vazquez-Mayagoitia, Q. Wu, T. Van Voorhis, A. A. Auer, M. Nooijen, L. D. Crosby, E. Brown, G. Cisneros, G. I. Fann, H. Fruchtl, J. Garza, K. Hirao, R. Kendall, J. A. Nichols, K. Tsemekhman, K. Wolinski, J. Anchell, D. Bernholdt, P. Borowski, T. Clark, D. Clerc, H. Dachsel, M. Deegan, K. Dyall, D. Elwood, E. Glendening, M. Gutowski, A. Hess, J. Jaffe, B. Johnson, J. Ju, R. Kobayashi, R. Kutteh, Z. Lin, R. Littlefield, X. Long, B. Meng, T. Nakajima, S. Niu, L. Pollack, M. Rosing, G. Sandrone, M. Stave, H.

Taylor, G. Thomas, J. van Lenthe, A. Wong, and Z. Zhang, "NWChem, A Computational Chemistry Package for Parallel Computers, Version 5.1.1" (2009), Pacific Northwest National Laboratory, Richland, Washington 99352-0999, USA.

11. L. M. Woods, Ş. C. Bădescu, T. L. Reinecke, *Phys. Rev. B* **2007**, *75*, 155415(1-9).

12. A. Rochefort, J. D. Wuest, *Langmuir* **2009**, *25*, 210-215.

13. S. Grimme, *J. Comp. Chem.* **2006**, *27*, 1787-1799.

Annexe 3

Partie supplémentaire de l'article 5

Supporting Information

Tampering with Molecular Cohesion in Crystals of Hexaphenylbenzenes

Eric Gagnon,[†] Shira D. Halperin,[‡] Valérie Métivaud,[†]
Kenneth E. Maly,[‡] and James D. Wuest[†*]

[†]*Département de Chimie, Université de Montréal, Montréal, Québec H3C 3J7 Canada*
[‡]*Department of Chemistry, Wilfrid Laurier University, Waterloo, Ontario N2L 3C5 Canada*

Content **Page**

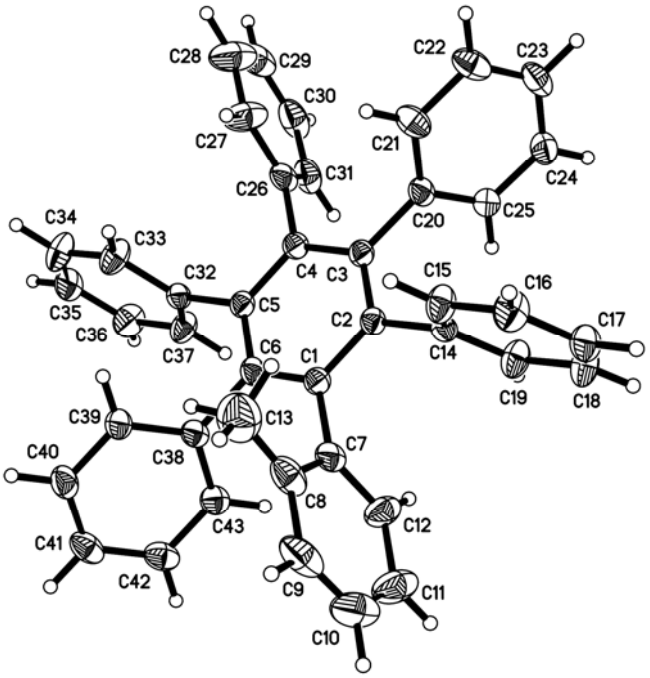

Figure S1. ORTEP view of the structure of crystals of 1-(2-methylphenyl)-2,3,4,5,6-pentaphenylbenzene (**3b**) grown from chlorobenzene. The ellipsoids of non-hydrogen atoms are drawn at the 30% probability level, and hydrogen atoms are represented by a sphere of arbitrary size.

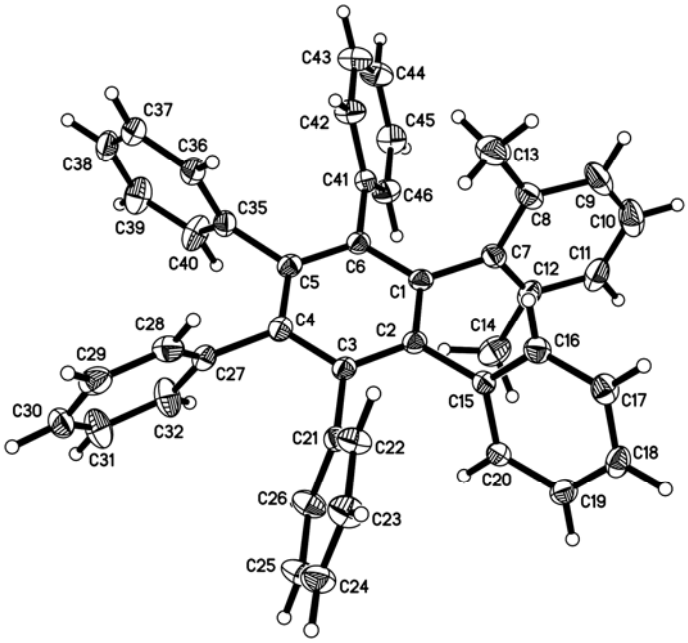

Figure S2. ORTEP view of the structure of crystals of 1-(2,6-dimethylphenyl)-2,3,4,5,6-pentaphenylbenzene (**3c**) grown from toluene. The ellipsoids of non-hydrogen atoms are drawn at the 30% probability level, and hydrogen atoms are represented by a sphere of arbitrary size.

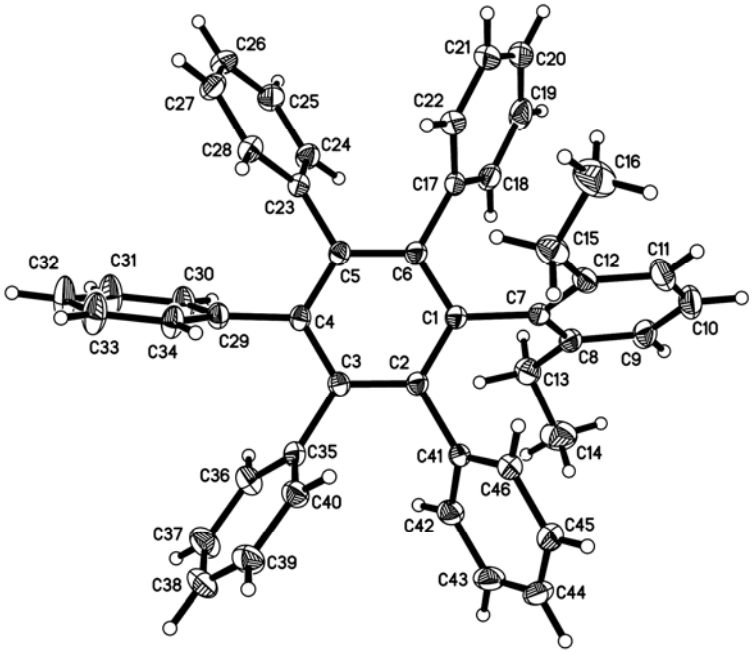

Figure S3. ORTEP view of the structure of crystals of 1-(2,6-diethylphenyl)-2,3,4,5,6-pentaphenylbenzene (**3d**) grown from toluene/hexanes. The ellipsoids of non-hydrogen atoms are drawn at the 30% probability level, and hydrogen atoms are represented by a sphere of arbitrary size.

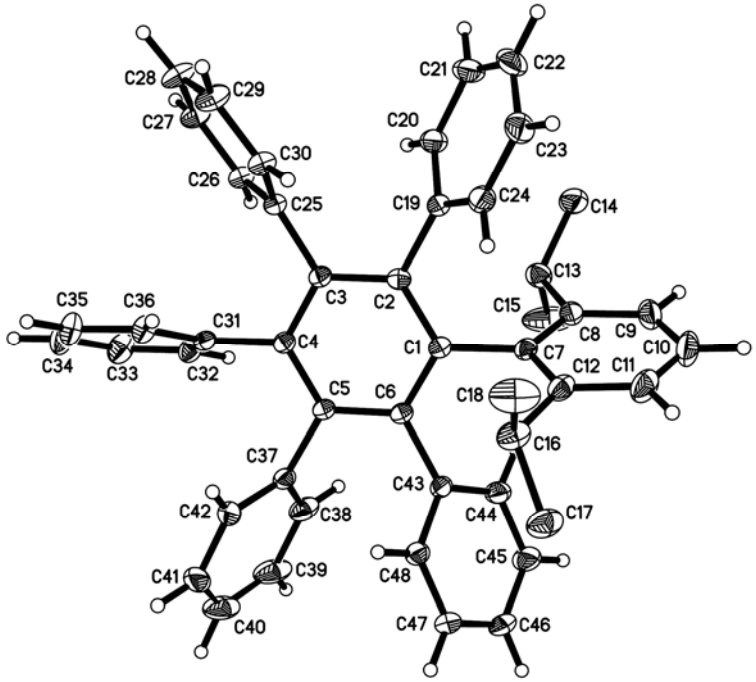

Figure S4. ORTEP view of the structure of crystals of 1-(2,6-diisopropylphenyl)-2,3,4,5,6-pentaphenylbenzene (**3e**) grown from toluene/hexanes. The ellipsoids of non-hydrogen atoms are drawn at the 30% probability level, and hydrogen atoms are represented by a sphere of arbitrary size.

Homogeneity of Bulk Crystalline Samples

In all structural studies, experimental powder X-ray diffraction patterns were recorded for each bulk crystalline sample and then compared with those calculated from single-crystal X-ray diffraction data. In all cases, these comparisons confirmed that the single-crystal specimens selected for structural analysis were representative of the bulk crystalline samples from which they were chosen.

Experimental powder X-ray diffraction patterns were recorded at 25 ºC in reflection mode on a Bruker D8 Advance powder X-ray diffractometer equipped with a VÅNTEC-1 linear position-sensitive detector, using Ge-monochromatized Cu $K\alpha_1$ radiation generated at 40 kV and 40 mA. Calibration of the instrument was done with a NIST 1976 corundum sample. For each experiment, the bulk crystalline sample was ground, the resulting powder was placed in a sample holder (PMMA holder ring), and the surface of the powder was flattened with a glass plate. Data were collected in Bragg-Brentano geometry in the range $2° < 2\theta < 50°$ with a step size of 0.016º and a counting time of 2s/step.

Structural data from single-crystal analyses were used to calculate theoretical powder X-ray diffraction patterns with the aid of Mercury software. Peak fitting and the refinement of lattice parameters were carried out using TOPAS software (Bruker), and Pawley fitting was applied to the powder X-ray diffraction patterns. All experimental and calculated diffraction patterns were plotted in the most pertinent range ($5° < 2\theta < 35°$). The x-scale of the experimental pattern was shifted to minimize the slight angular shift due to the effect of temperature.

PXRD Data for Compound **3b**

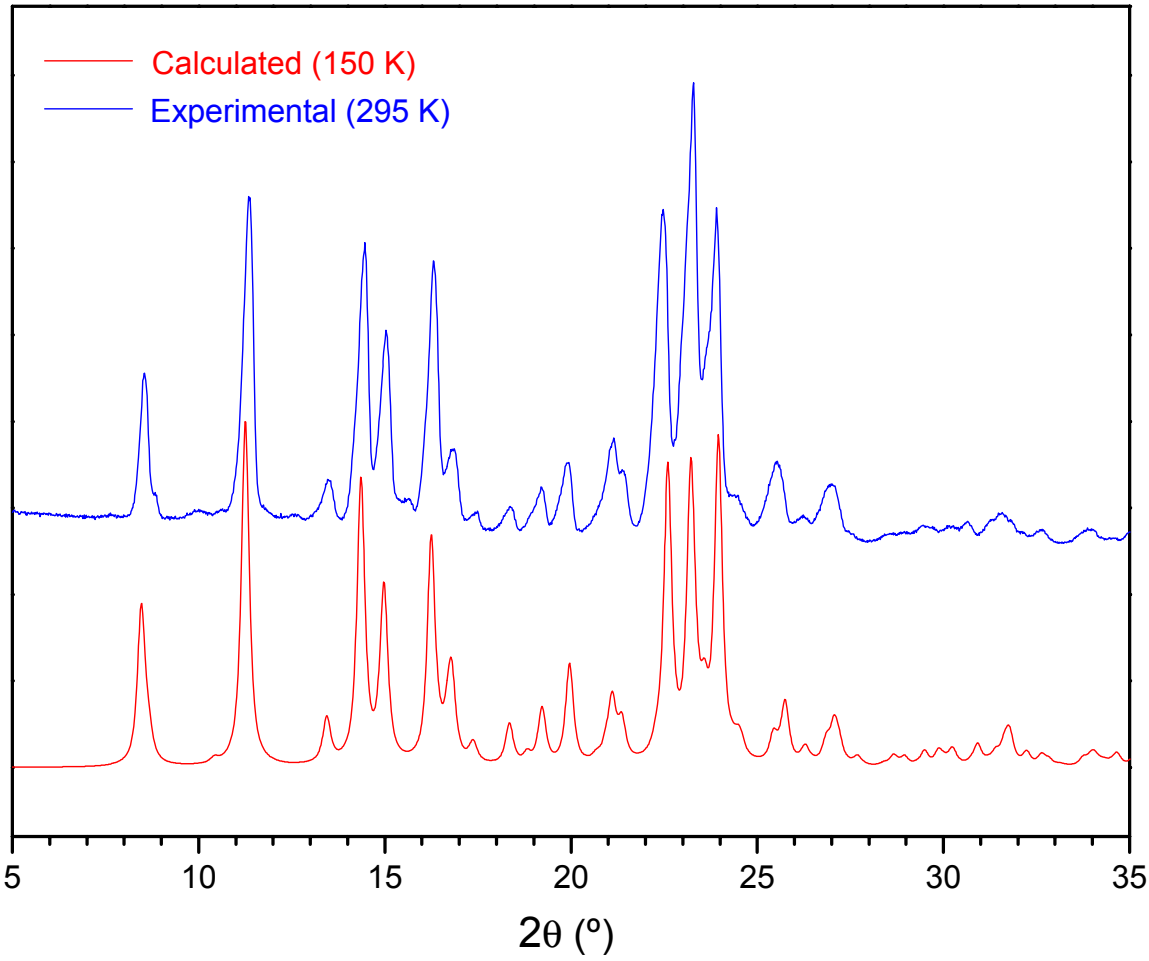

Figure S5. Comparison of experimental and calculated powder X-ray diffraction patterns of compound **3b**.

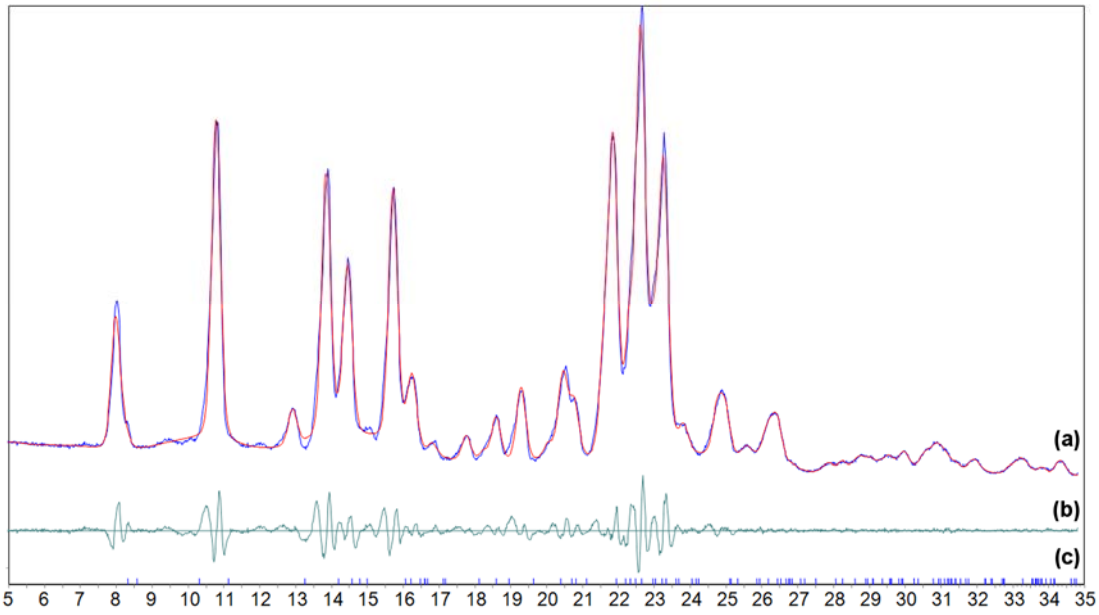

Figure S6. (a) Simulated powder X-ray diffraction pattern of crystals of compound **3b** (red curve) as determined by Pawley fitting of the experimental powder X-ray diffraction pattern (nearly superimposed blue curve). (b) Difference between experimental and calculated intensities. (c) Position of calculated reflections.

Table S1. Crystallographic Data for Compound **3b** as Determined by Pawley Fitting of Powder X-Ray Diffraction Data at 295 K.

Compound	$C_{43}H_{32}$
temperature (K)	295
crystal system	orthorhombic
space group	$Pna2_1$
a (Å)	12.4098 (29)
b (Å)	11.7731 (34)
c (Å)	21.1504 (45)
α (º)	90
β (º)	90
γ (º)	90
V (Å^3)	3090.1 (13)
Z	4

PXRD Data for Compound **3c**

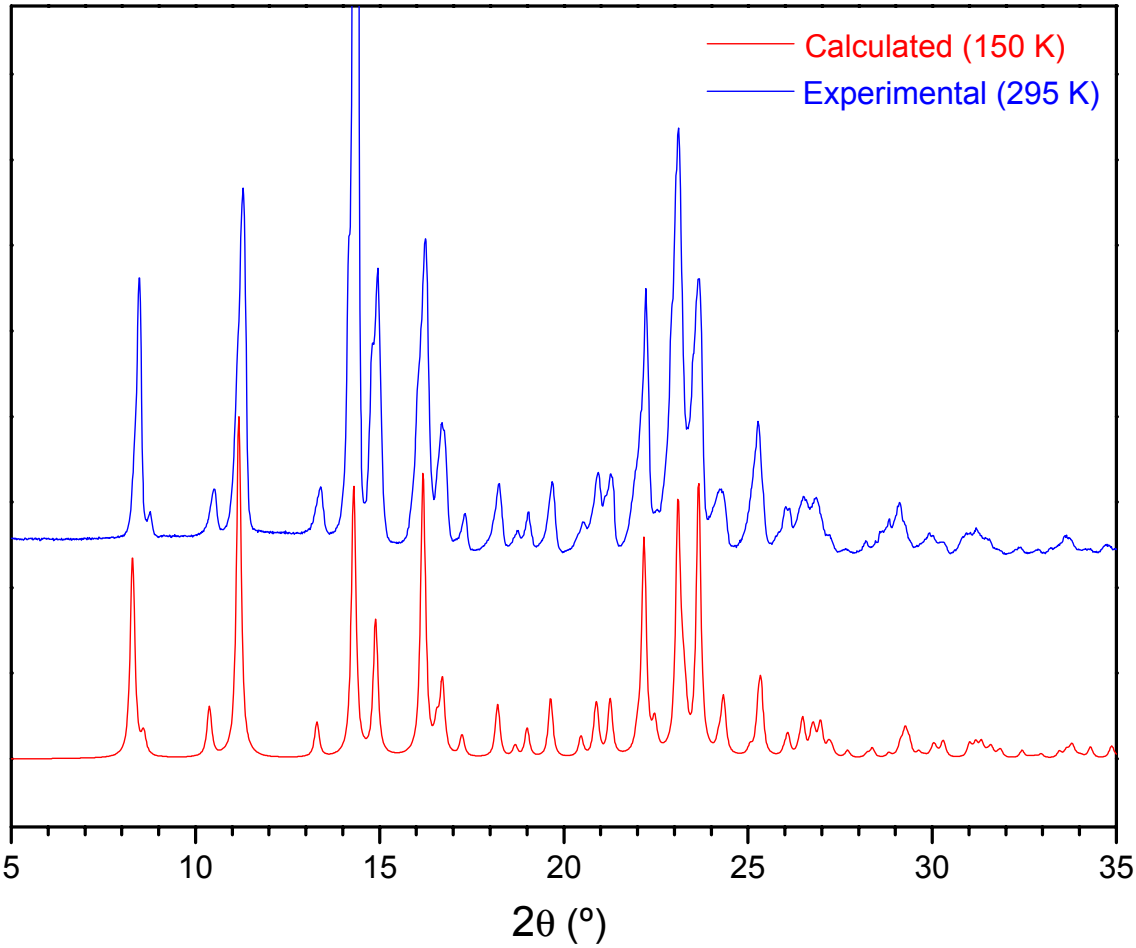

Figure S7. Comparison of experimental and calculated powder X-ray diffraction patterns of compound **3c**.

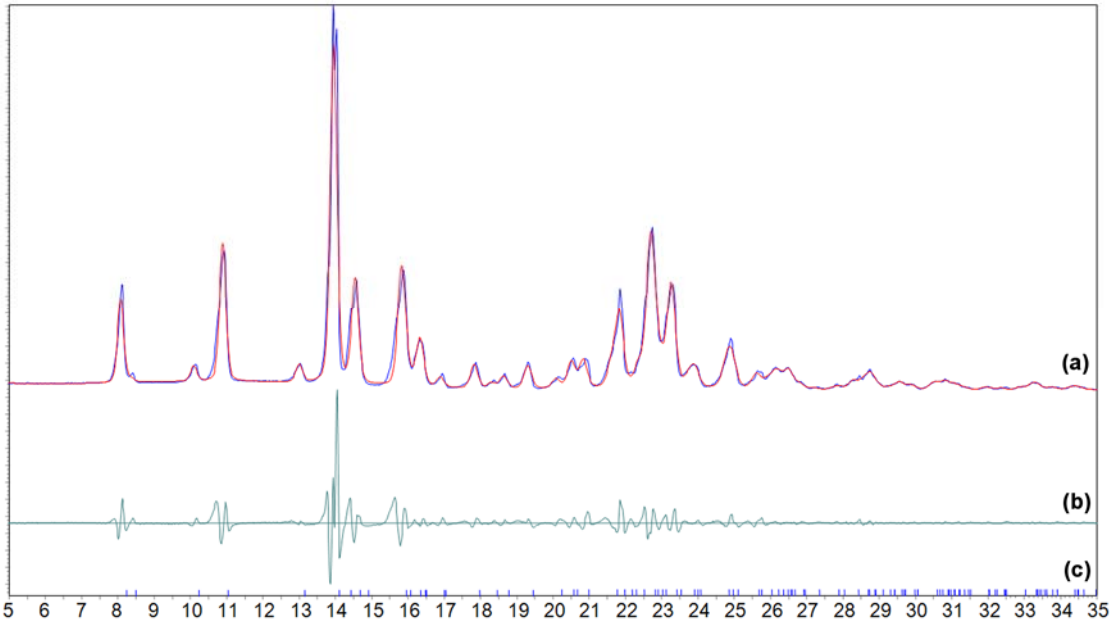

Figure S8. (a) Simulated powder X-ray diffraction pattern of crystals of compound **3c** (red curve) as determined by Pawley fitting of the experimental powder X-ray diffraction pattern (nearly superimposed blue curve). (b) Difference between experimental and calculated intensities. (c) Position of calculated reflections.

Table S2. Crystallographic Data for Compound **3c** as Determined by Pawley Fitting of Powder X-Ray Diffraction Data at 295 K.

Compound	$C_{44}H_{34}$
temperature (K)	295
crystal system	orthorhombic
space group	$Pna2_1$
a (Å)	12.5493 (32)
b (Å)	11.8791 (45)
c (Å)	21.4742 (67)
α (º)	90
β (º)	90
γ (º)	90
V (Å^3)	3201.3 (18)
Z	4

PXRD Data for Compound **3d**

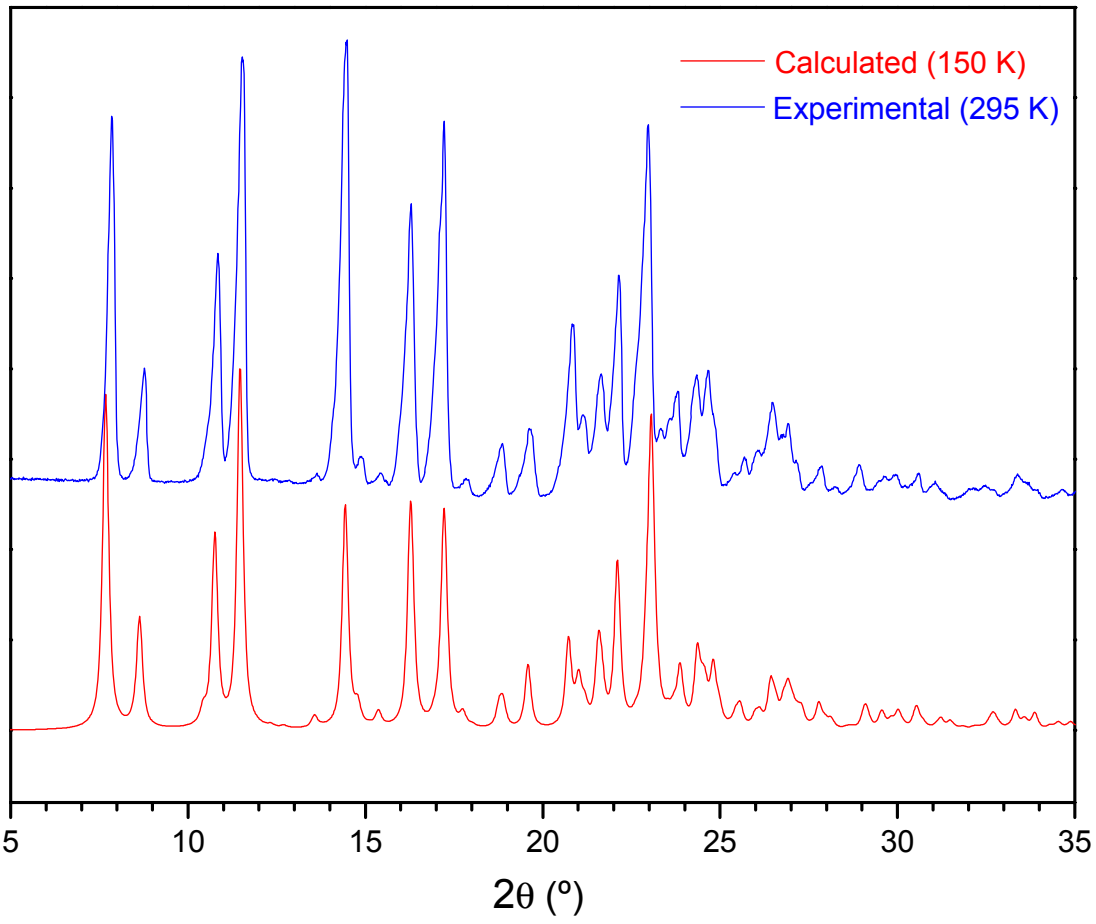

Figure S9. Comparison of experimental and calculated powder X-ray diffraction patterns of compound **3d**.

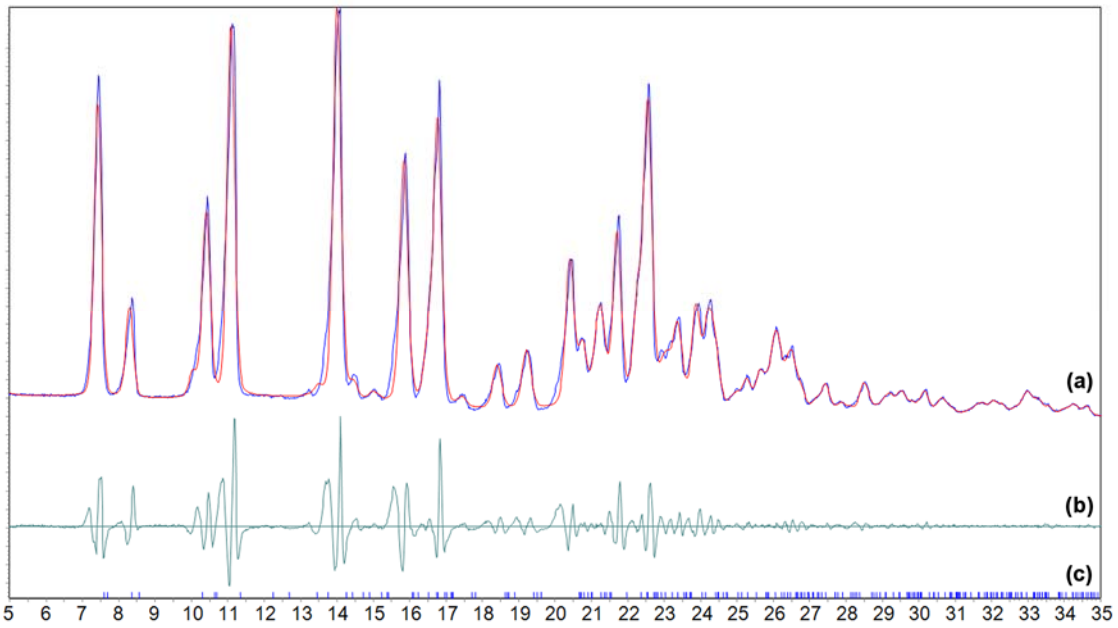

Figure S10. (a) Simulated powder X-ray diffraction pattern of crystals of compound **3d** (red curve) as determined by Pawley fitting of the experimental powder X-ray diffraction pattern (nearly superimposed blue curve). (b) Difference between experimental and calculated intensities. (c) Position of calculated reflections.

Table S3. Crystallographic Data for Compound **3d** as Determined by Pawley Fitting of Powder X-Ray Diffraction Data at 295 K.

Compound	$C_{46}H_{38}$
temperature (K)	295
crystal system	monoclinic
space group	$P2_1/n$
a (Å)	12.535 (13)
b (Å)	11.889 (13)
c (Å)	23.200 (37)
α (º)	90
β (º)	98.15 (12)
γ (º)	90
V (Å^3)	3422.6 (76)
Z	4

PXRD Data for Compound **3e**

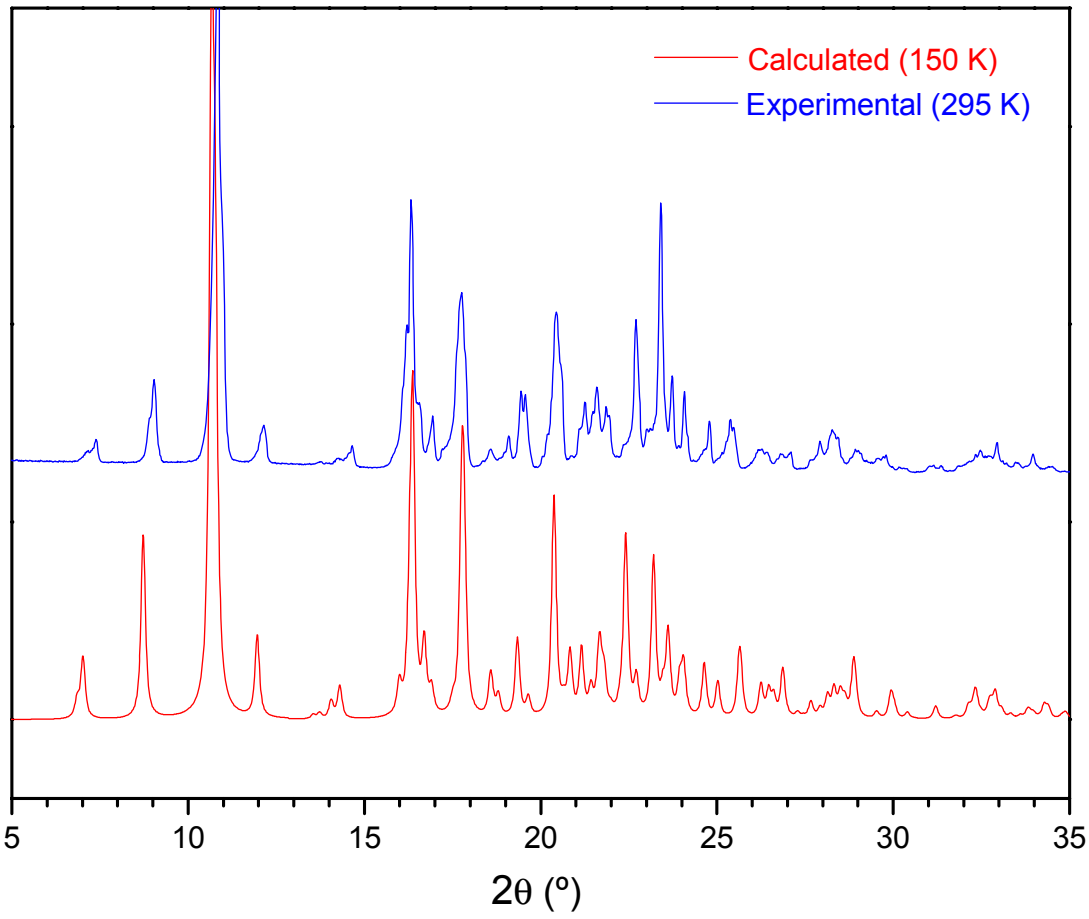

Figure S11. Comparison of experimental and calculated powder X-ray diffraction patterns of compound **3e**.

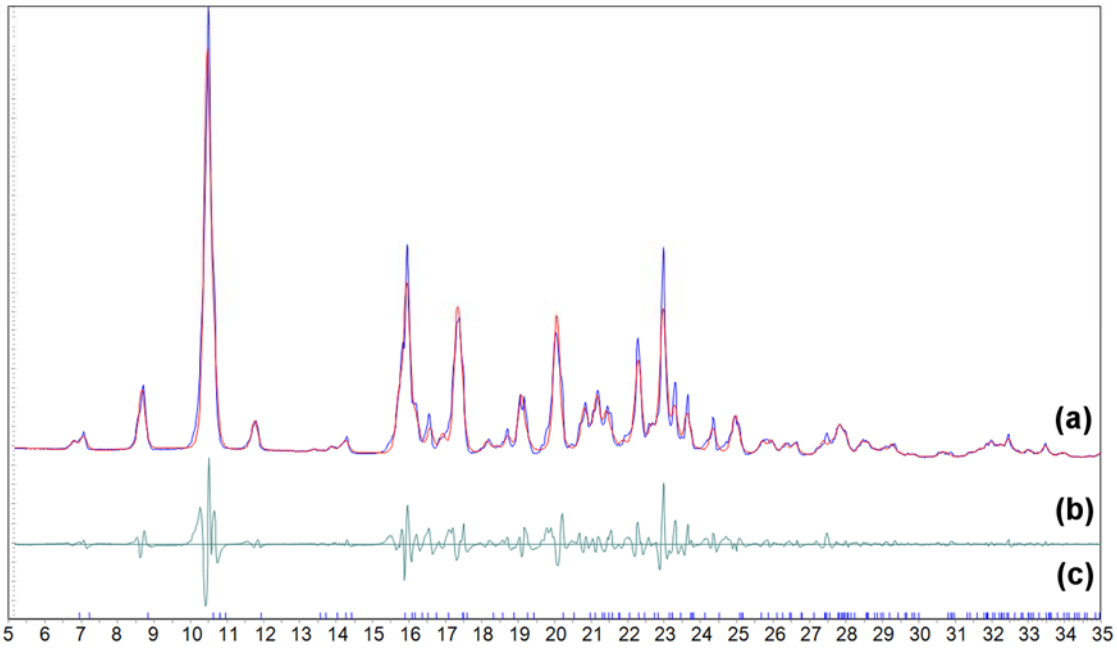

Figure S12. (a) Simulated powder X-ray diffraction pattern of crystals of compound **3e** (red curve) as determined by Pawley fitting of the experimental powder X-ray diffraction pattern (nearly superimposed blue curve). (b) Difference between experimental and calculated intensities. (c) Position of calculated reflections.

Table S4. Crystallographic Data for Compound **3e** as Determined by Pawley Fitting of Powder X-Ray Diffraction Data at 295 K.

Compound	$C_{48}H_{42}$
temperature (K)	295
crystal system	monoclinic
space group	$P2_1$
a (Å)	12.8232 (30)
b (Å)	11.0875 (45)
c (Å)	13.3414 (32)
α (º)	90
β (º)	102.489 (17)
γ (º)	90
V (Å^3)	1851.96 (98)
Z	2